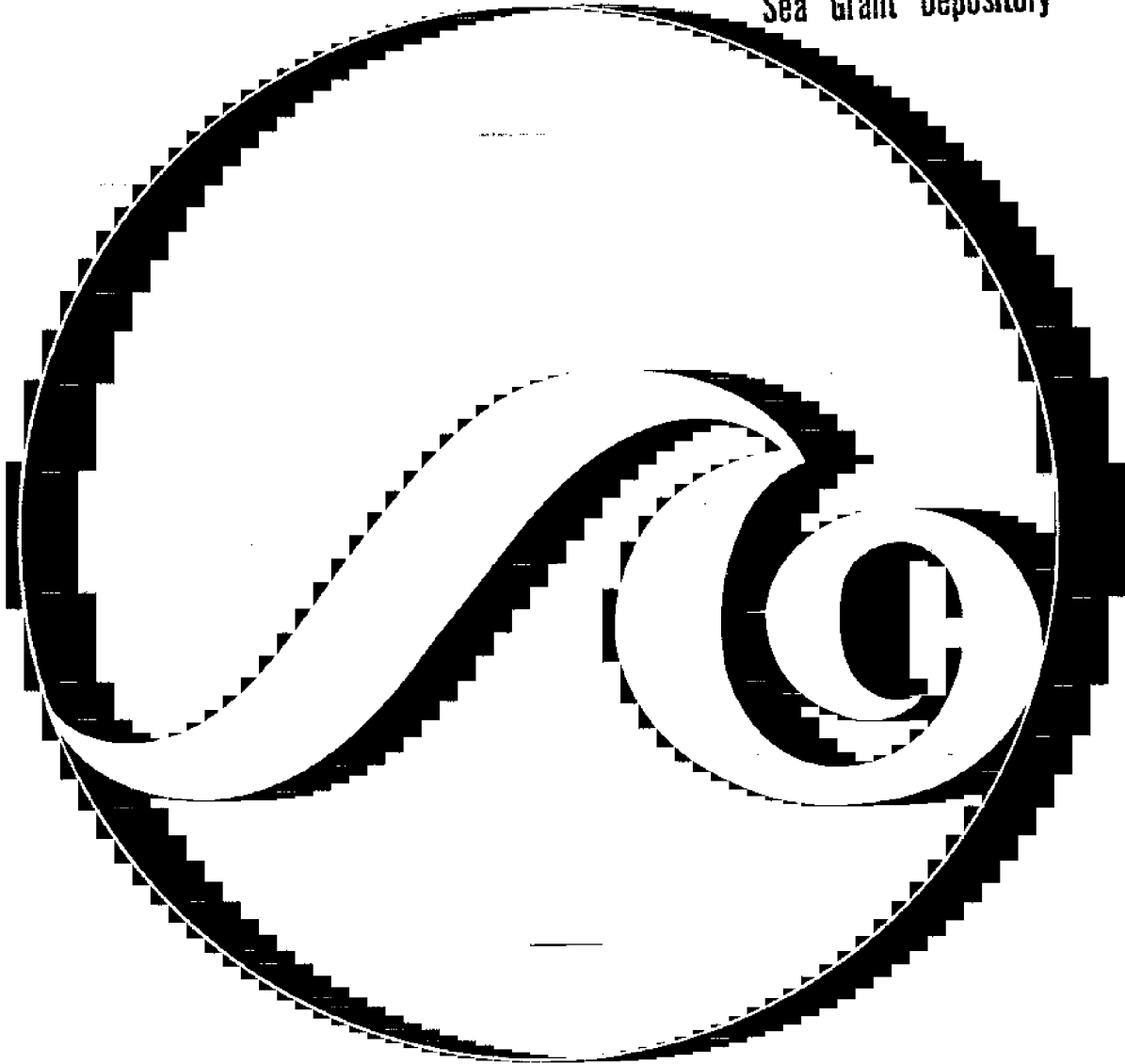Gregory B. Baecher
Mark Chan
Thomas S. Ingra
Thomas Lee
Louis R. Nucci

Geotechnical Reliability of Offshore Gravity Platforms

GEOTECHNICAL RELIABILITY
OF OFFSHORE GRAVITY PLATFORMS

by

Gregory B. Baecher

and

Mark Chan

Thomas S. Ingra

Thomas Lee

Louis R. Nucci

TABLE OF CONTENTS

ACKNOWLEDGMENTS

RELATED REPORTS

Baligh, Mohsen M., Amr S. Azzouz, Robert T. Martin. CONE PENETRATION TESTS OFFSHORE THE VENEZUELAN COAST. MITSG 80-21. 163 pp. $8.00.

Levadoux, Jacques-Noel and Mohsen M. Baligh. PORE PRESSURES DURING CONE PENETRATION IN CLAYS. MITSG 80-12. 310 pp. $8.00.

Baligh, Mohsen M. and Jacques-Noel Levadoux. PORE PRESSURE DISSIPATION AFTER CONE PENETRATION. MITSG 80-13. 368 pp. $8.00.

Baligh, Mohsen, M., Vitoon Vivatrat and Charles C. Ladd. EXPLORATION AND EVALUATION OF ENGINEERING PROPERTIES FOR FOUNDATION DESIGN OF OFFSHORE STRUCTURES. MITSG 79-8. 268 pp. $8.00.

MIT/Marine Industry Collegium. TOWARDS IMPROVED TECHNIQUES FOR PREDICTING SOIL STRENGTH: OPPORTUNITY BRIEF #16. MITSG 79-17. 19 pp. $3.50.

The MIT Sea Grant Marine Resources Information Center maintains an inventory of technical publications. We invite orders and inquiries to:

Marine Resources Information Center
MIT Sea Grant College Program
Building E38-302
Massashusetts Institute of Technology
Cambridge, MA   02139
(617) 253-5944

PREFACE

The research reported in this volume began as an ambitious attempt to
quantify risks in offshore structures, in particular gravity platforms,
deriving from uncertainties in geotechnical bottom conditions and models of
foundation performance. The work has led to something different, for among
the early conclusions of the research were that (a) present reliability
analysis techniques and present statistical procedures for interpreting
geotechnical data are inadequate to quantify overall risks, and (b) many of
the uncertainties in offshore construction are inductive and not amenable to
quantified analysis. Argument against these conclusions is sure to be reg-
istered by those favoring subjective probability approaches, but for the
present work such procedures were not seriously investigated. This is not
to suggest these approaches to be inappropriate, only that the objectives
of the present work were directed at generic procedures for analyzing risk
and reliability, and not with the requirements of a particular project and
designer.

What has developed in the present work is an approach to the use
of reliability techniques in analyzing those aspects of the design of off-
shore facilities that are benefited by such analyses, and a generic analysis
of such uncertainties. The predictions of risk and reliability that result
are, of course, partial. They do not include such things as negligence and
gross error, or do they include modes of performance about which basic
mechanistic understanding is lacking. However, for the purposes of explora-
tion, design and regulation they provide quantified analyses that allow
partial optimizations and rational bases for decisions.

The results of this work, therefore, do not fulfill all the original
objectives, because certain of these in hindsight were not fulfillable.

Of course, this too is a conclusion. However, current techniques of risk and reliability analysis provide a strong analytical framework for dealing rationally with many uncertainties of offshore design. This report presents those capabilities, and summarizes data and analyses supporting this conclusion.

This report is a summary of work carried out between August 1977 and August 1979, under funding by MIT Project Seagrant.

1. INTRODUCTION

As with any engineering project, offshore facilities inevitably involve risks and are designed in the face of uncertainties. The recent surge in offshore development, particularly the move to deeper waters and more hostile environments, has led to a situation with even larger uncertainties than those of onshore counterparts. These uncertainties arise from environmental loadings (e.g., storm wave and earthquake), from inadequately understood physical mechanisms (e.g., structural and soil response), and from insufficient data to precisely characterize offshore sites (e.g., bottom parameter or storm recurrence rates).

These uncertainties are normally dealt with by designing for adequately high factors of safety against chosen design loads. This is done to assure that the available resistance of a structure is subtantially greater than the loads it normally experiences, and also higher than the extraordinary loads which may occur in the life of the structure. However, because the loads actually to be experienced by the structure as well as the structural and foundation response to those loads are known only imperfectly, no matter how high the design factor of safety some probability remains that realized loads will exceed realized resistance, leading to partial damage or total collapse of the facility. The consequent costs of such failures can exceed the immediate structural damage, through oil spillage, other environmental impact, loss of service of the facility, and in certain cases human injury or death.

The questions, then, are what is the magnitude of this probability of damage or collapse, what are the significant sources of uncertainty, and what is the marginal cost of reducing risk? The work reported here deals
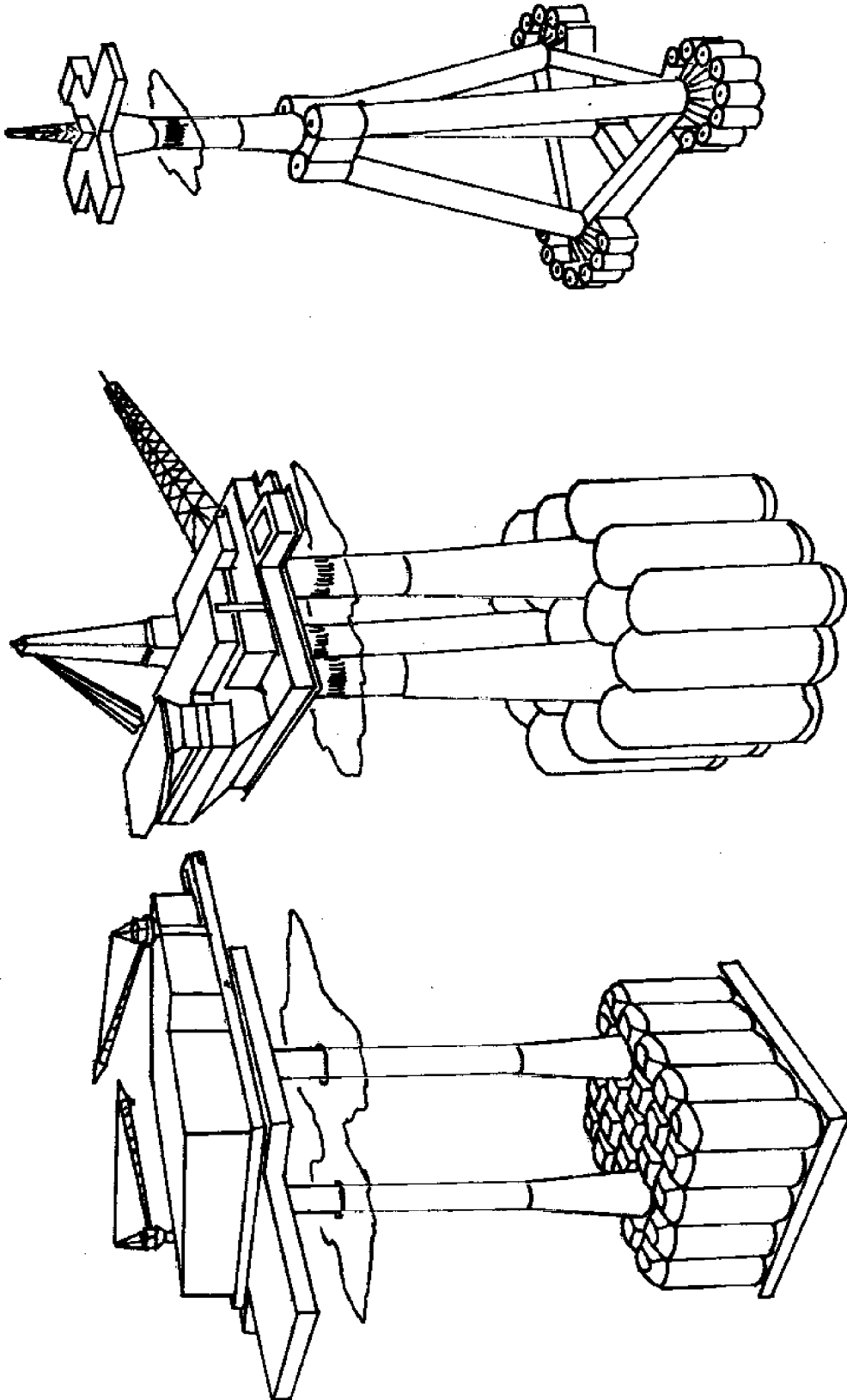
Figure 1.1 -- Various deep water gravity platform designs.

specifically with geotechnical sources of risk. That is, with the principle sources of uncertainty affecting predictions of foundation performance, and with the aggregate uncertainty they lead to. To limit the breadth of coverage, the work has focused on gravity-type platforms, founded on the ocean bottom, held in place by their weight. Several types of gravity platforms in place or under construction are shown in Figure 1.1. While many offshore platforms are not of this type, being founded rather on driven piles, much of the present work applies to them as well.

The evolution of offshore construction has progressed rapidly. Beginning as extensions of nearby on shore facilities, offshore towers have now been placed in over 300 m of water. While the early decades of offshore development, particularly in the Gulf of Mexico, proceeded at a moderate rate into deeper waters, the last decade has seen a tripling of the depths in which structures have been placed (Figure 1.2). This means that the long history of empirical validation and trial and error design which normally characterize geotechnical engineering are missing in much offshore work. The problem is, of course, compounded by new development in environments such as the North Sea, Alaska, and potentially the Antarctic. This means that much of the new design is based on modeling, usually numerical, and on extrapolation from sparse data bases.

The problem of risk offshore is complicated by the design philosophy of many owners and constructors of offshore platforms. Given the commercial nature of these ventures and limited design lives, there is understandably little incentive for the highly conservative design practice common in other large civil projects, for example, dams or bridges. Offshore facilities tend to be designed with an attempt to rationally balance financial risk of failure against marginal design modifications.
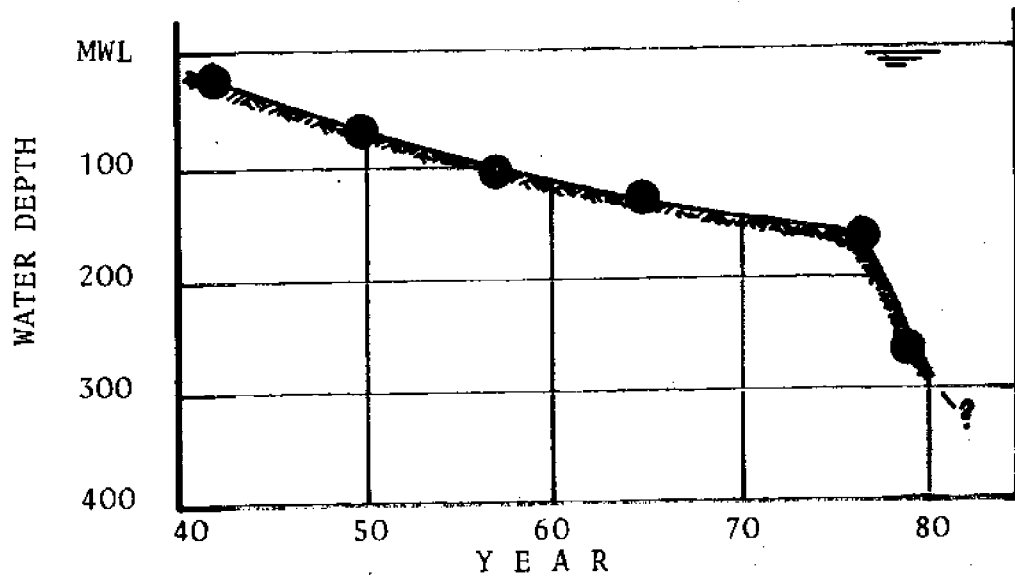
Figure 1.2 -- Progression of offshore construction
to greater depths.
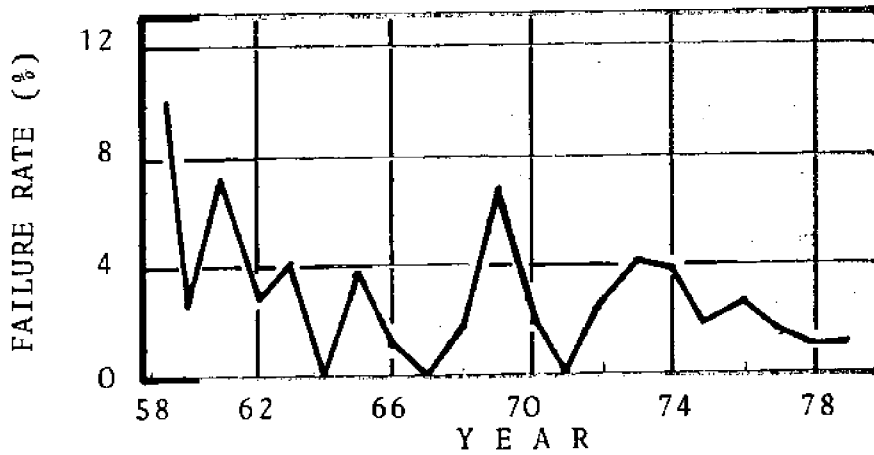
Figure 1.3 -- Failure rate of fixed offshore
platforms (from Moan, 1977).

Nevertheless, the historical performance of offshore facilities has been fairly good. There have been no substantial failures of major gravity platforms, and the record of failures for pile supported platforms is shown in Figure 1.3. However, the historical record for the former is only slightly more than 10 years, with the total numbers of such towers increasing geometrically as time goes on.

In United States waters, platform design has been performed primarily in accordance with the recommended guidelines of the American Petroleum Institute (API RP ZA, 1978), and more recently of the American Concrete Institute. The API guides are essentially extensions of American Institute for Steel Construction design rules (AISC, 1970), modified by offshore experience. The ACI guides are new design rules based heavily on the performance of structures in the North Sea, more of which are concrete than in the Gulf of Mexico and other shallow regions. Neither of these codes has the strength of law, and the U.S. Federal Government through the Department of Interior and Department of Energy is now taking a more active stance in regulating offshore construction. Recommended guides like those of the API and ACI have also been proposed in other countries, for example, by Det Norsk Veritas and Fédération Internationale de la Précontrainte (FIP)

ORGANIZATION OF REPORT

This main part of the report is organized in five broad chapters (Figure 1.4). The first presents an overview of the sources of geotechnical uncertainty in offshore structures, previous quantitative analysis of those uncertainties, and the philosophy of formal methods in geotechnical reliability analysis. The second and third examine the basic uncertain variables, dealing with environmental loads and load effects, and with site characterization and parameter estimates, respectively. Chapter 5 is an extended discussion of
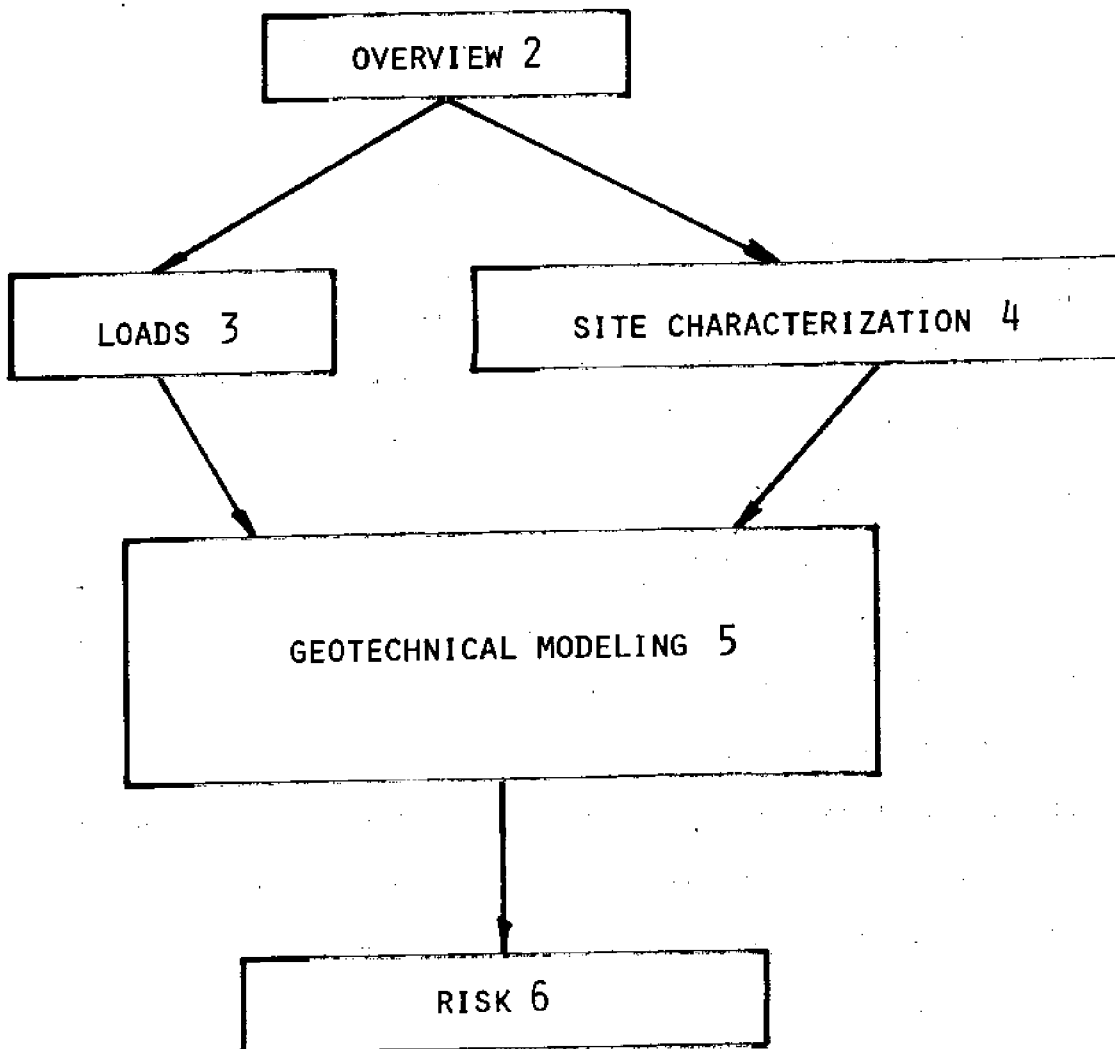
Figure 1.4 -- Organization of Report.

the problem of modeling foundation performance, and the uncertainties of that undertaking. Finally, Chapter 6 considers the aggregation of these uncertainties into overall estimates of risk and reliability.

To illustrate the analyses and methods developed in the course of the work, a specific site on the southern flank of Georges Bank has been chosen for discussion (Figure 4.12). This site had been studied earlier by Laszlo (1976), and was chosen for its location offshore New England, the availability of data, and its inclusion in potentially developable tracts (Bureau of land Management, 1976). Specific information on the site has been introduced as needed throughout the report.

2.   RISK ANALYSIS OF OFFSHORE STRUCTURES

Offshore structures are designed to withstand loadings they may exper-
ience during their design life. That design is aimed at ensuring that for
all mechanisms of failure that a structure may experience, the available re-
sistance to failure exceeds the realized loads. No matter how detailed the
process of modeling and design, and no matter how sophisticated the analysis
of empirical data or performance, design remains an inductive task. Risk
analysis, too, remains an inductive task. The methods of risk analysis,
like other methods of engineering science, are tools for aiding human judg-
ment and do not replace it.

2.1   Risk Analysis

Risk analysis techniques are in many ways accounting schemes. The
purpose of these techniques is to maintain logical (i.e., deductive) consis-
tency among empirical observations, physical theory, and engineering opinion
in drawing conclusions about the performance of a facility. This is not an
unimportant task or one that is otherwise easily accomplished, despite
common wisdom. A large literature on the analysis of uncertainties and
human decision making attests to the difficulties of intuitively dealing
with, let alone aggregating uncertainties (Hogarth, 1975). Geotechnical
engineering is no exception (Nordquist, 1979).

Given this task, risk analysis must be a logically structured, consis-
tent, explicit format for combining information from all available sources
and deducing conclusions which follow objectively within that format. The
format itself, however, incorporating a number of assumptions and sources of
information can never be said to be wholly objective.

Criteria against which risk analyses must be based are (e.g., Latai, 1977):

1) The results must be useable. The answers provided to questions must be both important and relevant to decisions that have to be taken.

2) The analyses must reflect profound understanding of the systems being studied. The questions answered must be clear and their answers, to the extent possible, complete.

3) The analyses must be replicable. Independent groups analyzing the the same systems with the same method must arrive at nearly the same results.

These criteria are not easily satisfied, and much of what now passes for risk analysis in civil construction only partially achieves these goals.

The basic procedure for risk analysis consists of four steps:

I. Enumerate failure modes or "limiting states."

II. Select physical theories and develop models for predicting the interaction of events and processes.

III. Estimate probabilities associated with events, processes, and series of events and processes.

IV. Establish measures for the consequences of failures.

To do these four things, the problem being analyzed must be very well understood. The ways in which the system can fail must be describable and the consequences of failure must be identifiable. The problem must also be well structured. The task of completing steps I through IV is almost entirely inductive. The risk analysis itself only provides a reference for organizing the results and combining them to draw consistent conclusions.
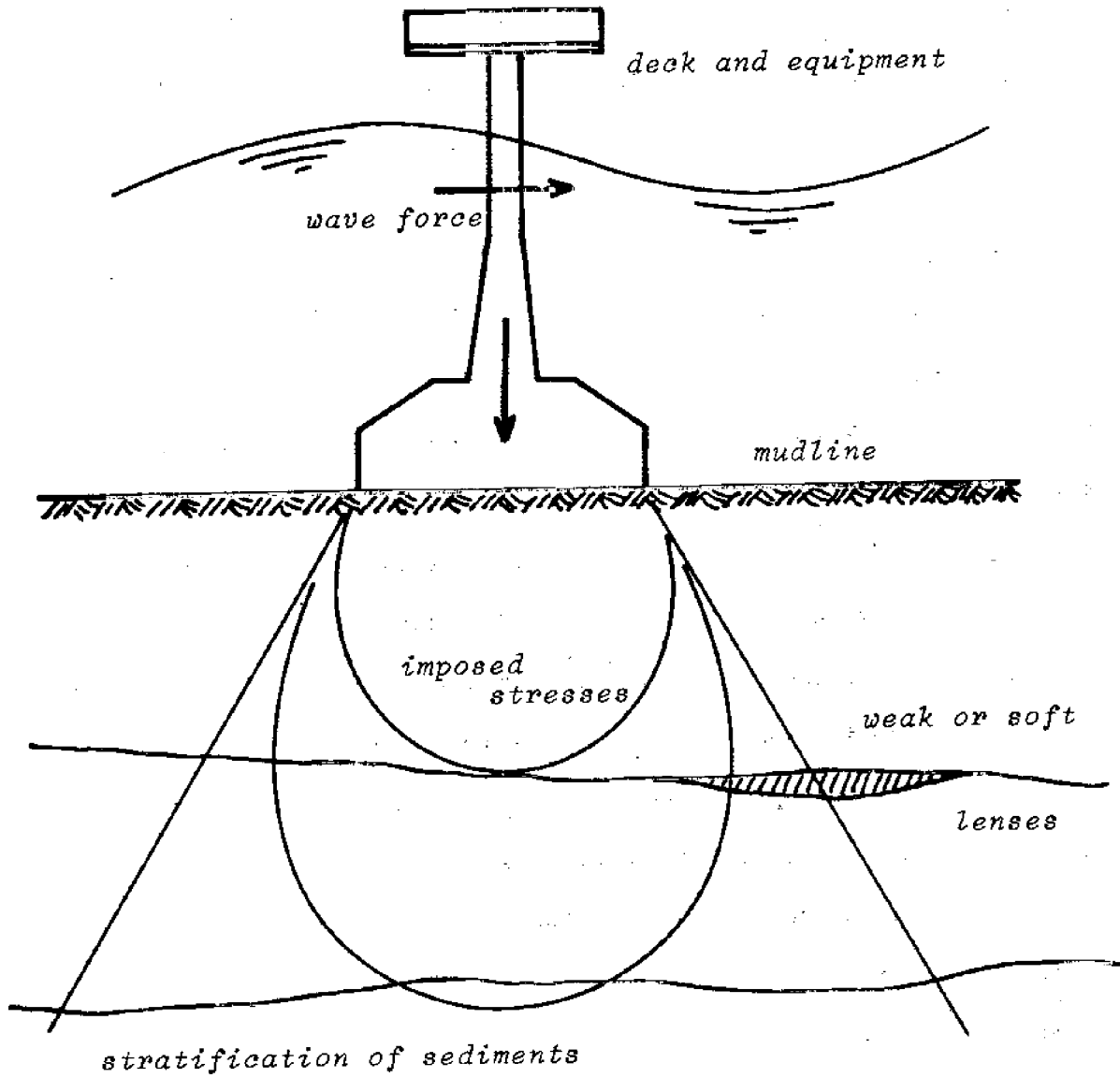
Figure 2.1 -- Typical Profile view of offshore gravity platform

2.1.1 Enumerating Failure Modes

The common objection to risk analysis is that there is no way to account for omissions -- failure modes unthought of, or event dependencies overlooked. This is true of risk analyses as of any other engineering analysis. The resulting quantifications of risk are always conditional on the modeling assumptions introduced and are therefore quasi lower bounds. This is not a limitation of risk analysis, per se, but of deductive logic generally.

As opposed to many man-made systems like electronics, foundations for offshore structures are "open" systems. That is, they exist within a larger environment and possess an essentially infinite number of potential failure modes. Most of these cannot be enumerated, and thus the set of modes analyzed is never exhaustive. The modes of failure chosen for analysis are those thought to be important (Figure 2.2), but, they can only be identified by (i) the experience of a failure, (ii) constructing and operating on a model to deduce mechanisms of failure (within the context of the model), or (iii) intuitive reasoning. There is no way of insuring that an important mechanism of failure has not been omitted. In onshore practice, this situation, in combination with the difficulty of modeling certain behaviors, has led to the well known "observational approach." This approach has more limited application offshore.

2.1.2 Estimating Probabilities

The estimation of probabilities requires that events, processes, and parameters be precisely defined. Such definitions are not innate, but depend on the use to which the probabilities are to be put. In this case they depend on the models of site conditions and foundation behavior adopted. Parameters, even those purported to quantify physical properties like undrained strength, are only partly innate. In large measure they are
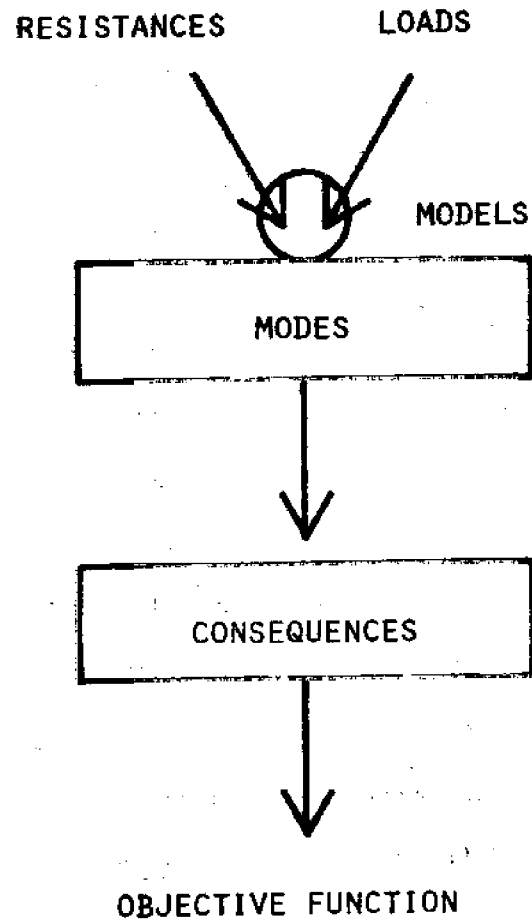
Figure 2.2

artifacts of and inseparable from the geotechnical models they are used in (e.g., Lambe, 1973; Baecher, 1979a).

Although ostensibly based on in situ information and historical data, behind the facade of geotechnical and oceanographic technology parameter estimates are highly subjective (Baecher, 1978). The amount of site information is insufficient to precisely define spatial properties of the sub-bottom, and often allows only the first few moments of spatial or temporal averages to be calculated. Just as for failure modes, geologic or hydrographic anomalies must be conceived of before their probabilities of existing can be calculated. Section 4 covers these points in greater detail.

2.1.3 Establishing Consequences

Just as for failure modes, establishing consequences is an inductive problem in that from the essentially infinite number of effects caused by adverse behavior of a structure only a limited number are selected as important for analysis. Those that are unthought of, naturally, are not weighted in making decisions.

For the purpose of design-decision in civil construction, consequences are commonly divided into three classes: financial, environmental and social, which in turn are subdivided in a tree-like hierarchy until a set of objectives is obtained that either cannot be further subdivided or is operational at its level of detail. This set of subobjectives should be complete, in that it includes all consequences that bear on a decision; and clear, in that each subobjective has unambiguous meaning.

To each subobjective some scale of measurement must be assigned, which in current usage are normally termed 'attributes'. An attribute should be comprehensive in that important differences in the degree to which

FIGURE 2.3 -- MODES OF FOUNDATION FAILURE

BEARING CAPACITY

OVERTURNING

DIFFERENTIAL SETTLEMENT

SLIDING

EXCESSIVE SETTLEMENT

LIQUEFACTION
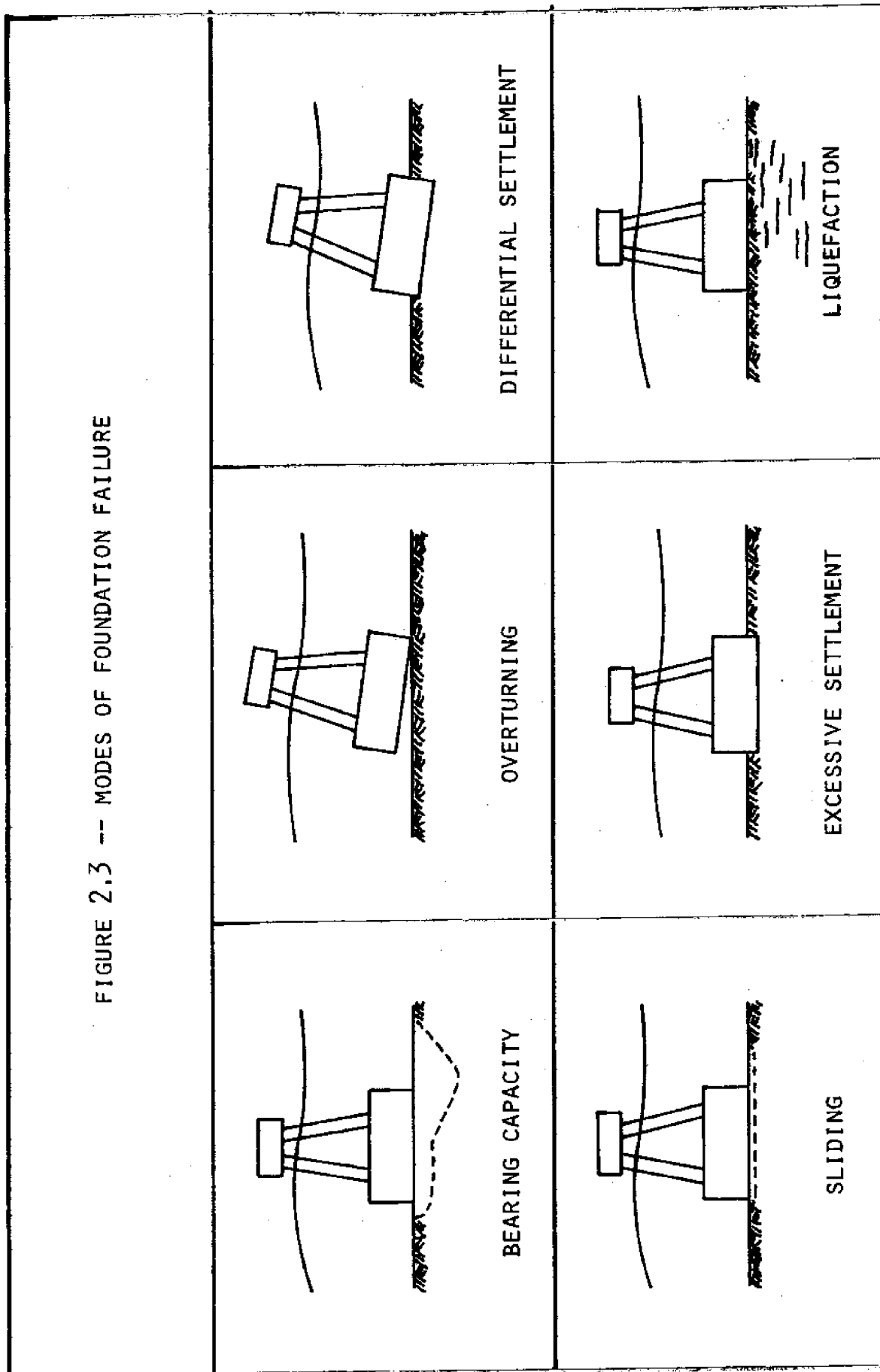
a subobjective is achieved are reflected in numerical changes in the attributes, and vice versa. However, an attribute must also be useable, in that measurement along it is possible; and understandable in that its values carry meaning to the analyst or designer. Thus, appropriate attributes are often difficult to define, and are often only partial correlates to the consequences or subobjectives one actually wishes to measure.

Perhaps the central problem in developing an objective function for risk analysis is combining "non-commensurate" consequences into a scalar measure to be compared across design alternatives. A number of approaches have evolved during the past twenty years (e.g., Zelan, 1973; Keeney and Raiffa, 1975), but several practical problems remain. These problems were seen as outside the scope of the present study, however, and are not further addressed.

Most work to date on reliability analysis for offshore structures has used the single dimension of financial cost for an objective function, and minimizing expected cost as the criterion of optimality. Little work seems to have been done on risk aversion, although one-dimensional utility theory seems an obvious vehicle in future applications.

2.2   Sources of Uncertainty

Geotechnical engineers in the course of their work are forced to deal with uncertainties seldom tolerated in most branches of civil engineering Unlike man-made materials, soil and rock masses are naturally variable and little information is available with which to characterize them. Properties measured in the laboratory may only approximately apply to in situ conditions, and the mathematical models which most branches of engineering rely upon are in geotechnical engineering rather poor.

2.2.1 Uncertainties Offshore

A schematic overview of the uncertainties entering risk analyses for offshore structures is shown in Figure 2.4. As a first approximation they are divided between loads and load effects on the one side, and foundation response (resistance) on the other.

Along the load side one begins with some historical record of environmental conditions, e.g., observed wave heights, wind speeds, seismic accelerations, etc. From these a recurrence model is postulated and statistical techniques used to infer parameter values. Then a load effects (load transfer) model is assumed, its parameters estimated from testing or theory, and the recurrence of environmental conditions propagated through to obtain the recurrence of foundation loads.

Along the foundation response side one begins with general geological data and direct or indirect measurements at a proposed site. Some model of physical response is postulated to transform these measurements into mechanical properties of the bottom sediments, and then a general conception of the local geology is used as a background against which to construct a characterization of the site for design. From this characterization engineering properties are estimated for use in analysis and design.

The two streams of analyses are brought together in a geomechanical model(s) of the proposed structure and its foundation (Figure 2.5). This model is a simplified view of the real physical processes at work, chosen to display the important interrelational properties among events and objects of an adopted theory, to which in turn reality is thought to conform. For such predictions as general stability against static strength failure and deformation under induced stresses, well developed theories and associated

Figure 2.4 -- Schematic overview of uncertainty and risk analysis for an offshore platform.

historical record

statistical inference of environmental loads

load effects

model

exploration data

site characterization

parameter estimation

risk profile (analyzable)

professional uncertainties & poorly understood modes

overall risk
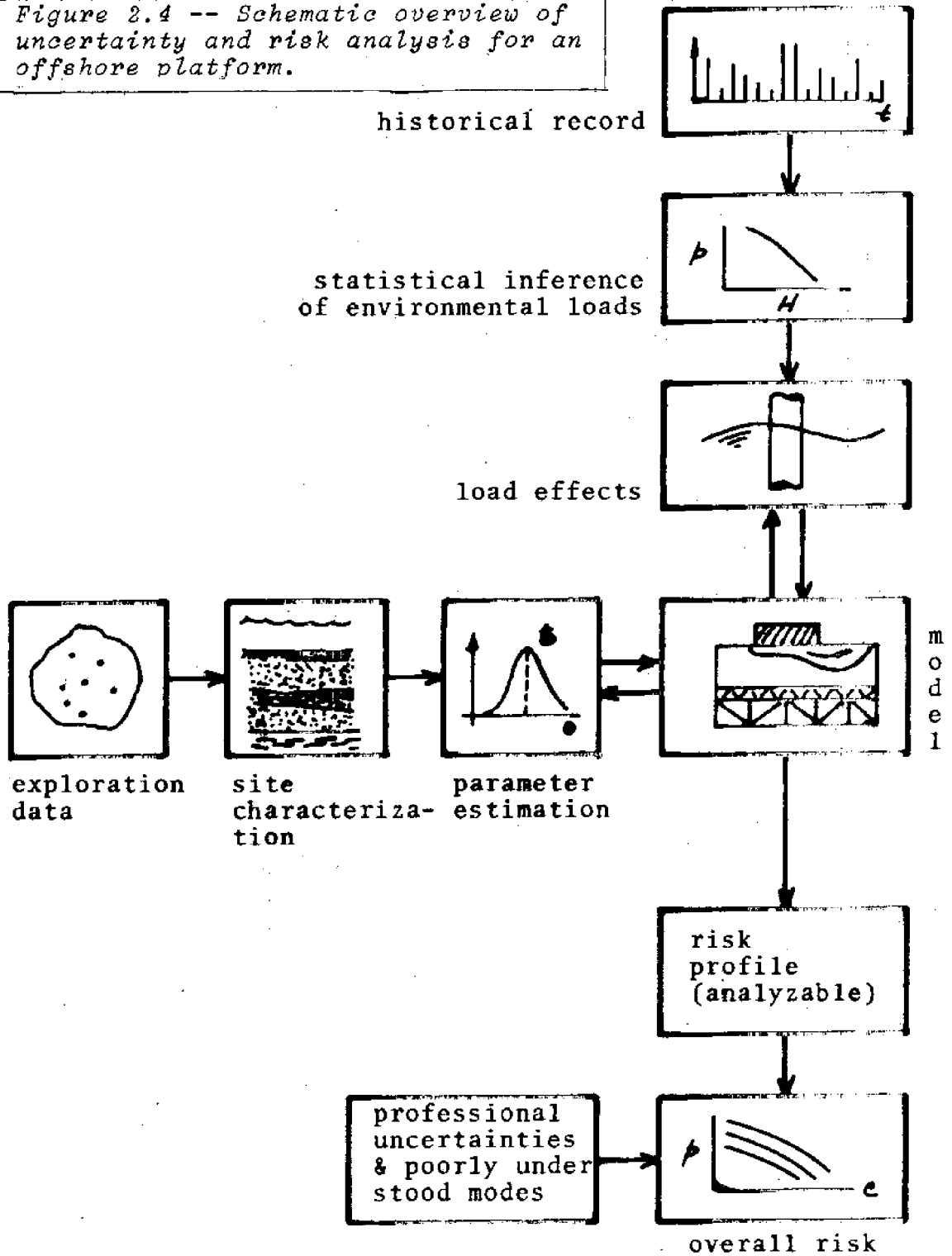
models exist. For other predictions, such as liquefaction of cohesionless sediments under cyclic loading, theoretical understanding is poor and widely accepted models do not exist.

From the calculations a combined risk profile is predicted which is a quantification of those contributions to risk that can be directly analyzed. To these must be added professional uncertainties and judgment about modes of behavior that cannot be directly analyzed, to reach a final summary of risk of adverse performances. For design decisions this final summary must be combined with some objective function to determine actions that are in some sense optimal.

2.2.2 Types of Uncertainty

This outline illustrates types of uncertainties associated with geotechnical engineering. Formal analysis cannot treat all of them, and must approach those it does treat in different ways, possibly using different techniques. As such, formal analysis is an aid to experienced judgment, and should be used only when it will provide insight or help maintain logical consistency among analyses.

A separation will be maintained between inductive, deductive, and inferential uncertainties. Usually, uncertainties are separated merely between inductive and deductive, but the inclusion of inferential uncertainty as a separate class is convenient.

Inductive uncertainties are traditionally said to involve movement from the specific to the general. From observations on a finite number of realizations of some process one is led to general conclusions on the process itself. Inductive reasoning is usually associated with the formation

of scientific theories, as for example, postulating the theory of effective stress from laboratory experiment but it is also the reasoning leading to the development of a geological concept of a site from borings, geophysics and geomorphology. Whether peat lenses are suspected in a coastal profile and therefore searched for is a matter of inductive reasoning.

Deductive uncertainties are generally said to be those moving from the general to the specific. From knowledge of the mechanisms underlying some process and estimates of the parameters of the process, specific outcomes or realizations are predicted (deduced). If the logical steps are correctly followed, the conclusions follow objectively from the premises. Deductive reasoning is usually associated with mathematical logic, for example using the theory of effective stress to predict consolidation behavior, but it is also the reasoning leading to a predictions of FS from models and parameter estimates. Predicting the chance of finding a peat lens of assumed size and shape at a site is a matter of deductive reasoning.

Inferential uncertainties are generally thought of as those in estimating designed properties or parameters from a limited number of observations. They are somewhat similar to inductive uncertainties, and some authors group the two together. Inferential uncertainty is usually associated with statistical reasoning, as for example, in estimating strength parameters from experiments. In this example, the assumption of homogeneity and modes of failure to be analyzed would be inductive, the estimation of parameters from borings and tests inferential, and the predictions of a FS from the model and parameter estimates deductive.

Returning to the previous outline, the roles of these types of uncertainties can be seen. Deciding what problems to analyze, selecting

theories to apply, and hypothesizing the overall geological conditions are inductive problems. If one is to believe Hume, these problems cannot be made logical. They involve generating hypotheses and assigning initial degrees of confirmation to those hypotheses, and these are not logical undertakings. They are also not illogical; rather one might call them 'alogical' (e.g., Salmon, 1964). The point is, these uncertainties cannot be formally analyzed. They are the starting point from which analyses of uncertainty must begin. For example, to predict the chance that significant liquefaction will occur in sand profile, one must induce theories explaining liquefaction and develop logical relations (models) for combining field evidence at a particular site. Predicting liquefaction in absence of a theory cannot be done formally, expect by adopting the hypothesis that it is a totally random phenomenon, and extrapolating the historical frequency. But, even then an inductive leap of faith is being taken.

Predicting bearing capacity from Terzaghi's superposition involves deductive uncertainty. A model is available, parameters estimates are available, and a prediction is mathematically deduced. Uncertainty in the parameters c' and ϕ' is propagated through the model, and possibly uncertainty in $N_\gamma)$, and finally a statement of deductive uncertainty in the predicted bearing capacity results. However, this uncertainty is conditioned on a number of strong assumptions. For example, a sand stratum may be assumed homogeneous, the theory upon which the model is based is assumed to hold, as well as other things. Since there is uncertainty in all of these conditioning assumptions, the deductive uncertainty is only partial -- although one cannot definitely declare it a lower bound.

Estimating c', ϕ' parameters, permeabilities, and the like is inferential. From a limited number of observations the parameters are estimated, usually statistically. In principle, the inferential uncertainty can be reduced arbitrarily close to zero by increasing the sample size, but this is not actually the case. Actually, bias errors enter the problem of inference, and these bias errors must usually be identified inductively.

Formal methods of analysis can be brought to bear on deductive and inferential uncertainties, but not on inductive uncertainties. One cannot ask that reliability techniques and statistical theory answer questions that cannot be formally answered. These may be the questions one most wants answered -- what is the chance we've omitted some important failure mode, missed some important subsurface condition; or made a mistake -- but they can only be dealt with by conservatism and robustness of design.

2.2.3 Taxonomy of Geotechnical Uncertainties

The outline above also illustrates a number of specific uncertainties common to geotechnical problems.

First, the geological subsurface is *spatially variable*. Sometimes this variation is called inherent or natural randomness, but for reasons discussed below these terms are misleading. The subsurface is spatially variable in that it is composed of different materials which are stratified, truncated, and in other ways separated in discrete bodies. It is also spatially variable in that within an apparently homogeneous body, material properties vary from point to point. With sufficiently many observations spatial variation can be characterized to any arbitrary level of precision.

With an infinite number of observations the variation could be known exactly. Obviously, however, the number of observations is limited by cost and time, so uncertainty remains about material properties and classification at points not observed. In reliability analysis these are often represented by stochastic processes.

Second, because the number of measurements at a site is limited there is inferential or *statistical uncertainty* in the engineering properties and model parameters used in analyses. Measurements vary from specimen to specimen or boring to boring because the in situ properties are spatially variable and because the act of measuring itself introduces errors. As sample sizes (numbers of observations) increase the precision with which parameters can be estimated increases, and further, the relationship between sample sizes and estimate precision can often be expressed mathematically. In principle, statistical uncertainties can also be reduced to any arbitrary level by increasing the number of observations.

Third, most testing procedures in geotechnical engineering introduce *bias errors* in addition to random error. That is, systematic differences between measured and actual properties usually exist. Ladd (1977) describes a number of these in soil property measurement. Bias error cannot be reduced by repeated testing and cannot be inferred by logical deduction from the results of a testing program. However, biases can be inferred from comparisons of predicted and observed performance, but as with Bjerrum's (1963) field vane strength correction, the bias so inferred comes from all sources in the analysis (i.e., from measurement techniques, mechanical models, definitions of failure, and the like). These bias calibrations cannot always be transferred to new applications without complete revision.

Fourth, theories and simplifications are required to predict performance from property measurements and these introduce *modeling uncertainty*. Model uncertainty is generated because there are uncertainties over the theory assumed to apply to the physical process being studied, there are uncertainties in the structural relations adopted within the model, there are boundary and initial conditions chosen, and there are errors introduced by numerical or mathematical approximations. Model uncertainty in geotechnical analyses is widely thought to be large (e.g., deMello, 1979), and is often used as an argument for not using formal methods in the analysis of uncertainty. This view seems somewhat inconsistent with itself, but is returned to below.

Fifth, one never knows -- and epistomogically, can never know -- what has been left out of an analysis. That is, there is uncertainty due to *omissions*. Any analysis is partial. The real world has properties and interrelationships that can never entirely be included in an engineering analysis. The question is whether these things left out of the analysis are important. This is the same for probabilistic and deterministic analyses. Unless conditions are hypothesized, they cannot be included in predictions. Many of the major failures of constructed facilities are due to omissions. For example, Malpasset Dam, Tacoma Narrows Bridge, Vijont Reservoir.

Last, while this report concentrates on geotechnical uncertainties, the *external loads and conditions* to which a structure is subject are also uncertain. These are uncertainties in addition to the first five, and in problems like seismic safety can occupy a significant place in the total uncertainty.

deformation model

strength model

finite element idealization
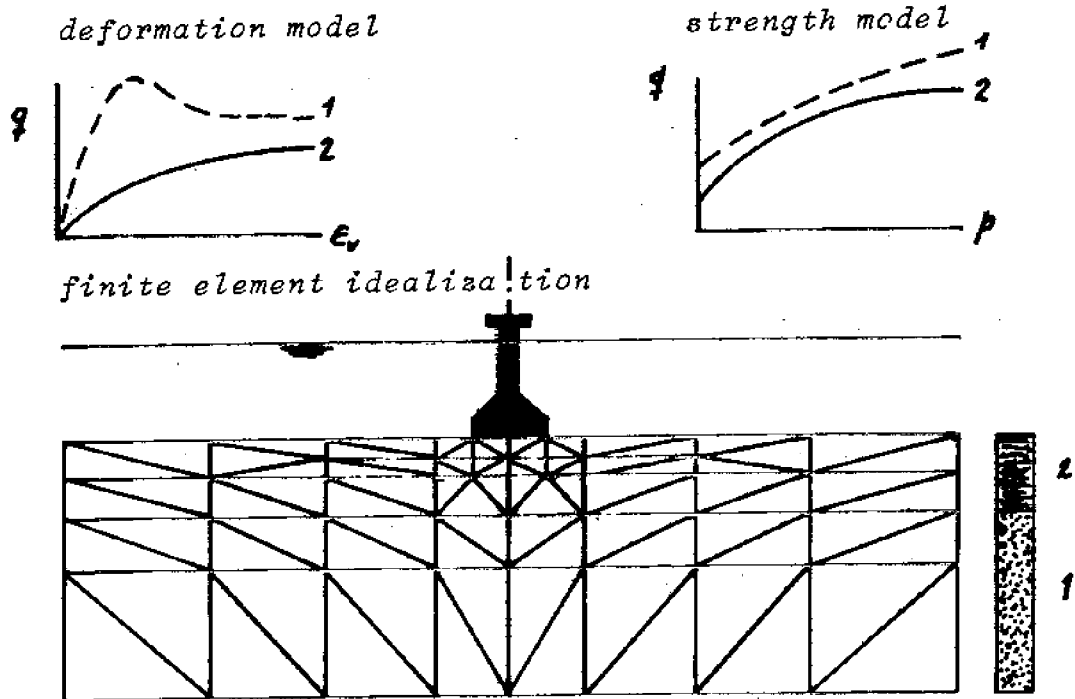
Figure 2.5 -- Geotechnical model of gravity platform
for use in engineering analysis.

PARAMETERS

INPUT
(ENVIRONMENTAL
LOADS)

MODEL

OUTPUT
(PREDICTIONS)
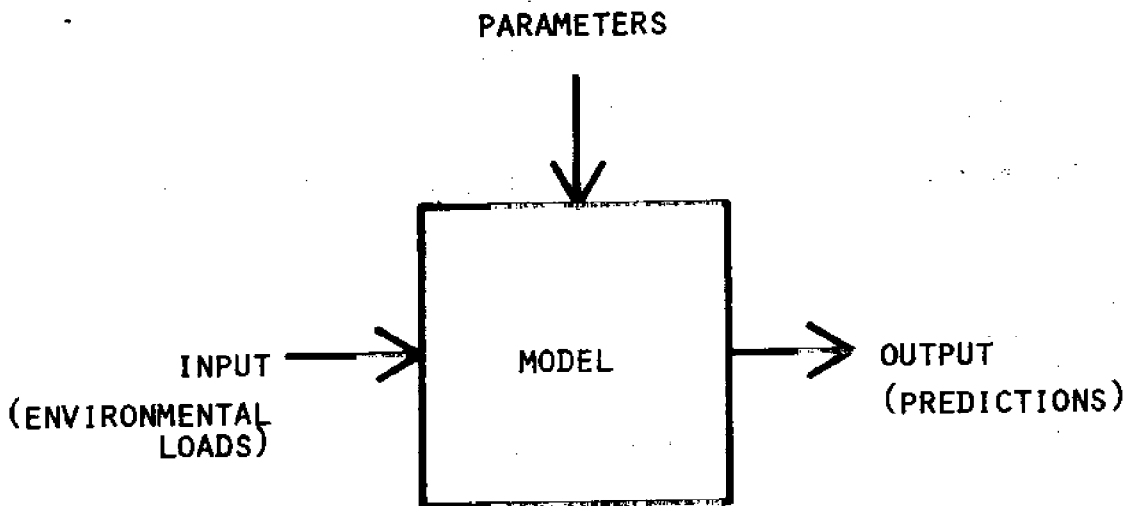
Figure 2.6 -- Abstraction of modeling.

2.3   Previous Work on Offshore Risk

The amount of previous work on geotechnical reliability of offshore structures is limited. This reflects more the state of geotechnical reliability analysis in its entirety than the advancement of offshore geotechnics. For example, the recent report of the ASCE Committee on Reliability of Offshore Structures (1979) concluded that (p. 15) "Offshore geotechnical problems appear to be well suited for reliability technology due to the natural vagarities of soil deposits, the variability of field and laboratory tests, and the uncertainties involved in the analysis of soil and foundation behavior in offshore environments. At the present time design and analysis are both fundamentally deterministic, ... Probabilistic methods have just begun to be applied to offshore geotechnical problems."

Much of the work in geotechnical (and structural) reliability analysis for onshore facilities is applicable offshore, and is reviewed as needed in other parts of this report. Here, only that work expressly devoted to offshore structures is reviewed.

Early work on offshore reliability analysis, primarily of structural systems but also of pile performance, was presented by Marshall (1969) in a paper which remains useful. Marshall's interest in the 1969 paper was primarily pile supported structures in the Gulf of Mexico. He divided the structural response of these platforms into three subcomponents -- the structural frame, axially loaded piles, and laterally loaded piles -- and presented distributional information on each (Figure 2.6). However, no attempt was made to combine these into probabilities of system resistance. Uncertainty in wave loading for a given wave height was expressed by a probability distribution over the ratio of actual (i.e., measured) load to predicted load for given waves heights, measured on platforms exposed to Hurricane Carla.

For a given wave loading the system probability of failure was taken as the sum of the three component probabilities. The return period wave and factor of safety for design were optimized using expected financial cost-assuming total failures. Philosophically, the approach owes much to the earlier work of Freudenthal (1956) and Borgman (1963). An upperbound on the total probability is taken to be the sum of the individual failure mode probabilities, implicitly recognizing the possible correlation among uncertainties in the FS's for different modes. However, no method is developed for other estimates. A schematic of the general design philosophy is shown in Figure 2.9.

Marshall's work seems to have led directly to later work by Bea (e.g., 1973, 1975) and probably influenced the work of Stahl. Bea's main concern in his published work has been the selection of environmental criteria for platform design, that is, design waves, storms, earthquakes, winds, etc. Like Marshall, Bea has considered lumped parameter analyses and specified probability distributions over ratios of actual to predicted strength of structural or foundation elements, and actual to predicted loads from waves or earthquakes (Figure 2.6). Optimization is by minimizing expected cost considering only total failure on the risk side (Figure 2.7).

Stahl has concentrated on the structural reliability of steel platforms in an approach very much like Freudenthal's. This work has been reported in a series of papers (1974, 1976, 1977). Probability distributions are specified on load parameters and on resistances and the probabilities of loads exceeding resistances calculated. These analyses primarily deal with individual structural elements under simple loadings, and little attention is directed to foundation response. Stahl has strongly supported a risk analysis approach to design decision and has proposed that a balancing of
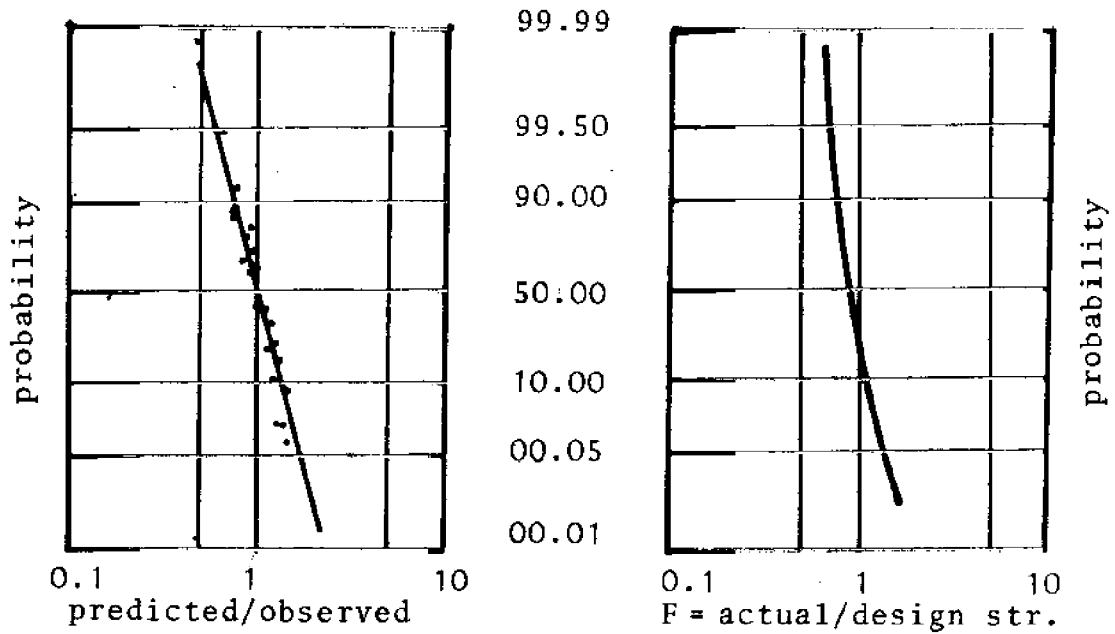
Figure 2.7 -- Typical input (axial pile capacity) and output (probability of pile failure) from Marshall's early work.
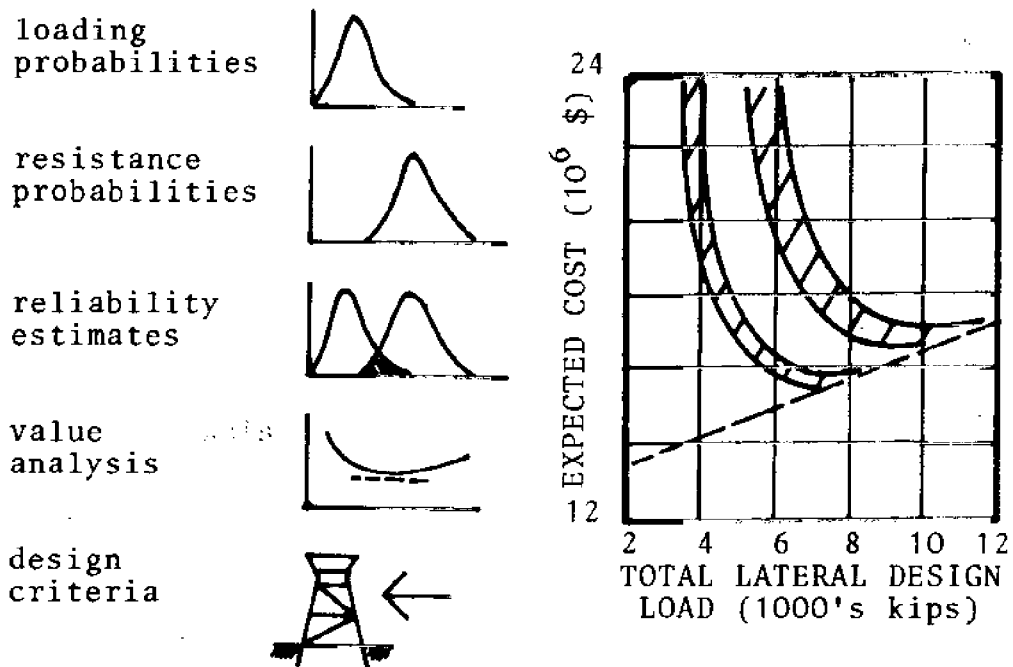
Figure 2.8 -- Outline of Bea's approach, based on direct calculation of probabilities that resistances are less than realized loads subsequently used in optimization analysis based on minimizing expected cost.

design and fabrication cost against expected losses due to failure be used in design. These ideas are strongly reflected in the ASCE committee report (1979).

More recent work in offshore reliability has been undertaken by Moses (1979 a, b), under support of Amoco. This work is a departure from that of Marshall, Bea, and the early work of Stahl. However, Stahl has had direct influence on this work.

Moses' approach is Bayesian, and consists of two parts. The first is an analysis of the structural system making up a platform. This is a second-moment analysis based on the means and variances of element resistances. The second is an empirical calibration of the reliability predictions against observed survivals and failures. This is based on Bayesian inference, and up-dates estimates of load and resistance correction factors. This work is mostly theoretical, and in principle is not limited in application to off-shore structures.

Others who have contributed to the structural reliability analysis of offshore structures include Flint and Baker (1976), who take a somewhat broader view of risk analysis, and who apply so-called level II methods of reliability theory (Flint, et. al., 1976), Fjeld (1978), and Moan (1979).

At the same time Bea and Stahl were presenting application of reliability methods to primarily structural aspects of offshore platforms, Kraft was working on reliability aspects of platform foundations. His work was presented in a series of papers (e.g., Kraft and Murph, 1975; Focht and Kraft, 1977), which while similar in spirit to the earlier structural work, is different in application. Kraft's work derives from a background in geotechnical reliability (e.g., 1968), and is not simply a transfer of technology in structural reliability.

Kraft considers specific modes of failure and attempts to develop second-moment information on the distribution of safety factors for each. Uncertainties in the analyses are primarily attributable to uncertainties in soil properties, geotechnical models, and imposed loads. On the resistance side these uncertainties are handled by a series of mutually independent random correction factors (Table 2.1). This procedure is similar to that suggested by Yuceman (1974) for reliability analysis of slopes. The probability of failure is computed assuming FS to be log Normally distributed, and the contention maintained that for probabilities of failure in the range $10^{-2} \leq p_f \leq 10^{-4}$ the sensitivity to distribution shape is slight.

More recently, Höeg and Tang (1978) have published a statistical analysis of site characterization data for North Sea structures, and a reliability model for skirt penetration. This work is divorced from the earlier structural reliability work, and like Kraft's work is entirely devoted to geotechnical problems. The analysis considers uncertainty in bottom parameters, although does not formally evaluate them statistically, and uses second-moment reliability analyses. For stability analysis the uncertainty in nominal factor of safety is computed using random correction factors (Table 2.2), but deformation uncertainties are not considered. The authors do note, however, that Bayesian inference can be applied to calibrating the reliability model for survivals (and implicitly failures).
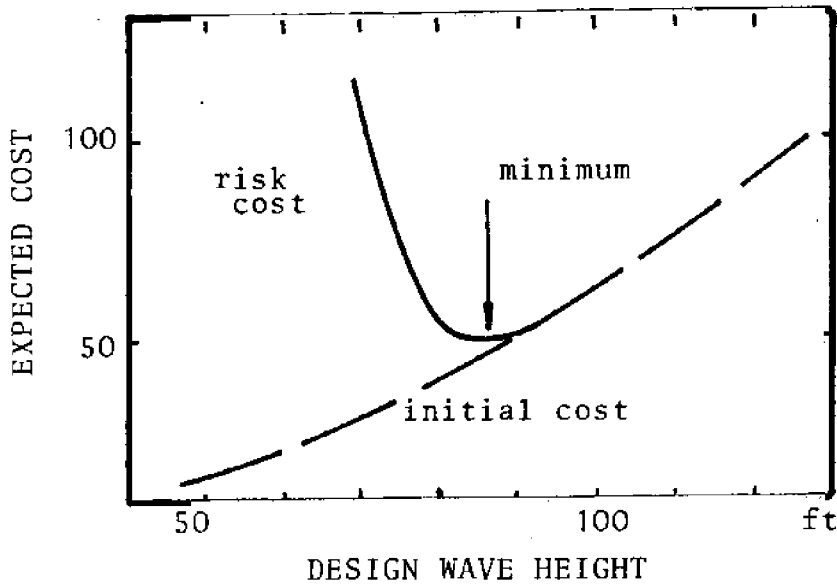
Figure 2.9 -- Cost optimization as design criterion (after Stahl, 1977).

Table 2.1:   From Kraft and Murff (1975)

Random Correction Factors for Predicting Factors of
Safety for Geotechnical Performance

	Expected Value	$C.O.V.$
Disturbance deuto stress release in sampling	1.05	0.03
Technical disturbance	1.50	0.11
Soil anisotropy--bearing	0.90	0.03
--sliding	0.80	0.14
Shearing rate	1.10	0.02
Cyclic loads	0.70	0.10
Strain softening	0.95	0.02
In-situ stress	1.05	0.01
Fissures	1.00	0.00
Bearing	1.55	0.12
Sliding	0.97	0.21

Table 2.2: from Hoeg and Tang
(1978)

Random Correction Factors for Stability Analysis

Factor	Mean	COV
Model uncertainty	1.0	0.03
Cyclic loading	1.05	0.03
Conductor effect	1.01	0.01
Erosion effect	0.98	0.01
Depth of embedment	1.0	0.025
Load factor	--	0.23
Undrained strength*	--	0.22

*Undrained Shear Strength	CPT only	CPT & Lab
Spatial variability	0.03	0.03
Insufficient samples	0.03	0.04
Calibration of CPT to laboratory	0.20	--
Laboratory compared to field	0.21	0.21
TOTAL	0.29	0.22

2.4   Present State of Offshore Geotechnical Reliability Analysis

From this brief review of previous work on risk and reliability analyses

of offshore structures it seems clear that the development and application

of such techniques is in its infancy. To date, most of the very difficult

problems of infering bottom conditions and assessing the uncertainties of

geotechnical predictions have not been addressed. This reflects primarily

the state of general geotechnical reliability analysis and not merely its

application to offshore structures. If anything, the offshore industry is

a spearhead of this work. The primary limitations of previous work have

been neglect of spatial variation in bottom conditions, simplistic analysis

of modeling uncertainty, and lack of attention to system behavior of offshore

foundations. It would be overly ambitious to suggest that these difficulties

can be quickly overcome, but significant contributions to the problem of

quantifying offshore risks are within grasp.

3. ENVIRONMENTAL LOADS

Reliability analysts must always concern themselves not only with uncertainties in resistance and response but also with imposed loads. For offshore structures the most important uncertainties in loads are those due to loads imposed by the environment, namely: wind, hurricanes, and tornadoes; waves, currents, and tides; earthquakes, and tsunamis; accidental loads; and in special cases, ice. No attempts were made in the current research to further the state-of-the-art of quantifying uncertainties in environmental loads, or of predicting their expected values. However, to assess the relative importance of geotechnical uncertainties to overall reliability an appreciation was needed of how large other contributors to overall uncertainty are.

This section summarizes current levels of uncertainty in predictions of environmental loads, concentrating attention on the most important of these--wave loading. The discussion is based on methods of analysis used in practice rather than emerging techniques in the literature, because first, these are the ways loads are forecast, and second, the empirical accuracy and precision of emerging techniques has yet to be verified.

Uncertainties in forecasting loads on an offshore structure may be grouped in three classes. First, there are those uncertainties arising out of the stochastic models used to characterize wave heights, wind speeds, earthquake ground motion, or other physical processes. From such models one arrives at an expression of annual or design life exceedance probabilities, autocorrelations of magnitudes in time or space (e.g., wave height) and cross correlations (e.g., of wave height and period). Within the chosen modeling these uncertainties are taken to be "natural," and can

normally be calculated once a set of model parameters have been specified.

Second, there are uncertainties arising out of the statistical esti-mation of the parameters of the stochastic models. These statistical uncertainties reflect the finite historical record of observations of the physical processes and associated sampling variation. They may also re-flect the uncertainty inherent in extrapolating observations made in one geographical location to predictions at another. These latter uncer-tainties, however, are not necessarily within the realm of traditional statistical procedures.

Third, there are uncertainties in translating physical occurrences to imposed loads. These uncertainties are usually said to involve the transfer function, e.g., in calculating wave loads from wave heights and periods. These uncertainties have to do with the models developed for re-lating environmental phenomena to load effects, and with the accuracy and precision with which the parameters of such models are known for a specific candidate design.

These three sources of uncertainty combine to yield the overall uncertainty in load predictions. As discussed in more detail below, in the present work this synthesis was made using two methods: Bayesian predictive distributions and propagation of variance techniques (e.g., first-order second-moment analysis, FOSM). The Bayesian technique uses the whole prob-ability relation to calculate the predictive distribution on load parameters as

$$f(s) = \iint_{\theta x} f(s \mid x) f(x \mid \theta) f(\theta) dx d\theta \qquad (3.1)$$

where $f(\theta)$ denotes the pdf, s the load parameter, x the natural phenomenon, and θ the parameters of the stochastic model of x. The FOSM technique uses the second-moment relations of means and variances based on Taylor series expansions of the relations among variables.

3.1 Stochastic Occurrence Modeling

In modeling sea states and subsequently the occurrence of wave loadings it is convenient to distinguish between long and short term descriptions. Long term descriptions are those summarizing storm occurrences and parameters, typically as discrete or point processes in time; while short term descriptions are those based on stationarity assumptions conditioned on the sea-state parameters of the long term descriptions. For the purposes of geotechnical modeling long term descriptions are typically the basis for predicting design life load exceedance probabilities, whereas short term descriptions are typically the basis for predicting dynamic response (e.g., development of excess pore pressures, cyclic strain softening).

3.1.1 Long Term Description

The data base upon which long term descriptions of the sea state rest comprise three types of information: 1) visual observations, 2) instrumental observations, and 3) hindcasts. Visual observations normally exist over a longer time period than do instrumental observations, but the bias and random errors of these observations (i.e., measurement cali-bration) are not known. Instrumental observations usually exist for only short time histories, and therefore their statistical uncertainty can be large. Hindcasts, made by combining historical storm wind speeds with a

theory of wind generated waves, provides a long historical record (of storm waves), but carries large calibration errors (Marshall and Bea (1976) estimate a bias of 0.8 and a c.o.v. of 30%).

It has been common to summarize long term variation of the sea state in the single parameter, characteristic wave height H_c. This might be a visually estimated height or some statistical measure like significant wave height H_s. More recent work, however, tends toward a description using a characteristic wave height, average mean period $\bar{T}$ and principle wave direction $\bar{\theta}$. Within this model the parameters $(H_c, \bar{T}, \bar{\theta})$ exist for every instant in time, and the instantaneous pdf is

$$f(H_c, \bar{T}, \bar{\theta}) = f(H_c|\bar{\theta}) f(\bar{T}|H_c, \bar{\theta}) f(\bar{\theta}) \quad . \tag{3.2}$$

The pdf $f(H_c|\bar{\theta})$ has been suggested to be best modelled by Weibull, Normal, or Gumbel Type I distribution, and in studies within which H_c and $\bar{T}$ are assumed independent the marginal distribution on $\bar{T}$ is often also taken to be Weibull, Normal, or Gumbel Type I. Little work appears to have been done on dependence of H_c and $\bar{T}$ in long term descriptions.

For design, particularly of the foundation, the probability of encountering extreme sea states in specified periods of time (e.g., design life) is of interest. By design these probabilities are necessarily small, and predictions must be extrapolated sometimes far from the existing data base.

Given that the exceedance probabilities are small, the distribution of number of exceedances of some extreme sea state H is commonly taken to be Poisson distributed with mean $\lambda(H)$ per unit time t,

$$p(n|\lambda(H),t) = \frac{1}{n!} \exp(-\lambda(H)t)(\lambda(H)t)^n \quad . \quad (3.3)$$

λ_H must be estimated from historical data and given the rarity of occurrence can contain significant statistical error.

To overcome this error some assumption or reference period must be taken by which to extrapolate observations of smaller H_c up to the higher values of H. The most common of these (e.g., Thom, 1971) is to assume some distributional form for the maximum H_c per year, and then to use extreme value theory to extrapolate. Thom uses a Gumbel type I (i.e., double expo-nental) type distribution for the distribution of annual peak H_c. From this a distribution of exceedance probabilities of given H in specified time periods is calculated. For the purposes of calculating reliability under a load, this distribution of exceedance probabilities suffices, unless cumulative effects of multiple storms are considered important.

The statistical uncertainty in estimates of exceedance probabilities based on the largest annual wave approach can be calculated directly from the sampling properties of, e.g., the double exponential distribution.

As discussed by Kimball (in Gumbel, 1958) the likelihood function for double exponential sampling cannot be factored into a kernal and therefore an analytical maximum likelihood estimator and a natural conjugate for Bayesian updating are not available. Nevertheless, from a frequentist view iterative and approximate sampling variances and distributions are available, and from a Bayesian view direct enumeration is always possible.

A convenient result due to Kimball is an approximate solution for the sampling variation of H_p, the wave height with (1-p) exceedance probability for the maximum likelihood estimate of the distribution parameters. Let

the double exponential pdf of maximum wave height H be

$$f(H) = \alpha\, e^{-\alpha(H-u)}\, e^{-\exp(-\alpha(H-u))} \tag{3.4}$$

with maximum likelihood estimators of α,u found iteratively from the expressions

$$e^{\hat{\alpha}\hat{u}} \Sigma\, e^{-\hat{\alpha}H_i} = N \tag{3.5}$$

$$\frac{\Sigma H_i e^{-\hat{\alpha}H_i}}{e^{-\hat{\alpha}H_i}} + \frac{1}{\hat{\alpha}} = \frac{1}{N} \Sigma\, H_i \tag{3.6}$$

with N, the sample size; and $(1/N)\Sigma H_i$, the mean annual observed maximum wave height. Then the sampling distribution of H_p is asymptotically Normal with variance

$$\sigma^2_{H_p} \simeq \frac{[1+(1-\gamma+y)^2/(\pi^2 6)]}{N\,\hat{\alpha}^2} \tag{3.7}$$

where $y = \hat{\alpha}(H-u)$ and γ is Euler's Constant   (0.5772156...).

3.1.2 Short Term Description

Short term descriptions of   states normally assume the water surface elevation to be a realization from a stationary (in time), homogeneous (in space) Gaussian random field, the defining parameters of which depend on the long-term description. Specification of the field requires joint pdf's of the elevations at arbitrary numbers of locations (in time and space), which for the stationary, homogeneous Gaussian case are sufficiently summarized in the mean (assumed zero) and autocovariance function. Usually,

the autocovariance function is replaced by the uniquely related spectral density function, since the latter has more convenient mathematical properties and ties directly into dynamic response analysis.

Wave Heights

Considering the water surface to be a Gaussian random field leads immediately to solutions for the probability distribution of wave height, exceedance probabilities as functions of time, and other important predictions for assessing potential loads on an offshore structure. These results are well known and have been in the literature for 30 years (e.g., Rice, 1944; Longuet-Higgins, 1957; Cartwright and Longuet-Higgins, 1956).

For a stationary Gaussian one-dimensional process $H(t)$ and an arbitrary level h the probability of one upcrossing in time interval δt has been shown by Rice (1944) to be

$$\Pr\{n=1 | \delta t\} = (m_2/m_o)^{\frac{1}{2}} \exp\{-h^2/2m_o\} \delta t + o(\delta t)\}$$

(3.8)

where m_k is the kth moment of the spectral density function of the process $f(\omega)$ defined over frequency

$$m^k = \int_o^\infty \omega^k f(\omega) d\omega,$$

(3.9)

and $o(\delta t)$ is a term of order δt^{-1}. Thus the expected number of upcrossings per unit time $\lambda(h)$ becomes

$$\lambda(h) = (m_2/m_o)^{\frac{1}{2}} \exp\{-h^2/2m_o\}$$

(3.10)

and for upcrossing of the mean

$$\lambda(o) = (m_2/m_o)^{\frac{1}{2}} \quad . \tag{3.11}$$

The mean time between successive upcrossing $E(T)$ is the reciprocal of $\lambda(o)$,

$$E[T] = (m_2/m_o)^{-\frac{1}{2}} \quad . \tag{3.12}$$

These upcrossing probabilities allow calculation of the distribution of extreme wave heights, by setting the cdf of h_{max} equal to the probability of not crossing an arbitrary level in time t. The expected number of upcrossings of h in time t is simply $\lambda(h)t$, and asymtotically for large h the number n approaches a Poisson distribution (Cramer and Leadbetter, 1967),

$$F(h_{max}|t) \simeq e^{-\lambda(h)t}$$

$$\simeq \exp\{-\lambda(o)te^{-h^2/2m_o}\} \tag{3.13}$$

given that $h/\sqrt{m_o}$ is large. This result does not rest on a narrow-band assumption. The distribution of all maxima (Figure 3.1), and not simply the largest maxima is Rayleigh distributed,

$$F(h) = 1 - \exp\{-h^2/2m_o\}$$

a result which has been derived in several ways (e.g., Cartwright, 1958; Cartwright and Longuet-Higgins, 1956; Bonneau, 1971; Ochi, 1973).
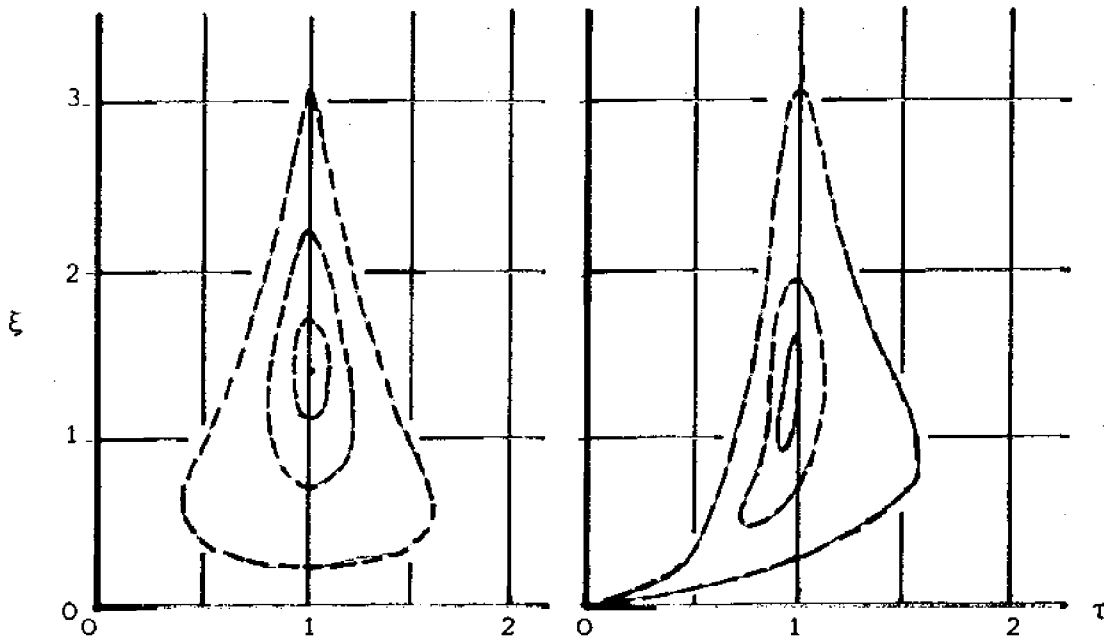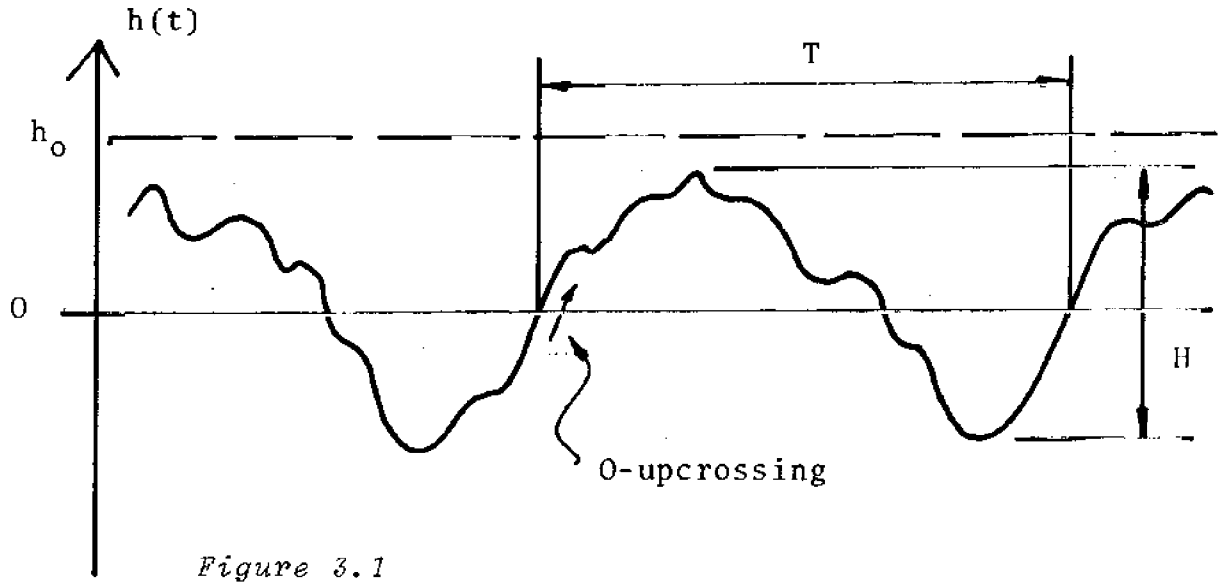
Figure 3.1

Figure 3.3 -- Theoretical joint pdf of wave height and period (from Battjes, 1977).
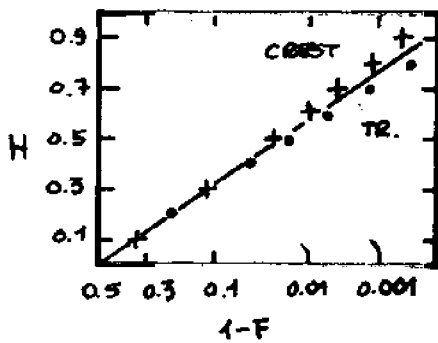

Figure 3.2 -- Variation of observed water surface elevation from Gaussian assumption. Data (+) are positive standardized heights, and (•) are negative.

For narrow band processes the wave height, h, or maximum range of h(t) between zero-upcrossings, is approximately $H \approx 2h_{max}$, thus H is also Rayleigh distributed (Figure 3.1). For wide band processes this need not follow. In such processes the correlation between consecutive h_{max} and h_{min} may be small and though they are assumed to be marginally Rayleigh distributed, their difference may not be. Corrections to the Rayleigh distribution for H have been given by Haring, et al. (1976), who report about 10% empirical reduction in H_o : $1 - F(H_o) = 10^{-3}$ compared with the Rayleigh cdf.

Jahns and Wheeler (1972) conclude on the basis of hindcasting and empirical data that the Rayleigh distribution of h signficantly under-estimates the actual probability of occurrence of large maxima; however, that the poor correlation between peak and following trough in broad band processes decreases the exceedance probabilities of H. Similar evidence has been presented by Nolte and Hsu (1972), Thompson (1979), Haring, et al. (1976), and Forristall (1978), among others. Recently, Nolta and Hsu (1979) have presented a statistical filtering procedure for minimizing the influence of these biases on prediction.

The reason for these biases is that real sea states are not sufficiently narrow band (<0.3/E[T]) for the Rayleigh distribution to be a good approximation. Also h(t) seems to diverge from the Gaussian assumption for large positive and negative deviations (Figure 3.2). In general, a 10% over-prediction of H for given exceedance probabilities seems to be somewhat agreed upon.

Because the load effect on an offshore structure depends on both wave height and period, the joint distribution of H, T is of importance. In general, less work has been done on this joint dependency than on H alone, but certain models are available. The summary here follows Battjes (1978) and is brief.

Bretschneider (1959) proposed for developed sea states that H and T be taken independent and each marginally distributed as Rayleigh variables. Specifically, for the normalized variables $\xi = \frac{1}{2}H/\sqrt{m_o}$ and $\tau = T/E[T]$,

$$f(\xi,\tau) = [\xi e^{-\frac{1}{2}\xi^2}] \cdot [4\Gamma^4(1.2)\tau^3\exp\{-\Gamma^4(1.2)\tau^4\}] \quad . \quad (3.14)$$

Recent empirical work, however, (e.g., Earle, et al. 1974) fails to confirm this distribution using hurricane Camille data. Battjes, et al. (1972) have suggested a bivariate Rayleigh pdf including a covariance term.

Wooding (1955) and Longuet-Higgins (1957) derived a theoretical joint distribution for narrow band Gaussian processes based on Rice's (1944) results for the envelope of a random process. Renormalizing the period to

$$\zeta = \frac{(m_1/m_o)T - 1}{(m_o m_2/m_1^2 - 1)^{\frac{1}{2}}} \quad (3.15)$$

the distribution becomes

$$f(\xi,\zeta) = [\xi\exp\{-\frac{1}{2}\xi^2\}] \cdot [\frac{\xi}{\sqrt{2\pi}} \exp\{-\frac{1}{2}\xi^2\zeta^2\}] \quad (3.16)$$

That is, $f(\xi) \simeq$ Rayleigh and $f(\zeta/\xi) \simeq N(o,\xi^{-1})$. Contours of this joint pdf are shown in Figure 3.3.

Cavanié, et al. (1976) have also derived a theoretical joint distribution for narrow band Gaussian processes by considering the joint distribution of h(t) and $\ddot{h}$(t). The resulting density is (Figure 3.3)

$$f(\xi,\tau) = \frac{2\alpha^3\xi^2\tau^{-5}}{\sqrt{2\pi}\epsilon(1-\epsilon^2)\mu^4} \exp \frac{-\xi^2\tau^{-4}}{2\epsilon^2\mu^4}\{\mu^2\tau^2-\alpha^2)^2 + a^2\alpha^4\} \quad (3.17)$$

where

$$\epsilon = 1 - m_2^2/m_o m_4$$

$$\alpha = \frac{1}{2} \left[1 + (1 - \epsilon^2) \right]$$

$$a = \sqrt{\epsilon^2/(1-\epsilon^2)}$$

$$\mu = E[T]/E[T_m^+] \tag{3.18}$$

where $E[T_m^+]$ is the mean time between positive maxima, $(1/\alpha)(m_2/m_4)^{\frac{1}{2}}$. For large ξ, the marginal pdf $f(\xi)$ is asymptotically Rayleigh.

For all cases the marginal distributions of wave height are about the same. The marginal distributions on period, however, differ somewhat. As can be seen in Figure 3.3, the distributions of Wooding and Longuet-Higgins and the distribution of Cavanié, et al. become similar for large ξ. considerably more empirical work is needed on this problem, however.

3.1.3 Combined Exceedance Probabilities

To estimate wave exceedance probabilities for the design life of a structure the long term description of the temporal variation of characteristic parameters $(H_c, \bar{T}, \bar{\theta})$, and the short term description of a stationary, homogeneous sea state having those parameters must be combined.

Considering maximum wave height H, the conditional cdf of H given $(H_c, \bar{T}, \bar{\theta})$ is from Equation (3.13),

$$F(H|H_c) = 1 - \exp\{ -\frac{2H^2}{H_c^2} \} \qquad (3.19)$$

where H_c is conventionally defined either as $H_{1/3}$, the mean of the largest 1/3 of the wave height, or $4m_o^{\frac{1}{2}}$. For narrow band Gaussian processes these are identical. If $f(H_c)$ is the distribution of H_c over time, then the marginal cdf on H becomes simply

$$F(H) = \int_{H_c} [1-\exp\{ -\frac{2H^2}{H_c^2} \}] f(H_c) dH_c \qquad , \qquad (3.20)$$

with direct generalization to larger numbers of sea state parameters. This expresses the probability that any one peak is of less than height H.

Commonly, however, only sea states for which $H_c \geq H_o$ are considered (i.e., storms), and the occurrence of such states are considered a Poisson process with parameters λ. Then the distribution of H for $H_c > H$ becomes

$$f(H) = \int_{H_o}^{\infty} [1-\exp -\frac{2H^2}{H_c} \}] f(H_c|H_c \geq H_o) dH_c \qquad (3.21)$$

From Equation 3.10 the expected number of exceedences of H within a storm of duration D and characteristic wave height H_c

$$\lambda(H/D) = (m_2/m_o) \exp\{ - 2H^2/H_c^2 \}D \qquad (3.22)$$

and the cdf of the largest wave height is

$$F(H_{max}) = e^{-\lambda(H/D)} \qquad (3.23)$$

Thus, for n storms of differing H_c the cdf of largest wave height becomes

$$F(H_{max}|n) = \int_{H_o}^{\infty} \exp\{-\lambda(H/D)\}^n f(H_c|H \geq H_o) dH_c \qquad (3.24)$$

A difficulty arises in application because the storm duration is itself a random variable, and to date the models for the pdf of duration are poorly verified by empirical data. Most analyses begin by noting the average duration above some level H_o, as being $(1-F(H_o))$ times the total time period divided by the expected number of storms with $H_c \geq H_o$, then make a distribution assumption for D and estimate the parameters from historical data. For example, Vik and Houmb (1978) use a Weibull pdf, Nolte and Hsu (1979) use an exponential pdf, and occasionally a Normal pdf is suggested. Theoretical solutions for dieussions of a random process above an arbitrary level are difficult to formulate.

Once a distribution for storm durations is obtained it is incorporated in Equation 3.24 by integrating the conditional pdf of H_{max} over the pdf of D. Because this is itself difficult, and because f(D) is not well grounded, one of two approximations is usually introduced. The first is to approximate the average duration as above, and then estimate the average number of waves per storm k as

$$E[k] \simeq E[D]/E[T] \qquad , \qquad (3.25)$$

implying a loose form of narrow band assumption. Then from Equation 3.24 an extreme value distribution on the largest wave per storm can be calculated and similarly on the largest in n storms. The second approximation (e.g.,

Thom 1971; Schueller and Choi, 1977) is not to consider sea state at all, or to implicitly assume that $\Pr\{n>1 | t = 1\text{year}\} \to 0$, and simply take the largest wave per year as the basic random variable. The common assumption is that this largest yearly wave is Weibull or Double Exponential Distributed, and from extreme value theory the exceedance probabilities for largest annual wave an calculated for various design lives.

3.2 Transfer Functions

For a given wave height, period, and other environmental conditions some model must be introduced to predict resulting loads on the structure. Such a model is here called the loading transfer function. As with any modeling this transfer introduces uncertainties (Section 5.1).

Current predictions of wave forces on offshore structures are commonly based on Morison's equation (1950), in which the horizontal force on a vertical cylinder extending from the sea bottom and piercing the surface is divided into two parts: (1) An inertial force taken linearly proportional to fluid particle acceleration, and (2) a drag force taken proportional to the square of fluid particle velocity and in its direction,

$$dF = \frac{1}{2}C_D \rho D \underline{u} |\underline{u}| + \frac{1}{4}C_M \rho \pi D^2 \underline{a} \qquad (3.26)$$

in which dF is the differential force along the cylinder, C_D a drag coefficient, C_m an inertia coefficient, ρ the fluid density, $\underline{u}$ fluid particle velocity, and $\underline{a}$ fluid particle acceleration (Figure 3.4). This force acts in the direction of the wave motion and varies along the depth of the cylinder due to changes in u and a. The total horizontal force
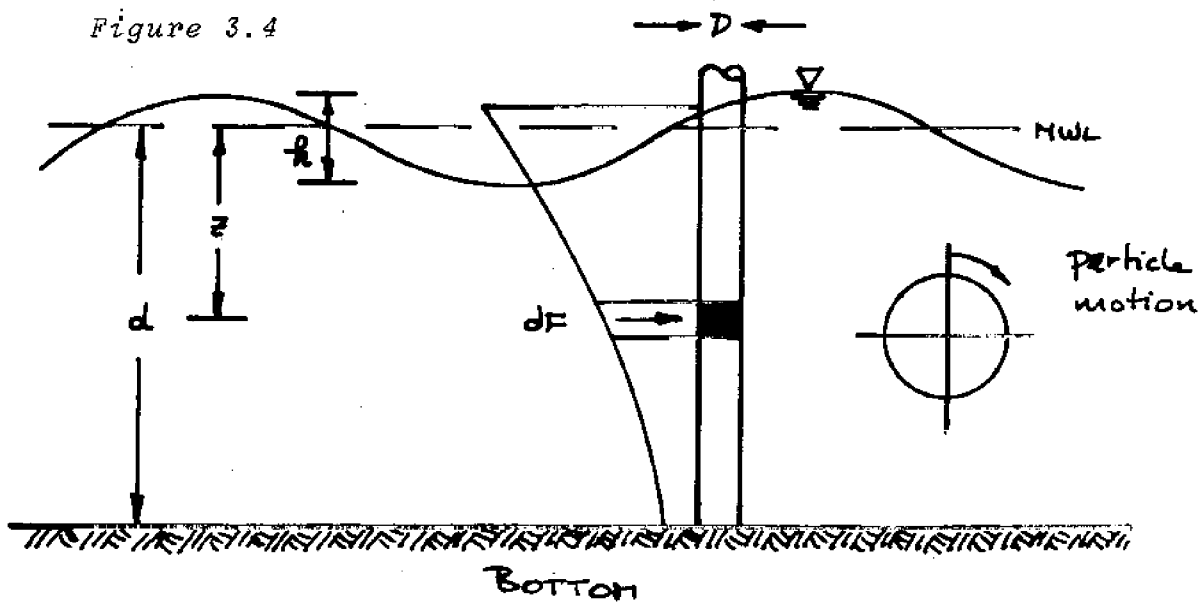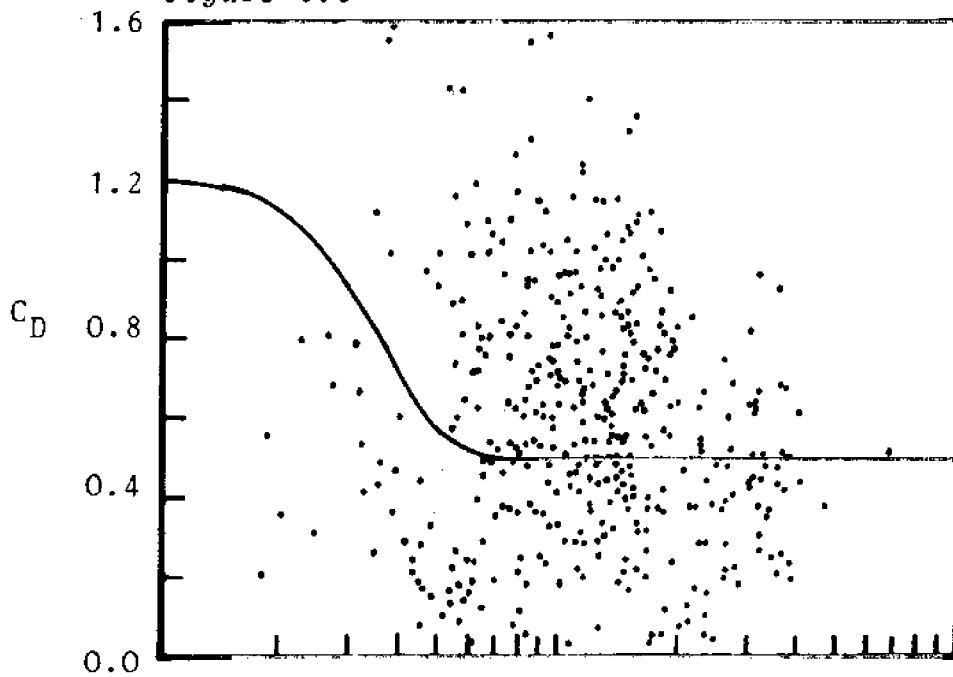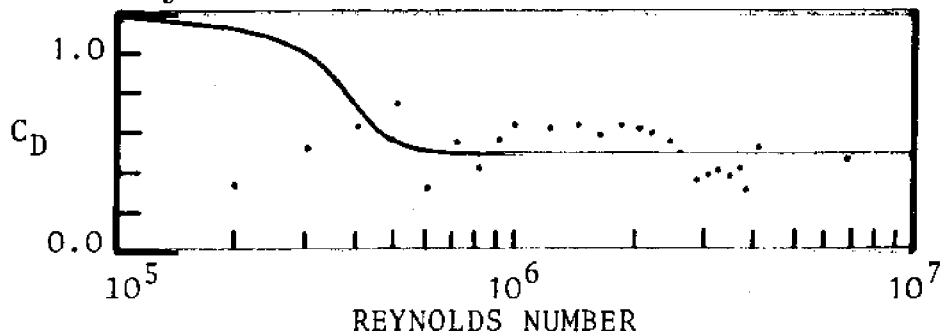
Figure 3.4

Figure 3.5

Figure 3.6

REYNOLDS NUMBER

on the cylinder is the integral of dF acting at some level z depending on the distribution with depth.

The derivation of Morison's equation is based on a large number of simplifying assumptions. Among these are that only a single pile is considered, and that the pile diameter, D, is small compared with the wave length, L. Thus, the kinematics of wave flow are considered unchanging over the cross section. Flow is assumed rectalinear, even though particle motion is actually orbital, and the cyliner is assumed to be at right angles to the directions of $\underline{u}$ and $\underline{a}$. The effect of wave history is ignored, as are lateral (i.e., lift) forces on the cylinder. Obviously, the basic linear decomposition of drag forces due to fluid viscosity and decrease in pressure behind the cyliner, and inertial forces due to acceleration of the displaced volume is also assumed valid.

The intent in noting these well known assumptions is only to suggest the underlying reasons for model uncertainty in predicting loading transfer.

To use Morison's equation an estimate of particle velocity and acceleration must be made as a function of depth. These predictions are usually made on the basis of one form or another of wave theory, rather than from empirical analyses. These are usually linear. This also introduces uncertainty, as the theoretical $\underline{u}$ and $\underline{a}$ may differ from those realized. Composition of uncertainties in drag and inertia coefficients made using wave theory and simultaneous observation of $\underline{u}$, $\underline{a}$ seem to confirm this contention (e.g., Kim and Hibbard, 1975). However, it should be noted that the variation between linear and non-linear wave theory in predicting forces is small, except for high h/D (e.g. > 0.8) (Raman and Veukatanar-Asaiah, 1976); Chakrabarti, 1975). The variance between observed and predicted is larger.

To include lift forces the Morison equation is usually addended with the term

$$F_L = \frac{1}{2}C_L \rho D u^2 \quad , \tag{3.27}$$

acting horizontally perpendicular to the direction of $\underline{u}$. C_L is the lift coefficient and summarizes the effects of eddies forming around the cylinder and separating from it. Experimental work indicates that for Keulegen-Carpender numbers, $\underline{u}T/L$, less than about 5, these lift forces are negligible (Chakrabarti, et al.1976). T is the wave period. However, for $\underline{u}T/D$ of the order of 15 the total forces including the lift component can be as large as 60% higher than that predicted from Morison's equation, and acts in a direction oblique to $\underline{u}$.

The effect of multiple cylinder groups on individual cylinder forces has been studied by Chakrabarti (1978), Spring and Monkmeyer (1975), and Twersky (1952). These studies have all been theoretical and have not been extensively verified experimentally. The conclusions of these studies is that for center to center cylinder spacings of greater than about 2.5 or 3 diameters,and for either cylinders in a single row, three in equilateral triangle, or four in a square, the difference between single cylinder forces when alone and in a group are small. For closer spacings the increase in single cylinder force can become large.

Present practice treats Morison's equation as a semi-empirical model (i.e., black box), by estimating C_D, D_M, and C_L empirically and allowing uncertainty in the coefficients to include the uncertainty of the model itself. Thus, unsurprisingly, the uncertainty in these coefficients is
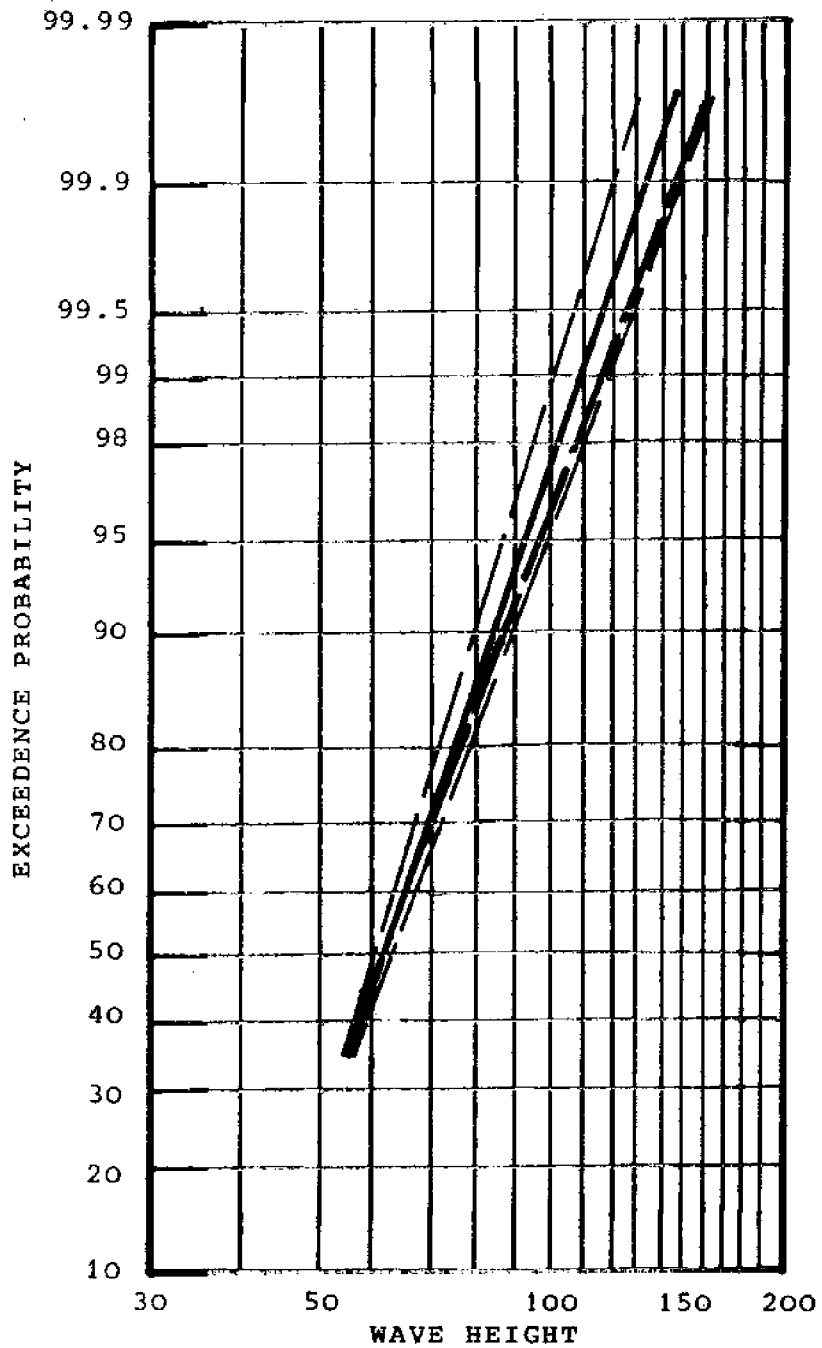
*Figure 3.7 -- Wave height exceedence
probabilities for annual maximum.
Solid curve, best estimate; broken
curve, including statistical uncer-
tainty.*

large. Furthermore, the estimates of the coefficients depend on the procedure used to make them. Morison, et al.'s approach was to set the measured force equal to either the drag or inertial force when the other was theoretically zero. Keulegan and Carpenter (1958) decomposed the measured force into Fourier components and used the amplitudes of these to estimate the coefficients. Current practice is to fit Morison's equation to measured forces through some least squares criterion. These various methods yield different estimates of C_D, C_M unless the measured forces are given identically by the postulated model, which of course they are not. For example, Sarphaya (1975) has studied one dimensional oscilating flow over a cylinder and found a 4% consistent difference in coefficient estimates made by Fourier decomposition and least squares. The question of coefficient estimates is therefore a statistical one, and some error about the best estimates will exist even for infinite data series.

Estimates of C_D and C_M vary considerably from wave to wave, as shown in Figure 3.5, and are a function of two dimensionless numbers, the Reynolds R_e and Keulegan-Carpenter KC numbers.

$$R_e = uD/\nu$$

$$KC = uT/D \qquad\qquad (3.28)$$

where ν is the kinematic viscosity of the fluid, and KC is sometimes called the period number. When averaged over a number of waves this scatter is naturally reduced (Figure 3.6), although a large residual error remains. Current practice is to take C_D to lie between about 0.7 and 1.0, and C_M between 1.5 and 2.0. The associated coefficients of variation are of the
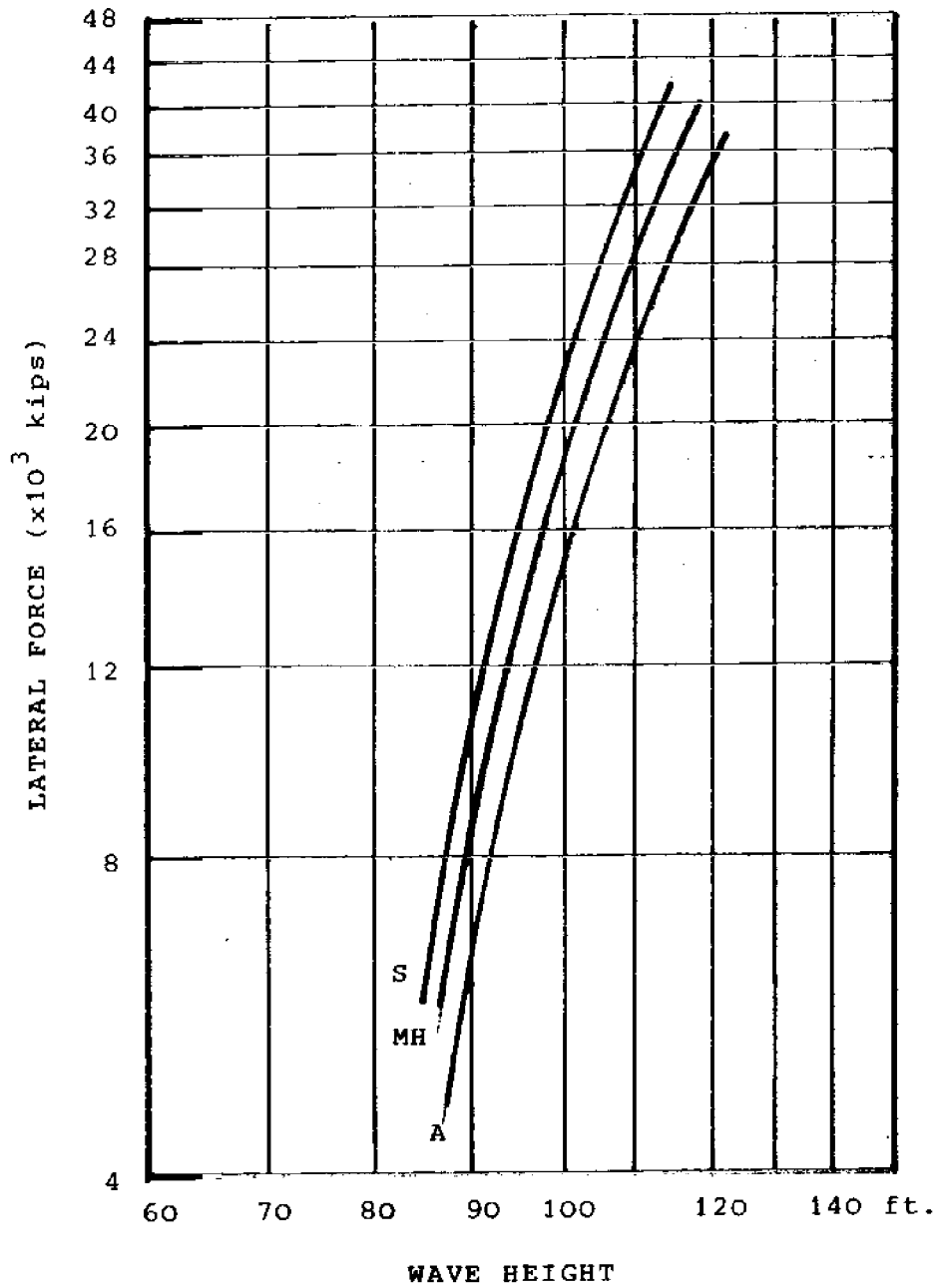
Figure 3.8 -- Loading transfer functions using Airy, Solitary Wave, and Mitchell-Havelock formulations.

order of 35% for C_D and 40% for C_M (Schuéller, 1976).

The effect of uncertainties introduced by using (linear) wave theory to predict $\underline{u}$ and $\underline{a}$, as compared with direct observations, is seen in Kim and Hubbard's results (1975). By measuring $\underline{u}$ and $\underline{a}$ simultaneously with force the observed coefficients of variation in C_D and C_M were reduced to 24% and 22% respectfully. However, because wave thoery is used in practice for predicting forces these reductions in uncertainty do not apply.

As discussed by Ramberg and Niedzwecki (1979), the assumption of uniform force coefficients over the depth of the cylinder also introduces error. The conclusion of this work is that the assumptions of uniform C_D leads to over prediction of force, attributable to variations in the degree to which fluid particle movements approach the one-dimensional assumption. Again, the observed coefficients of variation for C_D, C_M determined from empirical analyses include such uncertainty.

3.3   Combined Wave Loading Uncertainties

In assessing the combined uncertainty in environmental loads on an offshore structure each of the contributions of stochastic, statistical, and loading transfer function must be included. In this section the combined uncertainty in wave loading for the Georges Bank site is considered.

From Section 3.1 the annual hazard exposure to wave heights is shown in Figure 3.7. This figure shows the cumulative distribution of wave height-based on best estimate stochastic parameters, and the predictive distribution incorporating statistical uncertainty.

From Section 3.2 the load transfer function and its associated uncertainty are shown in Figure 3.8 for the design platform. Wave
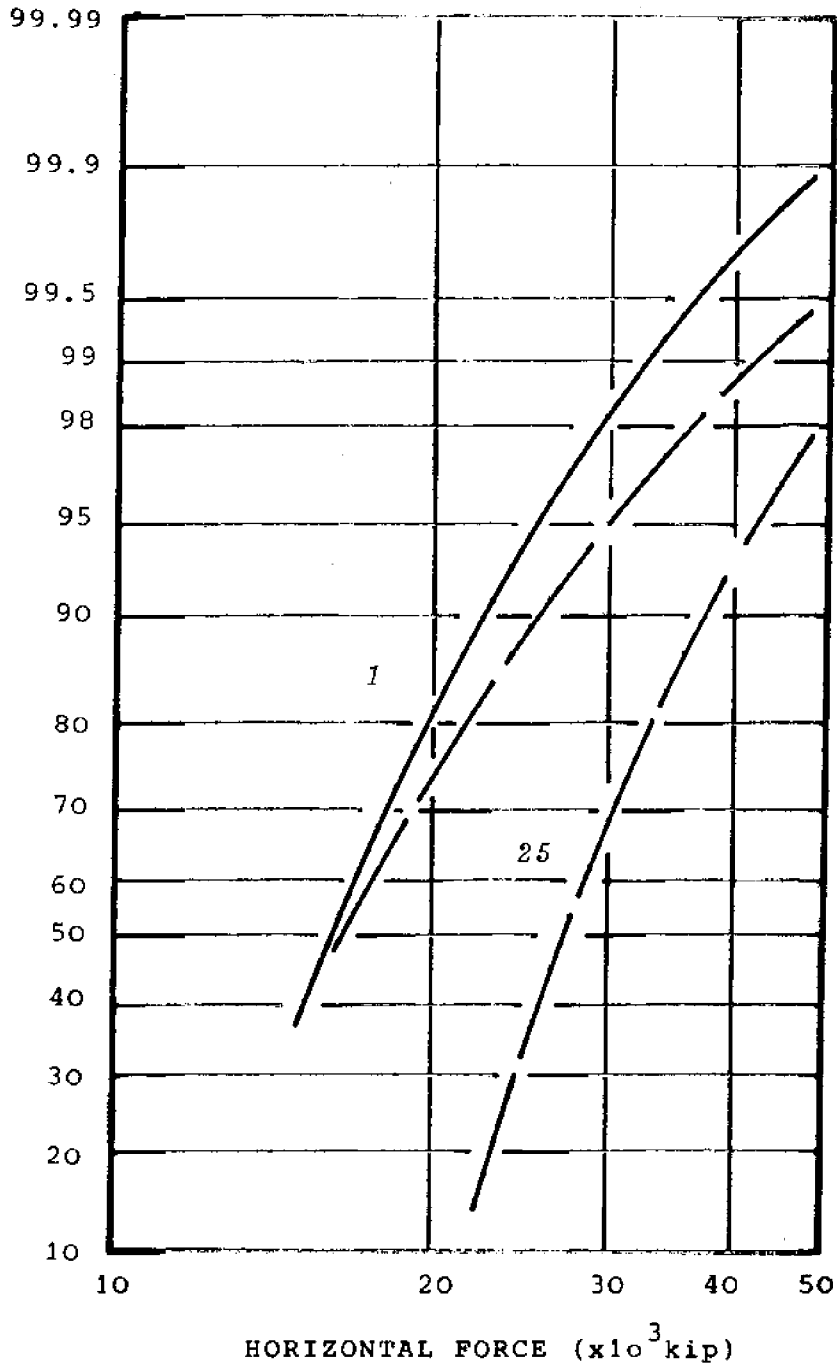
Figure 3.9a -- Exceedence probabilities for horizontal force on structure for one and twenty-five years. Broken lines include statistical uncertainty.

heights breaking over the platform deck are not considered in this analysis (Cf., Committee on Offshore Reliability, ASCE, 1979).

Combining Figures 3.7 and 3.8 techniques leads to the annual CDF of wave loading shown in Figure 3.9. This figure also shows CDF's for 25 and 50 year design lives. These distributions include both stochastic and statistical uncertainty.

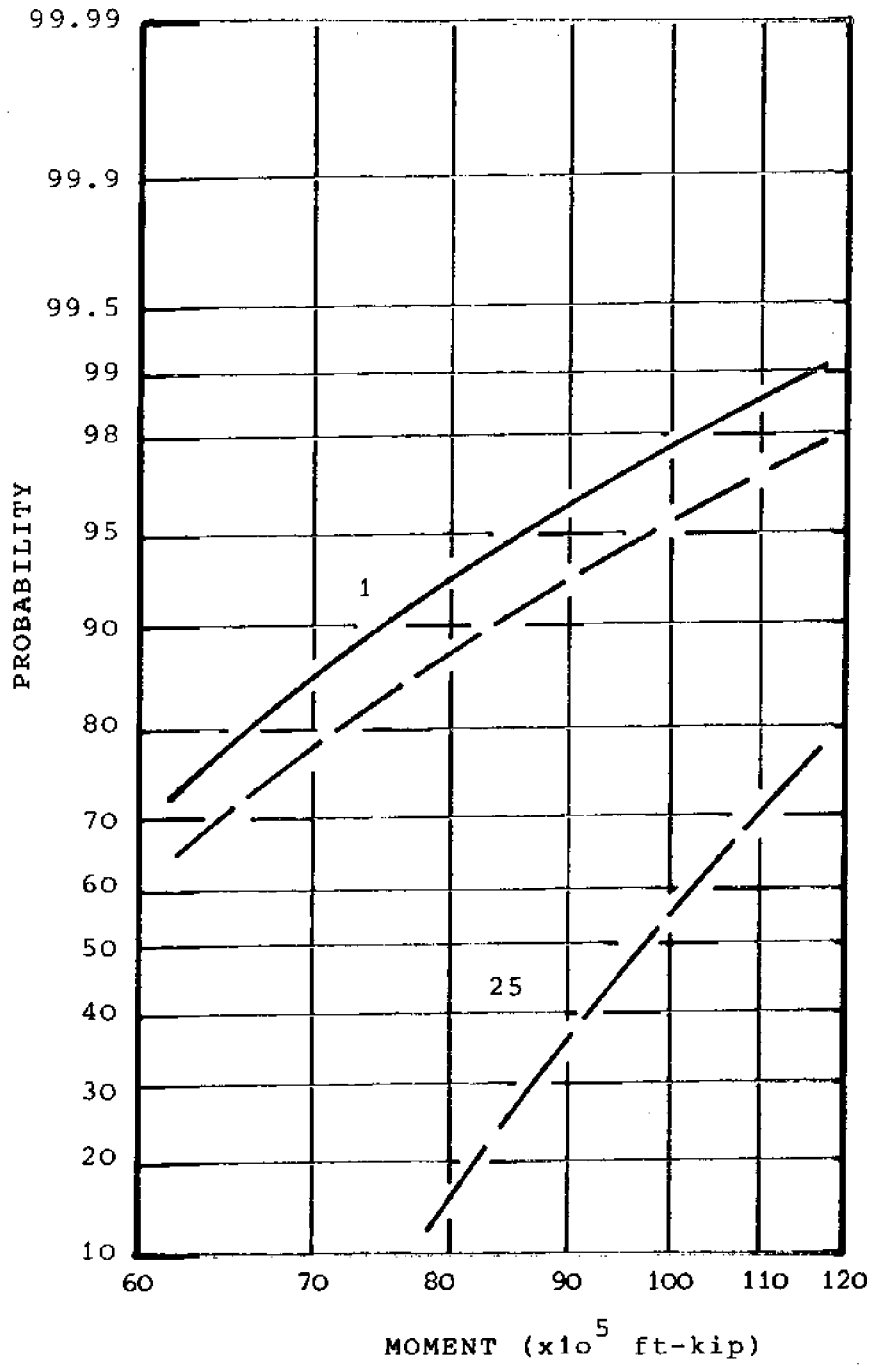*Figure 3.9b -- Exceedence probabilities for moment at mudline for one and 25 years. Broken lines include statistical uncertainty.*

4.   SOIL EXPLORATION

Uncertainties in bottom conditions and parameter estimates are caused by the spatial variation of bottom sediments, by limited numbers of measurements, by bias error in measuring sediment properties, by undetected geological details, and by poorly defined strata geometry.
Certainly, any problem of measuring sediment properties and inferring subsurface conditions that is difficult onshore is even more difficult offshore. The cost of site investigation is high, the technical difficulty of making accurate measurements great, and the number of direct observations limited.

4.1   Site Investigation Program

A typical site investigation program offshore begins with the collection of geophysical information (i.e., remote sensing) over a large region. Because there is often latitude in the exact siting of an offshore facility, this preliminary reconnaissance serves as a screening and site selection stage in which favorable conditions are more precisely located. Upon deciding on one or more favorable locations, further geophysical information is collected on a more intense pattern.

4.1.1 Accoustical Data

The most common offshore geophysical measurements for geotechnical purposes are accoustical, that is, high frequency seismic reflection surveys. Accoustical sources based on high power spark gaps ("sparkers") generate frequencies in the range 200 Hz to 1000 Hz, and penetrate to 300 or 400 m below the mudline, depending on sediment properties. Because of the comparitively low frequency of sparkers, however, the resolution of the returned signal is seldom better than about 5m, meaning that details of the subbottom geometry are not defined   and that the critical sediment zones

immediately below the seabed are difficult to evaluate. More resolution

can be obtained using higher frequency "boomers" or multi-electrode sparkers,

but these have correspondingly less penetration (i.e., greater attenuation).

A difficulty with accoustical data is how to interpret it. Returned

reflected signals show pleasingly precise delineations of "reflectors" in the

subbottom (Figure 4.1), but what precisely the reflectors represent, where

exactly they are, and what details fail to appear in the traces are difficult

questions to answer.

All acoustical data is expressed as time delays between transmission

and reflection. To change time delay into geometric information requires

that physical properties of the sediments (e.g., seismic velocity, density)

be known or assumed. Since these properties are known only imprecisely

without direct physical measurements, the geometry of stratification, lenses

and other details is only imprecisely inferrable from the acoustic profiles.

Therefore, acoustic profiles must always be calibrated by direct observations

of the subbottom sediments (i.e., borings), and they are therefore used at

particular sites more to interpolate among borings than to define the sub-

bottom itself. Even then, however, the spatial variation of sediment

properties adds uncertainty to geometric interpretations of the acoustical

data.

Some work has been done in attempting to correlate acoustical properties

of sediments to physical, particularly engineering, properties. This work

has met with little success. The only apparent correlation of signficance

is sonic velocity with sediment density (Figure 4.2), but even though den-

sity is an important index properties for sediments (e.g., Figure 4.3) the

level of correlation is insufficient to be of much use. Attempts to predict

properties like undrained shear strength or compressibility have produced
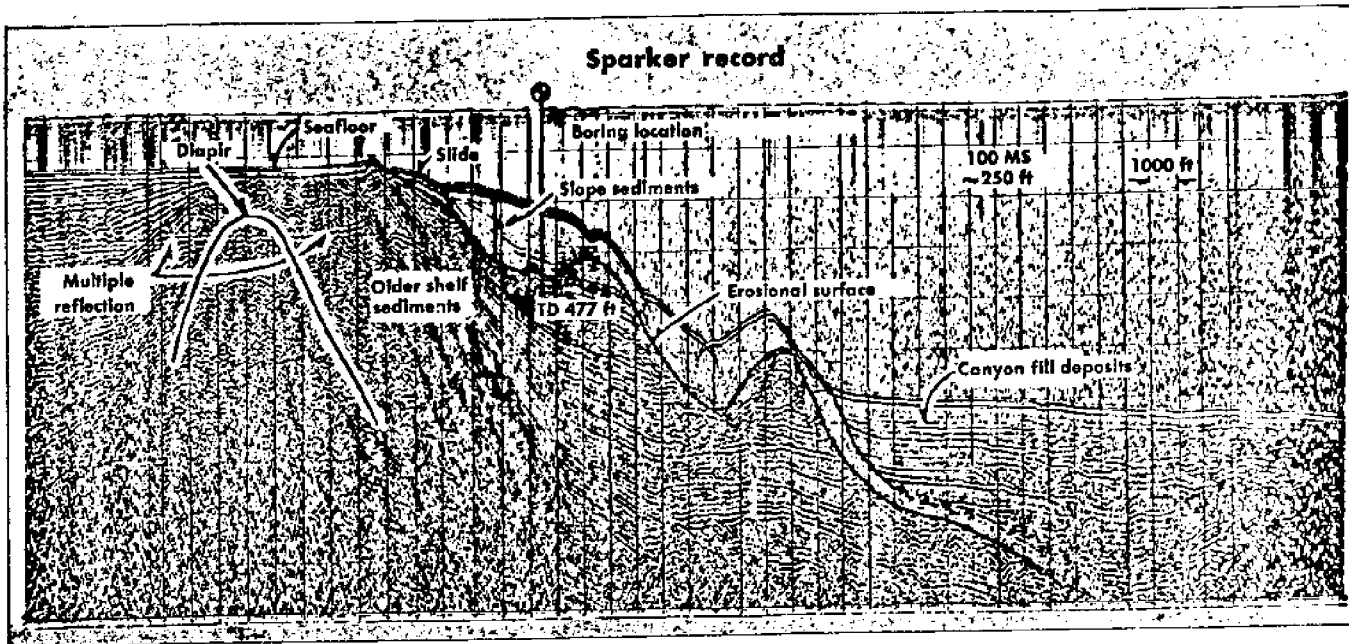
few results.

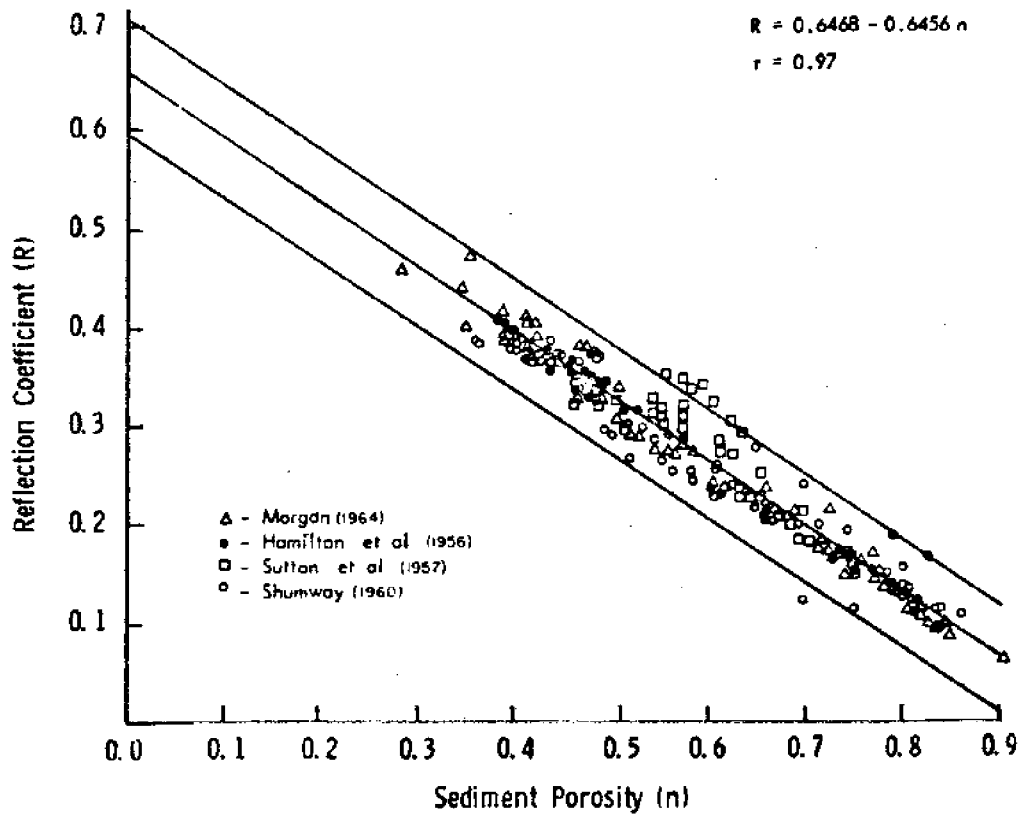*Figure 4.1 -- Typical acoustic log (after Kraft and Perkins, 1978).*

Figure 4.2 -- Correlation between porosity and reflection
coefficient for bottom sediments (From Faas, 1969).
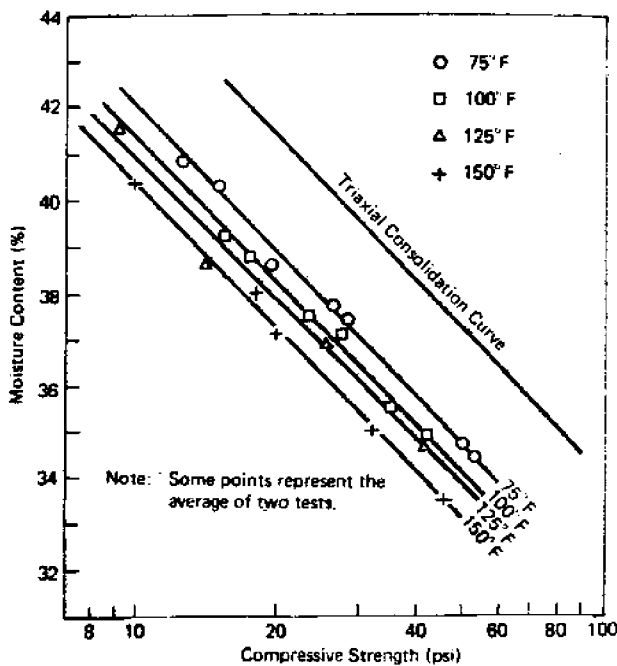
Figure 4.3 -- Relation
between sediment moisture
content and undrained
strength at various
temperatures for kaolinite
(From Sherif and Burrous,
1969).

The detection of anomalies in subbottom profiles is potentially the most important use of acoustical data. However, few carefully controlled experimental programs have been carried out. Proponents of geophysical techniques often point out the past successes of geophysical surveys in locating anomalies on or beneath the sea bottom. However, for inferrential purposes one must not only know the conditional probability that an anomaly in the data is an anomaly in situ, but also that an anomaly in situ produces an anomaly in the data. Since most field research on geophysics is based on an analysis of successes but not failures -- which in fairness is due to the fact that one doesn't know that an existing anomaly is undetected -- only the first of these two conditional probabilities is known. This means inferences of the probability of undetected details are not possible from the geophysical data.

4.1.2 Direct Measurements

The next and most important stage in site investigation is to gather direct information on the bottom sediments. This is done in three ways, using penetration probes, specimen sampling, and in situ testing.

The most rudimentary information is obtained by taking grab or similar samples of the bottom sediments near the mudline. These specimens are easy to obtain and cheap, but are highly or totally disturbed, and only provide information on very shallow strata. They allow classification of surface sediments, but contribute little other information of geotechnical significance.

Other procedures for near surface sampling allow less disturbed samples to be taken, but again are limited in their depth of penetration. The most common of these are gravity samples, which use the inertia of the falling

Figure 4.4 -- Gravity corer (from Noorany and Gizienski, 1970). From left: lowering freefall, penetration, retrival.
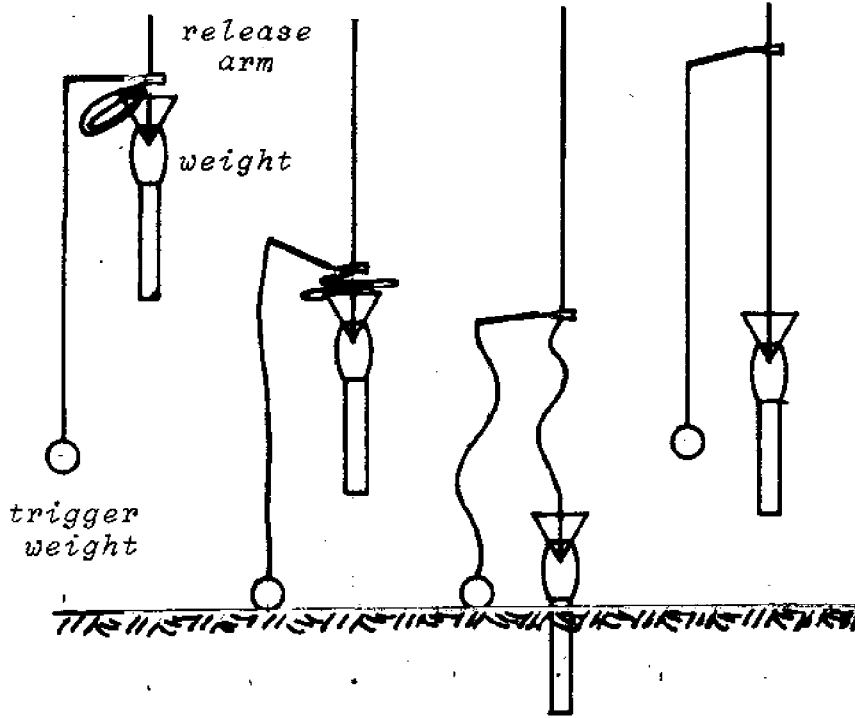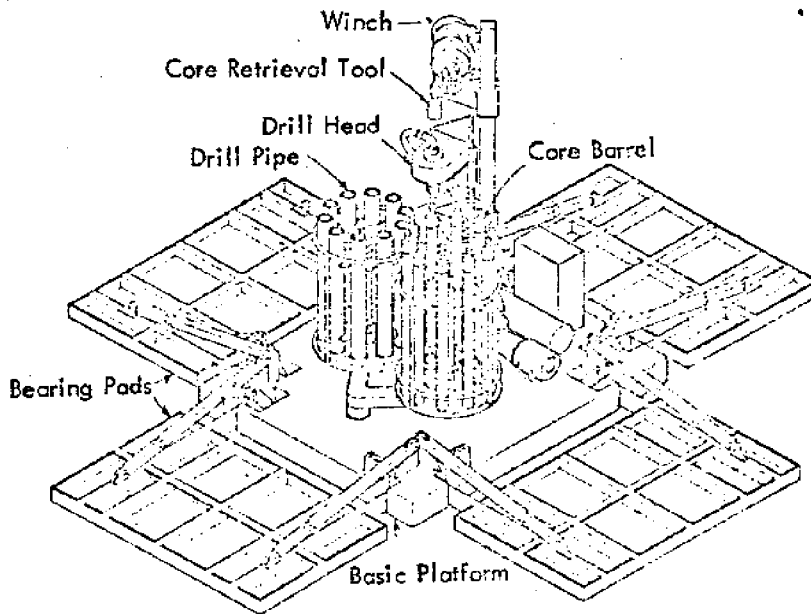

NCEL REMOTELY CONTROLLED SEAFLOOR CORER

Figure 4.5 -- (after Hironaka and Green, 1971).

sampler to drive the sampling tube into the bottom sediment (Figure 4.4).
There are several forms of gravity sampling devices, but they are all
limited to depths of one to two meters and all take rapidly intruded speci-
mens (i.e., "dynamic"). Therefore, the specimens so obtained are more
disturbed than those taken by intrusion. Similarly, vibracores taken
by vibratory penetration of a sampling tube have limited depth penetration
and introduce severe sample disturbance.

Deeper and less disturbed specimens are taken by borings, made either
from the water surface or from specially designed submersible drilling
stages (Figure 4.5). For borings off fixed structure or in calm seas,
common soil samplers (e.g., split spoons or thin walled tube samplers) are
typically used. These have the same drawbacks and advantages as when used
onshore. For drilling off floating structures or boats, wire line samples
are usually used. There are various sorts of these, but generally follow the
principle illustrated in Figure 4.6. Wire line sampling from drilling boats
can be made to depths of over 200 m (McClelland, 1942).

As with any geotechnical sampling, the specimens recovered are to some
extent disturbed (Figure 4.7). Measurements of physical parameters are made
by testing specimens in the laboratory, and are again subject to testing
errors both random and biased. An extensive discussion of these is given
by Ladd (1977). Index properties are usually measured, for example Atterberg
limits, and used to predict in situ properties through well known correlations.
As onshore, sands are exceedingly difficult to sample undisturbed.
Therefore, laboratory tests are made on reconstituted specimens and the results
expressed parametrically with relative density. The well-known error in
measurements of relative density (e.g., Tavernas, 1976) introduce considerable
uncertainty to predictions of in situ properties made this way.
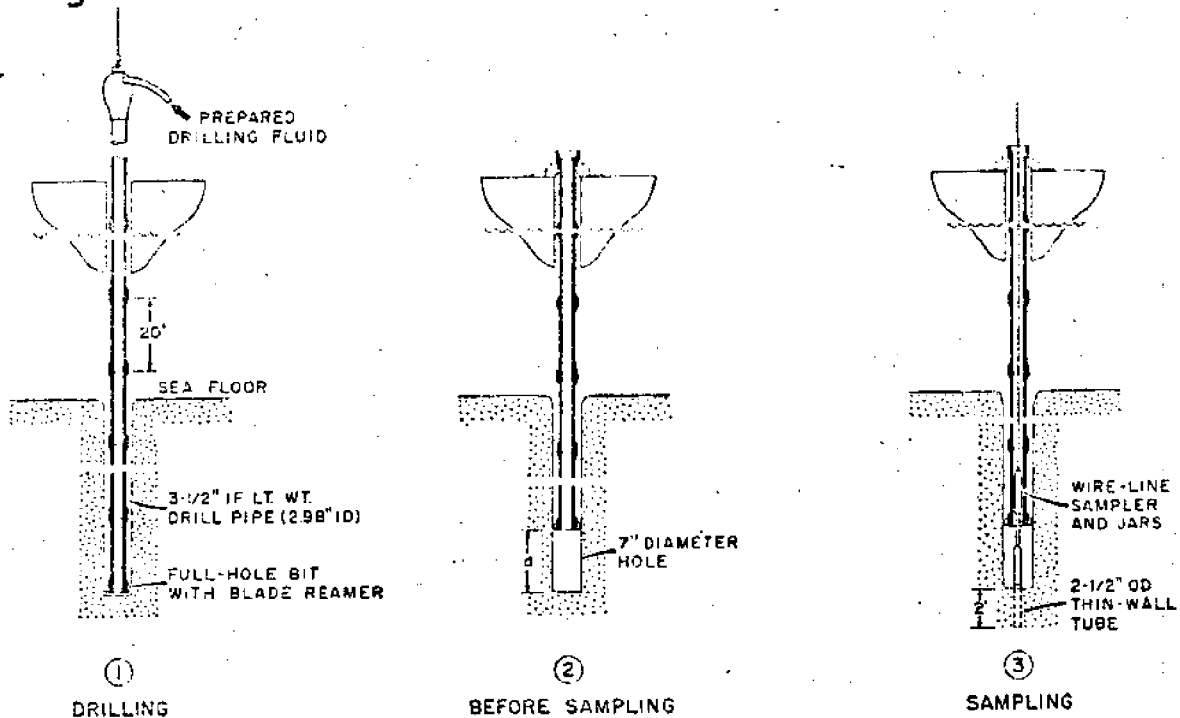
① DRILLING

-Rotary drill pipe, partially supported by draw-works line, moves vertically with drill boat.

-Drilling fluid and cuttings exit at sea floor.

-Continuous re-supply of drilling fluid maintains a clean hole.

② BEFORE SAMPLING

-Drill pipe is set in slips at boat deck, with bit held off bottom a distance, d, which varies as boat moves with sea. Mean value of d is usually about 5-ft.

-Hole diameter is about 7 in. Some cuttings accumulate at bottom.

③ SAMPLING

-Sampler is lowered to rest on bottom, its depth monitored by wire-line revolution counter.

-Sample tube is driven to desired penetration, usually 18 to 24 in, by wire-line operation of jars attached to sampler head.

WIRE-LINE SOIL SAMPLER

PREPARED DRILLING FLUID

20'

SEA FLOOR

3-1/2" IF LT. WT. DRILL PIPE (2.98" ID)

FULL-HOLE BIT WITH BLADE REAMER

7" DIAMETER HOLE

WIRE-LINE SAMPLER AND JARS

2-1/2" OD THIN-WALL TUBE

Figure 4.6 -- Schematic of a wire line sampler (after McClelland, 1972).
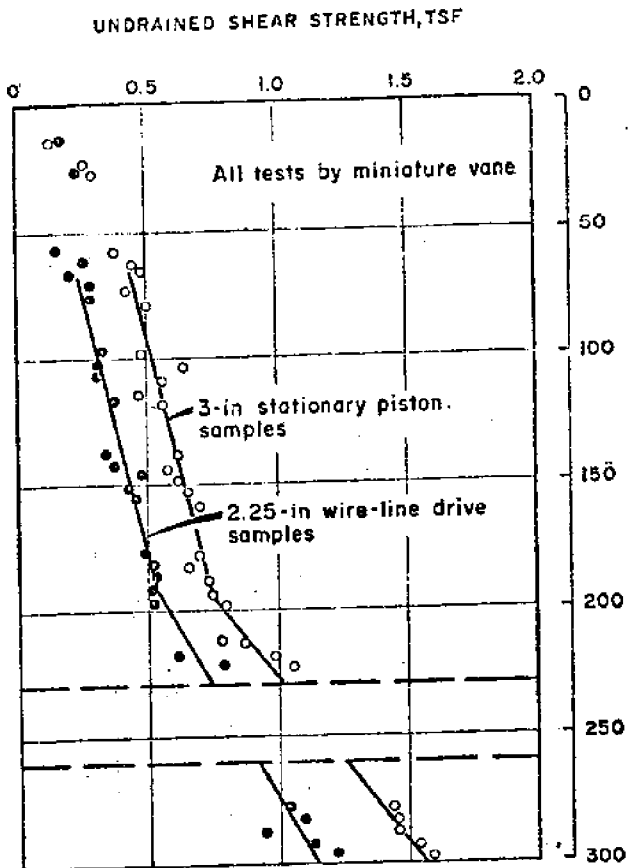
Figure 4.7 -- Sample disturbence: comparison between sampling types (from McClelland 1972, after Emrich, 1970)

UNDRAINED SHEAR STRENGTH, TSF

All tests by miniature vane

3-in stationary piston samples

2.25-in wire-line drive samples

DEPTH, FT

Increasing use is being made of penetration probes in offshore work, particularly core penetration (CPT). The advantages of such tests are that they are easier and faster than taking specimens, less expensive, and directly measure properties in situ. The disadvantage has traditionally been that the correlations between penetration resistance and geotechnical properties are poor (i.e., these must scatter in the data), and primarily empirical. Recent work on penetration testing, however, seems to be leading to theoretical relations among core resistance and engineering properties, and reducing scatter in the empirical relations (e.g., Vivitrat, et. al. 1979).

The CPT very simply measures the resistance of the sediments to penetration by a cone shaped probe of specified geometry (Figure 4.8). The resistance of the cone itself is always measured, and it is increasingly common to measure the drag resistance on the sleeve of the rod to which the cone is attached. From these measurements certain engineering properties can be inferred. Most directly, the CPT is used to infer undrained strength (friction angle or relative density in sands), but inferrence of deformation properties is also sometimes attempted. Recent work on piezometer measurements at the cone tip have indicated that it may also be possible to measure consolidation properties in clay from CPT results.

Finally, a number of other in situ tests of general use onshore are sometimes used offshore. Of these, the field vane is common. However, pressure meter tests and even plate load tests have been used on occasion, if not routinely (e.g., Höeg and Tang, 1978). Typically, the same magnitudes of correction factors and the same correlations are used for these tests onshore and off.
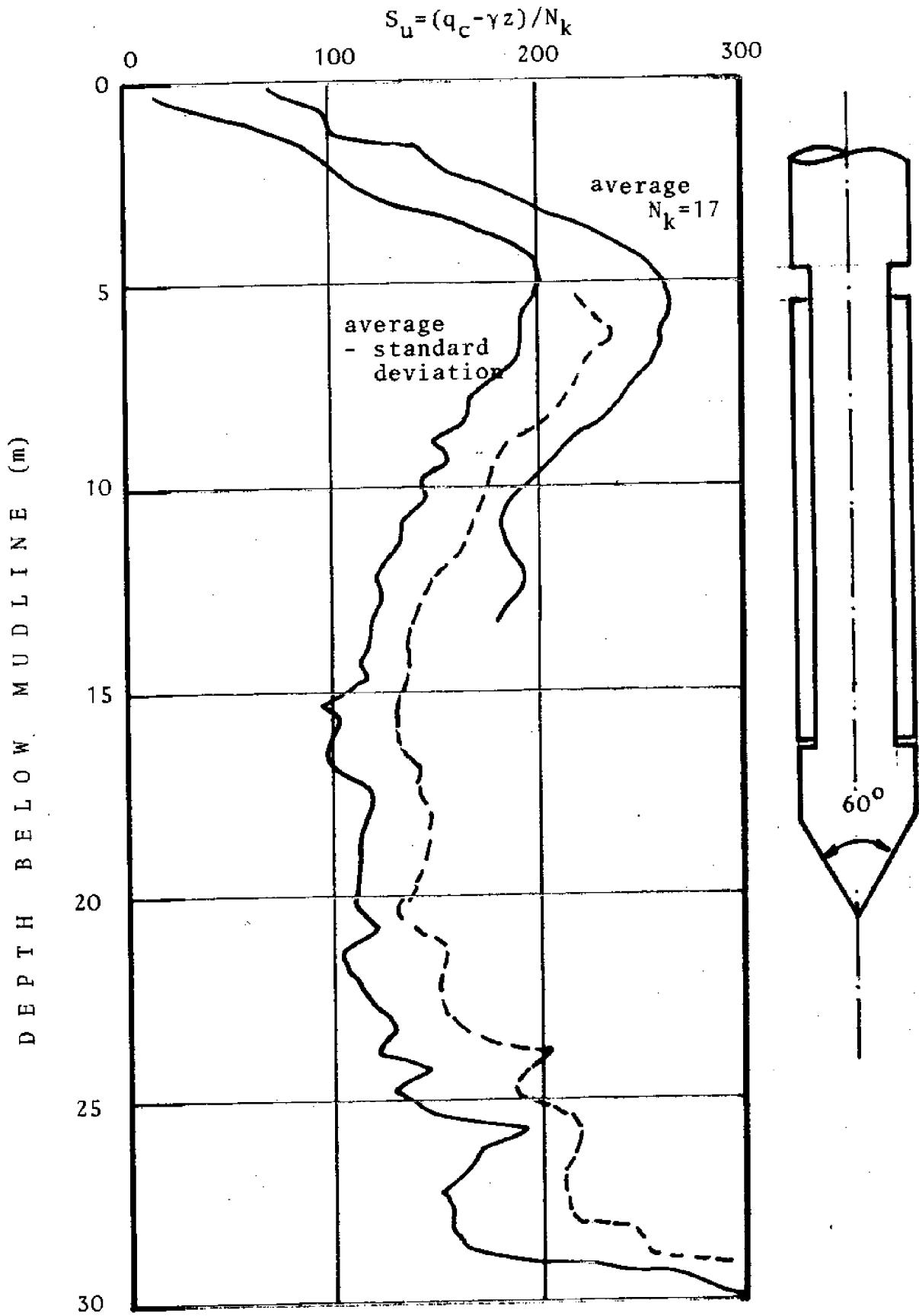
Figure 4.8 -- Typical cone penetration profile and instrument geometry.

4.1.3 Exploration Programs

Typical exploration programs for a large gravity platform are illustrated by those presented by Hitchings, et. al., (1976) and Høeg and Tang (1978). Course grid acoustic surveys might be run at 300 to 500 m spacing, followed by a fine grid at perhaps 50 to 100 m spacing. In the direct sampling and testing phase on the order of 10 to 15 penetrations and a like number of borings are made. Most of these are shallow, penetrating perhaps to 25 m; but a few must be deep, penetrating perhaps to 100 m beneath the mudline. The region of significant influence of the structure is from one to two diameters of the base, depending on the mode of performance, so this depth of investigation is mandatory.

Boring and probe layouts are shown in Figures 4.9, 4.10, and 4.11. The patterns are planned to give full spatial coverage of the site, such that trends or major inhomgeneities will be identified. However, they must also be planned such that cross calibrations are possible among specimen tests, in-situ measurements, and geophysical surveys. Since the exact final location of the completed structure is often uncertain, particularly with gravity platforms that are floated to the site and sunk, the pattern is often not specifically designed with respect to imposed stress distributions as in onshore site investigation. The investigation program typically requires 3 to 6 months from beginning to end, and in 1979 figures costs from one to two million dollars.

4.2 Offshore Sediment Profiles

Offshore sediments vary perhaps even more than onshore soils, from terrigenous detritus derived from continental runoff, to biogenic

Figure 4.9 -- Brent B drilling and probe pattern (after Höeg and Tang, 1978).
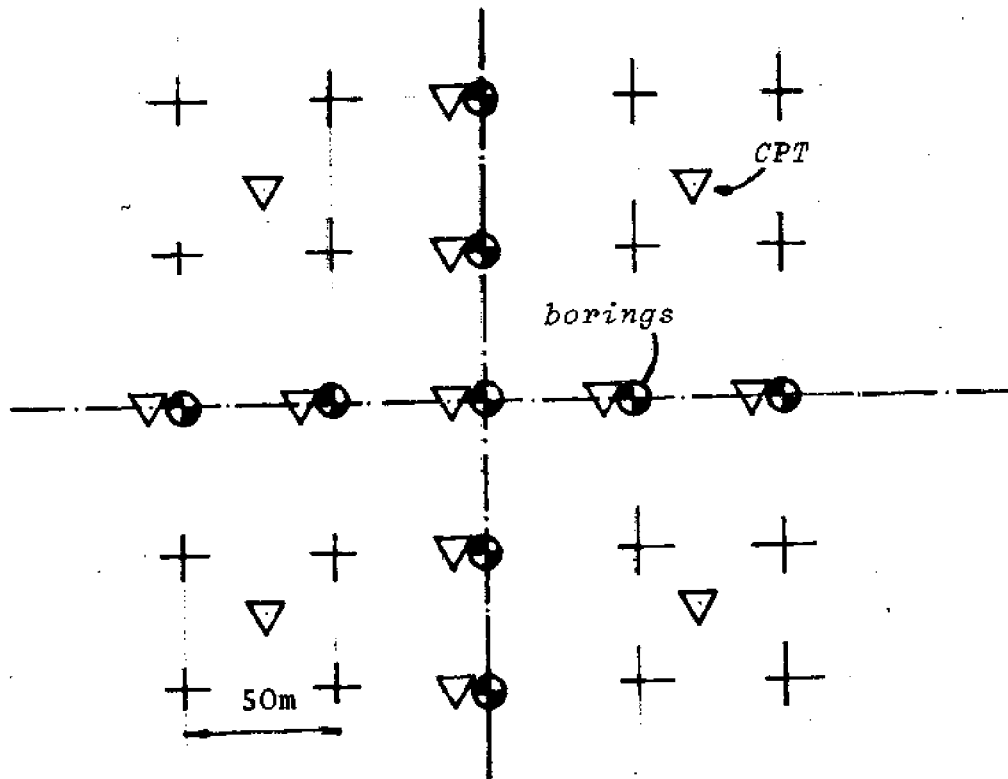
Figure 4.10 -- Soil investigation test pattern from Hitchings, Bradshaw, and Labiosa, 1976.
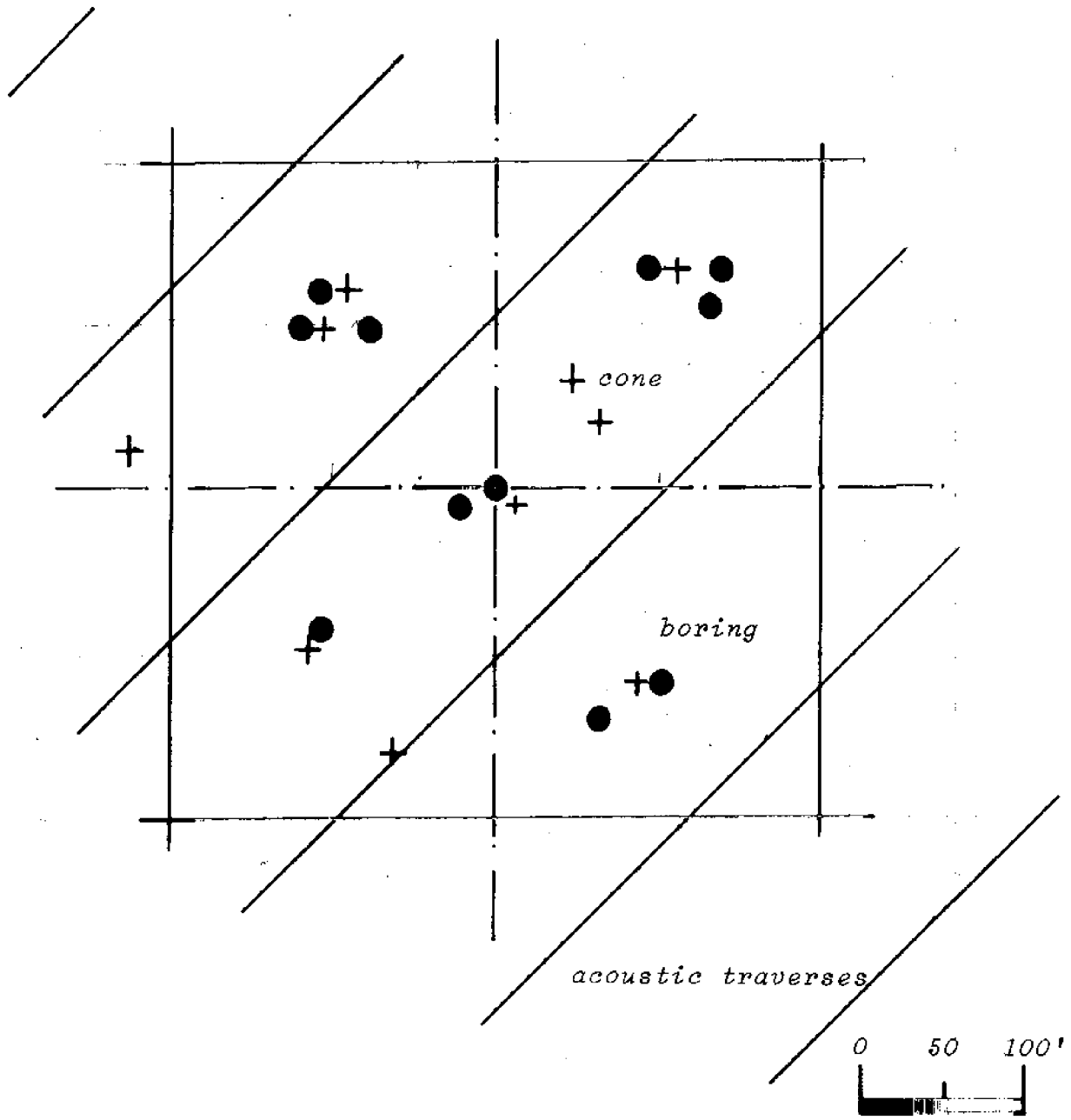
Figure 4.11

calcareuites and calcilutites derived from marine organisms. This section
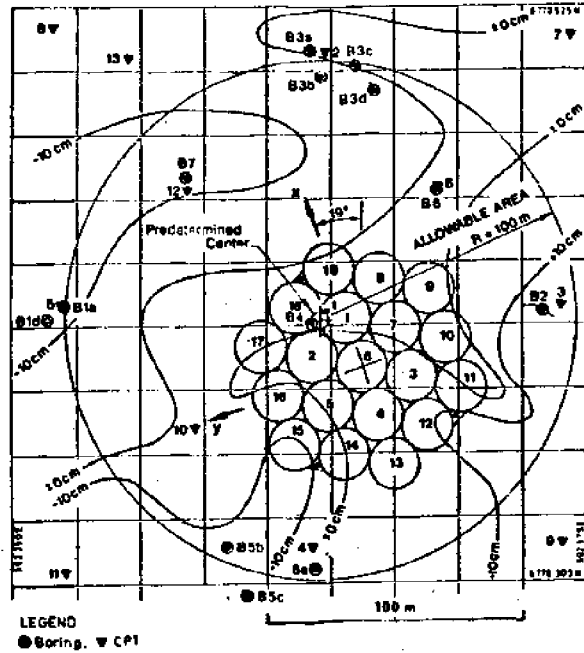discusses geotechnical conditions at the Georges Bank site, used as an example
in later chapters of the report. No attempt is made to more broadly cata-
gorize marine sediments. Such more general discussions are found in Noorany
and Gizienski (1970), Shepard (1948), and Richards (1967).

The site chosen for test applications is that previously considered by
Laszlo (1976). It lies on the southeast edge of Georges Bank in 100 m (300 ft.)
of water, approximately 40 km Northeast of Lydonia Canyon (Figure 4.12).
The bottom sediments at the mudline are mostly sand with some gravelly sands;
and geologically the site is near to boundary between Triasic marine sediments
and the older Avalon Platform (560 m.g.). Normal faults form the boundary
between these formations, and like the entire Georges Bank, a number of small
normal faults are within a few tens of kilometers.

The Georges Bank itself is a remnant of the coastal plane, isolated from
the surrounded continental shelf by erosion of the Gulf of Maine, Great South
Channel, and Northeast Channel. Late tertiary erosion modified by glacial
events are primarily responsible for the present bank morphology. Estimates
of Pleistocene deposition on the Bank vary greatly.*

During the Cretaceous and Tertiary the continental shelf was formed by
up- and outbuilding on the continental margin. Deposition was interrupted
at the beginning of the Tertiary by an episode of extensive erosion, resulting
in a non-conformity between Cretacious and Tertiary.

In late Tertiary a lowland formed Northwest of the present bank and
deepened into the Gulf of Maine. Two southward flowing drainage systems
formed east and west of the present bank, and by early Pleistocene much of
the Tertiary material to the west was removed by fluvial and glacial action.

*The geological history is based on Lewis and Sylvester (1975).

Figure 4.12
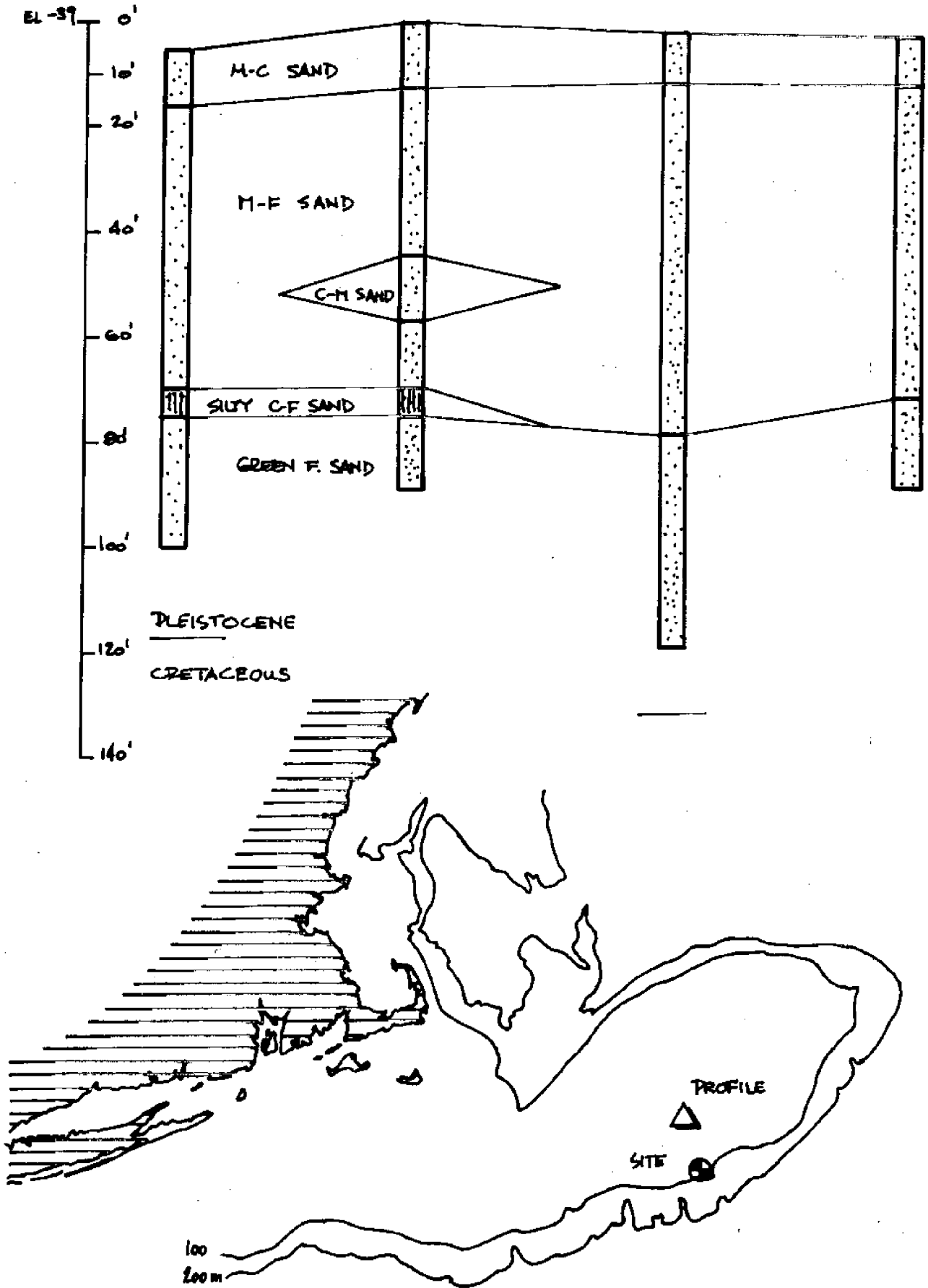
The present canyons on the south of the bank (Hydrographer, Welker, Oceanographer, Gilbert, and Lydonia) are probably the result of drainage outlets during periods of low sea level.

Early Pleistocene glaciation deepened the Gulf of Maine and provided large amounts of sediments. Prior to the final glacial episode a transgression of the sea planed the Bank forming a non-conformity, which was modified by subaerial erosion during the last glaciation. Many stream channels incise the non-conformity in the northeast corner of the Banks, decreasing in number eastward. These are probably the remains of a late Pleistocene drainage system which flowed eastward. Subaerial exposure appears to have lasted long enough to produce complex cut and fill relations in materials overlying the non-conformity.

Very little direct information on geotechnical properties has been gathered near the site, or on Georges Bank. Deep geophysics surveys (e.g., seismic refraction) have been run, but these give essentially no information on sediments near the sea bottom. The available sources of geotechnical information from which data have been taken are shown in Table 4.1. No direct physical property data was taken during the present course of study.

The best direct information comes, first, from borings and standard penetration tests (SPT) performed by Moran, Proctor, Mueser, and Rutledge for the Texas Towers Study. In particular, borings were made from drilling barges on the Nantucket and Georges Shoals, bordering the Great South Channel. Second, the best direct information comes from the Atlantic Margin Coring Project, performed by the USGS. This study resulted in acoustic survey of Georges Bank, and in six borings on the Bank. The location of all of these borings are shown on Figure 4.13, the acoustical survey grid in Figure 4.14.

Table 4.1   Sources of Geotechnical Information
             on Georges Bank Site Used in Present
             Study

Year of Data	Report or Project
1959	Texas Tower Feasibility Study (Bureau of Yards and Docks, USN)
1973	Atlantic Generating Studies (Dames and Moore)
1973,4	Wilkinson Basin Studies (Richards)
1975	Shallow Sedimentary Study of Georges Bank (Lewis and Sylwester - U.S.G.S.)
1976	Atlantic Margin Coring Project -- Preliminary Report (U.S.G.S.)

Figure 4.13 -- Georges Bank site boring locations. Circles, USGS; triangles, Texas Towers project.
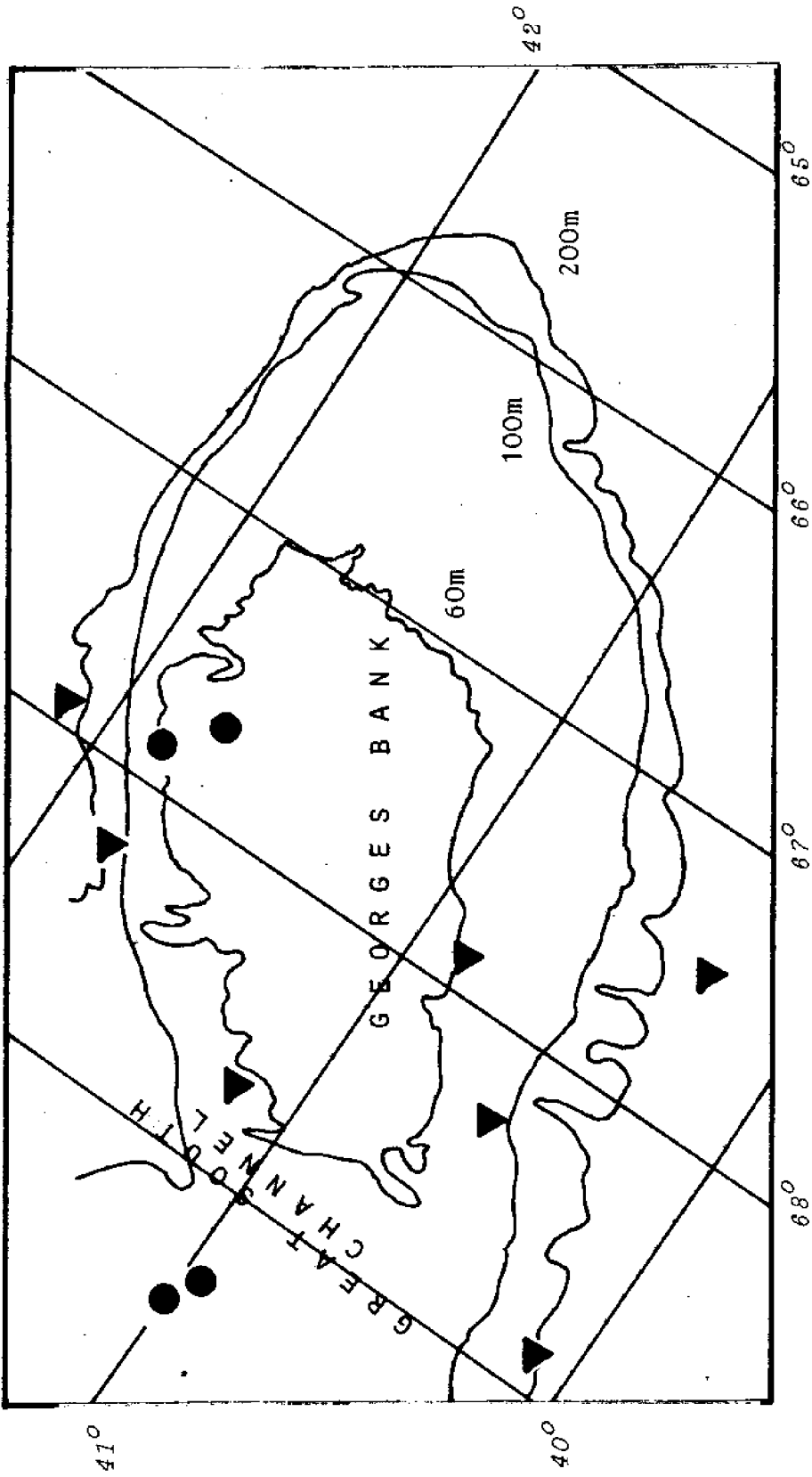
As a cursory overview, the Georges Bank tracts and the test site in particular have gray Pleistocene gravelly sands to a depth of 50 to 100 m below the mudline. Toward the flanks of the Bank these Pleistocene sediments grade into silty sands and silty gravelly sands. The Pleistocene sediments are terrestial detritus, without any apparent appearance of carbonate sands or silts, in keeping with the general nature of the sediments of the Northern Atlantic States (Hathaway, et. al.,1979). Beneath the Pleistocene sands lie Miocene clayey silts and silty sands to an unexplored depth. Borings made on the Bank in connection with the AMCP extend only slightly more than 100 m below the mudline. Typical profiles from the Texas Towers project and AMCP are shown in Figures 4.15 and 4.16.

4.3   Uncertainties in Site Characterization.

Given the limited number of observations, measurement errors, and other factors obscuring the characterization of site conditions, attempts are now being made to quantify ("rationalize") the uncertainties of parameter estimation, mapping, and general site exploration. The objective of such an approach, reviewed and extended in the following subsections, is to arrive at a useable description of uncertainty for assessing reliability and risk. This is not a straightforward task. The uncertainties of site characterization cannot be made entirely objective and many traditional methods of statistical inference require rethinking in application to geological exploration.

The following sections provide first an epistemological background for statistical site characterization, and then an overview of problems and current approaches to quantification. Later subsections address each of three principal tasks in site characterization: parameter estimation, formation mapping, and anomaly detection.

Figure 4.14 -- USGS seismic traverses on the Georges Bank (from Lewis and Sylvester, 1975.)
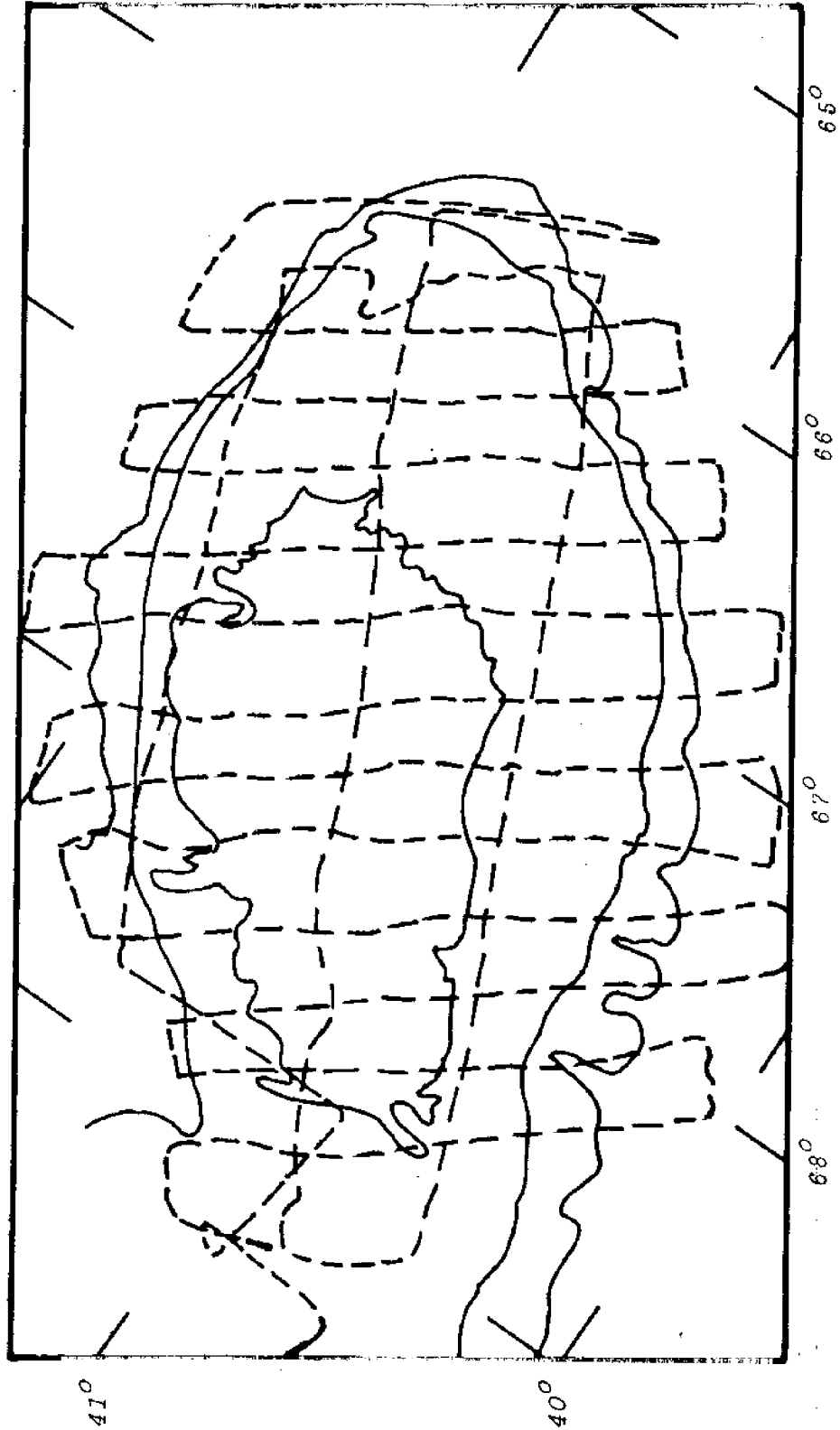
4.3.1 Inductive Basis of Site Characterization

The application of probabilistic modeling to site characterization has been seen by many as an opportunity to make objective a process traditionally seen as subjective. While probabilistic modeling may provide insights into the problem, and may for well defined questions provide quantitative answers, at the basis of geological exploration are epistemological questions which probability theory cannot answer. While important questions in exploration and characterization are amenable to probabilistic modeling, not all are. There are fundamental limitations to the "rational approach" which must be recognized.

As in any inferential task, the data of site characterization do not "speak for themselves". They may, in conjunction with some model of how they arise, lead one to alter what was suspected or believed to some new belief; but at its underpinings geological exploration is an inductive undertaking, and the uncertainties of site characterization are therefore necessarily subjective.

The conclusions of site characterization rest on three stages of considerations. First, in order for probabilities over hypotheses or parameters to be inferred, the hypotheses or parameters must be thought of. That is, they must be imagined through some process of inductive reasoning. Then, the extent to which the hypotheses or parameters are believed must be considered. That is, initial degrees of confirmation must be assigned to the hypotheses or parameters before any data are analysed. Finally, the data themselves are evaluated in light of the hypotheses to modify the initial degree of confirmation. That is, the degree to which the data are or are not consistent with the hypotheses or parameters leads to either increased or decreased belief in the latter.
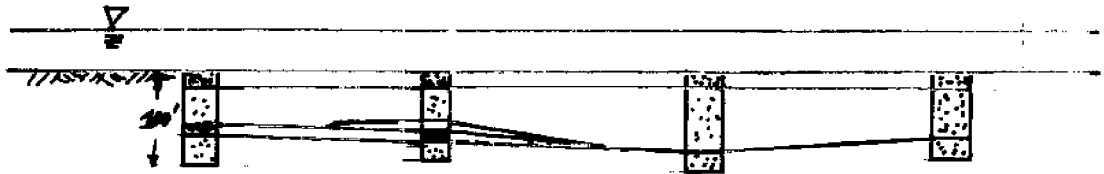
Figure 4.15 -- Inferred profile from Texas Towers exploration program.

Figure 4.16 -- Inferred profile from USGS drilling program (Hathaway, et al., 1979).

gravels

gravelly sands

fine sands

sands with shells or fragments

silty sand

clay
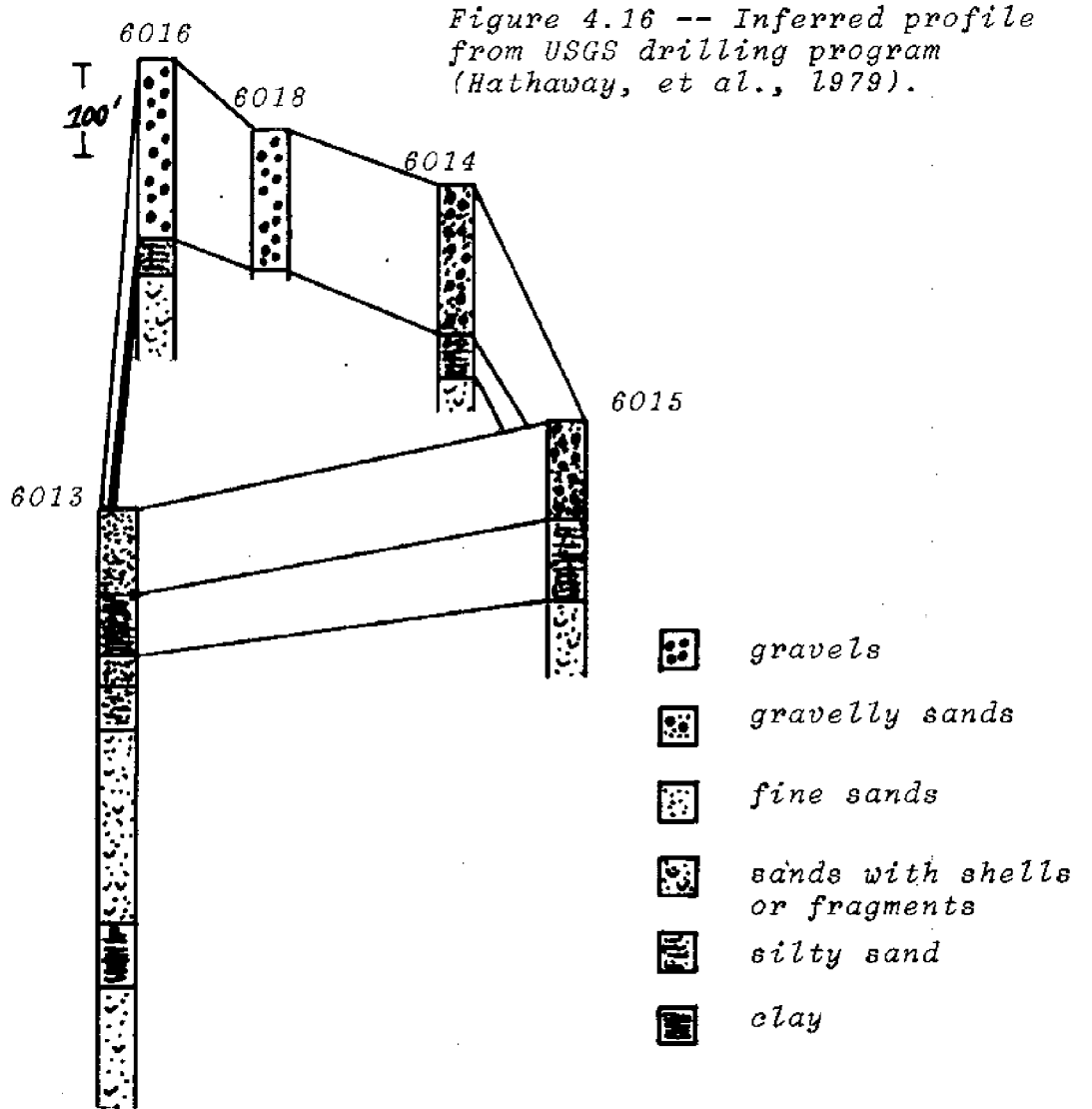
Only the last of these three stages can be considered objective, in the sense that a set of mathematical relationships can be specified from which conclusions necessarily follow. The first two stages are purely inductive, and if Hume is to be believed, "non-logical". This means that the conclusions of site characterization contain much more than the records themselves. Hypotheses are the result of exploration, and uncertainties manifest in the degree to which these are or are not confirmed by observations. Therefore, the uncertainty reflects ignorance, it has little to do with natural randomness.

Figures 4.17a, b illustrate this subjectivity better than many more words could. Each shows a map of the same area of Northern Canada, but drawn 35 years apart. It would be unlikely that the differences were caused by actual changes in the distribution of minerals and rocks, but interestingly they are also not changed by differences in information. The data bases for the two maps are the same. What did change between 1923 and 1958 was geological theory, and this change led to a reinterpretation of the physical observations. This sort of uncertainty, between the map of 4.17a and that of 4.17b, is not a statistical problem but a problem of induction.

The influence of initial degree of confirmation is shown in Figure 4.18. Here the probability of an undetected anomaly in a sediment profile after exploraton has failed to find it is plotted as a function of its probability prior to exploration and of the efficiency (extent) of the exploration program. Efficiency here is measured by the conditional probability that the anomaly would be found if it existed. Only if this efficiency is high (say, > 80%) does the confirmation of the hypothesis of an anomaly existing become insensitive to prior, mostly subjective information.

GRANITIC

BASIC INTRUSIVES

CRYSTALLINE LS.

GRANITIZED
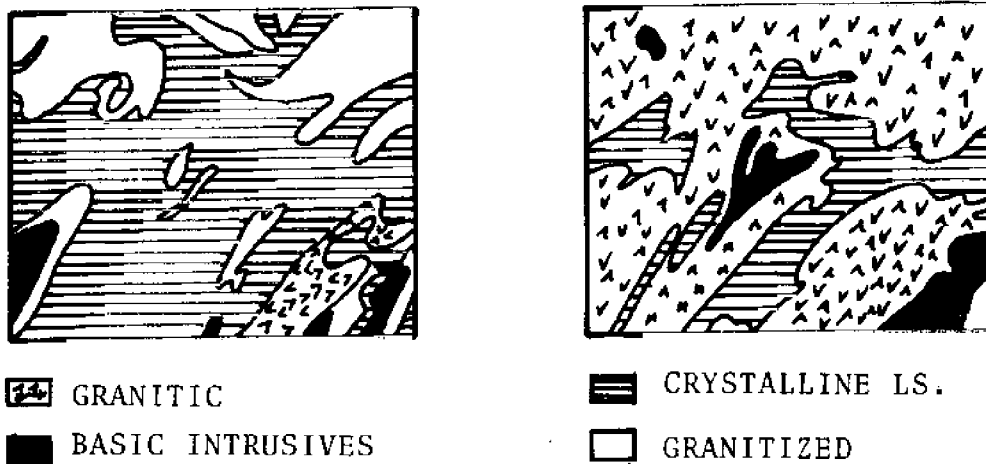
Figure 4.17 -- Two maps of the same area of Canada mapping thirty years apart. Map on left dates from 1958, that on right from 1923. Data base is the same for both maps. Taken from Harrison, 1963.
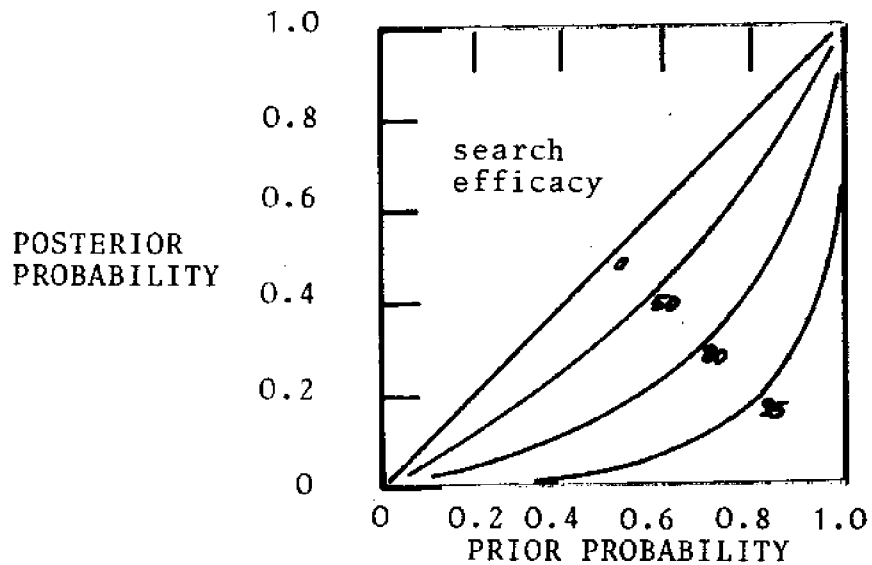
Figure 4.18 -- Relationship between prior probability of an anomaly existing and the posterior probability if none is found during exploration, as a function of the search efficacy (i.e., conditional probability of finding an existing anomaly).

In most geotechnical applications this efficacy is more in the range of 20 to 30%.

The implication of Figures 4.17a, b and 4.18 is that only parts of site exploration and characterization can be statistically modelled. This does not diminish the importance of such modeling, but emphasizes that one must distinguish between what can and what cannot be modelled in engineering analysis. The role of statistical analysis is to logically specify how observations modify prior probabilities of hypotheses or parameters to posterior (after data) probabilities.

4.3.2 Development of Statistical Site Characterization

While hypothesis formulation and initial degrees of confirmation are subjective, the support offered by field data can be statistically modelled.

It is important to briefly distinguish among schools of probabilistic thought. Probability theory is a mathematical construct predicated on axioms within which "probability" is a primitive term. Properties of probability are specified, but its meaning is not. This has led to a number of philosophical interpretations, generally grouped into two schools: the frequentist school, which holds probability to be the relative frequency of an event within a long series of similar trials; and the degree-of-belief school, which holds probability to be the degree to which one believes in the probable occurrence of an event or the truth of a proposition.

The rise of rationalism and the development of the British school of statistics from about 1880 to 1940, and the resurgence of interest in belief starting about 1926, lead to strongly held opinions on the philosophical basis of probability. The distinction between frequency and belief as

complimentary rather than competing philosophies is today not very popular. Yet, one could argue, that frequency and belief are distinct and that their commonality through mathematical probability theory is the extent of their connection.

The practical implications of the philosophical distinction between frequency and belief are the following:

- Within frequentist thought probabilities are not defined on the state-of-nature. A fault exists at a particular site with probability 0 or 1. Whether or not a certain exploration program detects the fault is admissable of probabilistic description, since it can be conceived of as a frequency. But one time events or specific realizations cannot. In frequentist theory, one can only make statements of the following type: "if a fault exists, this exploration program has a 35% chance of finding it."

- Degree-of-belief philosophy allows probabilities on unique events. One can in this case say, "the probability of a fault existing at the site is 60%." A difficulty with belief theory however, is that the issue of belief prior to evidence must be explicitly considered. By disallowing probabilities on "nature" frequentist theory sidesteps this issue.

Degree-of-belief theory is heavily dependent on one familiar equation, Bayes' Theorem:

$$P(H|E) \propto P(H) \, P(E|H) \quad .$$ (4.1)

The probability of an hypothesis, H, conditioned on evidence, E, is proportional to the product of the marginal probability of H, and the conditional probability of E. Because the marginal probability of H is usually that prior to observing E, it is called the "prior" probability. The conditional probability of the evidence is called the likelihood of H. The decomposing equation shows the unification Bayesian methods bring to inference. The entire evidence of field data enters through the likelihood function, which is the probabilistic model for how observations occur. Pre-existing (in part subjective) information enters through the prior distribution.

Uncertainty in predictions

Subsurface data are ultimately used to make predictions about performance. Therefore, the extent of exploration and the types of data to be collected, depend on the relationship of subsurface uncertainty to predictive uncertainty. If better subsurface information would not influence decisions, there is no sense collecting it.

Predictions are made in three ways,

- Extrapolating historical frequency,
- Extending natural law, and
- Quantifying human judgment.

The first two are discussed here.

To extrapolate frequencies or extend laws requires an abstraction of the real world, a model, into which site specific information generally enters as parameter values. There are two purposes in modeling: to understand reality and to predict it. These functions are not always served best

by the same model. The frequency of 'heads' in tosses of a coin is accurately predicted by simple Bernoullian theory. However, sophisticated dynamic analysis, yielding less predictive accuracy, probably yields more insight. In analyzing exploration, models play the same role as in analyzing stresses, and suffer the same limitations. Use of elastic theory is much like use of the normal distribution.

As a first approximation, predictive uncertainty can be divided into three categories:

- Parameter uncertainty -- ignorance of, or inability to measure soil and rock properties;

- Model uncertainty -- simplication and approximation in abstracting reality;

- Changed conditions -- overlooking important mechanisms or geological details.

Site characterization information enters predictions through parameters and boundary conditions. As used here, model uncertainty applies only to the geotechnical models for strength, deformation, and flow, and not to boundary conditions or identification of important mechanisms.

Strategic modeling of site exploration

The applicability of probability theory to site exploration lies in its facility for handling two questions:

- How much effort should be expended in exploring a site and how should it be allocated to return the most information?

- What inferences can be drawn from exploration data, and what are the uncertainties associated with those inferences?
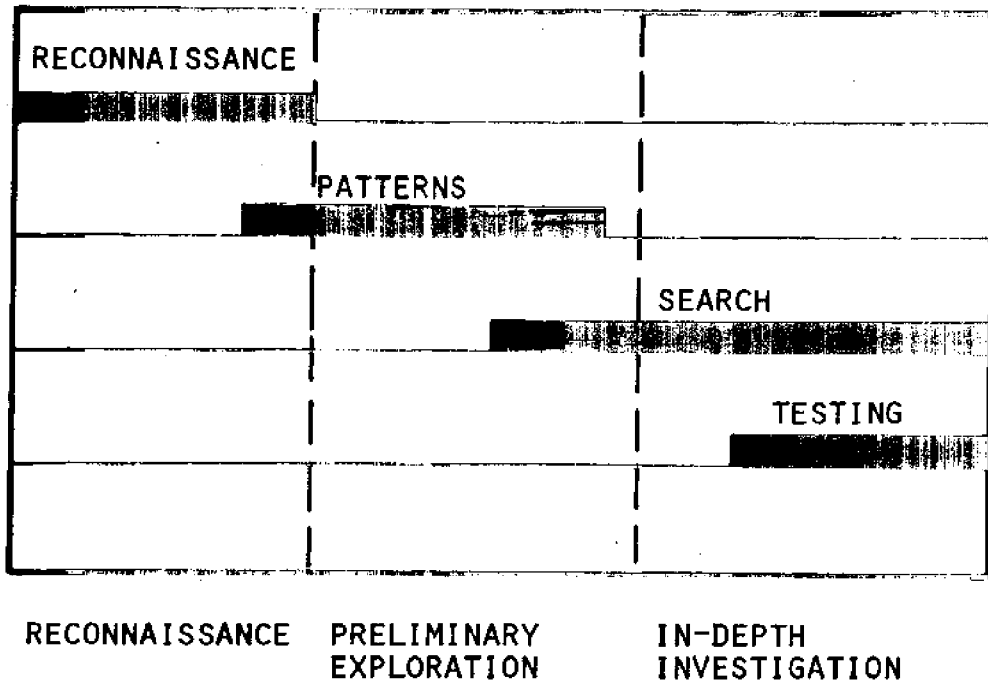
Figure 4.19 -- Problematic taxonomy of site investigation tasks.
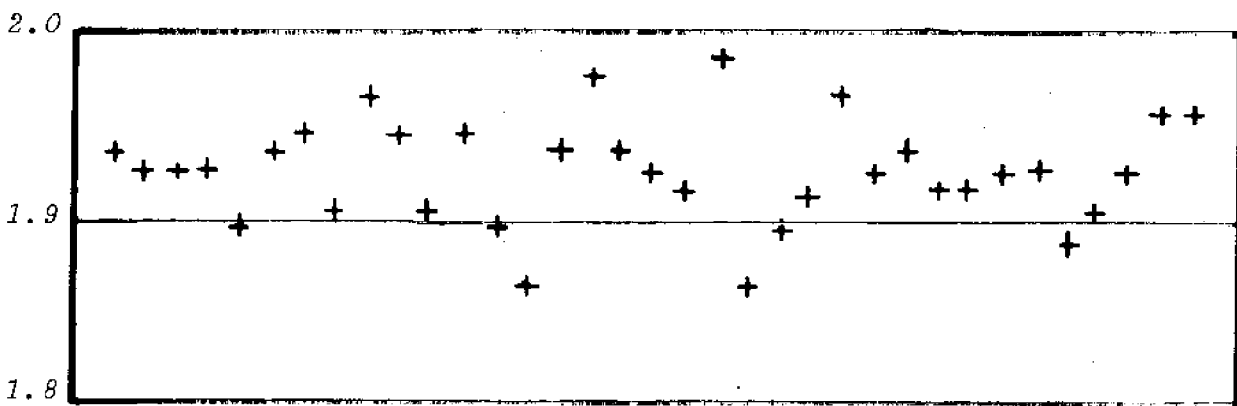
Figure 4.20 -- Spatial variation of dry density in compacted clay dam core. Data correspond to average dry density in each 40cm compaction lift, in vertical direction.

The traditional temporal division of exploration into reconnaissance, preliminary, and in-depth investigation is not particularly useful in strategy optimization, because the division is not along functional lines. Thus a new taxonomy, one based on classes of problems, might be introduced. This is not a replacement for the traditional taxonomy, just a new way of viewing the same problem. Figure 4.19 shows one possibility. Exploration is divided into four categories of problems:

- *Reconnaissance:* Reviewing existing qualitative information and subjective opinion to form initial hypotheses about site geology and possible inhomogeneities.

- *Pattern Recognition and reconstruction:* Recognizing geological forms and extrapolating to areas not actually observed (i.e., mapping).

- *Search:* Finding geological details, or reducing the posterior probability of adverse details to acceptable limits. Locating "non-stationarities" in statistically homogeneous fields.

- *Sampling Homogeneous Material Properties :* Using field and laboratory tests to infer in situ material properties related to strength, deformation, and permeability. Sampling and characterizing pervasive inhomogeneities (e.g., joints).

The strength of this characterization is that it provides an organizing reference for the problems of exploration, in which functionally similar tasks are grouped together. The remainder of Section 4 summarizes uncertainties associated with pattern recognition, search, and sampling material properties; presents techniques for quantifying these uncertainties; and estimates of them.

4.3.3 Parameter Estimation

Estimation of the strength, deformation, and permeability properties of homogeneous zones or strata is made difficult by two sources of uncertainty. The first is spatial variability of the sediment properties, which leads to variation among observations at different location, and just as importantly leads to the problem of selecting an equivalent deterministic (i.e., spatially uniform) property for use in numerical modeling (Figure 4.20). The second is measurement error, which leads both to bias and random fluctuation on top of the spatial variation (Figure 4.21).

Spatial Variation

The now commonly used model of spatial variation of sediment properties is the stationary random field. A vector of soil properties $\underline{y}$ is represented by a mean trend over space $\underline{t}(\underline{x})$ plus a random error term $\underline{\epsilon}(\underline{x})$, where $\underline{x}$ is the basis of the space. Thus (Figure 4.22),

$$\underline{y}(\underline{x}) = \underline{t}(\underline{x}) + \underline{\epsilon}(\underline{x}) \tag{4.1}$$

The error term $\underline{\epsilon}$ is assumed to be autocorrelated in the space $\underline{x}$, and possibly cross-correlated among the various soil properties $\underline{y} = \{y_1, \ldots, y_k\}$. In the geotechnical literature work on sampling from correlated random fields has been presented by Lumb (1974, 1975), Vanmarcke (1977), Alonzo (1976), and in a series of papers by Veneziano (with Faccioli, 1975; Kitanidis, 1977; Queiroz, 1977). This work is related to sampling problems in geology (Matheron, 1971, Agterberg, 1970), hydrology (Rodriquez-Iurbe, 1974; Bras, 1974), groundwater flow (Bakr, et. al., 1977; Wilson, 1978), time series analysis (Box and Jenkins, 1970), and other fields (e.g., Matern, 1960; Whittle, 1963). Veneziano (1979) has recently presented an overview.
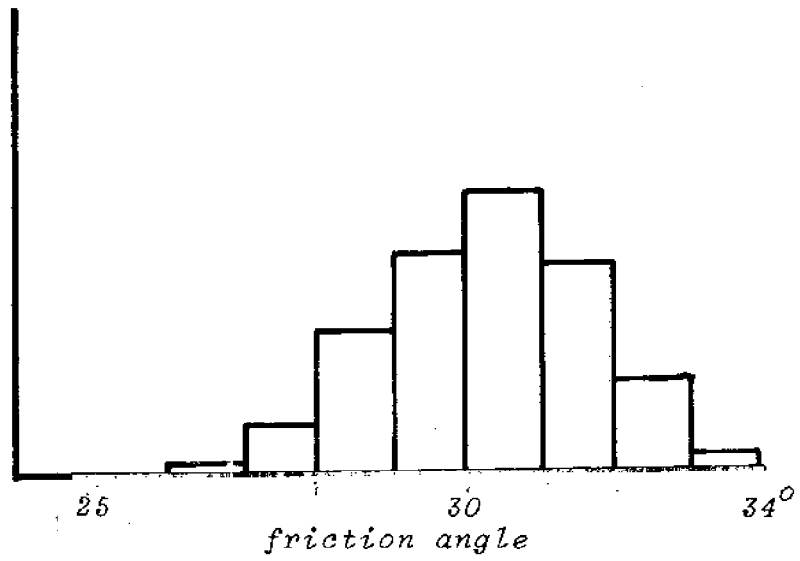
Figure 4.21 -- Scatter of measured values
of friction angle
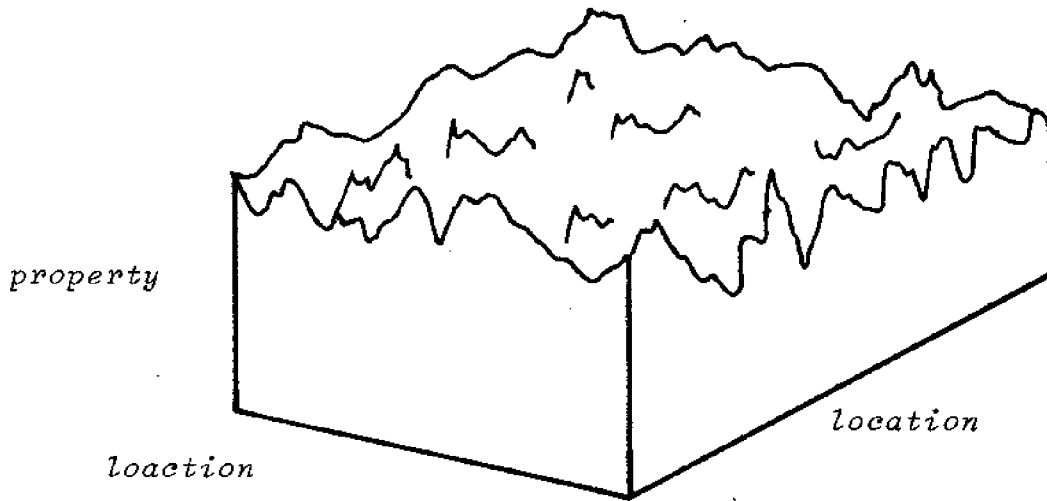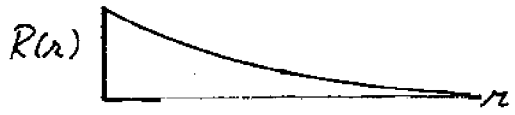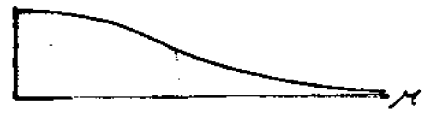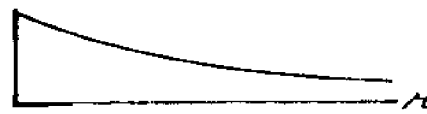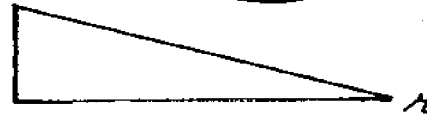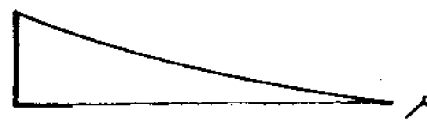
Figure 4.22 -- Abstraction of the spatial
variation of sediment properties at a given
elevation.

A random field $\underline{y}(\underline{x})$ is said to be stationary in the strict sense if the joint density function of $\underline{y}(\underline{x}_1), \ldots, \underline{y}(\underline{x}_m)$ depends only on the relative locations of $\underline{x}_1, \ldots, \underline{x}_m$, and is therefore invariant with respect to changes in the reference. This is a strong assumption, and usually difficult to verify. A weaker assumption is to say the field is stationary in the weak or broad sense, meaning that the mean $t(\underline{x})$ and autocovariance function $R(\underline{r})$ are invariant to changes in the reference (i.e., are the same everywhere). This latter assumption is usually made for sediment properties. Stationarity might be thought of as the stochastic equivalent of deterministic homogeneity, and in fact some workers use "homogeneity" to mean what is here called stationarity when dealing with spatial (rather than temporal) variables.

The feature of central importance in random field sampling is the autocovariance function, $R(\underline{x}_i, \underline{x}_j)$ describing the covariance of soil properties at locations $\underline{x}_i$ and $\underline{x}_j$. Under the assumption of stationarity this function depends only on the vector separation distance between $\underline{x}_i$ and $\underline{x}_j$, to be denoted $\underline{r}$, and not on the exact locations of $\underline{x}_i$, $\underline{x}_j$. Normalizing $R(\underline{r})$ by $R(\underline{o})$, the point variance of the sediment property, leads to the autocorrelation function describing the correlation among properties at various separations. The autocovariance function is of importance because it substantially influences both the sampling properties of the field, and the variance in predictions of physical behavior.

Given that soil properties are generally expected to be more similar when measured at neighboring locations, and to become less and less similar as their spatial separation increases, monotonically decaying $R(\underline{r})$ are usually assumed. Typical functions are shown in Table 4.2. The simpler

TABLE 4.2 — COMMONLY USED AUTOCORRELATION FUNCTIONS FOR SCALAR RANDOM FIELDS.

$R(r)$	SHAPE R^2
e^{-r/r_o}	
$e^{-(r/r_o)^\alpha}$	
$\dfrac{a\,e^{-r/r_o}}{a+1}$	
$e^{-r/r_o}\cos\beta r$	
$e^{-(r/r_o)^2} I_o(\beta r)$	
$1-\beta r$	
$1-\frac{3}{2}\beta r + \frac{1}{2}\beta^3 r^3$	

of these, for example the exponential and squared exponential, have been verified by field observations (e.g., Lumb, 1975; Hilldale, 1971; Höeg and Tang, 1976) (Figures 4.23 and 4.24).

The extent of autocorrelation is commonly indexed by an "auto-correlation distance" r_o, defined such that $R(r_o) = (1/e)\sigma^2$. The meaning of this index can be seen in Figure 4.25. Long r_o imply wavy spatial variations, whereas short r_o imply rapid fluctuation. In the former case an observation, such as at x_o in Figure 4.25a, gives information about sediment properties quite far from its own location; in the latter case it does not. However, the reverse consequence is also of importance; observations at x_o and x_1 contain redundant information when r_o is large, and therefore cannot be treated as independent in drawing inferences about $y(\underline{x})$.

Despite the importance of $R(\underline{r})$ in sampling and predicting physical processes, it is an artifact of the modeling. There is nothing innately random about sediment properties. The stochastic model is an expression of ignorance about subbottom conditions, not random variation. Therefore, depending on how this spatial variation is divided between a deterministic mean trend $t(\underline{x})$ and the random component $\varepsilon(\underline{x})$, the autocovariance function and the point variance will change (Figure 4.26).

Table 4.3 summarizes typical point variances and correlation lengths for various sediment properties, when sampled at individual sites. These correlation lengths result from assuming a spatially constant mean. Figure 4.27 shows the autocorrelation function inferred for shallow (3.6m) cone resistance at the Brent B site in the North Sea (Höeg and Tang, 1978). As can be seen, r_o in the range 15 to 60 m is typical.

Figure 4.23 -- Autocorrelation of SPT blow count for a dune sand (after Hilldale-Cunningham, 1971).
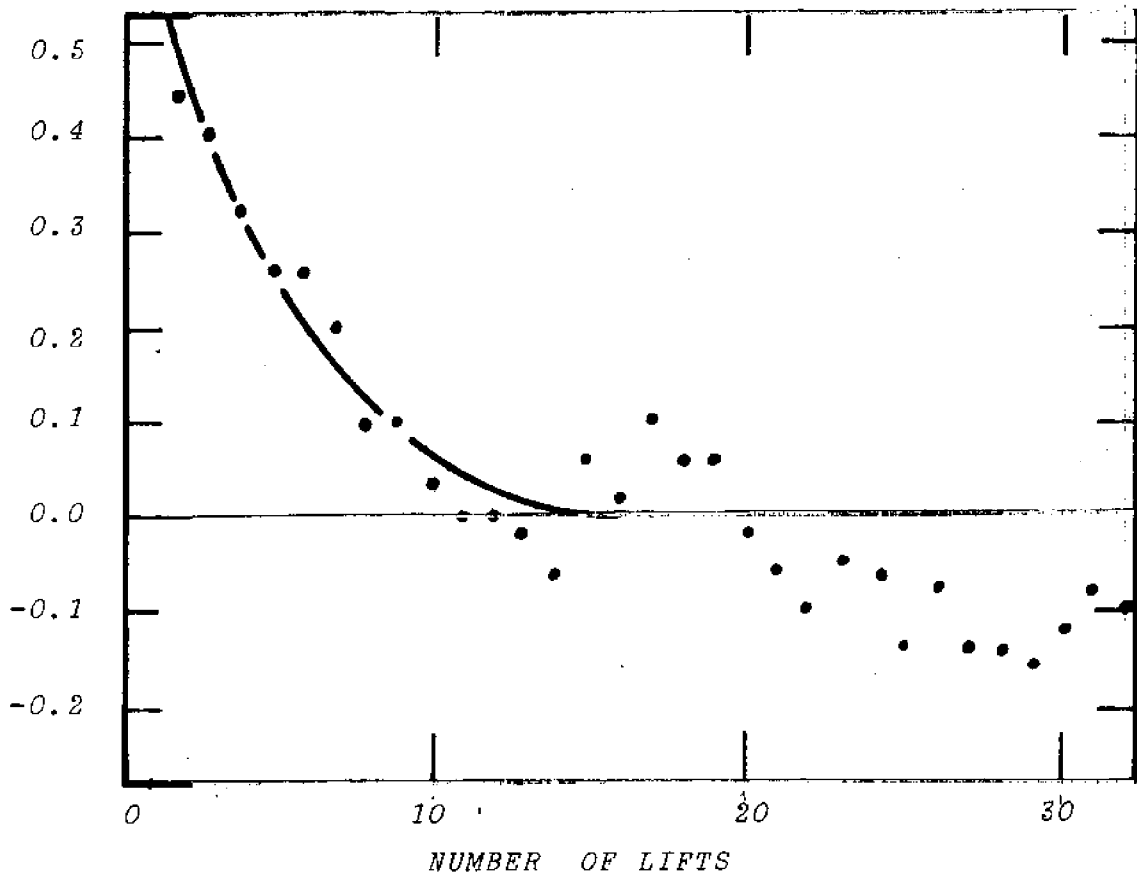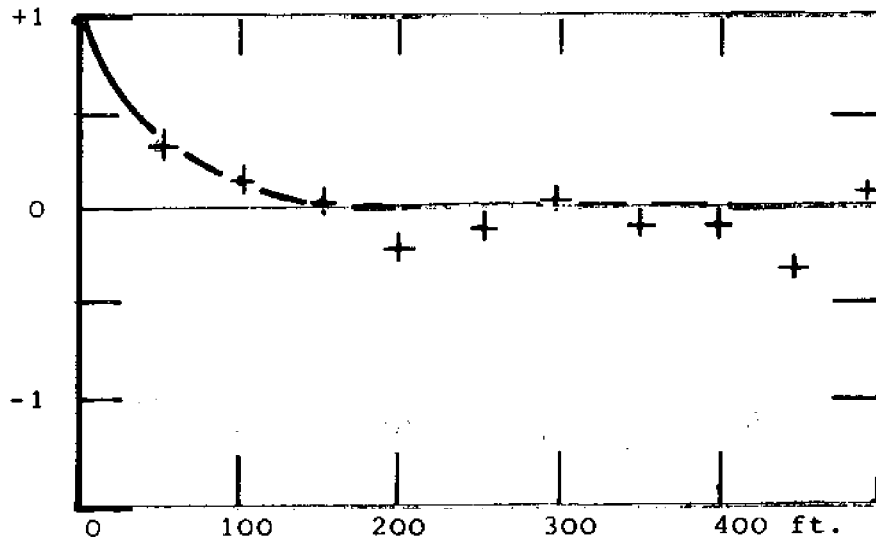
Figure 4.24 -- Autocorrelation for data of Figure 4.20. Total data length N=183.

Table 4.3 -- Typical variances and autocorrelation lengths for sediments.

MATERIAL	PROPERTY	r_0	SOURCE
coastal sand	CPT	5m	Tokheim (1976)
compacted clay (dam core)	dry density (horizontal layers)	5	Wünch, et al.(1980)
	(vertical)	5	--"--
North Sea Clay	CPT	30	Höeg and Tang (1978)
dune sand	SPT	20	Hilldale-Cunningham (1971)
Plastic clay	dry density (vertical)	1.3	Vanmarke and Fuleihan (1975)
Clean sand	CPT	0.36	Alonzo and Kreizek (1975)
clay	CPT	1.91	--"--
silty loam	w/c	0.16	--"--

Table 4.4 -- Empirical distribution function for various soil properties.

Material	Property	pdf	Source
compacted clay core	dry density	Λ	Wünch, et al. (1980)
sand	pile capacity	Λ	Baecher and Rackwitz (1980)
dry sand	bearing capacity	Λ	Ingra and Baecher (1978)
silt	e_0	N	Schultze (1975)
silt	uniformity coefficient	Ex	--"--
Sands (various)	n, e	N	--"--
silts(")	n, e	N	--"--
clays(")	n, e	N	--"--
marine clay	S_u	N	Lumb (1966)
silty sand	tan ϕ'	N	--"--
clayey silt	--"--	N	--"--
clayey silt	S_u	N	Singh (1971)
various	c', ϕ'	ß	Lumb (1970)

distributional forms: N = Normal, Λ = logNormal, ß = Beta.
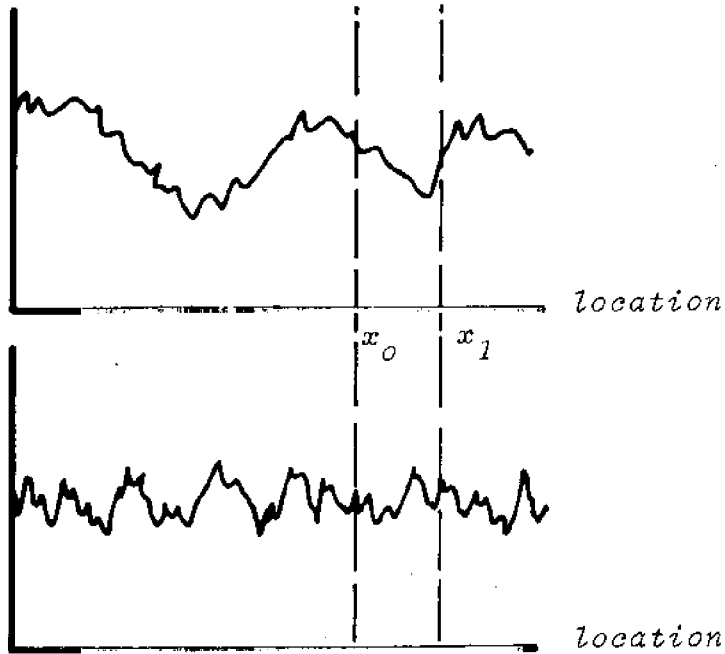
Figure 4.25 -- Comparison between spatial variation with high autocorrelation distance (above) and low autocorrelation distance (below).
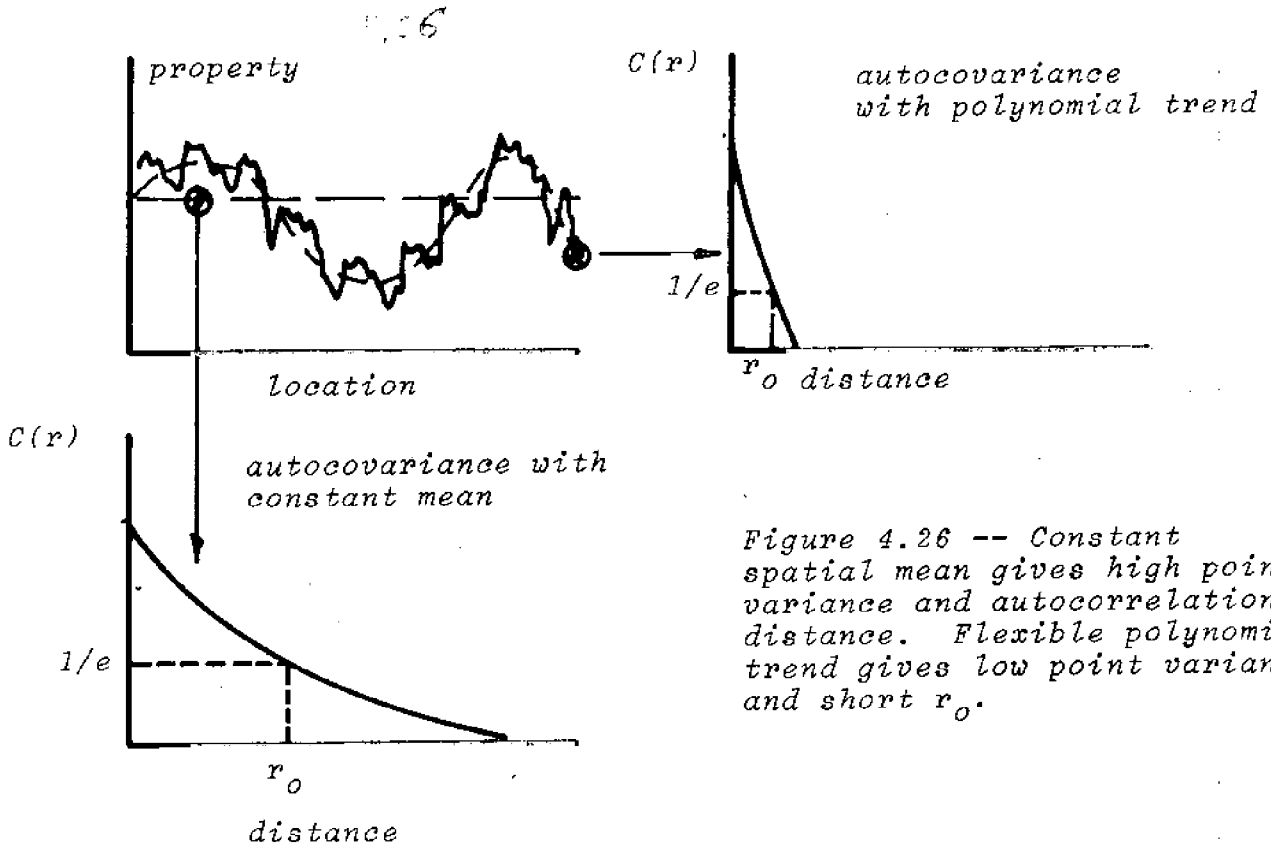
Figure 4.26 -- Constant spatial mean gives high point variance and autocorrelation distance. Flexible polynomial trend gives low point variance and short r_o.

Estimates of Mean Sediment Properties

Estimates of mean sediment properties from a finite number of observations follows fairly well known statistical results. For the case of widely spaced measurements such that the correlation among measurements approaches zero, simple application of Bays' Theorem yields a posterior (i.e., after sampling) distribution on $t(\underline{x})$, now assumed spatially constant,

$$f'(t|\underline{z}) \propto f^O(t)L(\underline{z}|t), \qquad (4.2)$$

where $\underline{z} = \{z_1,\ldots,z_n\}$ are the observations, $f^O(t)$ is the prior (i.e., before sampling) distribution on t, and $L(\underline{z}|t)$ is the likelihood (i.e., conditional probability) of $\underline{z}$ given t.

The assumption is commonly made that variation of sediment properties is Normally distributed, in which case for a diffuse prior, $f^O(t) \propto$ constant, the inferred posterior on t is also Normal (Table 4.5). However, for a broad class of distributions the probabilities distribution of the sample mean, $(1/n) \Sigma z_i$, given t is asymtotically Normal with mean t and variance $\sigma2/n$ (i.e., the sampling distribution), and although not correct statistically is used as a proxy distribution for t.

In application, the variance σ^2 must itself be estimated from the observations. Since the posterior distribution of t depends on σ^2, inferences must first be drawn on the joint distribution $f'(t,\sigma|\underline{z})$, and then integrated over σ to yield the marginal posterior on t,

$$f'(t) \propto \int f^O(t,\sigma)L(\underline{z}|t,\sigma)d\sigma \qquad (4.3)$$

The well known result (e.g., Raiffa and Schlaifer, 1961) is a Student t distribution on t. This result is shown graphically in Figure 4.38 for

a sample of water content measurements.

For not widely spaced observations the variance of Figure 4.28 is a lower bound. Because the observations report redundant information, the uncertainty in the inference on t must be greater than in the independent case. The sample mean $\bar{z} = \Sigma z_i/n$ remains an unbiased estimator in the relative frequency sense, but the variance of the distribution of the sample mean $\bar{z}$ increases to

$$v\{\bar{z}|t\} = \frac{1}{n^2} \sum_{i=1}^{n} \sum_{j=1}^{n} C[z_i, z_j] \qquad (4.5)$$

The exact increase in this variance depends on the pattern of observations with respect to the autocovariance function $R(\underline{r})$. For example, with the Brent B observation pattern (Figure 4.9) and the corresponding $R(\underline{r})$ (Figure 4.27), the increase in variance from independent to correlated observations is about 50%.

This increase in likelihood function variance, and therefore in inferential uncertainty can be reduced somewhat by differentially weighting each z_i according to its correlation with other observations. For example, adopting the linear estimate

$$\hat{z} = \Sigma w_i z_i \qquad , \qquad (4.6)$$

where $0 \leq w_i \leq 1.0$, and $\Sigma w_i = 1.0$; the weights $\underline{w} = \{w_1, \ldots, w_n\}$ can be optimized to produce the smallest variance in Equation 4.5. Introducing the Lagrange constraint $\lambda(\Sigma w_i - 1) = 0$ and differentiating with respect to $\underline{w}$ yields the optimal weights $\underline{w}^*$,
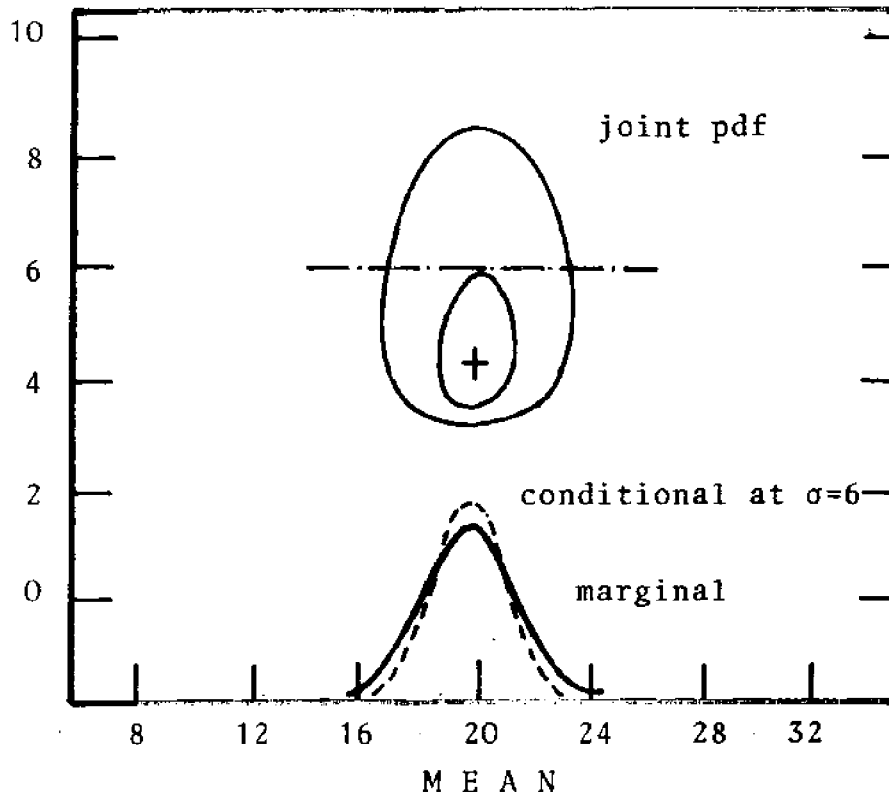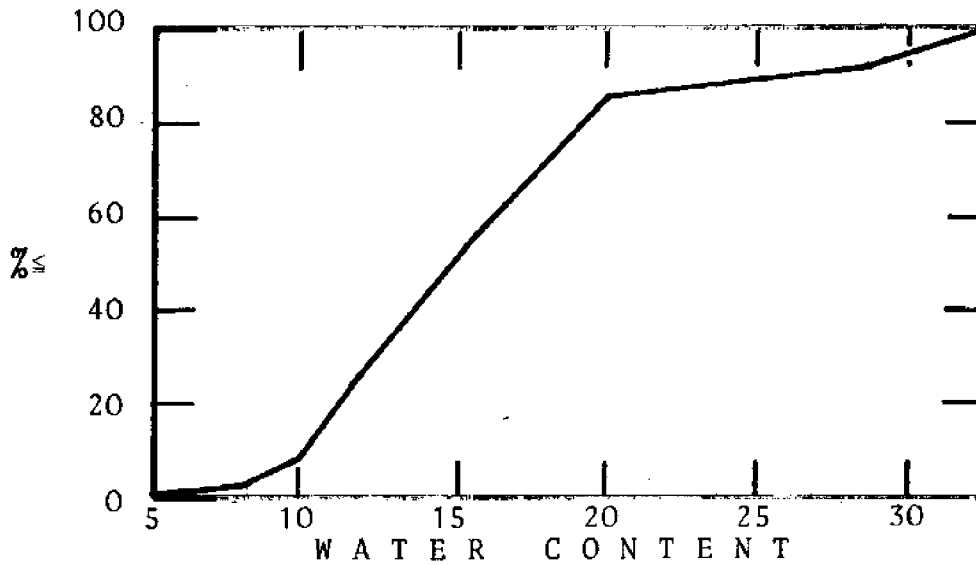
Figure 4.28 -- Water content data for the Munich Tertiary Silts and inference of mean and standard deviation. After Peintinger, 1979.

$$\left\{ \begin{matrix} w^* \\ \lambda \end{matrix} \right\} = \left[\begin{matrix} \underline{\underline{C}} & \underline{1} \\ \underline{1} & 0 \end{matrix} \right]^{-1} \left\{ \begin{matrix} \underline{0} \\ 1 \end{matrix} \right\} \quad , \tag{4.7}$$

where $\underline{\underline{C}}$ is the covariance matrix of the observations.

Applying 4.7 to the Brent B pattern yields the weights show in Figure 4.29. This reduces the estimate variance by about 7.1% compared with the simple arithmetical average. Note that adding a 14th boring, with its corresponding cost, and assuming it to be independent of the other observations, would only reduce the variance about 7.9%.*

Estimates of Autocovariance Function

Among the more important insights gained by reliability modeling in soil mechanics is the strong influence of spatial variation of strength, deformation, and permeability properties on physical behavior. Despite this importance of spatial variability, the use of rigorous statistical procedures for estimating autocovarience uncommon in present applications. This reflects in part the mathematical difficulty of these procedures, but perhaps more simply the general neglect of statistical uncertainty in geotechnical analyses. This section summarizes a few of the more useable statistical results for estimating spatial variability.

The spatial variability of physical properties will be represented by a stochastic process $\underline{Z}(x_1, x_2, x_3) = \underline{Z}(\underline{x})$, in which $\underline{Z}(\underline{x})$ is a vector of properties at location $\underline{x}$ in space. Individual realizations of the process are denoted here by the lower case symbol $\underline{z}(\underline{x})$.

---

* Appendix 4.3 contains further discussion of optimal estimation.
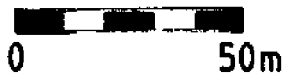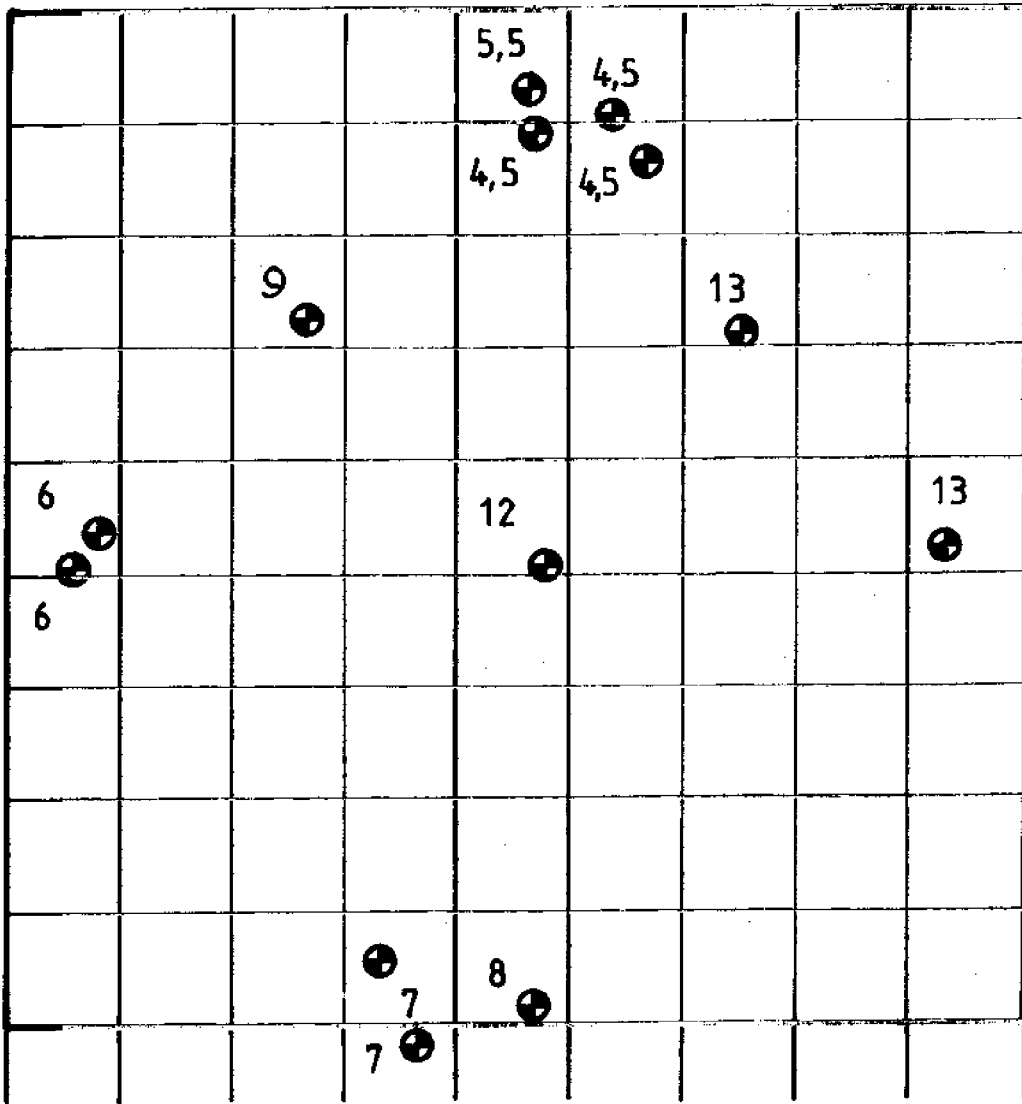
WEIGHTS x100
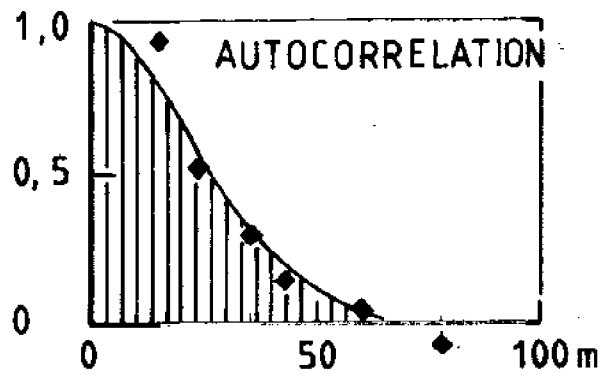
Unless otherwise noted, the process $\underline{Z}(\underline{x})$ is assumed to be second-order stationary, in that the mean $E\{\underline{Z}(\underline{x})\} = \underline{\mu}$, variance $V\{\underline{Z}(\underline{x})\} = \underline{\mu}$, and auto-covariance function

$$C\{\underline{Z}(\underline{x}_i), \underline{Z}(\underline{x}_j)\} = E\{[\underline{Z}(\underline{x}_i)-\underline{\mu}][\underline{Z}(\underline{x}_j)-\underline{\mu}]\} \qquad (4.6)$$

do not depend on location. For the case of vector $\underline{Z}$, both the variance and covariance function are matrices, the off diagonal terms of which reflect covariance or crosscovariance of the components of $\underline{Z}$.

For simplicity, and in keeping with current practice, two simplifications will be made. First, attention will be restricted to scalar properties Z, and the covariances among different physical properties (e.g., strength and deformability) will not be considered. In this case the variance becomes σ^2 and the autocovariance

$$C\{Z(x_i), Z(x_j)\} = C_{zz}\{x_i, x_j\} \qquad (4.7)$$

and obviously $C_{zz}(0) = \sigma^2$. Second, only one dimensional processes will be considered (e.g., soil properties in the vertical dimension, or along one horizontal direction). This, $\underline{r}$ becomes a scalar.

The spectral density function of the process $Z(x)$ is defined as the Fourier transform of the autocovariance function

$$f(\omega) = \frac{1}{2\pi} \int_{-\infty}^{\infty} e^{ir\omega} C_{zz}(r) \, dr \qquad (4.8)$$

and is an alternative way of representing the same spatial variation.

Given a set of N evenly spaced observations of $Z(x)$: $z(x_1)$, $z(x_{1+\delta})$, ... , $z(x_{1+(N-1)}\delta)$, the moment estimator of the mean μ of $Z(x)$ is the sample mean (Figure 4.30).

$$\bar{z} = \frac{1}{N} \Sigma \, z_i \tag{4.9}$$

where z_i is used to denote $z(x_i)$, $i=1, \ldots , N$. This estimate is unbiased in that $E\{\bar{z}\} = \mu$, and has variance.

$$V\{\bar{z}\} = \frac{\sigma^2}{N} \sum_{r=-N+1}^{N-1} (1 - \frac{|r|}{N}) R_{zz}(r) \tag{4.10}$$

where $R_{zz}(r)$ is the autocorrelation function of $Z(x)$, $R_{zz}(s) = \frac{1}{\sigma^2} C_{zz}(r)$. This variance approaches 0 as $N \to \infty$, and thus is consistent.

The moment estimator of the process variance σ^2 is the sample variance,

$$V\{z_i\} = \frac{1}{N-1} \Sigma \, (z_i - \bar{z})^2 \equiv s^2 \tag{4.11}$$

which is also unbiased, and to a first approximation has sampling variance

$$V\{s^2\} \simeq 2\sigma^4/N \quad . \tag{4.12}$$

Thus, the estimate is also consistent.

The moment estimator of the autocovariance function $C_{zz}(r)$ is the sample autocovariance function $\hat{C}_{zz}(r)$,

Figure 4.30 -- Typical spatial variation of soil properties.

x_1 x_2 ... x_n
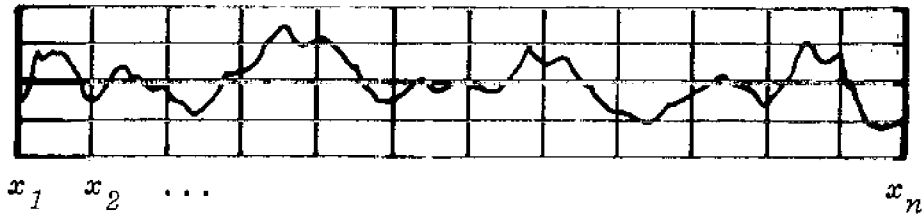
Figure 4.31 -- Sampling bias of moment estimator of autocovariance function for one-dimensional process.
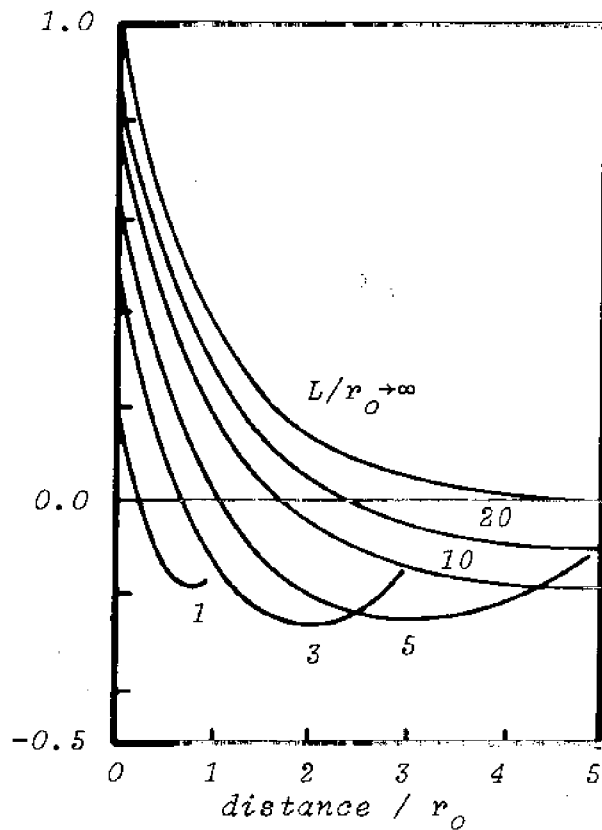
$$\hat{C}_{zz}(r) = \frac{1}{N-r} \sum_{i=1}^{N-r} z_i z_i + r \bar{z}^2 \qquad (4.13)$$

where r is measured in units of the separation δ.

The expected value of the sample autocovariance is

$$E\{C_{zz}(r)\} = C_{zz}(r) - [E\{\bar{z}_1 \bar{z}_{1+r}\} - \mu^2]$$

$$= C_{zz}(r) - \frac{\eta}{N-r} \qquad (4.14)$$

where

$$\eta = \lim_{N\to\infty} \sum_{r=-N+1}^{N-1} 1 - \frac{|r|}{N} C_{zz}(r)$$

$$\bar{z}_1 = \frac{1}{N-r} \sum_{i=1}^{N-r} z_i$$

$$\bar{z}_{1+r} = \frac{1}{N-r} \sum_{i=1+r}^{N} z_i \qquad (4.15)$$

This means that $C_{zz}(r)$ is only asyptotically unbiased, and in fact for finite N can be severely biased (Figure 4.31).

The sampling covariances of the estimates $\hat{C}_{zz}(r)$ are approximately (Bartlett, 1955)

$$C\{\hat{C}_{zz}(r), \hat{C}_{zz}(r+\delta)\} \approx \frac{1}{N-r} \sum_{\nu=-(N-r)+1}^{N-r+\delta-1} \{1 - \frac{\gamma(\nu)}{N-r-\delta}\} \phi(\nu) \qquad (4.16)$$

where

$$\gamma(\nu) = \begin{cases} \nu & 0 \leq \nu \\ 0 & \delta \leq \nu \leq 0 \\ -\nu - \delta & -(N-r)+1 \leq \nu \leq -\delta \end{cases} \qquad (4.17)$$

$$\phi(\nu) = C_{zz}(\nu) C_{zz}(\nu+\delta) + C_{zz}(\nu+r+\delta) C_{zz}(\nu-r) + \kappa_{\nu,r}, \qquad (4.18)$$

in which $\kappa_{\nu,r,\delta}$ is the fourth order cumulant (Kendall and Stuart, 1976) of z_i, z_{i+r}, $z_{i+\nu}$, $z_{i+\nu+\delta}$. For Gaussian processes $\kappa_{\nu,r,\delta} = 0$, and in general is ignored.

These equations illustrate the difficulty of estimating autocovariance functions. Unless the actual autocovariance is known, neither the estimator bias nor variance is known exactly. Although this is usually the case with statistical estimators, because $\hat{C}_{zz}(r)$ is strongly biased for short data records, it can not be easily used to approximate either the bias term or the sampling variances.

While the sample covariance function $\hat{C}_{zz}(r)$ is at least a consistent estimator of the true covariance function $C_{zz}(r)$, the same is not true of the sample spectral density function, in that (Parzen, 1961),

$$\lim_{N \to \infty} E\{e^{ir\hat{f}(\omega)}\} = (1 - irf(\omega))^{-1} \qquad (4.19)$$

for every real number r and frequency ω. Thus,

$$\lim_{N \to \infty} \Pr\{\hat{f}(\omega) > \epsilon\} = e^{-\epsilon/f(\omega)} \qquad , \qquad (4.20)$$

which means that asymptotically $\hat{f}(\omega)$ is exponentially distributed with mean and standard deviation $f(\omega)$; $f(\omega)$ does not converge probabilistically as $N \to \infty$.

Because $\hat{C}_{zz}(r)$ is a consistent estimator of $C_{zz}(r)$, however,

$$\lim_{N \to \infty} \int_{-\infty}^{\infty} e^{ir\omega} \hat{f}(\omega) \, d\omega = \int_{-\infty}^{\infty} A(\omega) f(\omega) \, d\omega \qquad , \qquad (4.21)$$

so that for every bounded continuous function A( )

$$\lim_{N \to \infty} \int_{-\infty}^{\infty} A(\omega) \hat{f}(\omega) \, d\omega = \int_{-\infty}^{\infty} A(\omega) f(\omega) \, d\omega \qquad , \qquad (4.22)$$

and this weighted estimate is consistent. Thus, one can form the weighted covariance estimator

$$f(\omega) = \frac{1}{2\pi} \sum_{r=-\infty}^{+\infty} e^{ir\omega} w(r) \hat{C}_{zz}(r) \qquad , \qquad (4.23)$$

where the weighting function w(r) has the properties,

$$0 \le w(r) \le w(0) = 1$$

$$w(-r) = w(+r), \text{ all } r$$

$$w(r) = 0, \ |r| > M \qquad . \qquad (4.24)$$

In practice a number of weighting functions $w(r)$ have been used, each having slightly different sampling properties (Figure 4.32). As discussed by Jenkins (1961), it is important to remove the process mean before calculating $\hat{C}_{zz}(r)$ (and $I_N(\omega)$, below). The function $w(r)$ is called the lag window and M the lag number. The spectral window $W(\omega)$ corresponding to $w(r)$ is found by taking the Fourier transform,

$$W(\omega) = \frac{1}{2\pi} \sum_{r=-\infty}^{+\infty} e^{ir\omega} w(r) \qquad (4.25)$$

and

$$W(-\omega) = W(\omega)$$

$$\int_{-\pi}^{\pi} W(\omega) \, d\omega = 1 \qquad (4.26)$$

Substituting terms leads to

$$\hat{f}(\omega) = \int_{-\pi}^{\pi} W(\omega-\omega_\nu) \, I_N(\omega_\nu) \, d\omega_\nu \qquad (4.27)$$

or

$$\hat{f}(\omega) = \frac{2\pi}{N} \sum_{\nu=-(N-1)/2}^{N/2} W(\omega-\omega_\nu) \, I_N(\omega_\nu) \qquad (4.28)$$

where

$$I_N(\omega) = \frac{1}{2\pi N} \left| \sum_{j=1}^{N} z_j e^{ij\omega} \right|^2 \qquad (4.29)$$

Figure 4.32 -- Common lag windows w(k) and their corresponding spectral windows W(ω). Taken from Jenkins, 1961.

Originator	w(r)	W(ω)
1. Bartlett	1	$(1/\pi)(\sin(m+1/2)\omega/\sin(1/2)\omega)$
2. Bartlett	$1-r/m$	$(1/\pi m)(\sin^2(m/2)\omega/isn^2(1/2)\omega)$
3. Tukey	$1-2a+2a\cos\pi r/m$ (a = 0.23 suggested)	$(1/\pi)\left\{(1-2a)\sin(m+1/2)\omega/\sin 1/2\omega + a\left[\dfrac{\sin(m+1/2)(\omega+\pi/m)}{\sin 1/2(\omega+\pi/m)} + \dfrac{\sin(m+1/2)(\omega-\pi/m)}{\sin 1/2(\omega-\pi/m)}\right]\right\}$
4. Tukey	$1/2(1+\cos r/m)$	$(1/2\pi)\left[\sin(m+1/2)\omega/\sin 1/2\omega + 1/2\left\{\dfrac{\sin(m+1/2)(\omega+\pi/m)}{\sin 1/2(\omega+\pi/m)} + \dfrac{\sin(m+1/2)(\omega-\pi/m)}{\sin 1/2(\omega-\pi/m)}\right\}\right]$
5. Parzen	$1-r^2/m^2$	$(1/\pi m^2)\left\{\dfrac{1/2\sin(m+1/2)}{\sin^3(1/2)\omega} - \dfrac{(m+1/2)\cos(m+1/2)\omega\cos 1/2\omega}{\sin^2(1/2)\omega} - \dfrac{(m+1/2)\sin(m+1/2)\omega}{\sin(1/2)\omega}\right\}$
6. Parzen	$1-6r^2/m^2(1-r/m)$	$(3/4\pi m^3)(\sin(m/4)\omega/\sin(\omega/4))^4$
7. Daniell	$\sin(rh)/rh$	$(1/2h)(\omega_o-h < \omega < \omega_o+h)$

is the so-called periodogram of the data z_j, $j=1, \ldots, N$. Note, $I_N(\ )$ can also be found from

$$I_N(\omega) = \frac{1}{2\pi N} \left[\{ \sum_{j=1}^{N} z_j \cos \omega j \}^2 + \{ \sum_{j=1}^{N} z_j \sin \omega j \}^2 \right] \quad (4.30)$$

This estimator (4.28) is called the smoothed periodogram estimator.

Since the latter two estimators for $f(\omega)$ are mathematically equivalent, they share identical sampling properties. In particular,

$$E\{\hat{f}(\omega)\} \simeq \frac{2\pi}{N} \sum_{j=-M}^{+M} W(\omega_j) \, f(\omega_j) \quad , \quad (4.31)$$

where 2M is the width of the window and the variance is, without loss of generality, taken to be $\sigma^2=1$. If $f(\omega)$ does not vary greatly within $(j-M) \leq \omega \leq (j+M)$ Figure 4.3.3,

$$V\{\hat{f}(\omega)\} \simeq \frac{4\pi^2}{N^2} \sum_{j=-M}^{+M} W^2(\omega_j) \, f^2(\omega_j) \quad . \quad (4.32)$$

The estimator $f(\omega)$ can be shown to be approximately χ^2 distributed with the equivalent degrees of freedom (Koopman, 1974)

$$EDF = \frac{2 \, E^2\{\hat{f}(\omega)\}}{V\{f(\omega)\}} \quad (4.33)$$

which varies with the window chosen (Figure 4.34). This allows confidence limits on $\hat{f}(\omega)$ to be constructed and hypotheses on goodness of fit to be tested.

	$V\{\hat{f}(\omega)\}/f(\omega)$	EDF
1	$2m/n$	n/m
2	$2m/3n$	$3n/m$
3	$2m(1-4a+6a^2)/n$	$n/m(1-4a+6a^2)$
4	$3m/4n$	$8n/3m$
5	$16m/15n$	$15n/8m$
6	$0.542m/n$	$3.7n/m$
7	π/nh	$2nh/\pi$

Figure 4.33 -- Variance and equivalent degrees of freedom for various common windows (taken from Jenkins, 1961).
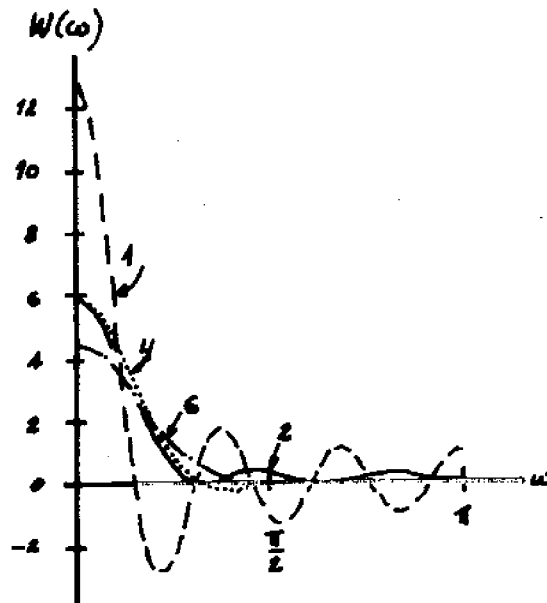
Figure 4.34 -- Various common windows corresponding to those of figure 4.33 (taken from Jenkins, 1961).

where A is the region within the sediment most influencing the behavior being predicted; $g\{\delta y_1\}$, $g\{\delta y_2\}$ are the influences of changes in the sediment properties at locations $\underline{x}_1$ and $\underline{x}_2$ or the prediction $g\{\cdot\}$; and $C[\cdot]$ is covariance.

This optimization confirms intuition. More weight is given to observations when they are (i) independent of other observations, (ii) in locations to which the prediction is sensitive, and (iii) correlated with nearby locations to which the prediction is also sensitive.

Measurement error

Sediment properties are difficult to measure without introducing bias, both because the instruments or procedures of measurement disturb the sediment structure and because many measurements are made through correlations with index properties. These correlations are partly theoretical, partly empirical, and change from one sediment profile to another. Much effort has been addressed to these bias errors throughout the history of modern soil mechanics (e.g., Ladd, 1976).

From a statistical point of view measurement errors are divided into a systematic or bais component and a random component (Figure 4.35). If the magnitude and direction of the systematic error is known, measurements can be directly calibrated. Thus, the only uncertainty remaining is the random one. The model for observation y of source property y_o becomes

$$y = y_o + b + u \tag{4.37}$$

where b is the (known) bias and u is a zero-mean random variable with
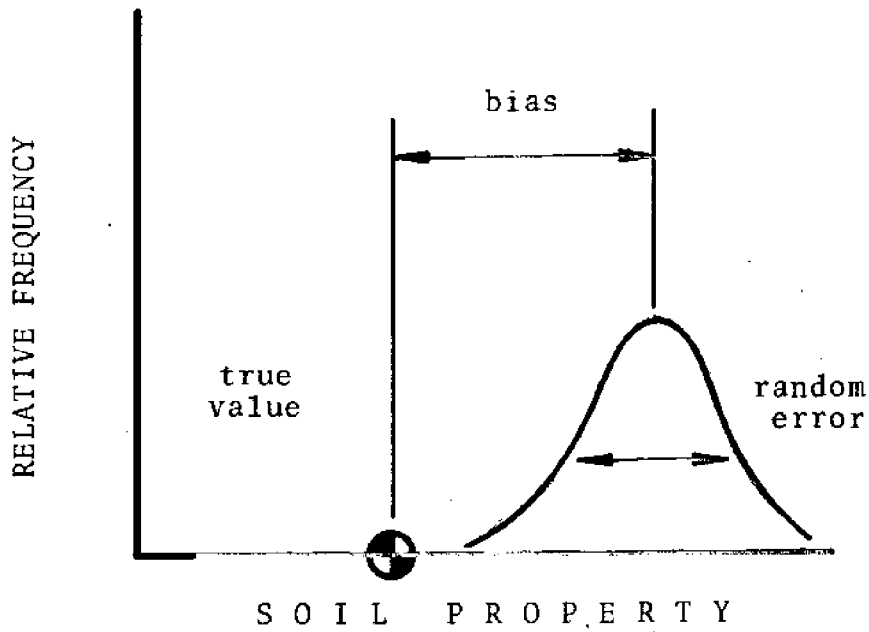
Figure 4.35
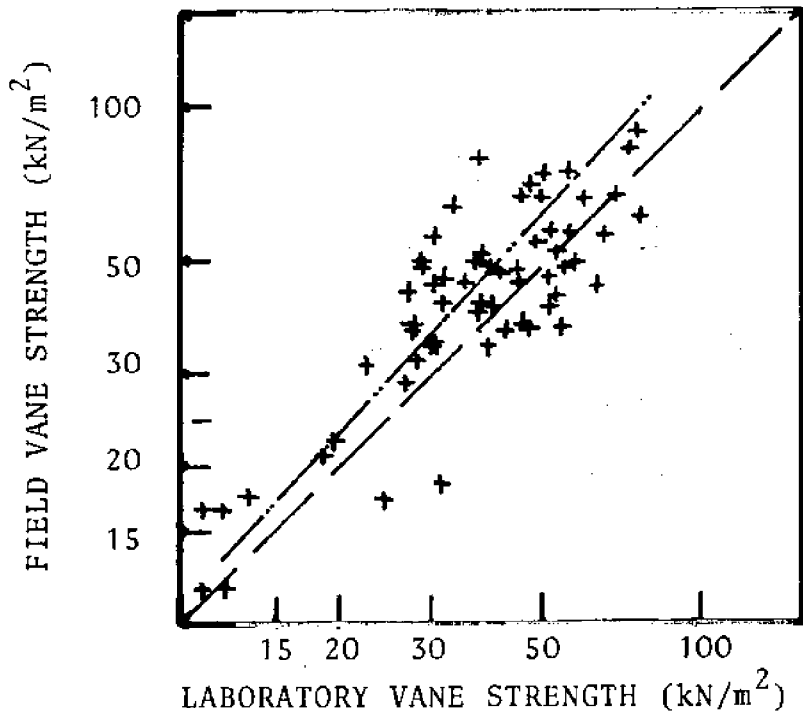
Figure 4.36 -- Systematic bias in measurement
of soil properties. Above, schematic description
of bias and random measurement error; below,
data from Lumb (1971) showing systematic differ-
ence between strength measured with field
and laboratory vanes.

variance σ_u^2 . Table 4.5 shows various biases and random errors reported in the literature for common measurements of sediment properties.

The situation is seldom so simple, of course. Usually b is not known with certainty, but only up to some probability distribution with mean $\bar{b}$ and variance σ_b^2. Then, the error in the measurement has variance $(\sigma_u^2 + \sigma_b^2)$. From the point of view of statistical modeling this characterization adequately reflects the measurement uncertainty, even if one is uncomfortable about grouping uncertainty over an unknown bias with "random" fluctuation. In fact, though, any such separation of measurement error is artificial since it is conditioned on the level of detail of the model for measurement error and on the extensiveness of the data base from which the calibrations are taken. Restricted data bases tend to show more bias and less random error, and the reverse for broad data bases. Reported variances like those of Table 4.5 already confound variation in bias across different sediment formations with random variation. A consideration that must always be faced in grouping σ_b^2 with σ_u^2 is correlation in the realized errors across the observations $\underline{z}$. If b is systematic, as assumed, then its realization will be the same for all observations within the same sediment mass and the model

$$y = y_o + \bar{b} + u_b + u \quad , \quad (4.38)$$

where $u_b \sim N(0, \sigma_b^2)$, will systematically over or under estimate all observations.

The introduction of random measurement error increases the variance of estimates of mean sediment properties and of the autocovariance function. For point estimates of the mean with widely spaced observations,

Table 4.5 -- Reported Coefficients of Variation for Various Soil Properties

Material	Property	COV	Source
Clay	liquid limit	5.9	Lumb (1)
	plastic limit	4 ±	
	clay content	11.4	
	specific gravity	0.5±	
	dry density	26.4	
Clay Shale	cohesion (direct shear, DS)	94.8	
	friction coef ficient (t), DS	45.6	
Cohesive Till	c -- DS	103.3	
	t -- DS	17.7	
"undisturbed"	c -- triaxial D	13.5	
	t -- triaxial D	1.6	
	c -- CU	19.9	
	t -- triaxial CU	9.8	
	c -- triaxial UU	18.8	
	t -- triaxial UU	22.3	
compacted	c -- D	24.0	
	t -- D	2.1	
	c -- CD	26.9	
	t -- CD	6.8	
	c -- UU	25.5	
	t -- UU	5.4	
Various Tills	UU	14.8	Morse (1)
		14.7	
		31.0	
		19.8	
		29.0	
Silt	e_o	21.6	
	n	89.4	
Gravelly Sand	e_o	29	
	n	16	
Coarse Sand	n	9.8	
	e_o	16	
Medium Sand	n	10	
	e_o	17.5	
Fine Sand	e_o	13.3	

Table 4.5 -- Continued

Material	Property	COV	Source
Marine Clay	c	18.4	Singh (1)
London Clay	c	16.2	
Sandy Clay	$\log(C_c)$	34.2	
Silty Sand	t	13.8	
Clay Silt	t	14.8	
	c	31.6	
	c	25.9	
Ottawa Sand (loose)	phi	14	
Ottawa Sand (dense)	phi	12.5	
Clayey Silt	c	51	
(unsoaked)	phi	22	
	s_u	19	
Clayey Silt	c	55	
(soaked)	phi	29	
	S_u	20	
Clayey Silt	c	64	
CH	c -- triaxial UU	15	
	phi -- UU	56	
CL	c -- UU	22	
	phi -- UU	19	
ML	c -- UU	71	
	phi -- UU	12	
CH	c -- DS	63	
	phi -- DS	10.4	
CL	c -- DS	3	
ML	c -- DS	2.5	
Road Subgrade	soil suction	24.2	Miura and Fujita (3)
	soil suction	23.2	
Average over	LL	6.37	Minty, Smith and
16 cohesive soils	PL	9.55	Pratt (3)
Road base coarse	CBR	17.4	Ingles (3)
	density	3.9	
	PI	75.0	
	S_u	36.8	
Plastic Clay	compression ratio	17 to 38	Vanmarke and
	t		Fuleihan (2)
Fine Sands	t	5 to 13	Schultze (2)
Gravel-Sands	t	5	
Coarse Sand	t	8 to 14	

1. First ICASP, Hong Kong.
2. Second ICASP, Aachen.
3. Third ICASP, Sydney.

Equation 4.10 becomes

$$V[\bar{x}] = \frac{\sigma^2 + \sigma_m^2}{n} \tag{4.39}$$

where σ_m^2 is the measurement error variance. The effect on estimates of the autocovariance is to reduce correlations among observations and to mask (hence increase the sampling variances of $R(r)$). Nevertheless, procedures for estimating this error are available for regularly spaced observations. Recent work by Veneziano (19xx) extends available techniques to include non-uniformly spaced observations.

Figure 4.37
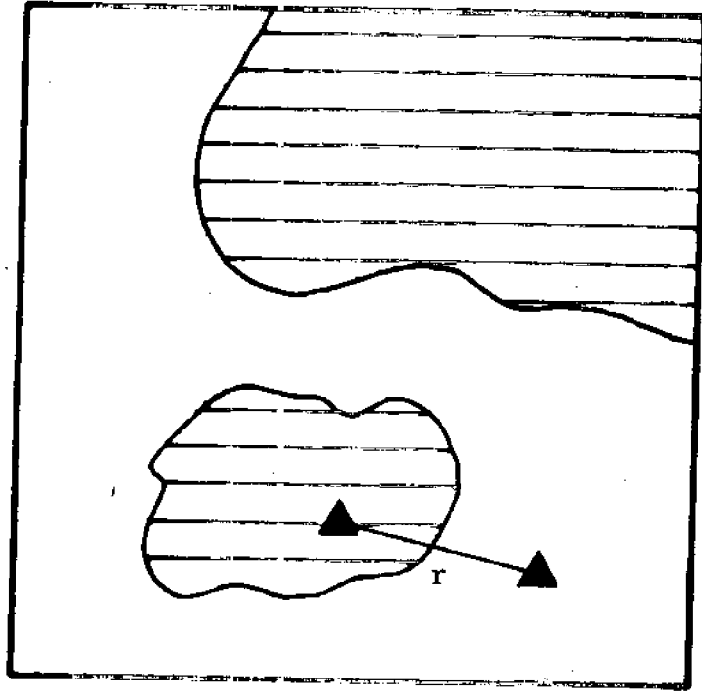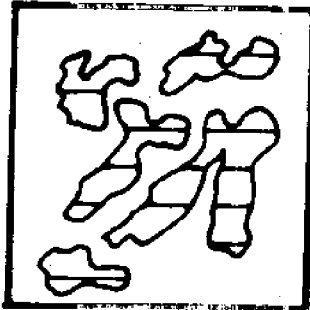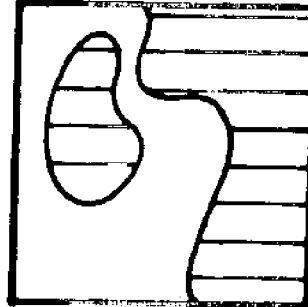
4.3.4 Mapping the Distribution of Bottom Sediments

One of the most difficult problems in site investigation to quantify is the uncertainty in qualitative distributions of sediments types, for example in mapping or in reconstructing profiles. As illustrated by Figure 4.17, this is a highly inductive task, based on familiarity with geological processes and history, and previous experience. Except by returning to previous cases and comparing predicted with actual distributions, errors in the intuitive contouring of sediment bodies are not immediately analyzable. Unfortunately, since even with past projects one never knows the true distribution of sediments, this is not possible.

On the other hand, errors in contouring sediment masses can be estimated for *fixed* classification procedures, if certain assumptions of randomness are made on the geological process of sedimentation. For example, if the sediment mass is contoured by nearest neighbor classification (i.e., any unobserved element in the mass is assigned to the same class as the nearest observation) and if the sediment mass is considered a discrete random field, then estimates of percent of area misclassified and the like can be made.

Following Switzer (1967) the spatial distribution of sediment-type-- i.e., zoning--can be considered a discrete correlated random field. In the two class case, or the so-called two-color map, a zero-one variable is associated with each point in space; zero if the sediment at the point is, say, clay and one if it is, say, gravelly sand. Then this random field is used to predict the class at unobserved locations, or to select optimal observation patterns.
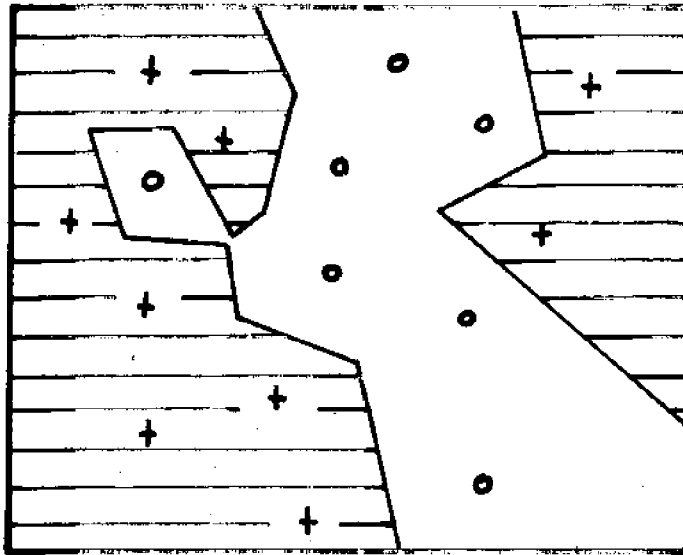
Figure 4.38 -- Typical nearest neighbor map for two-class problem.
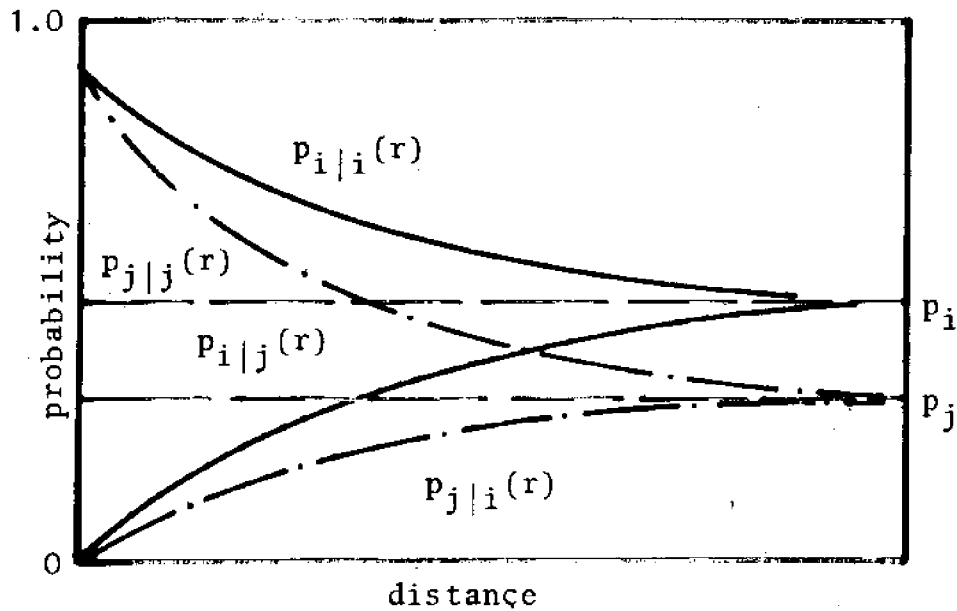
Figure 4.39 -- Decay of probability of class similarities or dissimilarities as a function of distance.

Probabilistically, if the classification at some point (x_o, y_o) in the horizontal plane is material i, then the probability of material i at some point (x_1, y_1) must approach 1.0 if the points are spatially close, and decay to the average fraction of material i, p_i, as the separation increases. A simple model is of the type

$$P_{i,i}(\underline{r}) = (1-p_i)e^{-\gamma r} + p_i \qquad (4.40)$$

where $P_{i,i}(\underline{r})$ is the probability of material i at some (vector) separation distance $\underline{r}$ given that the original location is of material i. If $P_{i,i}(\underline{r})$ depends only on $\underline{r}$ and not on (x_o, y_o), (x_1, y_1) then the field is said to be stationary. If $P_{i,i}(\underline{r})$ depends only on the scaler separation r, and not the vector $\underline{r}$, the field is said to be isotropic.

$P_{i,i}(r)$ is uniquely related to the autocovariance through the relation $R(r) = p_i P_{i,i}(r) - p_i^2$. The decay in probability reflected in $P_{i,i}(r)$ is an indication of the distance to which classifications can be extrapolated away from an observed point. The smaller the average zone size and the less smooth the boundaries among zones the more quickly $P_{i,i}(r)$ decays (Figure 4.37).

Now consider that observations of class at some finite number of points n are made, and that a sediment map is constructed using a nearest neighbor criterion (Figure 4.38). If an observation is of class i, then the probability of misclassifying a point at nearest neighbor distance r is $P_{j,i}(r) = \{1-P_{i,i}(r)\}$. Similarly, if an observation is of class j, then the probability of misclassifying at point at nearest neighbor distance r is $P_{i,j}(r) = \{1-P_{j,j}(r)\}$. For the two color case these functions are shown in Figure 4.39. If f(r) is the density function of nearest neighbor
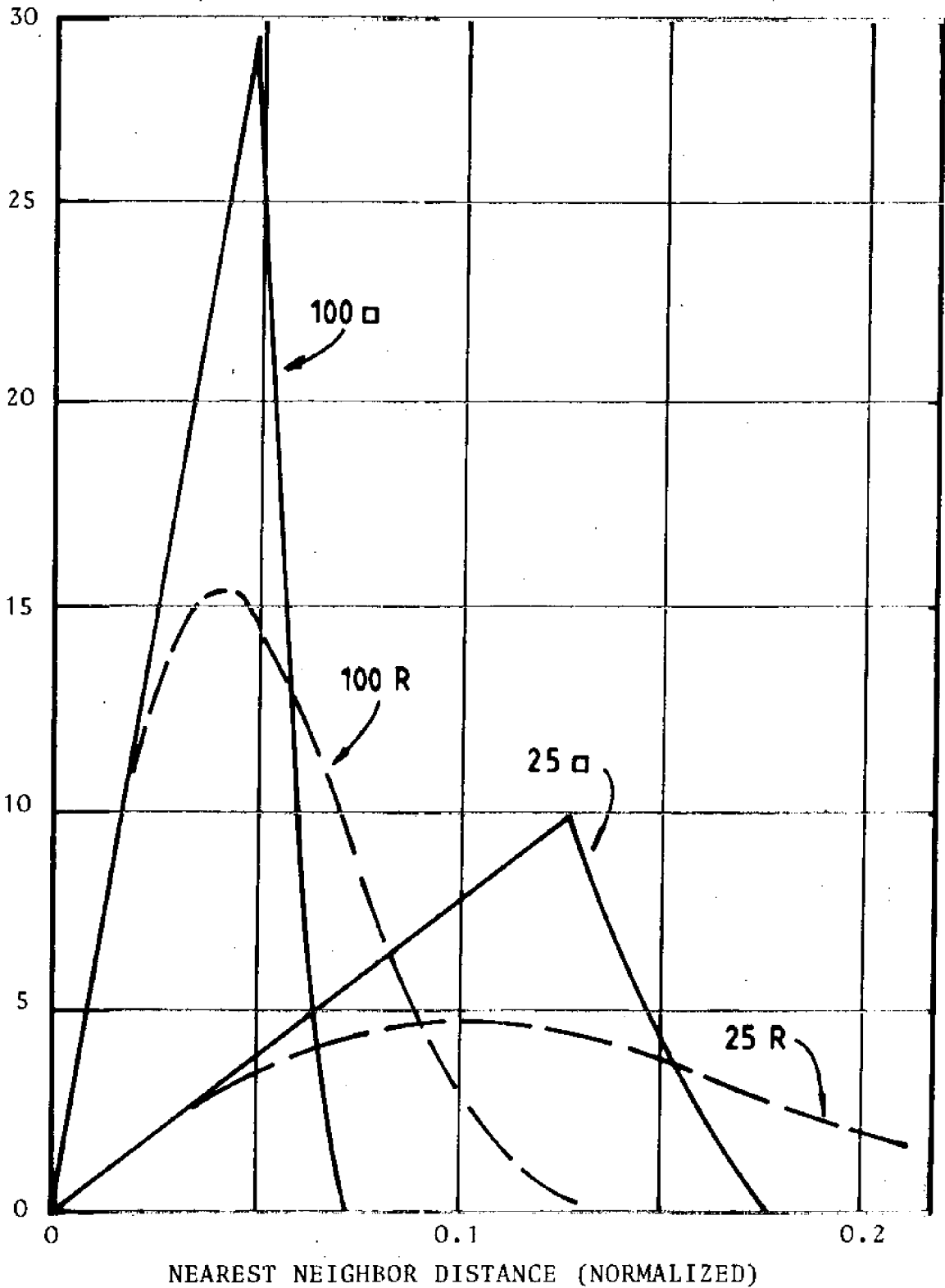
Figure 4.40 -- Nearest neighbor distances for square and random point observation grids as a function of sampling density (numbers per unit area).

spacings in the plane (or space) then the fraction of the constructed map misclassified is

$$J = p_i \int f(r) p_{j,i}(r) dr + p_j \int f(r) P_{i,j}(r) dr \quad . \quad (4.41)$$

where $p_i + p_j = 1.0$.

For random observation points Poisson distributed in the plane the neareast neighbor spacing is easily shown to be

$$f(r) = 2\Pi\lambda r \, \exp(-\Pi\lambda r^2) , \quad\quad\quad (4.42)$$

where λ is the spatial density of points (Figure 4.40). Similarly for square and hexagonally grided observations, $f(r)$ can be shown to be as in Figure 4.40. Therefore normalized charts can be developed to predict percent misclassified (Figures 4.41, 4.42). For other given observation patterns (e.g., Figure 4.43) the percent misclassified can be estimated once $f(r)$ is determined. However, such patterns do not allow normalized charts since the criterion of their genesis is not specified.

To test the classification theory, eight soil maps from extensively mapped regions were selected and used as base cases (e.g., Figure 4.43). The two-color distributions of sediment type as mapped were considered to be the true conditions, then observation points were randomly generated and nearest neighbor maps constructed from the results. Observation points were generated in Poisson fields, and in square and hexagonal grids. In total

Figure 4.41/2 — Theoretical error rates for square, triangular, and random point grids.
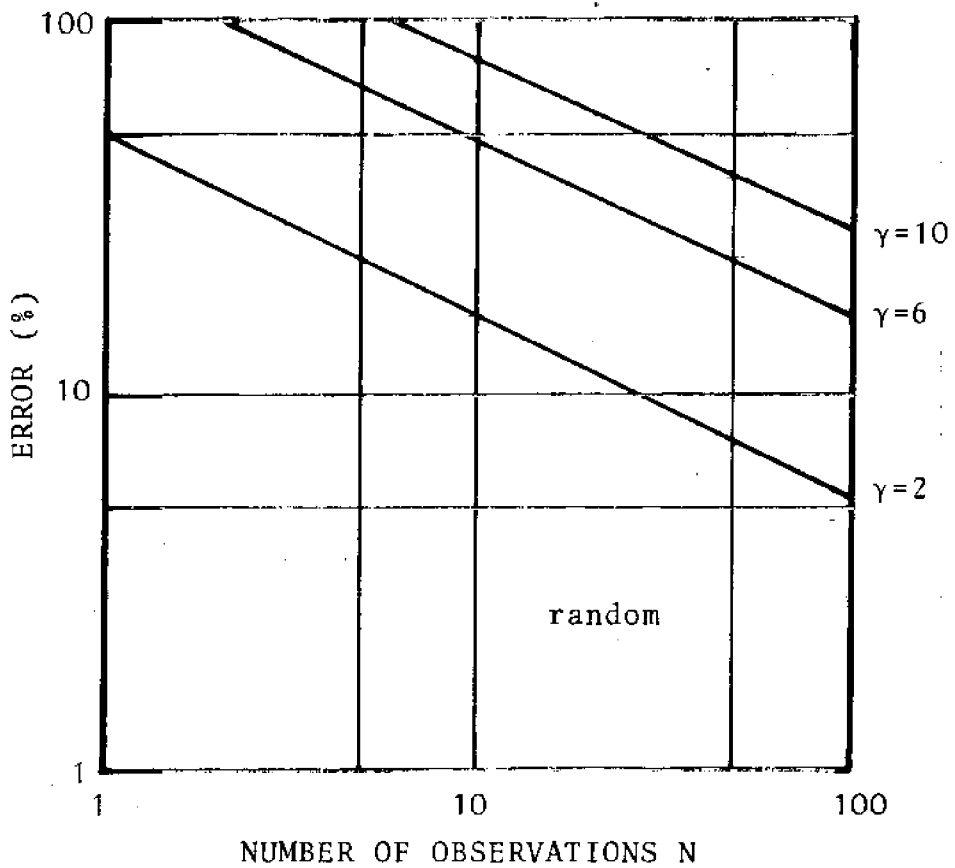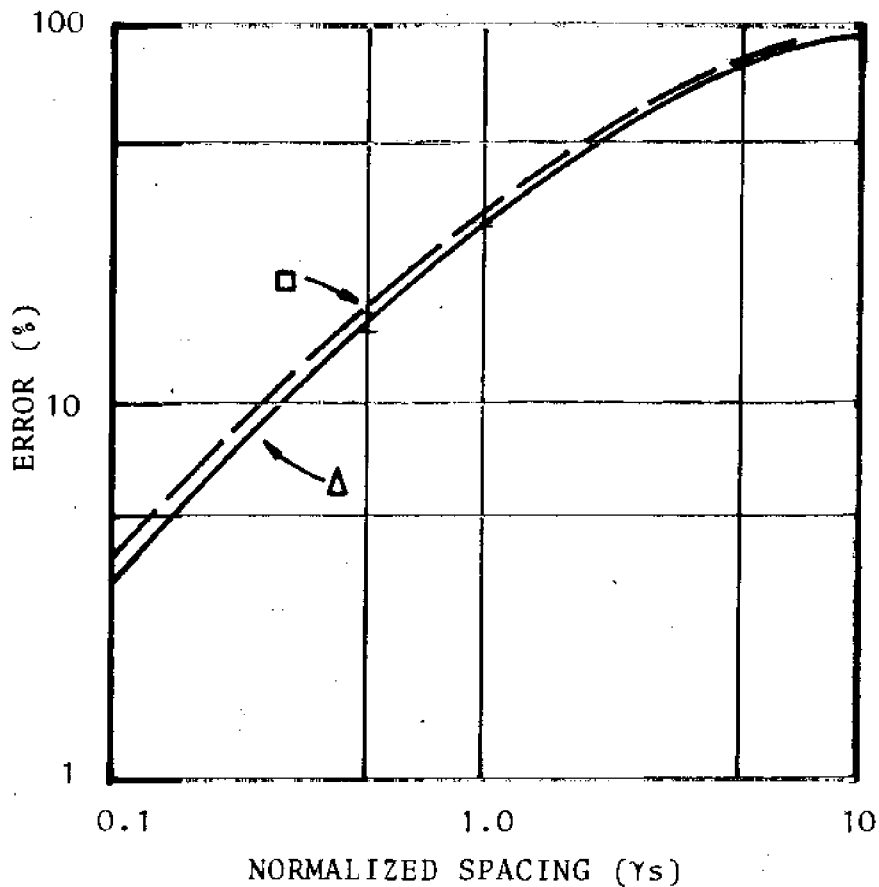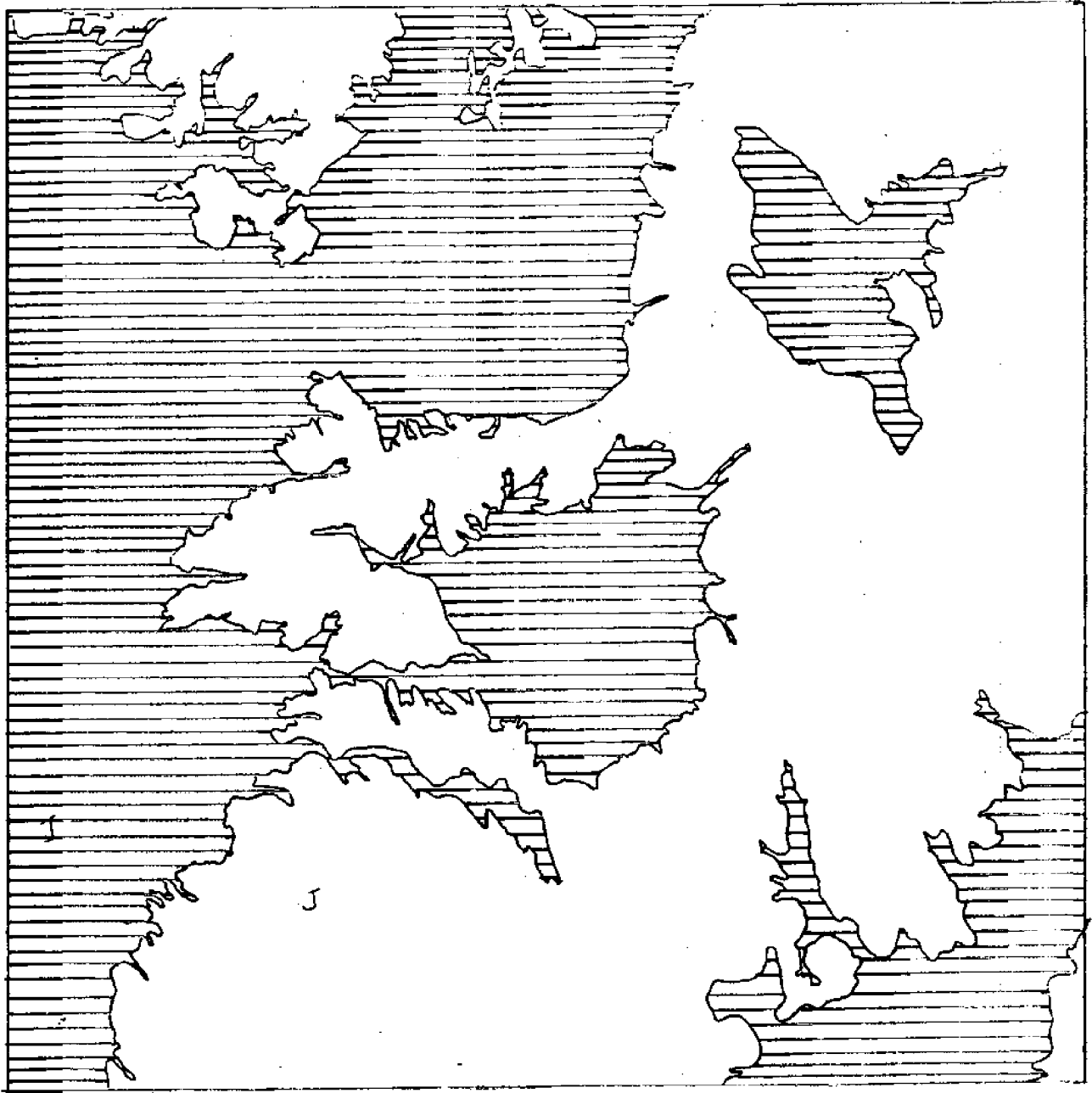
Figure 4.43 -- Typical base map for study of error rates in bottom sediment maps.

120 test maps were constructed of the eight base cases. For each test map
the percent misclassified was predicted from Figures 4.41, 4.42 and the
actual misclassified area planimetered. Results are shown in Figure
4.41. In general, the predictions of the theory seem accurate, and lead
to surprisingly large misclassified areas. Misclassified areas from 30 to
50 percent of the total map are not uncommon.

Several limitations of the present approach to mapping errors and of
the experiments intended to verify the theory must be mentioned. First, the
theory assumes no structural influence on the distribution of sediment types,
and no geological information to aid the mapping. The distribution of
sediments is assumed either to be or to behave like a random process. The
base case maps were selected to display isotropy of sediment distribution,
and therefore might be expected to be of areas with little structural
control. Nevertheless, these base cases do display apparently random dis-
tributions.

Second, the results of Figures 4.41, 4.42 give no indication of the
spatial distribution of misclassification, and the one measure "percent
misclassified" is difficult to relate to risk analyses or design decisions.
In fact, the misclassified areas occur as belts surrounding homogeneous
zones, so that the probability of misclassification near the middle of zones
can be very low. Although not contained in the present work, the probability
of misclassification at a point can be estimated by considering the classifica-
tions of surrounding observations (Figure 4.45). By Bayes' Theorem,

$$P\{i\} \propto p_i \prod_{a=1}^{n_i} P_{i,i}(r_a) \prod_{b=1}^{n_j} P_{j,i}(r_b) \quad , \tag{4.43}$$

Figure 4.44 -- Comparison of predicted and observed error rates for nearest neighbor mapping using square (□) and random (•) point grids.
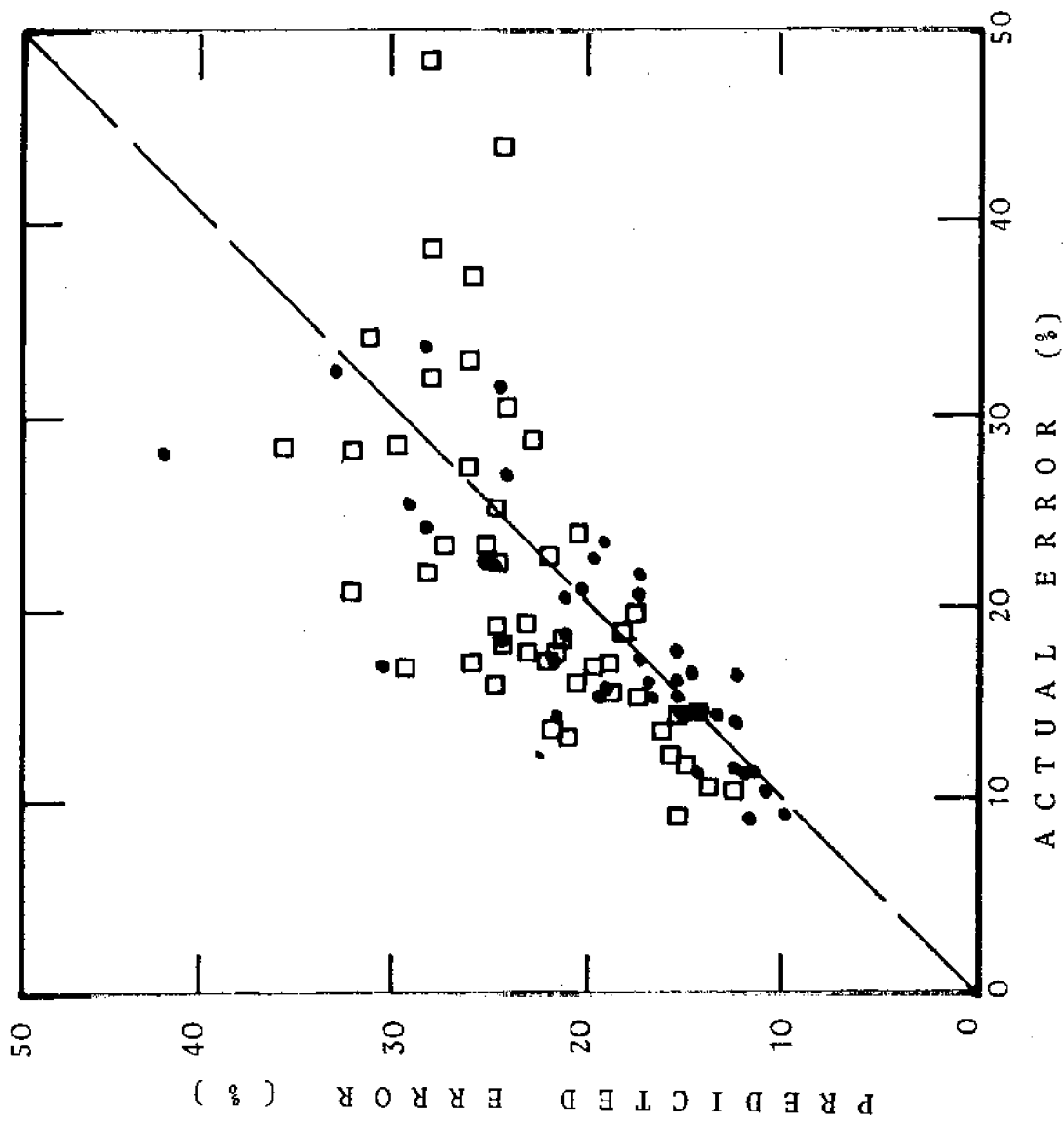
where $P\{i\}$ is the probability of the point in question being class i; n_i is the number of neighboring points of class i, and r_a, $a=1,\ldots,n_i$ their respective distances; and similarly for n_j and r_b. This procedure can be used to develop an entirely probabilistic map, if so desired (e.g., Baecher, 1972).

In the case of the base maps the decay parameter γ is precisely known because the true map is known. In normal problems of inference this is not the case. All that is known about the site is the observations. Therefore, γ must be estimated from them. In principle this is easily done, but given the form of Equation 4.40 applications are more difficult.

For a set of observations the likelihood can be expressed by considering all pairs of points,

$$(4.44)$$

$$L(\text{data}|\gamma,p_i) = \prod_{a=1}^{n_{ii}} P_{i,i}(r_a) \prod_{a=1}^{n_{ij}} P_{i,j}(r_a) \prod_{a=1}^{n_{ji}} P_{j,i}(r_a) \prod_{a=1}^{n_{jj}} P_{j,i}(r_a) \ ,$$

where n_{ii} is the number of pairs of observations comprising two i classes, and respectively for n_{ij}, n_{ji}, and n_{jj}. This can be maximized with respect to γ and p_i to obtain the maximum likelihood estimates, or can be used with Bayes' Theorem to infer a posterior distribution on (γ,p_i). However, the form of 4.44 leads to a high order polynomial and thus the solution must be by enumeration. Because p_i can be estimated from the fraction of observations of class i, the enumeration can be reduced to one dimension, but is still inconvenient.

A less satisfying procedure is to divide the distances between paired observations into intervals and for each interval evaluate the relative frequencies of ii to ji pairs, and jj to ij pairs. Since $P_{i,i}(r) + P_{j,i}(r) = 1.0$,
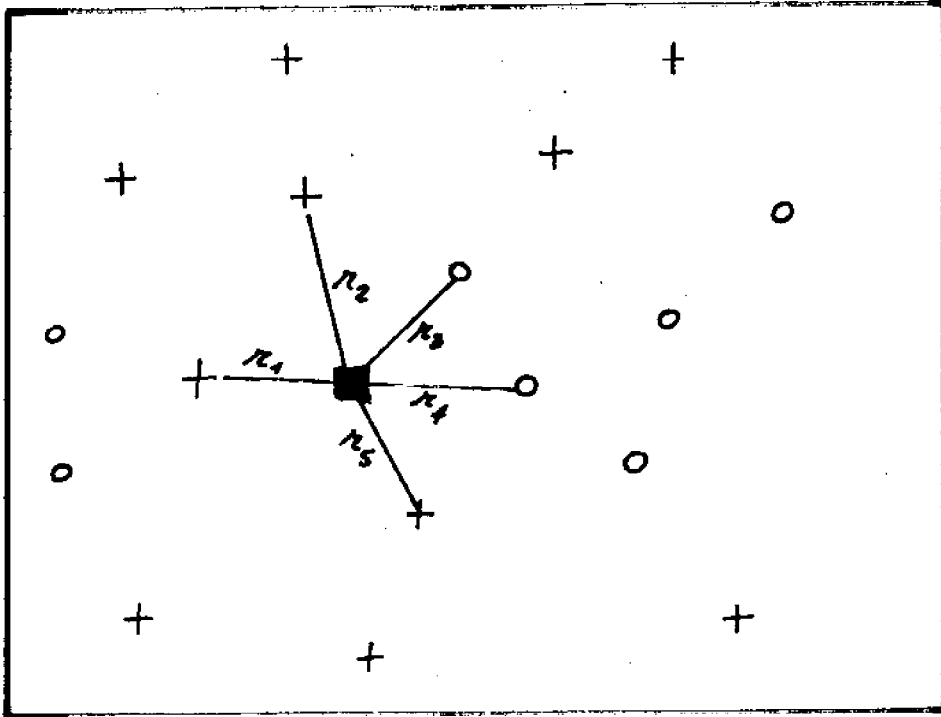
Figure 4.45 -- Optimal mapping using Bayesian estimate of classification at unobserved locations. Estimate based on joint likelihood of observations at distances r_1, r_2, ..., r_n given classification of unobserved location.

and similarly for jj and ij pairs, there frequencies can be plotted and curves fit to them to estimate γ and p_i. The procedure works, but the sampling variation of the estimators is difficult to untangle. Other procedures are discussed in Nucci and Baecher (1979).

The conclusion to be drawn from these analysis is that errors in zonation maps can easily be in the range of 30%, and possibly more. The influence of such errors on risk estimates is difficult to judge, except in quite specific problems. For example, in estimating unbalanced moments on the skirts of a North Sea structure Tang (1979) has brought up the problem of uncertain zonal boundaries. For such a problem the current analysis has direct application.

4.3.5 Finding Anomalous Details

This section is a review of current techniques for analyzing the search for adverse geological details, for optimizing allocations of effort, and for drawing inferences from the results of search programs. No attempt is made to redevelop mathematical foundations presented elsewhere, rather, emphasis is placed on assumptions and applicability.

The problem of search in geological exploration is to locate or detect a geological anomaly of particular, although perhaps probabilistic, description in an efficient way, subject to some initial probability distribution on its location and possibly in the presence of "noise" or uncertainty in interpreting field data. The problem of search strategy is how to allocate effort such that the probability of finding the anomolous conditions is minimized at a cost commensurate with the consequence of not finding it. Typical targets of geotechnical search include solution cavities, clay lenses, buried stream channels (e.g., high permeability zones beneath dams), abandoned underground workings, geothermal resources, mineral aggregate sources, and faults. Terzaghi's (1929) classic definition of minor geological details as, "features that can be predicted neither from the results of careful investigation... nor by means of a reasonable amount of test borings " is expanded here to include features of somewhat larger dimension and probability of detection.

Investigation for geological details or anomalous conditions must start with a suspicion that such conditions exist, what they might be like, and which locations (if any) are more likely than others. These are judgemental evaluations based on experience and knowledge of geology. Search theory is a tool by which these initial suspicions can be logically combined with field observations to draw deductive conclusions.

The basic model for search in geological and geotechnical exploration idealizes anomalous details as randomly located point targets with an associated size and shape distribution. For example, clay lenses might be modeled as ellipses in the horizontal plane, the centers of which form a Poisson or Negative Binomial point process, and the size of which is distributed, say, logNormally. Similar distribution assumptions would be required on obliquity and orientation. While insulting the geologist by simplicity, such models seem to adequately approximate the spatial character of many geological processes. Confirmation of this model has been provided by, among others, Kaufman (1963) for oil pools within individual plays, and by DeGeoffroy and Wignall (1970) for metallic mineral deposits. Nevertheless, the model is not a good representation for all geological entities, which must be kept strictly in mind. Within the past ten years substantial data have been collected on statistical properties of geological processes, particularly spatial characteristics. Much of this literature is summarized by Agterberg (1973). Many, perhaps most processes and formations in geology seem to follow well behaved distributions which are fairly consistent across different geological environments.

Uniform search

Let $f(x,y)$ be the density function (pdf) of target center location in the horizontal plane. If no information exists on location, $f(x,y)$ will be taken as uniform, and the optimal spatial allocation of effort will also usually be uniform. Uniform search will mean that, a priori, each infinitesimal element of the site has the same probability of containing an observation. In geotechnical exploration uniform search means grids.

Point grids

Random allocation is a baseline for the performance of grid patterns

of search. Consider a search strategy that randomly allocates observations

independently and with equal probability to each infinitesmal element

of the site. For a target area, A_t assumed known, and a site area A_s, the

probability of hitting the target with any one observation is A_t/A_s. Thus,

the probability of hitting the target with one or more of n observations is

$$\Pr(\text{find}/n) = 1 - (1-A_t/A_s)^n \doteq 1 - \exp\{-n(A_t/A_s)\} \qquad (4.45)$$

when $A_t/A_s \leq 0.2$ (Figure 4.45).

Points grids are search strategies that allocate observations at

regularly spaced points according to some prespecified geometric pattern.

Typical of such strategies are evenly-spaced boring arrays. Such strategies

are so common in geotechnical engineering that over the years empirical

rules have been developed for selecting appropriate spacings (e.g.,

Hvorslev, 1949). Grid patterns assure coverage of a site, are more effi-

cient than random strategies, and offer computational advantages when

analytically treating other facets of exploration such as mapping.

The probability of intersecting a target with a point grid depends

on the relation between two sets of factors: the size, shape, and

orientation of the target; and the spacing, geometry, and orientation of

the grid. Because grids are periodic, their performance characteristics

can be analyzed with reference to an individual cell (for uniform $f(x,y)$).

The conditional probability of finding an existing target is determined

by the fraction of the cell area in which, if the target center lies, at

least one observation will hit the target. For the case of random target size, orientation, or shape (within a family of shapes -- e.g., ellipses), probabilities of a find are obtained by integrating over the joint density function of these variables. Representative results for square and circular targets on square grids are shown in Figure 4.46 compared with random allocation. Results for elliptical and rectangular targets of various obliquities (i.e., ratios of dimensions) are shown in Figure 4.47 and 4.48. Elliptical targets with triangular (so-called hexagonal) grids are given in Figure 4.49.

Several conclusions are apparent from these figures. First, for low probabilities of a find, target and grid shape are unimportant. This has been shown by Santaló (1976) for the more general case of any bounded (not necessarily convex) figure. If the number of observations per unit cell is m, the expected number of hits, k, is

$$E(k) = m(A_t/A_c) \qquad (4.46)$$

where A_c is the area of the unit cell. For $Pr(k \geq 2) = 0$, the expected number of hits is the probability of a find. The target size for which the condition of only one possible hit holds depends both on the target and grid shapes. The second conclusion is that for regularly shaped targets, precise target shape at a given obliquity has little affect on probability of a find. The last conclusion is that for $\sqrt{A_t}/s$ below about 0.7, target obliquity has little or no effect on the probability of a find.

Extensive tables of grid search probabilities have been computed by Singer and Wickman (1969) and Savinskii (1965). There are inconsistencies

Figure 4.47

Figure 4.49

Figure 4.46

Figure 4.48
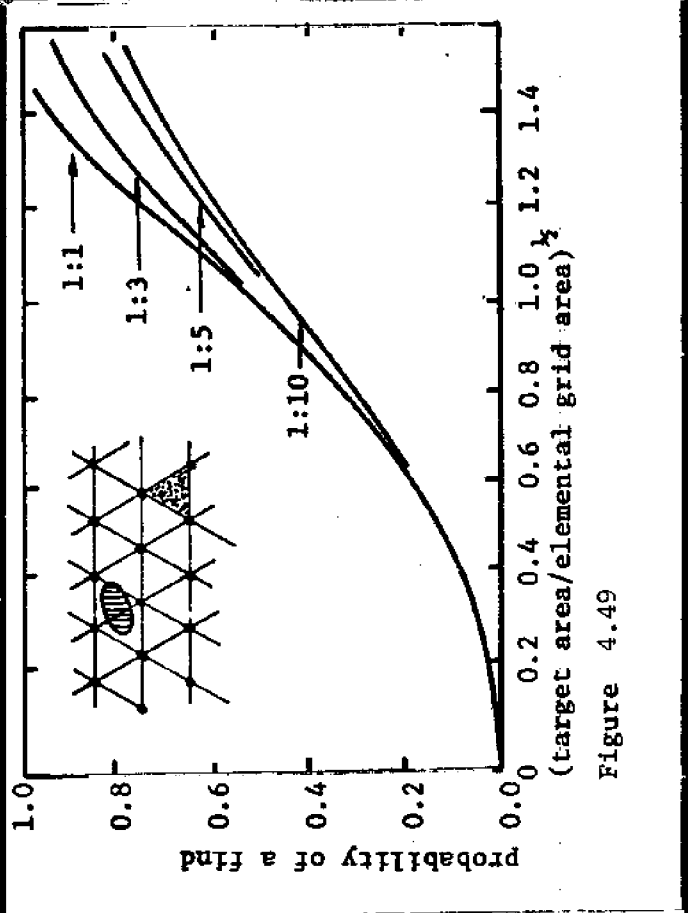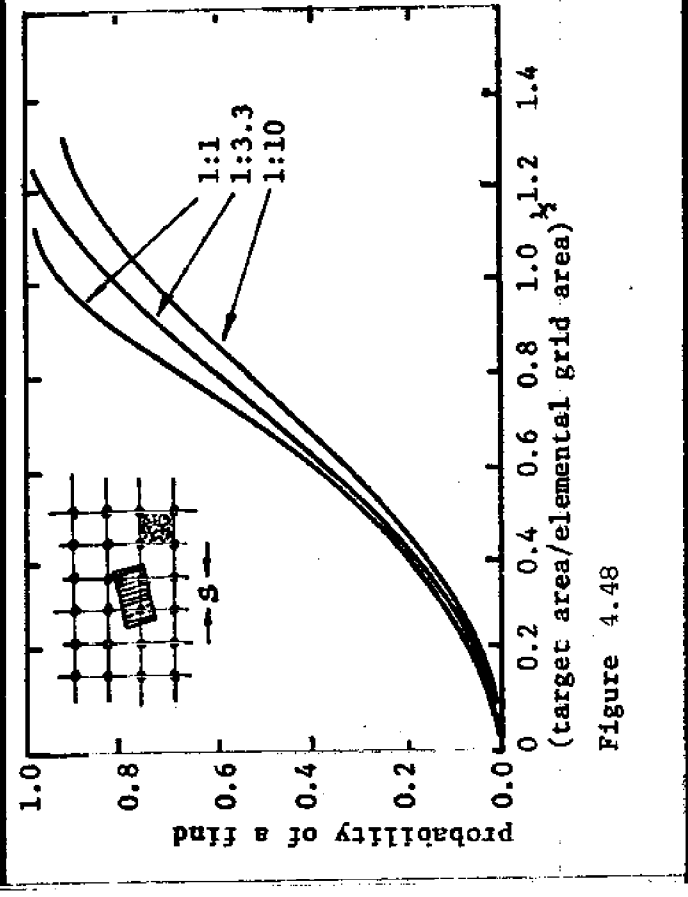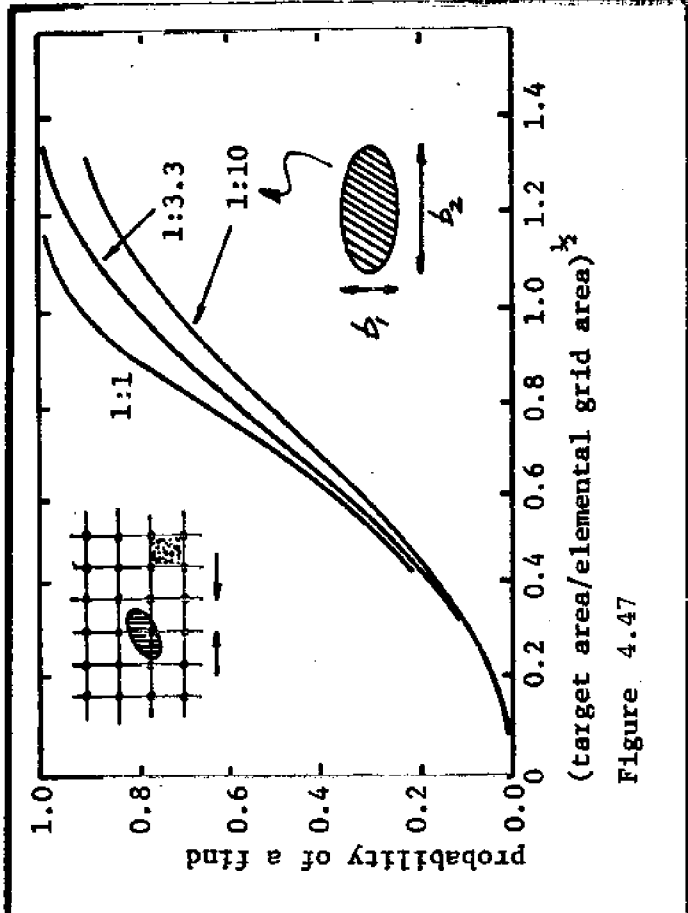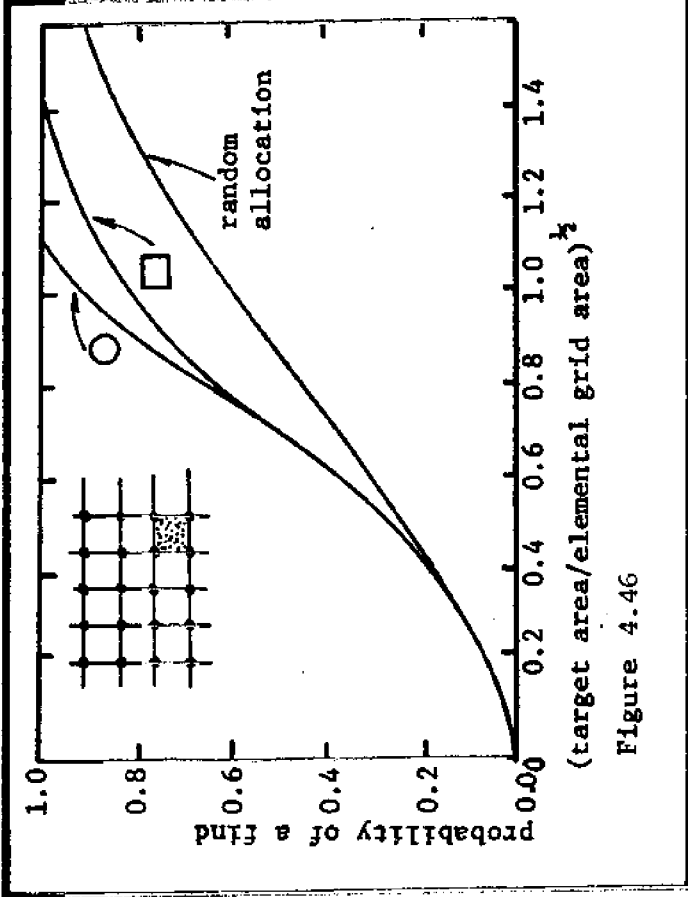
between these two tabulations. The former, apparently checked in light of these inconsistencies, would seem more reliable. Two issues of strategy may be concluded from these tabulations: The orientation of the long axis of a rectangular grid maximizing the probability of a find is parallel to the preferred orientation of the long axis of the target; and the grid obliquity maximizing the probability of a find is approximately equal to the target obliquity.

Line grids

Geophysical exploration tools are commonly allocated in line grids. Making the simplifying assumption that a find (or tentative find) is recorded if one of the lines transects the target, charts like those for point grids can be constructed using the same approach (Figures 4.50 and 4.51).

Although the assumption of only direct intersection resulting in a find is simplistic, in many applications the approximation may be sufficiently accurate. If this approximation is not sufficiently accurate, a lateral detection function (LDF) may be introduced, relating probability of a find to the minimum lateral distance between target and grid line. As this distance increases, the probability of detecting a target diminishes. Common LDF's are shown in Figure 4.52 (see Morse, 1974).

Introduction of a LDF leads to detection probabilities other than zero and one for certain fractions of the unit cell. The probability of a find is obtained by taking the expectation over these areas. Typical results, here for an exponential LDF with fixed range $b/2$, are shown in Figure 4.53. The rate of decay of the LDF, perhaps more than its exact form, can significantly influence the probability of a find in certain circumstances. Information of the LDF for a particular exploration tool and

Figure 4.51: Line Search

Figure 4.53

lateral detection function ∝ exp(-qd)

$q = \lambda s$

Figure 4.50: Line Search

Figure 4.52: Lateral detection functions
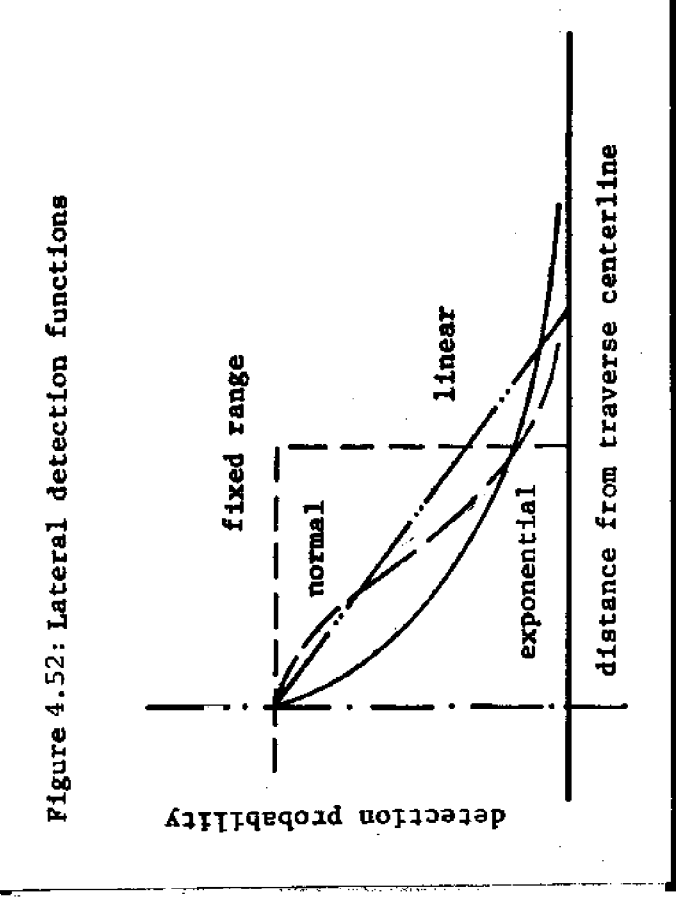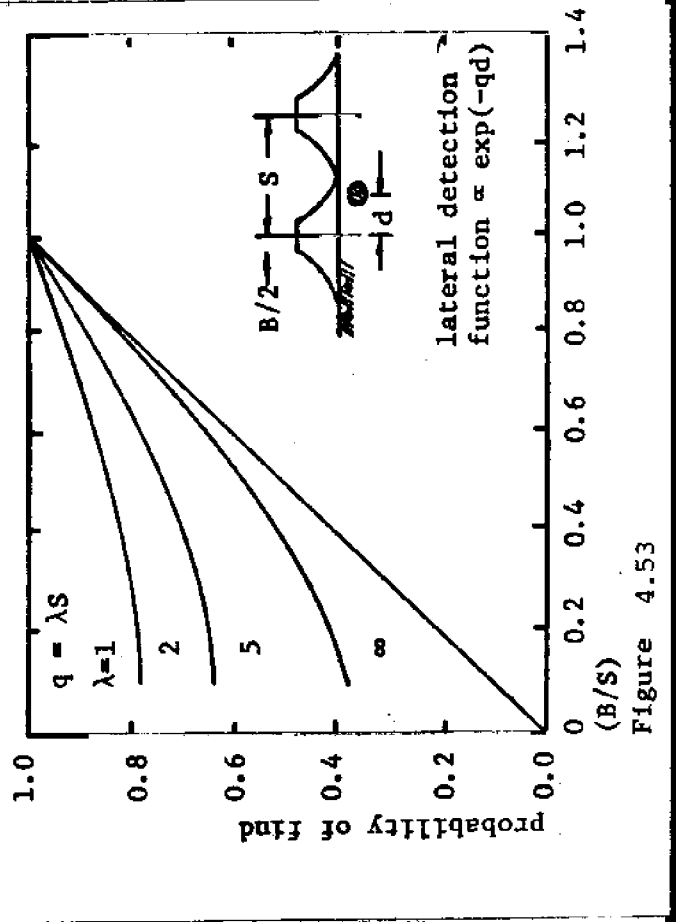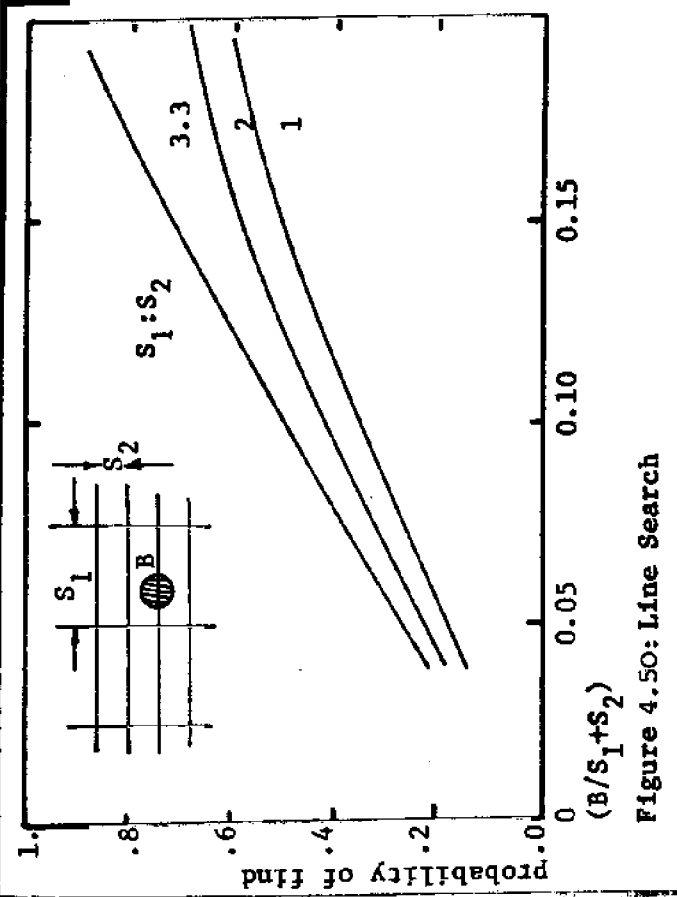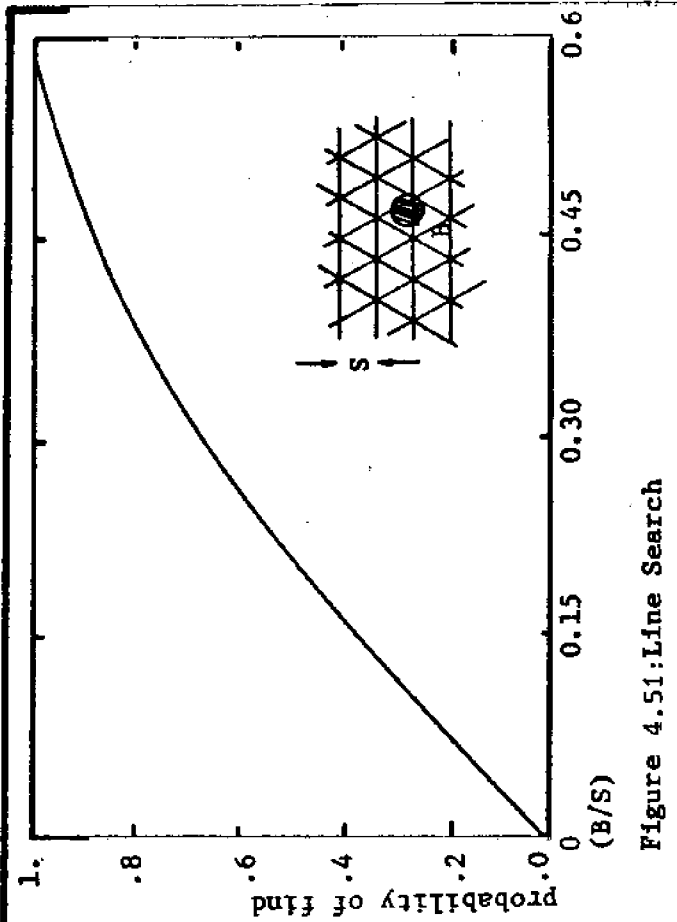
target type would have to be developed empirically, or estimated by physical reasoning. At present such information is difficult to obtain.

Inferences from uniform search

In the single target case, the probability of an undetected target after a search has been made is

$$p' \propto p^0 [1 - p_r (\text{find/search allocation})] \qquad (4.47)$$

where p^0 and p' are the prior and posterior probabilities (Figure 4.54). The dependence on prior probability is obvious.

For multiple targets the states of nature on which inferences are drawn are the parameters of the assumed distribution models for number and size (inferences on the size distribution of a single target would be made in the same way). A computational difficulty arises because number and size, even if independent a priori, are dependent in the likelihood and thus in the posterior distribution. This means many posterior distributions must be solved numerically.

Consider only the number n of targets as a random variable, with target size known. Prior information is encoded as a probability distribution over n. This can be done by assuming the targets mutually independent, in which case n is a Poisson r.v. with density parameter λ.*
The density parameter can be estimated from regional frequency data, if available, or subjectively. Alternately, λ can itself be considered uncertain, a pdf assessed over it, and a compound Poisson distribution used for n.

*Work in mineral resource modelling seems to indicate that the Negative Bionomial distribution (i.e., clumping of targets) is a better assumption. Whether this applies to geotechnical details has yet to be investigated. See e.g., DeGeoffroy and Wignal (1970), DeGeoffroy and Wu (1970), or Uhler and Bradley (1970).

Figure 4.54

PROBABILITY OF FINDING
EXISTING TARGET

Figure 4.55: Objective function surface
over grid spacing and anomaly size
bored in second stage, for optimal
two-stage allocation
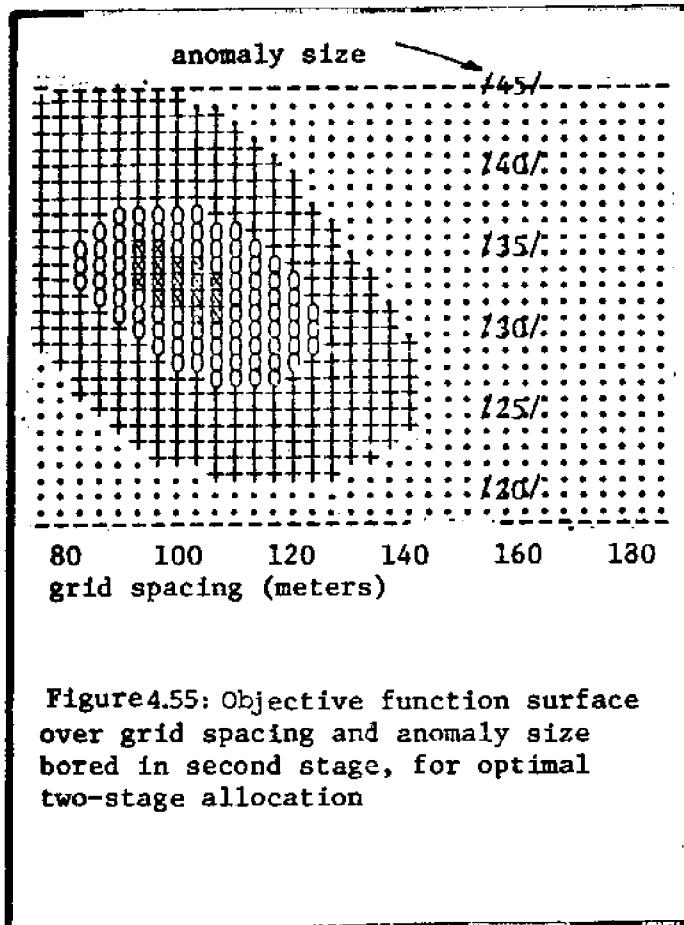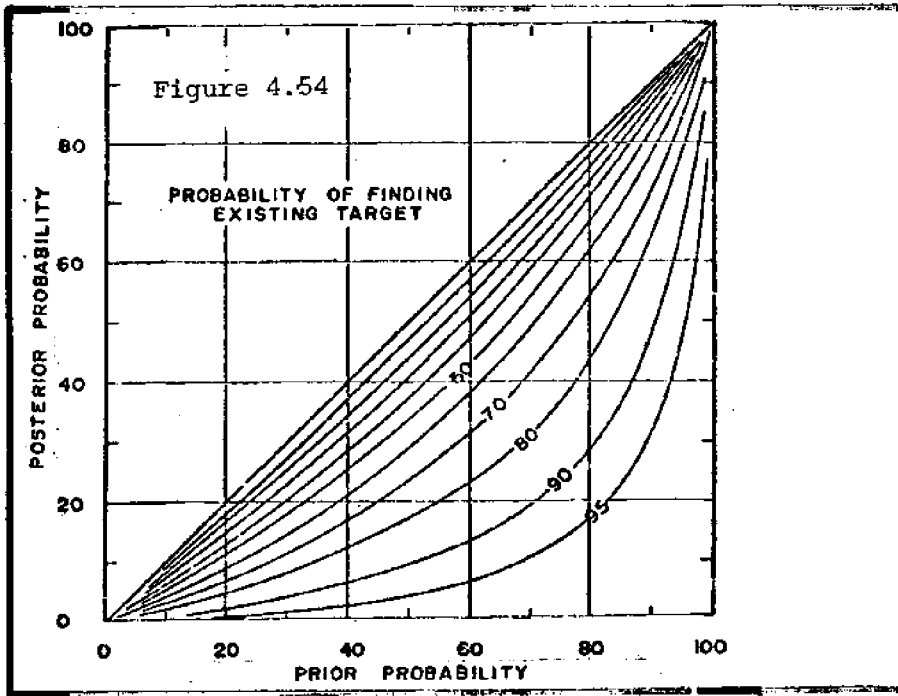
Let the intensity of exploration be such that the probability of finding any one target is p_f, then the posterior mass function (pmf) of number of targets when m is found are

$$p'(n \mid m, p_f) \propto \frac{\exp(-\lambda)\lambda^n}{n!} \binom{m}{n} p_f{}^m (1 - p_f)^{n-m} \qquad (4.48)$$

[Were λ considered the r.v. rather than n, updating would be by the likelihood of λ and p (n) found by integration.]

When no information on n exists prior to exploration either a uniform or non-informative distribution might be used. For variables with range $[0, \infty)$ the non-informative prior is usually taken proportional to 1/n (see, e.g., Jeffreys, 1960); prior ignorance is a controversial topic, however. Adopting the non-informative prior,

$$p'(n \mid m, p_f) \propto \binom{m - 1}{n - 1} p_f{}^m (1 - p_f)^{n-m} \qquad (4.49)$$

which is the Negative Binomial pmf -- a convenient result. Moments of n are:

$$E[n] = m/p_f, \text{ and } V[n] = m(1 - p_f)/p_f{}^2 \qquad (4.50)$$

Expected number of targets increases with the number found and decreases with the search efficacy.

With both number and size are r.v's p_f is no longer a constant. If the distribution of target size, b, is assumed to belong to some family of distributions $f(b \mid \underline{\theta})$, where $\underline{\theta}$ denotes the vector of parameters of the distribution, then

$$L(m|n,\underline{\theta}) = f(b|\underline{\theta})P_{fb}^{n}(1 - P_{fb})^{n-m} \qquad (4.51)$$

where P_{fb} is the probability of the search program finding a target of size b.

Two stage uniform search

In geotechnical and geological exploration two stages searches are common. These usually comprise an inexpensive, but imprecise screening stage like seismic refraction, with a more expensive but also more precise follow-up stage, like borings.*

Two-stage search with false targets (i.e., a noisy first stage) can be approached from several perspectives, and universal optimizations are difficult to formulate (Stone, 1972). Precise modeling depends on the operational strategy for selecting second-stage allocations (i.e., which anomalies are drilled). Optimization criteria are difficult because the amount of effort allocated in Stage 2 is usually a random variable depending on the Stage 1 outcome. For specific problems it is sometimes easier to specify a loss associated with missing targets and minimize total cost, than to maximize expected numbers of finds subject to stochastic constraints.

Consider the following example: Targets are random and independent with size distribution $f(b|\underline{\theta})$. Some geophysical tool is allocated on a parallel line grid, and every resulting anomaly greater than magnitude Δ is drilled. As the threshold magnitude Δ is decreased the detection probability increases, but so does the number of false target indications caused by noise. What first stage spacings should be used, and what anomaly magnitude Δ should be investigated?

---

*In other applications two-stage search has been investigated by Allais (1957) and Slichter (1955) for mineral exploration, and by Stone, et al. (1972) for naval salvage.

This is difficult to express as a constrained optimization but can easily be expressed as an expected cost minimization, if the cost of missing an individual target is specified. Let the regional frequency of targets be λ, and the detection probability be related to Δ as $P_r\{\delta_{target} \geq \Delta\} \propto \exp(-\alpha\Delta)$. Similarly, for Gaussian noise the number of level crossings above Δ is Poisson with density $\lambda(\Delta) \propto \exp(-\beta\Delta^2)$. The expected cost is a linear function of the expected number of missed targets and the expected stage-two exploration cost (Figure 4.55).

It should be noted that two-stage optimizations are possible, although more case specific than other techniques discussed here. As in the example, this modeling often requires the assessment of many parameters, and is therefore subject to noise of its own. The most difficult parameters to assess may be the "costs" of missing a target, as the exact relation between exploration inferences and design decisions is difficult to identify.

Non-uniform or optimal search

If the prior distribution $f(x,y)$ is non-uniform, the optimal allocation of search effort is also non-uniform. While formally optimized non-uniform allocations of effort are not common in geotechnical exploration, they have received attention in operations research, and have been applied to problems of mineral and oil exploration. The most well known optimal search allocations are those due to Koopman (1956), which bear his name, and the extension due to deGuenin (1961). The theoretical development of these techniques is readily available in the literature (e.g., Morse, 1974; Stone, 1972) and need not be repeated here. In essence optimal non-uniform allocations reduce to investing more effort where the target is

likely to be, and less where it is not. Depending on the situation, no effort at all might be allocated to regions of the site with low or even modest probability of containing a target.

The so-called detection function of an exploration tool plays a central role in non-uniform search. The detection function is the conditional probability of detecting (i.e., recognizing or finding) an existing target (i.e., conditional probability) as a function of the amount of search effort allocated to where the target is. While this would seem to have little meaning for borings, on closer inspection this is not the case. First of all, the probability of detecting certain details in borings is not 1.0 (e.g., faults). Secondly, one could think of borings not as individual entities but as a spatial density, in which case a detection function might look like Figure 4.47. For other types of exploration tools like geophysics or field reconnaissance, the detection function is more readily modelled as,

$$\text{pr}[\text{find at } x,y \,|\, \text{target at } x,y; \ \psi(x,y)]$$

$$\equiv D[\psi(x,y)]$$

$$= 1 - \exp[-\psi(x,y)] \qquad \qquad (4.52)$$

where (x,y) is the amount of effort allocated to (x,y).

Optimizing,

$$\text{pr}[\text{find}] \ = \int_x \int_y D[\psi(x,y)] f(x,y)\, dx\, dy \qquad (4.53)$$

subject to the constraint

$$\Psi = \int_x \int_y \psi(x,y)\,dxdy \qquad\qquad (4.54)$$

where Ψ is the total effort, leads to a simple graphical solution for the spatial allocation of effort (Koopman, 1956). In geotechnical practice the exponential saturation function is often inappropriate (Baecher, 1972), but deGuenin (1961) extended Koopman's results to any detection function displaying diminishing returns. For the latter optimization there is also a fairly simple graphical solution. Given the present availability of computers and programmable calculators, numerical solution is equally convenient.

DeGuenin's primary result is that the optimum spatial allocation of effort satisfies the condition

$$f(x,y)\frac{\partial}{\partial \psi(x,y)}\, D[\psi(x,y)] = \lambda = constant \qquad (4.55)$$

Based on this property, the graphical procedure for obtaining the optimal $\psi^*(x,y)$ is:

STEP 1: Select the initial value of λ and evaluate the quantity $\lambda/D'(o)$, where $D'(o)$ is the derivative of the detection function evaluated at $\psi(x,y) = o$. All points at which $\psi(x,y) > o$ satisfy the condition

$$f(x,y) \geq \lambda/D'(o) \qquad\qquad (4.56)$$

STEP 2: Limiting discussion to detection functions for which the derivative with respect to $\psi(x,y)$ is continuous, an inverse function

$$\psi(x,y) = g(\lambda/f(x,y)) \qquad\qquad (4.57)$$

exists. From λ and $f(x,y)$ and Equation 13, determine and graph $\psi(x,y)$.

STEP 3: Vary λ until the area under $\psi(x,y)$ equals the total effort .
The resulting distribution $\psi^*(x,y)$ is optimal.

If the importance of finding targets is different in different locations of the site, a utility function defined over the site can be introduced. The optimal condition becomes that of maximizing expected utility, which is mathematically similar to maximizing probability of a find, with $f(x,y)$ replaced by $f(x,y)u(x,y)$. In either case, the probability of a find (or expected utility) is an immediate result of the graphical solution, as is the posterior pdf of location.

Clearly, the optimal allocation depends on the prior pdf of location, which in most cases is subjective and poorly defined. However, the allocation depends on $f^o(x,y)$ only through the logarithm, and is therefore insensitive to minor imprecisions in the subjective assessment. The probability of a find, and the posterior distribution depend linearly on $f^o(x,y)$, however, and are more sensitive to imprecisions. The allocation derived by such optimizing procedures is for search effort defined continuously in both space and magnitude. Geotechnical tools are usually discrete in space, and therefore must be tailored to approximate the optimal solution. More work is needed on rules for making such approximations, and their affects on probability of a find.

Sequential search

In a sequential procedure the pdf of location is updated after each observation. In certain cases sequential procedures increase the probability of a find because observations are made on the basis of all available information.* At least four criteria of optimality might be used for sequential search: minimizing of expected amount of effort to find a target, maximizing the probability of finding a target with a given amount of effort, minimizing the conditional probability of an undetected target after a fixed amount of effort has been expended, and minimizing the expected amount of effort required to reduce the probability of an undetected target to a fixed level. Fortunately, each criterion leads to the same optimal sequence of observations (Baecher, 1972). The optimal strategy is myopic, at each stage the next observation is allocated such that the ratio of incremental probability of a find to incremental cost is maximized. Again fortunately, search is one of the few problems in sequential decision making for which myopic strategies are globally optimal (e.g., DeGroot, 1970). Cmf's of the number of observations to a find can be computed by enumeration, as can the cdf of cost, if spatially variable.

Sequential search procedures, aimed at finding minima, maxima or other properties of a continuous or trending field (e.g., the maximum depth of soil cover), are analyzed with techniques differing from the present ones. In continuous field cases spatial characteristics of the field are used to locate observations. Thus, observations are not independent of one another.

*In the special case of sequential non-uniform search with discrete stages of spatially continuous effort, sequential search can be shown to have no advantage over single stage search (Koopman, 1956; deGuenin, 1961).

While not discussed here, these problems are frequent in non-linear programming and related disciplines, for example, Wilde (1964) treats strategy optimization for deterministic surfaces. Veneziano and Faccioli (1975) treat special problems in strategy optimization for Gaussian random fields.

In sequential search as in one or two-stage searches, optimal stopping rules can be determined by straight forward decision theory techniques.

4.4 Magnitude of Errors in Site Characterization

Based on the above discussion of sources of uncertainty in site characterization, the following is concluded. The COV of averaged sediment properties for design due to spatial variation, statistical uncertainty, and random measurement errors should be expected to be about 30% and could rise to 50%. This does not include bias introduced by the procedures of measurement. The error rates in maps of sediment distribution defined as precent misclassified is expected to be on the order of 25%. Except in special applications, however, these errors are less important than those of parameter estimation due to spatial averaging. Finally, given the assumed regional frequency of clay-peat channels are typical exploration programs, the probability of an undetected anomaly is less than 1% and its expected horizontal diameter is about 4m.

Appendix 4.3

The linear estimate $\hat{z} = \Sigma w_i z_i$ presented in Section 4.3, is optimized to minimize the variance in estimates of the spatial mean t. However, if the use to which the inference is to be put is known, more appropriate criteria of optimality can be selected. For example, if the purpose of the inference is to predict the behavior of the platform through some mechanistic model $g\{y(\underline{x})\}$, where $y(\underline{x})$ is the realization of the random field in the space influenced by the platform, and if in the modeling $y(\underline{x})$ is replaced by an equivalent deterministic (i.e., uniform) parameter $\hat{y}$, then the estimator $\hat{z}$ for $\hat{y}$ can be optimized to minimize the variance of the prediction

$$\min_{\underline{w}} \; E[(g\{y(\underline{x})\} - g\{y\})^2] \quad . \tag{4.34}$$

Replacing $\hat{y}$ by $\Sigma w_i z_i$ and taking a Taylor's series expansion of the variance of $g\{y\}$ about its mean (i.e., $g\{y|(\underline{x})\}$ assuming $g\{\cdot\}$ is linear yields differentials of $g\{\cdot\}$ with respect to the sediment properties. Again assuming $g\{\cdot\}$ linear, these differentials of the function become functions of the differential, and setting the derivatives with respect to $\underline{w}$ equal to zero yields,

$$\left\{ \begin{array}{c} \underline{w}^* \\ \lambda \end{array} \right\} = \left[\begin{array}{cc} \underline{\underline{C}} & \underline{1} \\ \underline{1} & 0 \end{array} \right]^{-1} \left\{ \begin{array}{c} \underline{\Gamma} \\ 1 \end{array} \right\} \quad . \tag{4.35}$$

The influence factors $\underline{\Gamma} = \Gamma_1, \ldots, \Gamma_n$ are, respectively,

$$\Gamma_i = \int_A \int_A f\{\delta y_1\} g\{\delta y_2\} \{C[y_1, z_i] + C[y_2, z_i]\} dA_1 dA_2 \tag{4.36}$$

5.   GEOTECHNICAL MODELING

It is often said that two things distinguish soil mechanics from other branches of civil engineering: uncontrollable material properties and poor mechanical models.   Yet the magnitude of modeling error is seldom quantified.   In this section geotechnical models of stability and deformation are considered, to estimate the magnitude of uncertainty in predictions of behavior deriving from parameter uncertainty and model inaccuracy.

For both types of models empirical data analyses have been made to compare the predictions of simple widely used formulae with observations, and analytical approaches have been developed to assess the influence of spatial variation of bottom parameters.   Together, a first estimate can be made of the combined uncertainty of predictions.

A limitation of the present analyses is that they focus primarily on static behavior, whereas dynamic wave loading is an important concern offshore.   While limited attention is paid to dynamic analysis in Section 5.4, the empirical record against which to compare dynamic predictions is poor and fundamental mechanisms of soil behavior under dynamic loading are poorly understood (e.g., liquafaction under wave loading).   Thus, quantified conclusions on the uncertainties of predictions of dynamic preformance are in large measure speculative, and must be extrapolated by what we know of uncertainties in predictions of static performance.   This is a limitation of current practice which a formal analysis of uncertainty can do nothing for.

5.1   Epistemology of Modeling*

This section reviews the logical basis of modeling and the sources

of uncertainty in model predictions.

5.1.1 Logic of Modeling

Models can be viewed from a syntactic, semantic, or pragmatic perspec-

tive. Less precisely, a model can be thought of as exhibiting relationships,

truth, or usefulness. The distinction between syntactic and semantic

models is exclusive, while either may also be pragmatic.

The view adopted here is the syntactic, as summarized in Tarsky's

(1961) definition of a model as, "...a possible realization in which valid

sentences of a theory...are satisfied...." By this definition both a

mathematical (or symbolic) construction and reality itself would be said

to be models of a chosen theory. The theory is "a linguistic entity con-

sisting of a set of sentences" and is correct if internally consistent

according to the rules of mathematical logic (e.g., Suppes, 1961). A model

then is any set of objects and relations among or operations upon them

which conform to the theory.

Among models of the same theory certain isomorphisms exist, and these

isomorphisms are used to infer the behavior of one model from that of

another, even though there may be no interaction among models. While the

view is syntactic, it would appear pragmatic as well. From the pragmatic

view the central questions are, is reality a model of the chosen theory,

and what is the extent and character of isomorphisms between reality and

other models of the same theory?

---

* Work leading to the discussion of Section 5.1.1 has not been funded
  by Project SeaGrant.

The semantic view that models are correct (true) or exact representations of reality can be rejected almost a priori. However, it surfaces implicitly in hypothesis testing approaches to model uncertainty, and is therefore not without apparent adherents (Section 5.1.4). In the decision context models are used not because they are correct, but because they allow better decisions to be made (e.g., Veneziano, 1976). Models of ground deformation are neither right nor wrong, and neither true nor false. Predictions of reality based on model results reflect subjective opinion on the degree to which reality and the mathematical construction are both models (in the syntactic sense) of the same theory, and on the isomorphisms between reality and the construct. In application, a mathematical model is not constructed from reality itself, but from a chosen theory which reality is thought to satisfy.

A model, whether reality or a mathematical construct, comprises a rich variety of interrelational properties, some of which exceed the requirement of satisfying the valid sentences of a chosen theory. While isomorphisms among models of a given theory reflect the common interrelational properties they are constrained to exhibit, isomorphism may not extend to those interrelational properties not constrained by the theory. Therefore operations on a mathematical model may exploit properties which reality does not exhibit, and lead to conclusions that cannot be transferred.

Paraphrasing Ackoff (1962), we assign numbers to events and objects because they have interrelational properties that are well understood, and these interrelational properties can be used to deduce conclusions that were not otherwise apparent. Numbers, however, have interrelational

properties that events and objects may not share, and thus the deduced conclusions may not apply to reality.

These comments lead to the concepts of richness, power, and realism. *Richness* here means the capacity of a model to exhibit subtle variations in behavior. *Power* means the capacity to allow strong non-trivial inferences or extrapolations. *Realism* means strong and broad isomorphism with reality. These qualities are usually not maximized in a single model, so one may use a powerful model to extrapolate behavior, and calibrate it to a realistic model known to be strongly isomorphic with reality.

Within the context of the syntactic view, the central questions for application remain those based on induction, not deduction: is reality a model of the chosen theory, and how far do isomorphisms among models extend? Neither question admits a yes or no answer. Reality may be a model of a chosen theory only at some level of aggregation (e.g., jointed rock masses as models of Darcian flow), only under restricted conditions (e.g., low particle velocities modeling laminar flow), or only in an approximate way (e.g., Mohr-Coulomb strength criteria).

5.1.2 Information Content of Models

With the possible exception of simple curve fitting, the introduction of a theory from which a mathematical model is constructed introduces information to an analysis not contained in the observation themselves (Kaufman, 1979). This information is added by assuming reality to be a model of the theory.

An important question on the relation of data and professional opinion is the amount of information added by adopting a theory, and therefore a mathematical model. The theory reflects a history of empirical

observations, and therefore one measure of the information content of a theory is the total information contained in those observations (Cornell, 1979; Veneziano, 1979). While the set of observations confirming, say, Darcy's law cannot be enumerated in practice, one might assume that some sufficient statistic could be defined comprising this information. This might be the prior model credibility of the composite Bayesian approach (Section 5.1.4). While useful, this concept underrates the importance of induction in theory formulation (e.g., Salmon, 1966), and possibly carries the potential for leading the unwary into a semantic view of models.

A different approach to the amount of information in a chosen theory, and a mathematical model of it, is the degree to which the probability distribution over predictions is reduced by introducing the theory, as compared with that deriving solely from site specific observations (i.e., simple curve fitting or interpolation). This definition is akin to informational entropy.

Neither of these approaches by itself is satisfacotry. Both the power of a mathematical model and its realism (here, confirmation) should influence the amount of information it introduces. The statistical view (data record) deals with realism; the entropy view deals with power. A combination is required.

5.1.3 Uncertainty in Modeling

Decision analysts and Bayesian statisticians would hold that predictions of performance, whether they are assessed directly or come from mathematical modeling, are merely statements of subjective degrees-of-belief about the world. In quantifying the uncertainty in model predictions,

uncertainties in input parameters θ are assessed and then propagated

through the model. But a carefully assessed probability distribution

(pdf) over θ gives illusory satisfaction of having rationalized pro-

fessional uncertainties. Few decision analysts, let alone safety analysts,

would accept a model prediction, even though containing parameter uncer-

tainty, as a complete statement of uncertainty in the real world.

As a first cut, the sources of uncertainty in making prediction of

reality from mathematical models are the following:

- Theoretical Misunderstanding -- reality is a model in which not

  all the valid sentences of the theory are satisfied, or which

  has important interrelational properties exoginous to the theory.

- Structural Inadequacies -- objects and relations in the mathe-

  matical model are highly simplified compared to reality.

- Boundary and Initial Conditions -- the mathematical model un-

  like reality is isolated from an environment.

- Mathematical or Numerical Approximations -- simplifications and

  approximations are used to obtain quantified predictions.

- Omissions -- important facets of reality may not be reflected

  in mathematical models.

The amount of uncertainty contributed by these sources can be large,

and also biased. A common way of handling this bias is by calibrating

the mathematical model results to observations of reality through the

parameters. Thus, the estimates of θ, as expressed in the pdf $f(\theta)$,

incorporate not only the physical meaning of θ but also the model bias

(e.g., Lambe, 1973). An example of calibrating by modifying parameter

estimates is statistical filtering of process response (Gelb, et al.,

1974), i.e., "Kalman" filtering. In this case parameter estimates are not independent of the model, and cannot be assessed in isolation. This is an important point for site characterization studies.

A similar calibration of the mathematical model by altering $f(\theta)$ is seen in changes among domains of prediction. The linear Mohr-Coulomb failure criterion for rock is usually only an approximation to an empirically non-linear failure surface. Therefore the cohesion and friction coefficients used in analysis change with the normal stress of interest (Figure 5.1).

Attempts to quantify the contribution of uncertainties other than θ run afoul of two problems. Either the uncertainties cannot be known (e.g., omissions of important failure modes), or the uncertainties reflect an artifact of the modeling (e.g., boundary and initial conditions are chosen to calibrate the model, not usually to represent some physical aspect of reality).

5.1.4 Dealing With Model Uncertainty

Quantifying model error is more difficult than identifying its sources, and the contribution of certain sources cannot be established analytically (e.g., omissions). Therefore past attempts to handle model uncertainty have been primarily based on empirical validation.

In frequentist theory model uncertainty work has primarily concentrated on the issue of model selection: which of a set of models is "best," or is a model under consideration adequate? While hypothesis testing approaches imply the semantic view of models, it would be unfair to suggest that the modelers themselves subscribe to that view. Other
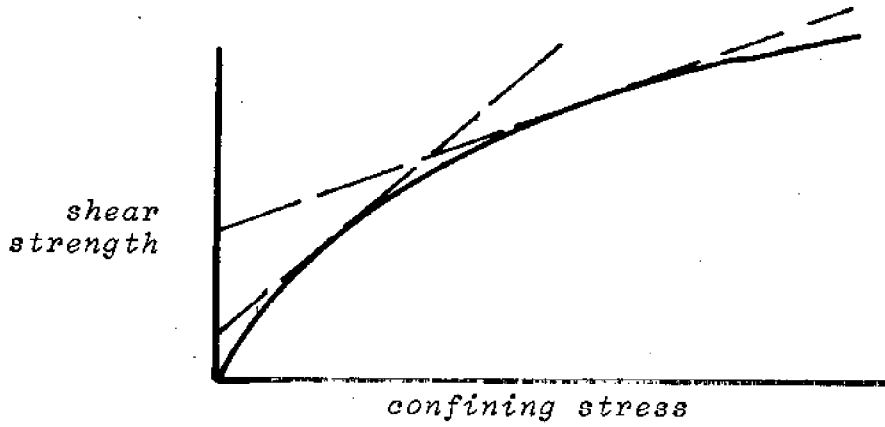
Figure 5.1 -- Linear approximation to the Mohr failure criterion.
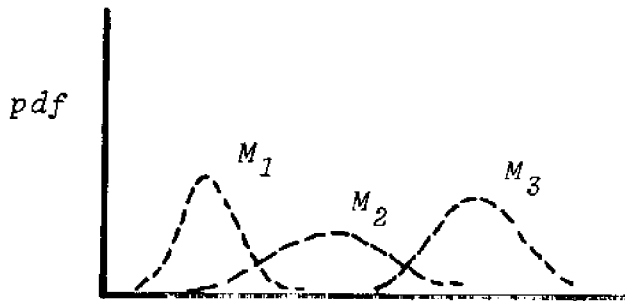
Figure 5.2 -- Predictions of three models
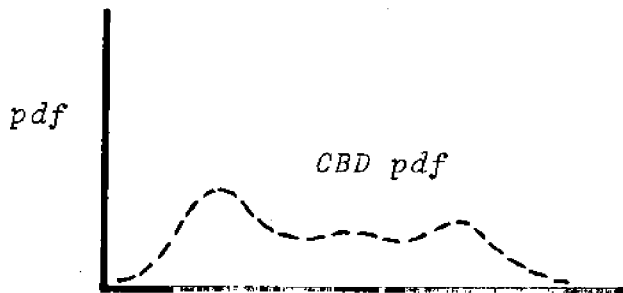
Figure 5.3 -- Composite Bayesian distribution based on the three model predictions.

techniques such as maximum R^2 or cross validation seek the model that best fits the data according to some prespecified, usually ad hoc, criterion. The frequentist techniques do not allow consideration across models.

Bayesian techniques of model validation are based on posterior probability. Given an inference set of models $M = \{m_1, \ldots, m_k\}$ and data $\underline{Z} = \{z_1, \ldots, z_n\}$, the best model is that which is most probable in light of $\underline{Z}$. The analysis can be extended to include a loss function for selecting the "wrong" model, and the selection treated as a decision. Note, however, the implied semantic view of models.

A more interesting problem is that of combining model predictions across models. This has been treated by Giesel (1969), Wood (1978), Grigoriu (1976), and Veneziano (1976) among others. The approach of these efforts has been what is here called the composite Bayesian distribution (CBD). The CBD is a linear weighted sum of the model predictions over M. Weights are taken proportional to the posterior probabilities (or densities) of the models, again implying the semantic definition. Let $\underline{S} = S_1, \ldots, S_h$ be zero-one parameters associated with $m_1, \ldots, m_k$, respectively, where $S_i = 1$ if m_i is the correct model, and zero otherwise. Clearly $\Sigma S_i = 1.0$. Letting $\underline{\theta}$ be the model parameter with respect to each model,

$$f'(\underline{S}, \underline{\theta} \mid \underline{Z}) \propto f^o(\underline{S}, \underline{\theta}) \, L(\underline{Z} \mid \underline{S}, \underline{\theta}) \quad . \tag{5.1}$$

The predictive density function over some prediction y is found by integrating (summing) over the models and parameters

$$f(y|\underline{Z}) = \int\int f(y|m_i,\underline{\theta}) \; f'(\underline{S},\underline{\theta}|\underline{Z})\,dmd\underline{\theta} \qquad . \qquad (5.2)$$

The difficulties with this approach are that it is implicitly semantic, and that it assumes independence of model predictions. It also exhibits the undesirable property that as the dimension of M increases, the predictive density function of (Y) becomes increasingly diffuse. By introducing a new model, uncertainty in the prediction increases even if the prediction of the added model is consistent with other model predictions, and even if the added model is based on a different theory. Thus, if three models yielded the predictions of Figure 5.2, the CBD might look something like Figure 5.3. This would not seem a particularly useful result. The problem is that the prediction may contain more information than is being exploited.

To answer these objections, a second approach to model aggregation has been introduced which is based on a joint likelihood concept (leung, 1979). The joint likelihood concept treats the model predictions as information, in a Bayesian sense, and defines a joint likelihood function over them. Thus the predictive density on y becomes

$$f'(y|\hat{y}_1, \; \ldots, \; \hat{y}_n) \; \propto \; f^0(y)L(\hat{y}_1, \; \ldots, \; \hat{y}_n|y) \qquad (5.3)$$

where $y_1, \ldots, y_n$ are the predictions of the n models and may be either
deterministic or probabilistic. The advantages of this approach are
that it treats model predictions as they are intuitively treated, it allows
for correlation among models, and it implies a syntactic view of models.
Furthermore, within this procedure the addition of new models reduces predic-
tive uncertainty in y, if the model results are consistent with one another.
That is, the additional model prediction adds information and therefore
confirmation to the prediction of y, rather than adding another random
error.

The importance of correlations among mathematical models is seen
in Table 5.1, in which the maximum likelihood estimate of the conditional
correlation coefficients among a number of foundation settlement models
and a number of pile capacity models are shown. The correlation can be
large because the individual formulae may be models of related or over-
lapping theories, even though the mathematical structure of the models
are different (e.g., most assume elastic stress distribution). This is
an important point: if model predictions are correlated, little new in-
formation is developed by performing parallel analyses. Furthermore, the
sources of dependence may be subtle.

Both the CBD and joint likelihood (JL) methods can be cumbersome
in specific applications, and both have been formulated for use with
empirical verification data. In principle, this need not be the case.
For the CBD approach the density function $f(\underline{s})$ could be taken directly
from expert opinion. Similarly, as Morris (1974) points out, the likelihood

Table 5.1 -- Conditional correlations among model predictions

PILE CAPACITY MODELS

	Eng'g News	Gow	Gates	Danish	P.C.	Hiley	Janbu
Eng'g News	1.0						
Gow	0.8	1.0					
Gates	0.2	0.3	1.0				
Danish	0.2	0.3	0.7	1.0			
Pac Coast	0.1	0.5	0.3	0.6	1.0		
Hiley	0.1	0.7	0.6	0.7	0.8	1.0	
Janbu	0.5	0.6	0.6	0.9	0.4	0.6	1.0

SETTLEMENT MODELS

	Elastic	B-DeB	B-DeB(c)	M	M(c)	S	TP	TP(c)
Elastic	1.0							
Buisman-DeB.	0.8	1.0						
Buisman-DeB.(c)	0.8	0.9	1.0					
Meyerhof	0.1	0.1	0.0	1.0				
Meyerhof (c)	0.3	0.1	0.1	0.8	1.0			
Schmertman	0.8	0.9	0.9	-0.1	0.1	1.0		
Terzaghi & Peck	0.1	0.1	0.1	0.9	0.8	-0.1	1.0	
Terzaghi & Peck (c)	0.1	0.1	0.1	0.8	0.9	0.1	0.8	1.0

function is always a subjective choice even if updated by data. The JL function of $\{y_1, \ldots, y_n\}$ could also be assessed from expert opinion. This seems a potentially fruitful area of work since very little has been done on quantification of model uncertainty and aggregation, and because considerable insight may be gained by further study.

5.2   Stability Modeling

Stability against strength failure of bottom sediments due to imposed platform loads are commonly analyzed by limiting equilibrium analysis, balancing imposed forces against the cumulative cohesive and frictional resistance mobilized over an hypothesized critical failure surface.   The most common semi-empirical model is Terzaghi's superposition of cohesive, overburden, and frictional resistances.   The empirical basis of this formula is well developed, and analyzed in Section 5.2.1.   Other models with which there are fewer verifying studies, but which nevertheless are in wide use offshore have been presented by Hansen (1970)   and Meyerhof (1963).

Analytical methods admitting consideration of spatial variability are mostly based on slope stability models using various methods of slices (e.g., Bishop, 1955; Morgenstern and Price, 1965).   Several $\bar{\phi} = 0$ analyses have been presented in the literature (e.g., Veneziano, et al. 1977), but the number of frictional analyses combining methods of slices with spatial variability is very limited (e.g., Alonzo 1976; Peintinger, et al., 1980).   A model based on modified Bishop Method was developed to establish the influence of spatial variability, and is presented in Section 5.2.2.

5.2.1 Semi-Empirical Formulae

Bearing capacity predictions based on Terzaghi's superposition method are partly theoretical and partly empirical. Many theoretical derivations have appeared in the literature as have the results of tests on model and prototype footings. This section addresses the uncertainty in bearing capacity predictions, inferred through statistical analyses of currently available data. The magnitude of aggregate uncertainty in bearing capacity is shown by example.

Previous Studies

While many studies of bearing capacity have been published, few have attempted to quantify uncertainty. Fewer still have based such quantification on large numbers of empirical data. Most studies approach uncertainty through modeling in which parameters are assumed spatially constant but not known with certainty.

Singh (1971), Höeg and Murarha (1975), and Kraft and Murff (1975) have published similar analyses of foundation stability. These analyses yield surprisingly high probabilities of failure (p_f) at commonly acceptable deterministic factors-of-safety (FS). Typically, probabilities are calculated under the assumption of Normal distribution of the safety margin, which is conservative and in part explains the high p_f's. Further, though, the authors cite the sensitivity of bearing capacity factors to effective friction angle as a primary source of uncertainty.

Höeg and Tang (1978) considered slip surface stability under an offshore gravity platform. In the undrained case they conclude that approximately 70% of the uncertainty in FS predictions are due to undrained strength. Another 25% they attribute to loads. The authors note, however,

that uncertainties deriving from poorly understood mechanisms (e.g., behavior under cyclic loads) cannot be directly included in calculations.

Theoretical Consideration

The ultimate bearing capacity of a shallow, concentrically loaded strip footing on a homogeneous soil is commonly determined from the Terzaghi (1943) superposition method. Combining the contributions of cohesion, surcharge, and unit weight, the superposition method yields:

$$q_v = \bar{c}N_c + qN_q + \frac{1}{2}\gamma BN_\gamma \qquad (5.4)$$

where:

q_v = ultimate bearing capacity for a vertical concentric load

N_c, N_q, N_γ = bearing capacity factors

B = foundation width

q = uniform surcharge around foundation

$\bar{c}, \gamma$ = effective soil cohesion and effective unit weight

The special case of interest here is the bearing capacity of a foundation initially on the surface of a cohesionless soil ($\bar{c}=0, q=0$). Accordingly, Equation (5.4) becomes:

$$q_v = \frac{1}{2}\gamma BN_\gamma \qquad (5.5)$$

Modification of Equation (5.5) for load eccentricity, load eccentricity, load inclination, foundation shape, and foundation size introduces several correction factors. Bjerrum (1973) suggests the form:

$$q_{v,\alpha} = \frac{1}{2}\gamma B N_\gamma R_\gamma S_\gamma I_\gamma E_\gamma \qquad (5.6)$$

where $q_{v,\alpha}$ is the vertical component of stress at failure for an inclined load. The terms R_γ, S_γ, E_γ, and I_γ are correction factors for foundation size, foundation shape, load eccentricity, and load inclination, respectively.

Theoretical bearing capacity factors, N_γ, for strip and circular or square footings differ by factors of two to four. The sensitivity of N_γ to friction angle is particularly notable with 5% deviations in friction angle causing almost 50% deviation in N_γ. Theoretical solutions for N_γ assume a unique value of friction angle. Substantial research indicates that the selection of one friction angle to model the behavior of sand is a major simplification (Ladd, 1977 , Lee, 1970 , Rowe, 1969 , Corforth, 1964; Nash, 1953) . The appropriate friction angle for selecting N_γ depends on: (1) the mode of failure, (2) friction angle anisotropy, (3) strain compatibility, and (4) curvature of the Mohr-Coulomb strength envelope. Terzaghi (1943), Meyerhof (1963), Hansen (1970), and Vesic (1973) suggest methods for selecting an appropriate friction angle.

Of particular importance in the extrapolation of small scale footing tests to large scale foundations is the curvature of the Mohr-Coulomb strength envelope. For model footings, stresses are low and the friction angle large. Field scale foundations produce higher stresses with a corresponding decrease in friction angle. As shown by Graham and Pollock (1972) spatial variation of the mobilized friction angle can be large.

Foundation roughness also effects bearing capacity. Meyerhof (1955) indicates the bearing capacity of a rough foundation ($\delta = \bar{\phi}$) is twice that

of a perfectly smooth foundation ($\delta = 0°$). Hansen and Christensen (1969) suggest a 50% decrease in N for $\delta < 20°$. For $\delta > 20°$ the foundation behaves perfectly rough regardless of $\bar{\phi}$. Chen (1975) indicates similar behavior for $\delta = 17°$.

Evaluation of Model Footing Tests

Data from many model tests exist for the bearing capacity, inclination, and eccentricity factors. Little information is available for the shape factor or effect of foundation roughness and size. Several difficulties arise in aggregating tests from various studies. Differences in: (1) test apparatus, (2) test procedure, (3) identification of failure load, (4) footing material and roughness, (5) control of soil density, and (6) measurement of friction angle, all effect comparison. Despite these difficulties, the present analyses treat experimental data as reported.

Figures 5.4 and 5.5 presents experimental results for rough footing with length width ratios (L/B) of one, and six. An L/B ratio of six is essentially a strip footing, while an L/B ratio of 1.0 corresponds to circular and square footings. Friction angles are from triaxial tests with confining pressures of one-half to two tons per square foot. Friction angles vary from 28° to 45°.

By inspection, N_γ is log-linear over the test range in both groups of data. Accordingly, linear regressions of $\ln(N_\gamma)$ on $\bar{\phi}$ were thought appropriate. Standard linear regression (i.e., least squares estimation) yields,

$$\ln(N_\gamma)_{L/B = 6} = 1.667 + 0.173\bar{\phi} \tag{5.7}$$

$$\ln(N_\gamma)_{L/B = 1} = 2.107 + 0.173\bar{\phi} \tag{5.8}$$

The sample size (n), correlation coefficient (r), and error variance (σ^2) are 130, 0.947, and 0.0425 for $L/B = 6$ and 145, 0.925, and 0.0864 for $L/B = 1$, respectively. Statistical tests (χ^2) show the residuals to be Normally distributed and homoscedastic.

The regression lines shown on Figures 5.4 and 5.5 are the expected values of $\ln(N_\gamma)$ given $\bar{\phi}$. The expected value and variances of N_γ itself, given $\bar{\phi}$ are (Aitchison and Brown, 1957),

$$E[N_\gamma] = \exp\left\{E[\ln(N_\gamma)] + \frac{1}{2}V[\ln(N_\gamma)]\right\} \tag{5.9}$$

$$V[N_\gamma] = \exp\{2E[\ln(N_\gamma)] + V[\ln(N_\gamma)]\} \cdot$$
$$\{\exp\{V[\ln(N_\gamma)] - 1\} \tag{5.10}$$

where

$$E[\ln(N_\gamma)] = \hat{a} + \hat{b}(\bar{\phi}) \tag{5.11}$$

$$V[\ln(N_\gamma)] = \sigma^2_{\ln(N_\gamma)} \tag{5.12}$$

Thus,

$$E[N_\gamma]_{L/B = 6} = \exp\{-1.646 + 0.173(\bar{\phi})\} \tag{5.13}$$

$$V[N_\gamma]_{L/B = 6} = (0.429)\exp\{-3.292 + 0.346(\bar{\phi})\} \tag{5.14}$$
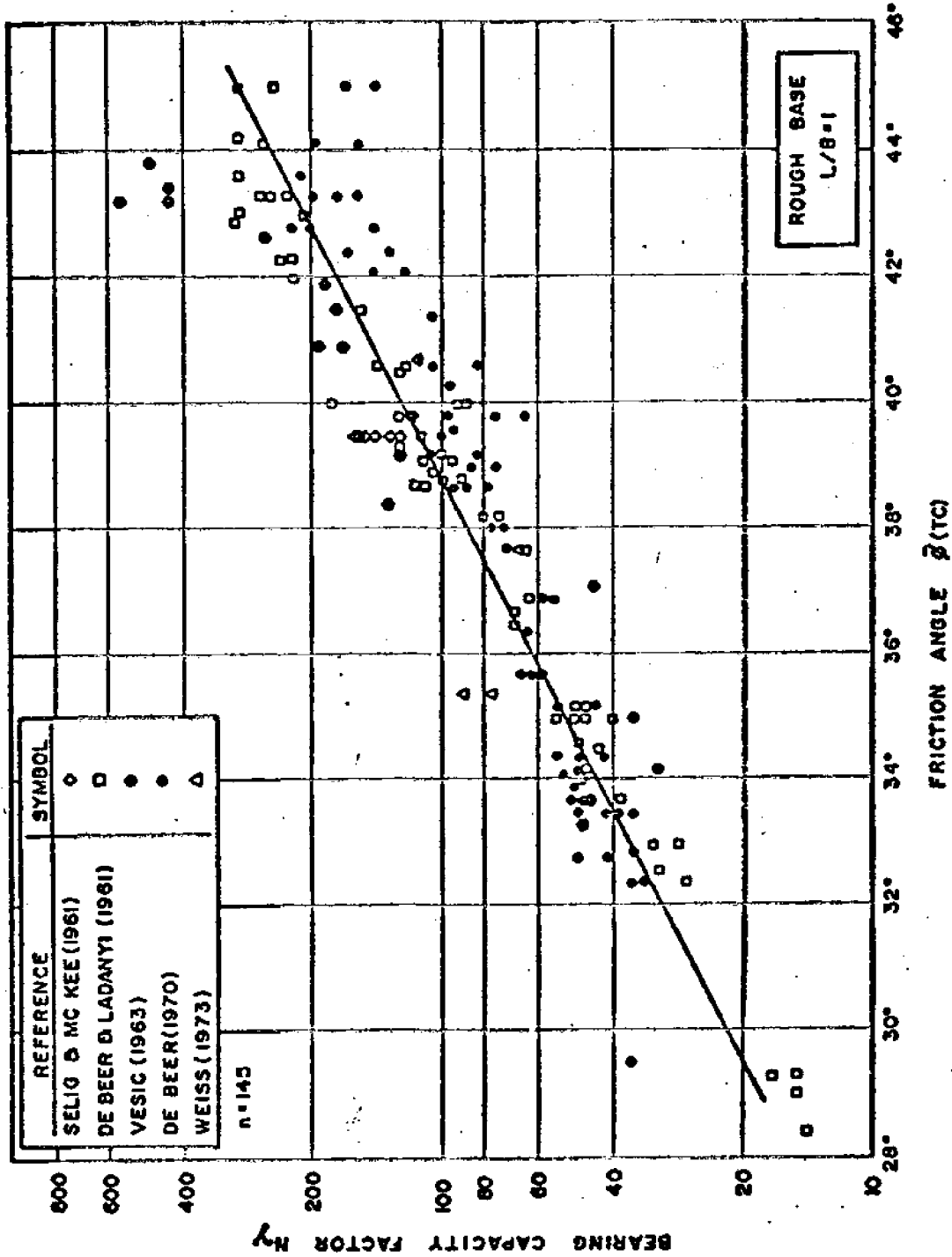
Figure 5.4 -- Experimental results for N_γ.
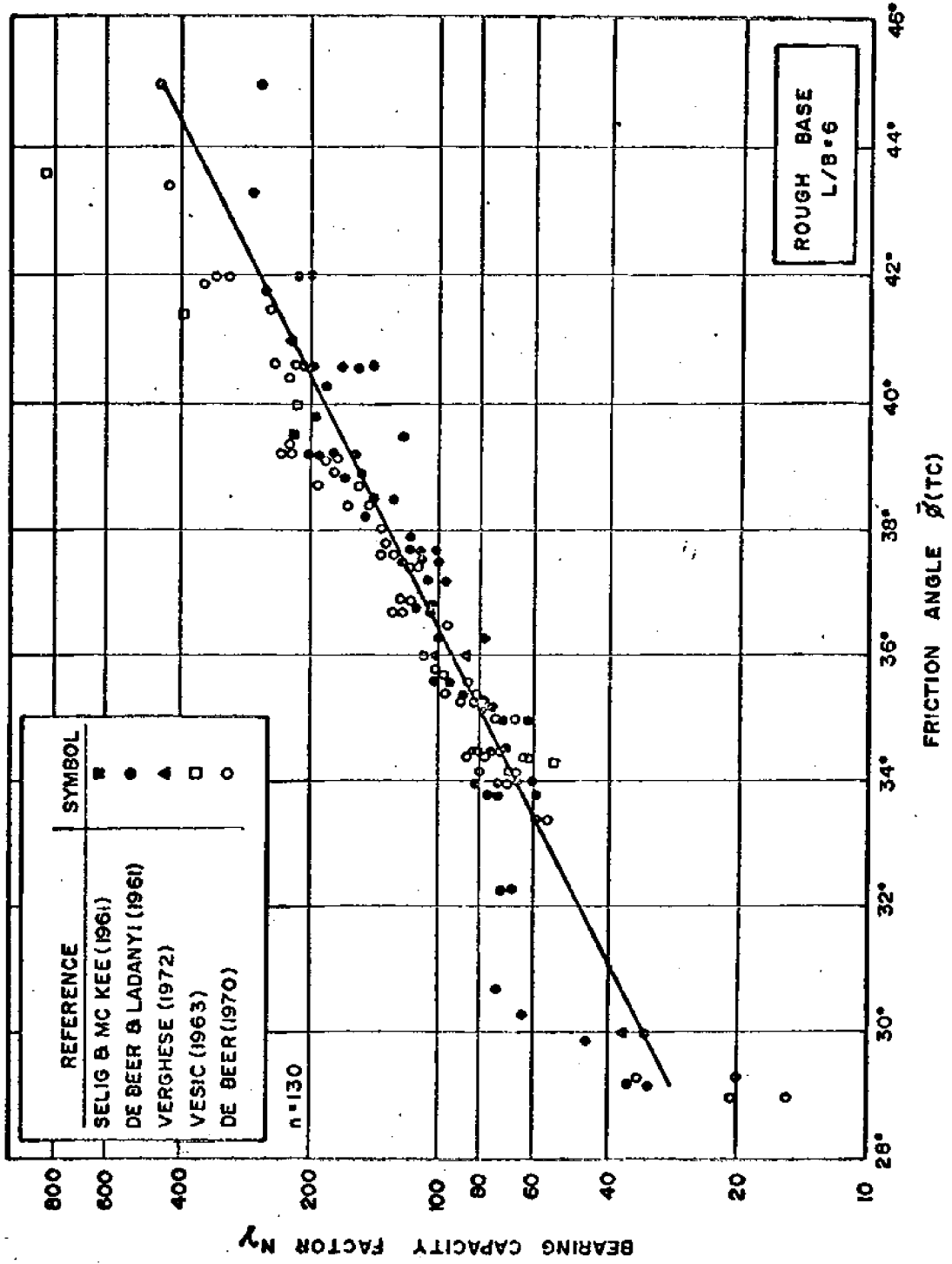
Figure 5.5 -- Experimental results for N_γ.

$$E[N_\gamma]_{L/B = 1} = \exp\{-2.064 + 0.173(\bar{\phi})\} \qquad (5.15)$$

$$V[N_\gamma]_{L/B = 1} = (0.0902)\exp\{-4.128 + 0.346(\bar{\phi})\} \qquad (5.16)$$

Figure 5.6 compares the $E[N_\gamma]$ with theoretical solutions. The $E[N_\gamma]$ is generally larger, by up to a factor of two. The slopes however, are similar.

Extrapolation of Equations (51.3) through (5.16) to field scale foundations requires consideration of size effects. Dimensions of the model strip footings range from 1.5" to 2.5". A representative value of 2" can be used for determining R . Similarily, dimensions of the circular and square models are about 4". To extrapolate these model dimensions to field scale foundations of 5' to 10' involves B_{field}/B_{model} ratios of 20 to 50. The reduction in bearing capacity, therefore, will be significant, and even with proportionally small error in R_γ, the absolute error will be great.

Experimental results for R_γ are shown in Figure 5.7. The Graham and Pollock (1972) scale dependent plasticity analysis for K' - 0.30 and K' = -0.20 is also shown. The experiments of Ovesen (1975) are from centrifuge tests. The experiments at small B_{field}/B_{model} ratios are from conventional model footing tests. Although the results are too inconsistent for meaningful regression analyses, they generally support the reduction indicated by Graham and Pollock.

Figure 5.8 summarizes model footings tests for the effect of load eccentricity. Analysis as a function of eccentricity ratio (E/B) indicates a least squares second order polynomial with expectation and variance:
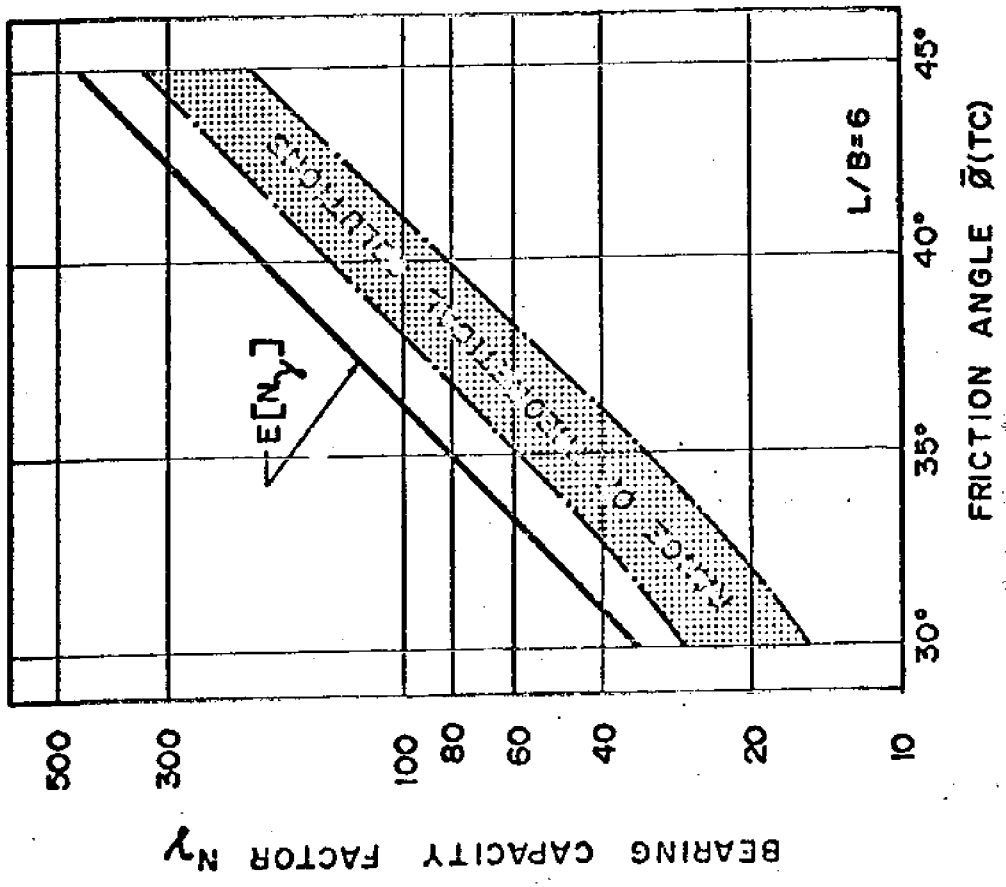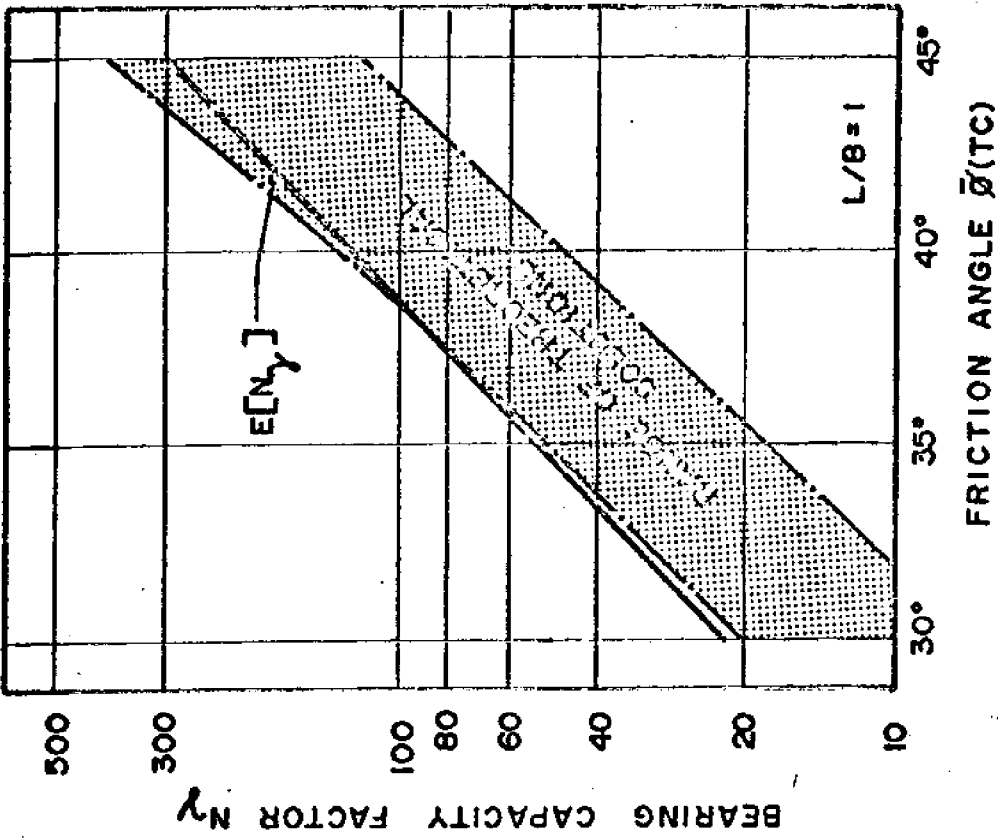
Figure 5.6 -- Comparison of expected N_γ with theoretical solutions.

$$\log R_\gamma = K' \log \frac{B_{field}}{B_{model}}$$
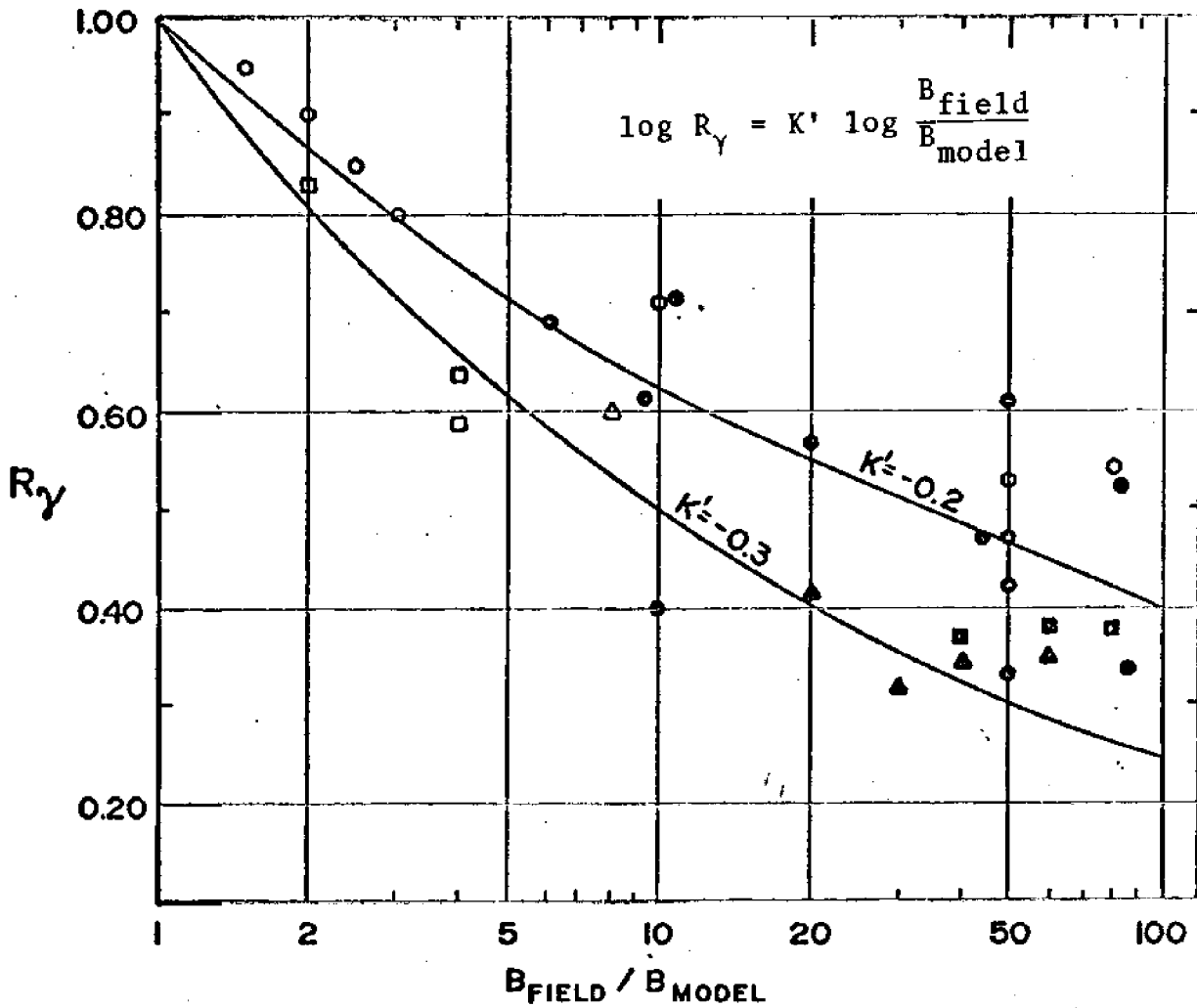
REFERENCE	SYMBOL	D_r
ANDERSEN (1972)	○	M.DENSE
GRAHAM & STUART (1971)	□	M.DENSE
GRAHAM & POLLOCK (1972)	△	M.DENSE
OVESEN (1975)	○	50%
	◖	95%
	■	77%
	▲	77%
	●	—

Figure 5.7 -- Experimental results for R_γ.

REFERENCE	SYMBOL	$\bar{\phi}$	L/B
RAMELOT & VANDEPERRE (1950)	◁		—
	◁		—
MEYERHOF (1953)	○	36°	—
	□	36°	6
	▣	48°	6
	▷	48°	1
	●	48°	—
EASTWOOD (1955)	◇		3
	◈		2.3
	◇		1.8
ZHARESCU (1961)	◐	37°	6
LEE (1965)	○	43°	—
	◕	43°	2
	◑	43°	3
PRAKASH & SARAN (1971)	▨		
DHILLON (1961)	○		
PURKAYASTHA & CHAR (1977)	◓	38°	2
IRSIA (1950)	▣	34°	—
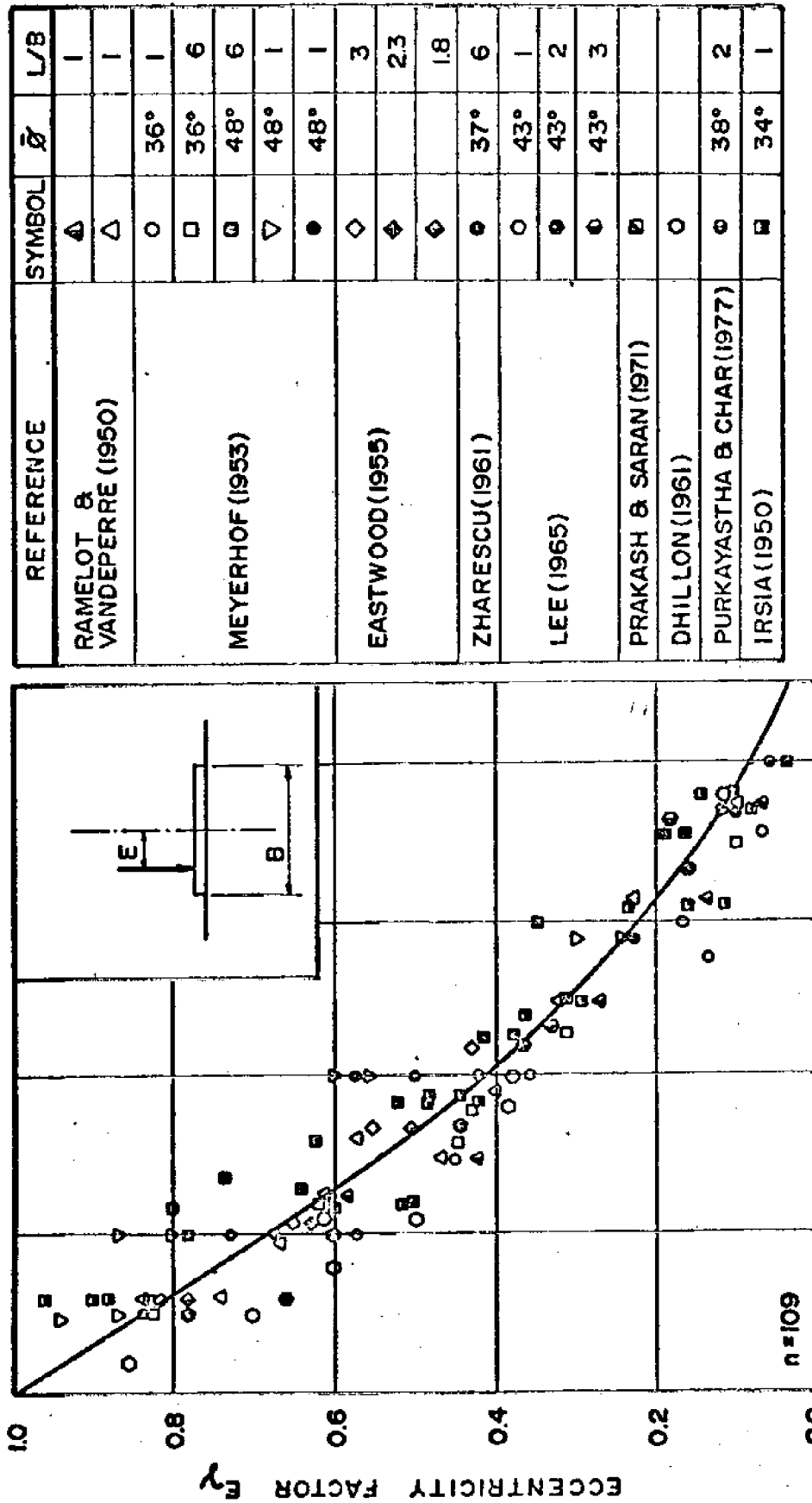
Figure 5.8 -- Experimental results for E_γ.

$$E[E_\gamma] = 1.0 - 3.50(E/B) + 3.03(E/B)^2 \tag{5.17}$$

$$V[E_\gamma] = 0.0058 \tag{5.18}$$

The regression was constrained to provide $E[E_\gamma] = 1.0$ for E/B = 0.

The tests indicate the effect of foundation shape. Strip footings apparently yield lower values of E_γ than other geometries. Regressions for L/B = 6 and L/B = 1 confirm a statistically significant difference. A significant difference also exists between the regressions and the Meyerhof (1963) solution. For E/B < 0.40, however, the absolute difference between all expressions is less than 0.10. As a matter of practical concern, Equations (5.14) and (5.18) satisfactorily describe the test results. Figure 5.12 summarizes the analysis. Purkayastha and Char (1977) report a statistical analysis indicating foundation size and friction angle have no influence on E_γ. Their least squares estimate of E_γ is also shown in Figure 5.8.

The experiments from several investigations of load inclination are shown in Figure 5.9. The values of Saran, et al. (1971) and Muhs and Weiss (1974) are consistently larger than other results. Despite this difference the tests are considered one sample. Regression analysis indicates a second order polynomial with expectation and variance:

$$E[I_\gamma] = 1.0 - 2.41(H/V) + 1.36(H/V)^2 \tag{5.19}$$

$$V[I_\gamma] = 0.0089 \tag{5.20}$$
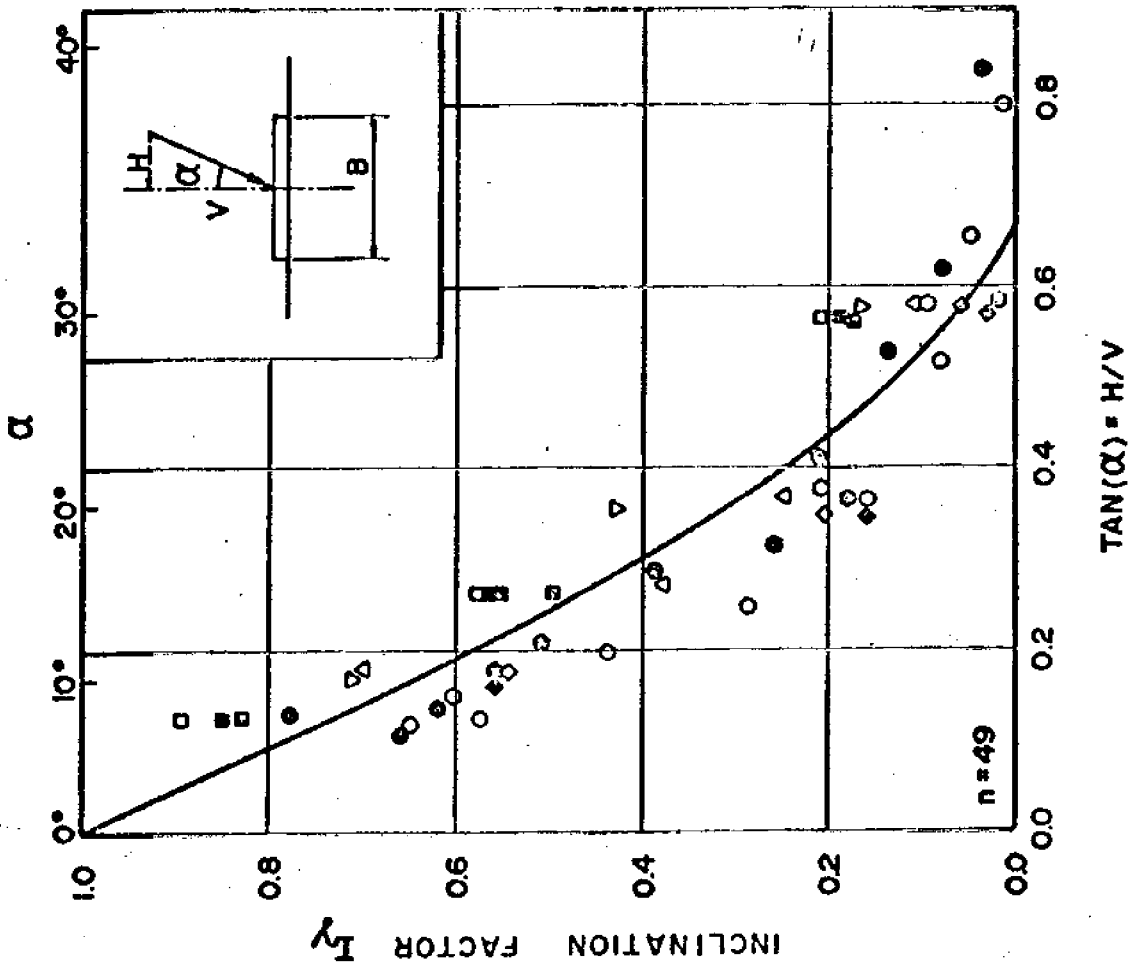
REFERENCE	SYMBOL	$\bar{\phi}$	L/B
MEYERHOF (1955)	○	45°	6
	◉	45°	—
TRAN-VO-NHIEM (1970)	△	26°	6
SARAN, ET AL (1971)	□	42°	—
	◪	42°	2
	◪	42°	4
	◪	42°	6
LEBEGUE (1972)	◇	35°	6
	◈	35°	6
	○	40°	6
	◈	40°	6
MUHS & WEISS (1974)	▽	40°	3

Figure 5.9 -- Experimental results for I_γ.

The regression was constrained to yield $E[I_\gamma] = 1.0$ for H/V = 0. No significant improvement results for high order polynomials.

Theoretical solutions suggest I_γ varies with friction angle and foundation shape. After reviewing experimental data and performing simple stability analyses, Andersen (1972) concludes I_γ is not a function of friction angle. Results for the few friction angles shown here concur with this finding. A trend does appear with foundation shape. Strip footings indicate smaller values of I_γ. The results of Meyerhof (1953) for L/B = 1 and L/B = 6 confirm a statistically significant difference. These results, however, are based on too few tests to yield a definitive relation. Accordingly, Equations (5.19) and (5.20) are still suggested to describe the test results.

In Equation (5.6) the effects of eccentricity and inclination are independent. This seems not to be the case in reality. Sixteen tests were found in which eccentricity and inclination were varied simultaneously (Figure 5.10). The bearing capacity in these tests is about 20% lower than that predicted using $E[E_\gamma]E[I_\gamma]$. However, the data are few. It should be noted that this joint effect is not a statistical covariance in the common sense, as only a single bearing capacity can be measured in any one test.

Sufficient consistent data are not available to evaluate the effect of foundation shape. Figure 5.11 presents several series of test results. Each entry represents the ratio of N_γ from several experiments for L/B = 6 and some other footing shape. The entry of DeBeer (1970), for example represents the ratio of N from 60 tests for L/B = 6 and L/B = 1. For geometries other than L/B = 1 or L/B = 6, DeBeer (1970), Hansen (1970), and Vesic (1973) recommend the arbitrary selection of a linear relation
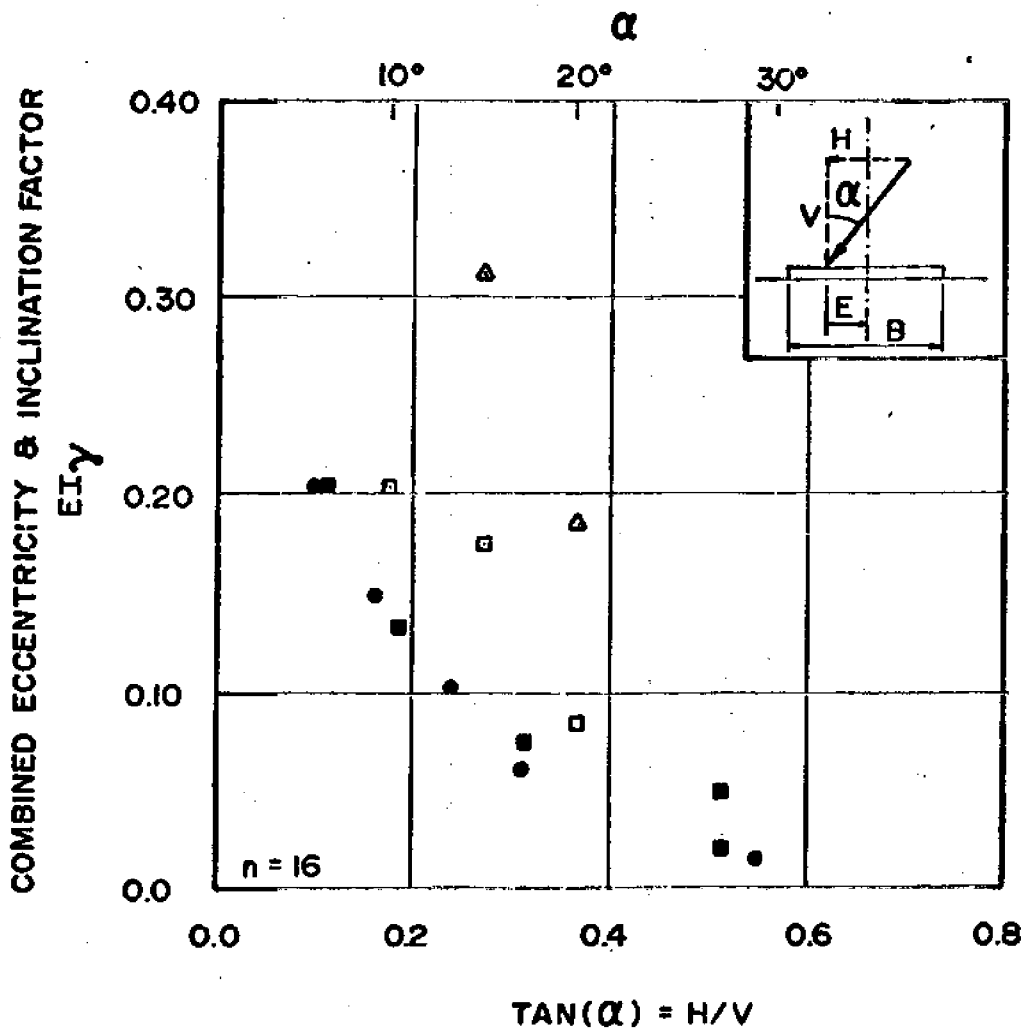
Figure 5.10 -- Experimental results for $E_\gamma I_\gamma^{\wedge}$.
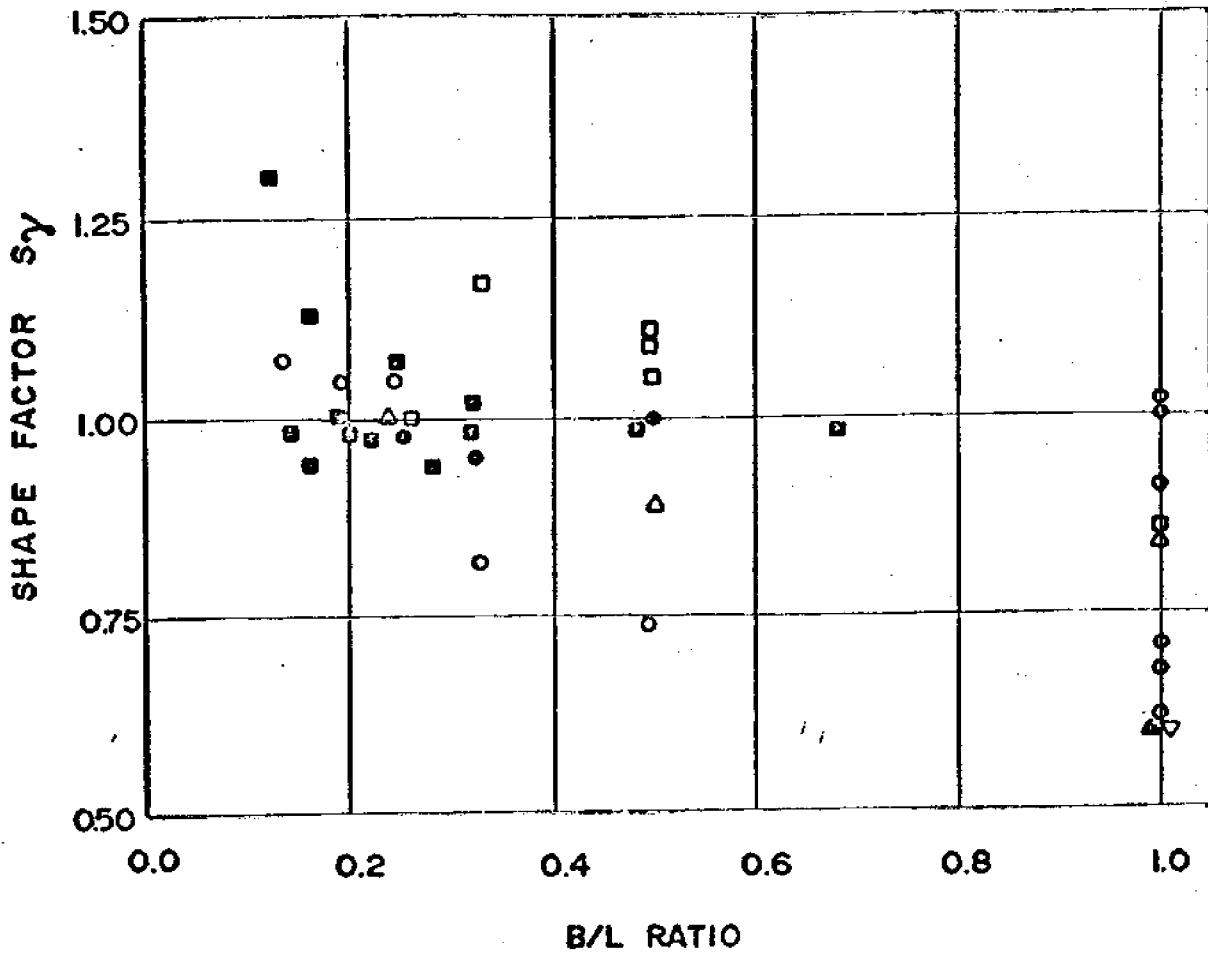
REFERENCE	SYMBOL	$\bar{\phi}$	BASE
GOLDER (1941)	◉	41°	S
EASTWOOD (1951)	▣	43°	S
DE BEER & LADANYI (1961)	▽	35°-45°	R
FEDA (1961)	△	39°	S
SELIG & MC KEE (1961)	○	39°	R
VESIC (1963)	○	35°-45°	R
DE BEER (1970)	▲	35°-45°	R
WEISS (1973)	□	35°-45°	R

Figure 5.11 -- Experimental results for S_γ.

independent of friction angle of the form:

$$S_\gamma = 1.0 - m(B'/L) \qquad (5.21)$$

where S_γ = 1.0 for strip footings and m = 0.40. The parallel regressions of N_γ for L/B = 1 and L/B = 6 support the independence of S_γ and friction angle. Comparing the regressions yields m = 0.383. There is no evidence, however, to indicate the relation is linear. Accordingly, for geometries other than L/B = 1 and L/B = 6 the evaluation of bearing capacity must still employ deterministic shape factors.

Few experimental results exist on the effect of foundation roughness. Two series of tests by Ko and Davidson (1973) and Meyerhof (1955) are inconsistent. Ko and Davidson show a 10% to 20% reduction and Meyerhof a 40% to 50% reduction from $\delta = \bar{\phi}$ to $\delta = 0°$. Concrete foundations, however, are usually considered perfectly rough. This practice is substantiated by several series of tests (Meyerhof, 1961; and Potyondy, 1961) indicating $\delta/\bar{\phi}$ for sand-concrete interfaces greater than 0.80. The effect of roughness on bearing capacity for concrete foundations can therefore be neglected.

Aggregation of Uncertainties

Consideration of theoretical solutions and model footing tests well establishes Equations (5.5) and (5.6) for the prediction of ultimate bearing capacity. Statistical evaluation of the bearing capacity and correction factors allows estimates of the uncertainty in this prediction.

If the true values of $\bar{\phi}$, E/B, and H/B are known, the uncertainty in bearing capacity is from model uncertainty alone. First-order second-moment approximation yields

$$E[q_{v,\alpha}] \simeq (\tfrac{1}{2}\gamma BS_\gamma R_\gamma) E[N_\gamma] E[E_\gamma] E[I_\gamma] \tag{5.22}$$

$$V[q_{n,\alpha}] \simeq \sum_{i=1}^{n} \sum_{j=1}^{n} \frac{\partial q_{v,\alpha}}{\partial X_i} \frac{\partial q_{v,\alpha}}{\partial X_j} C[X_i,X_j] \tag{5.23}$$

where x_i represents the parameters N_γ, E_γ, and I_γ and the derivatives are taken at the mean. Treating the parameters as uncorrelated:

$$V[q_{v,\alpha}] \simeq \sum_{i=1}^{n} \left[\frac{\partial q_{v,\alpha}}{\partial X_i}\right]^2 V[X_i] \tag{5.24}$$

For $L/B = 6$ and $L/B = 1$ the value of N_γ is available and S_γ is not necessary. Similarily, if the load is not eccentric or inclined, E_γ and I_γ are omitted.

Although Equations (5.22) through (5.24) are for known parameters, the expressions for $V[X_i]$ (Equations 5.14, 16, 16, 18, and 20) include some parameter uncertainty (σ_ϕ^2, $\sigma_{E/B}^2$, and $\sigma_{H/V}^2$) from the laboratory tests. In other words, not all the uncertainty is due to the models. For laboratory experiments with carefully placed sand and measured loads, however, the parameter uncertainty is assumed small relative to the model uncertainties $\sigma_{N_\gamma}^2$, $\sigma_{E_\gamma}^2$, and $\sigma_{I_\gamma}^2$.

In practice, the true values of $\bar{\phi}$, E/B, and H/V are seldom known. Uncertainty exists in $\bar{\phi}$ from spatial variations and from testing errors. Uncertainties in E/B and H/V arise from errors in estimating the magnitude and line of action of applied loads. The expressions for variance can be modified to include parameter uncertainty in the form:

$$V[N_\gamma]_{L/B=6} = \exp\{-3.292 + 0.346(m_{\frac{-}{\phi}}) + 0.030(\frac{2}{\phi})\}\cdot$$

$$\{\exp\{0.042 + 0.030(\sigma\frac{2}{\phi})\} - 1\} \qquad (5.25)$$

$$V[N_\gamma]_{L/B=1} = \exp -4.128 + 0.346(m_{\frac{-}{\phi}}) + 0.030(\sigma\frac{2}{\phi})$$

$$\{\exp\{0.086 + 0.030(\sigma\frac{2}{\phi})\} - 1\} \qquad (5.26)$$

$$V[E_\gamma] = 0.0058 + [6.06(m_{E/B}) - 3.50]^2\sigma^2_{E/B} \qquad (5.27)$$

$$V[I_\gamma] = 0.0089 + [2.72(m_{H/V}) - 2.41]^2\sigma^2_{H/V} \qquad (5.28)$$

Figures 5.12 and 5.13 illustrate the effect of parameter uncertainty on the standard deviation $(S[\cdot])$ of N_γ, E_γ, and I_γ.

For a deterministic applied vertical stress, $q_{v,a}$, a second moment analysis of the factor of safety yields:

$$E[FS] \simeq E[q_{v,a}]/q_{v,a}$$

$$V[FS] \simeq V[q_{v,a}]/q_{v,a}^2 \qquad (5.29)$$

If uncertainty exists in the applied load, the moments of the factor of safety are evaluated from:

$$E[FS] \simeq \frac{E[q_{v,a}]}{E[q_{v,a}]} + \frac{E[q_{v,a}]}{E[q_{v,a}]^3} V[q_{v,a}] \qquad (5.30)$$
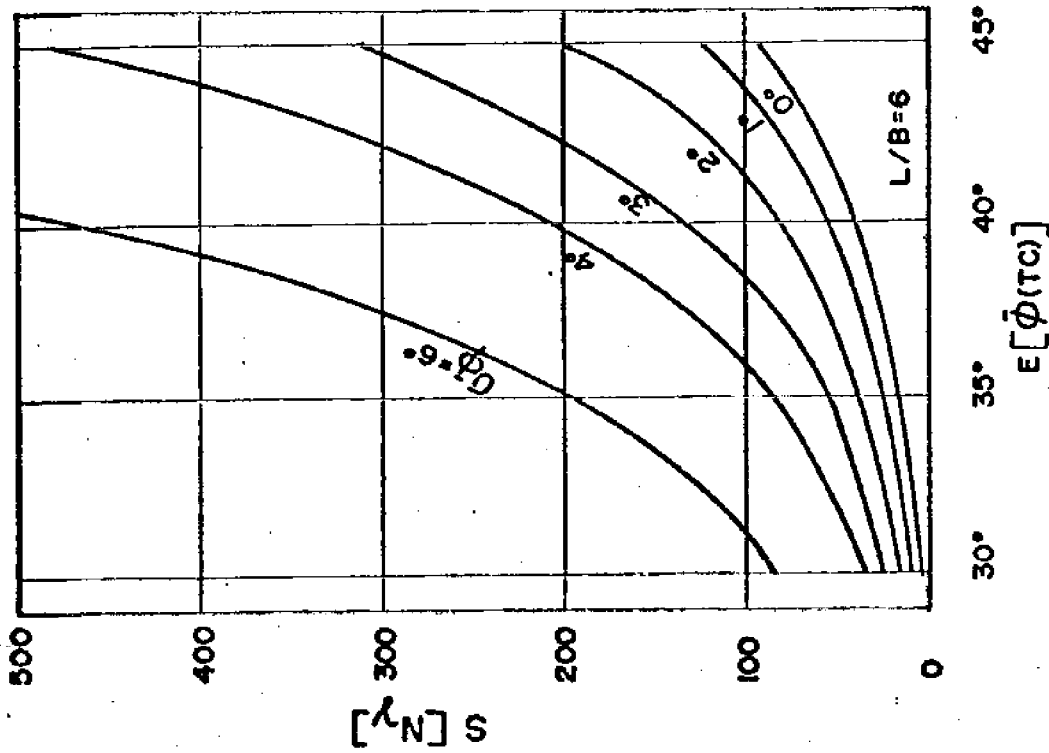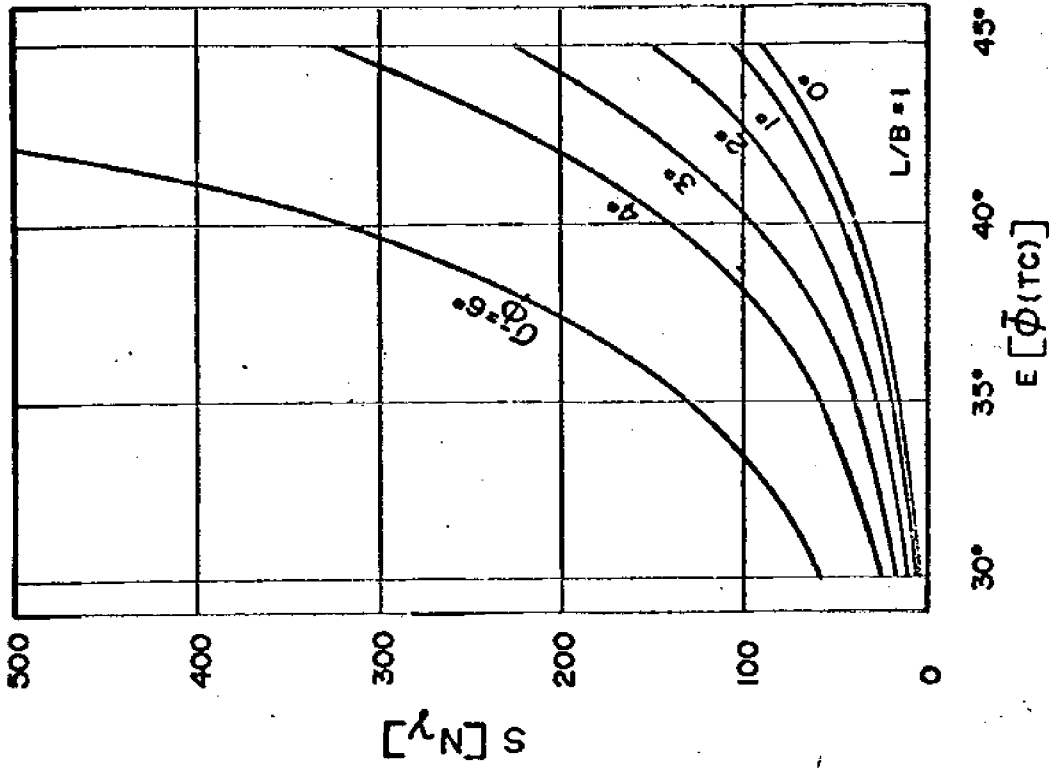
Figure 5.12. -- Effect of parameter uncertainty on the standard deviation of N_γ.
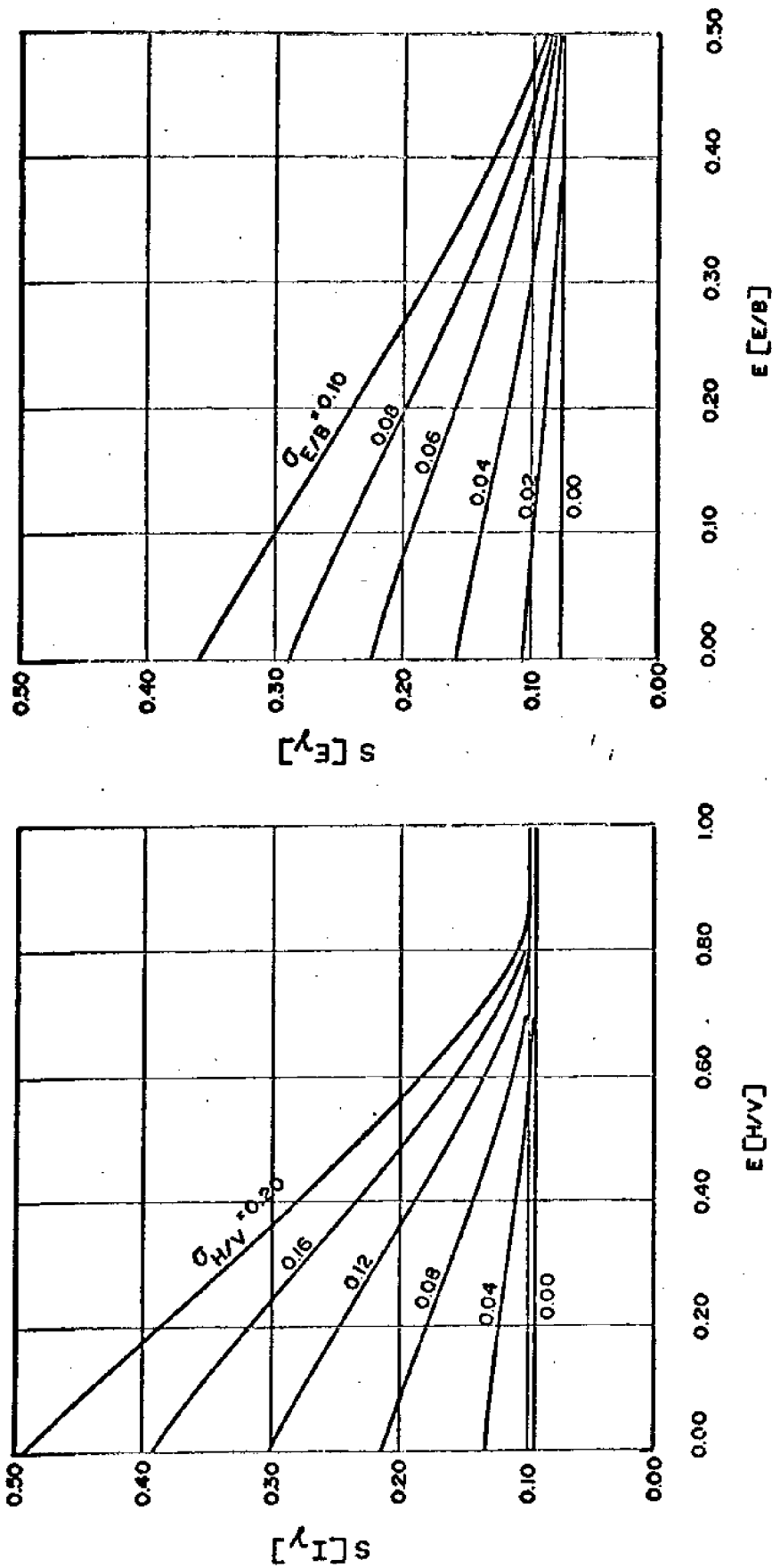
Figure 5.13 -- Effect of parameter uncertainty on the standard deviations of E_γ and I_γ.

$$V[\text{FS}] \quad \frac{V[q_{v,\alpha}]}{E[q_{v,a}]} + \frac{E[q_{v,\alpha}]^2}{E[q_{v,a}]^4} \quad V[q_{v,a}] \qquad (5.31)$$

assuming no correlation between $q_{v,\alpha}$ and $q_{v,a}$.

The following examples illustrate the effects of uncertainty on the bearing capacity factor of safety and probability of failure.

Example

Consider the basic cases of a strip and circular or square footing subject to a vertical, concentric load. From Equations 5.22 and 5.23 the expected value and variance of the ultimate bearing capacity are:

$$E[q_{v,\alpha}] \simeq (\tfrac{1}{2}\gamma BR_\gamma) \, E[N_\gamma] \qquad (5.32)$$

$$V[q_{v,\alpha}] \simeq (\tfrac{1}{2}\gamma BR_\gamma)^2 V[N_\gamma] \qquad (5.33)$$

For a deterministic applied stress the coefficient of variation of the factor of safety is:

$$COV[\text{FS}] = V^{\frac{1}{2}}[N_\gamma]/E[N_\gamma] \qquad (5.34)$$

$$= COV[N_\gamma] \qquad (5.35)$$

Equations (5.13) and (5.15) for $E[N_\gamma]$ and Equations (5.25) and (5.26) for $V[N_\gamma]$ give the coefficients of variation for factor of safety shown in Table 5.2.

Parameters			$E[FS] \sim \Lambda(m_{\ell n\ FS}, \sigma_{\ell n\ FS})$	
L/B	$\sigma_{\bar{\phi}}$	COV[FS]	$p_f = 10^{-4}$	$p_f = 10^{-2}$
6	0°	0.21	2.0	1.6
6	1°	0.28	2.8	2.0
6	2°	0.44	5.3	3.0
6	3°	0.69	12.3	5.0
1	0°	0.30	3.0	2.0
1	1°	0.36	4.0	2.4
1	2°	0.51	6.6	3.5
1	3°	0.74	14.5	5.8

Table 5.2 -- Comparison of COV(FS) and p_f for a vertical concentric function load.

Probabilities of failure, given $E[FS]$, and $COV[FS]$, are taken from a logNormal distribution on FS. This assumption reflects the logarithmic relation of N_γ to $\bar{\phi}$. The $[FS]$'s leading to $p_f = 10^{-4}$ and 10^{-2} are given for various $COV[FS]$'s. However, the sensitivity of p_f to distribution assumptions is shown in Figure 5.14. Increase in $COV[FS]$ due to uncertainty in $\bar{\phi}$ is shown in column two.

One must be cautious in expressing uncertainty as probability of failure. Unlike FS, which is widely accepted as an index of safety rather than a statement of deterministic truth, p_f is commonly interpreted to be what it says, the probability of failure. This is not true: p_f is a conditional probability of failure, given the model being used and a number of other strong assumptions. Thus, p_f too is only an index of safety. It is a more descriptive index than FS since it includes variance in the prediction, but it is not a global probability of failure. For this reason the realiability index, β, has been introduced, such that

$$\beta = \frac{E[FS] - 1.0}{\sqrt{V[FS]}} \qquad . \tag{5.36}$$

The uncertainty in predicted bearing capacity increases as additional correction factors are included. To illustrate the effects of inclination and eccentricity consider the specific example of a strip footing with the parameters: $\bar{\phi} = 37°$, $\gamma = 120\text{pcf}$, $B = 5'$, $H/V = 0.3$, $E/B = 0.1$, and $R = 0.43$. The appropriate correction factors for no parameter uncertainty are:
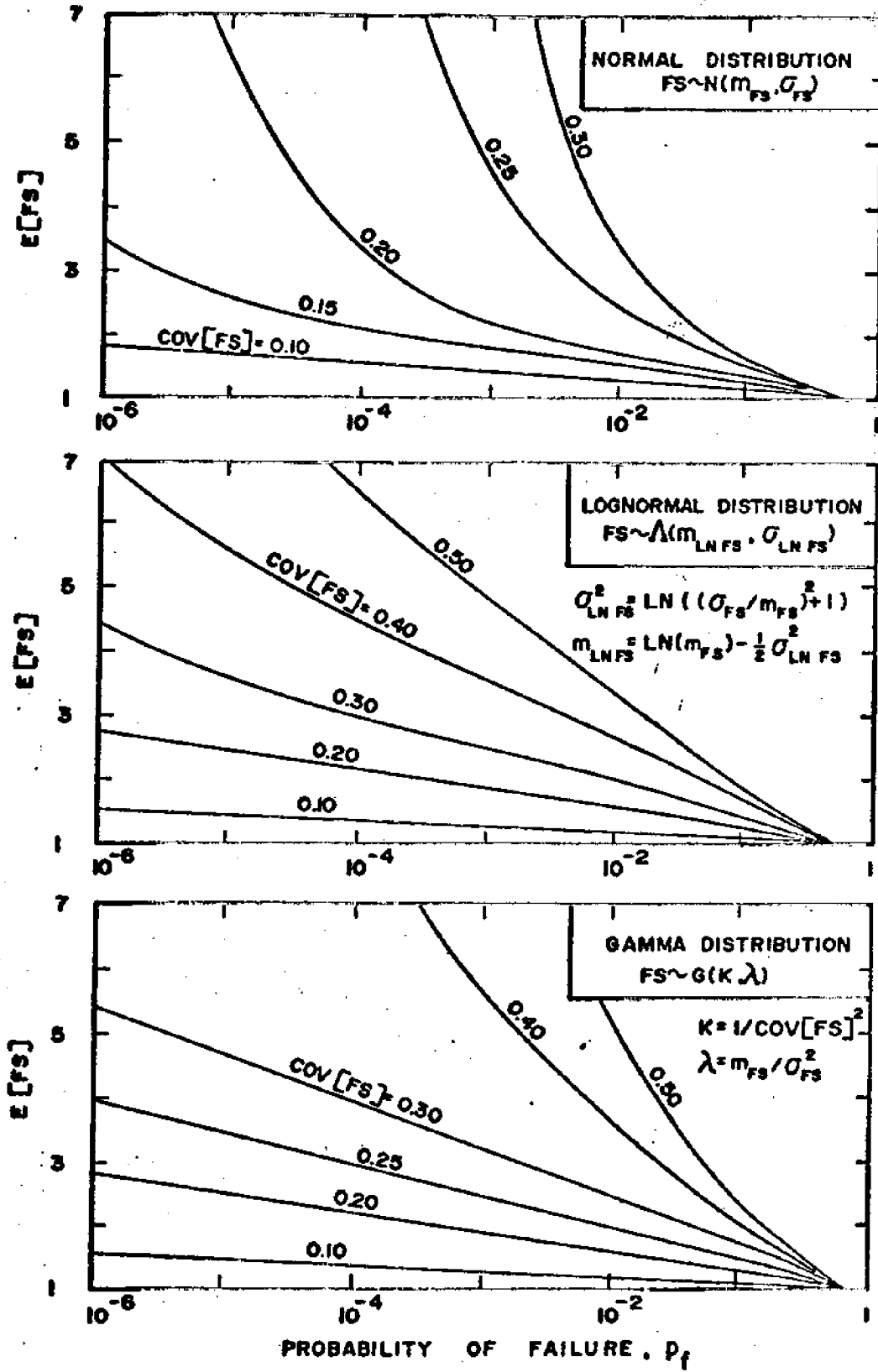
Figure 5.14 -- Probability of failure as a function of reliability index for Normal, logNormal, and Gamma pdf's.

$$E[N_\gamma] = 116 \qquad\qquad V[N_\gamma] = 579$$

$$E[E_\gamma] = 0.68 \qquad\qquad V[E_\gamma] = 0.0058$$

$$E[I_\gamma] = 0.40 \qquad\qquad V[I_\gamma] = 0.0089$$

From Equations (5.22) and (5.23),

$$E[q_{v,\alpha}] = 2.1 \text{ tsf} \quad (1.0 \text{ tsf})$$

$$V[q_{v,\alpha}] = 0.5 \text{ tsf}^2 \quad (0.12 \text{ tsf}^2)$$

$$COV[q_{v,\alpha}] = 0.34 \qquad (0.34)$$

where the parenthetical numbers correspond to the submerged condition. The addition of moderate load inclination and eccentricity, increases the uncertainty by 60% (o.34/0.21).

If parameter uncertainty is included as $\sigma_{\bar\phi} = 1°$, $\sigma_{E/B} = 0.01$, and $\sigma_{H/V} = 0.033$, the expectation remains the same but the correction factor variances increase to

$$V[N_\gamma] = 1040$$

$$V[E_\gamma] = 0.0066$$

$$V[I_\gamma] = 0.0114$$

and the coefficient of variation in the factor of safety increases from 0.34 to 0.40.

The uncertainty in FS also increases with uncertainty in the applied loads. Moreover, uncertainty in loads necessitates reconsideration of the definition of FS. For the previous conditions, failure surfaces as a

function of applied horizontal (H) and vertical (V) load are shown in Figure
5.15. These are the locii of $q_{v,\alpha} = q_{v,a}$; bounding lines are $\pm$ one
standard deviation. Again, $\sigma_{\bar{\phi}} = 0$.

For the expected loads of point A the FS against failure by increase
of the vertical load is 5.3; against failure by increase of the horizontal
load, 1.4. These FS's leave little feeling for the actual uncertainty
shown here as contours of a hypothesized joint distribution on H and V.
The uncertainty is whether the realized loads will fall outside the failure
envelope (see Section 6.3.2). Given the computational difficulty of
integrating over the density function of (H,V), relativity may be indexed
by the closest distance to the failure envelope measured in units of the
standard deviation (e.g., Rackwitz, 1976). Here, H and V are taken inde-
pendent with the same variances, however extension to correlated variables
with different variances is straight-forward. Including uncertainty in
both the loads and failure envelope, the reliability index becomes

$$\beta = \frac{380}{\sqrt{150^2 + 200^2}} = 1.52$$

where 380 is the minimum distance from A to the failure envelope and 150
and 200 are the standard derivations of load and failure envelope, respec-
tively.

Conclusions

An extention of the Terzaghi (1943) superposition method for bearing
capacity has been considered. Where possible, data have been analyzed with
statistical methods to draw conclusions on the uncertainty in the parameters
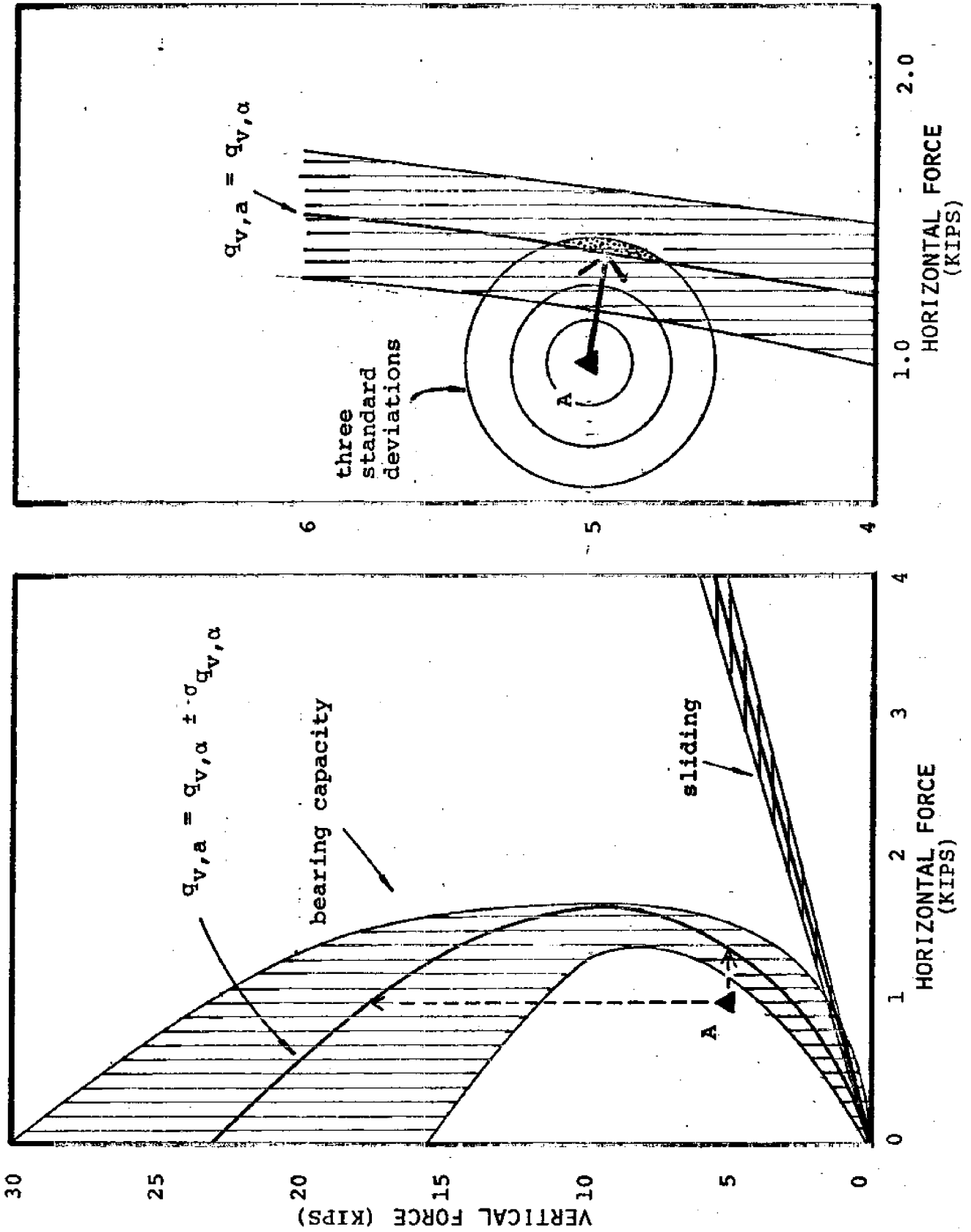
Figure 5.15 -- Failure surfaces for footing stability with an inclined load.

of that method. From this investigation the following conclusions are advanced.

(1) Theoretical consideration of ultimate bearing capacity of foundations on cohesionless soil leads to large variation among solutions. Variations by factors of two to four are typical. Proposals for N_γ and I_γ display greatest differences.

(2) Sufficient data exist to statistically analyze N_γ, I_γ, and E_γ. However, at present there are insufficient data to statistically analyze effects of foundation size, shape, and roughness on bearing capacity. At present levels of knowledge, substantial and unquantifiable uncertainty derives from size effect.

(3) Primary uncertainty seems to derive from the relationships of N_γ to $\bar{\phi}$ and I_γ to H/V. If $\bar{\phi}$ can be estimated to within $\pm 2°$ ($\sigma_{\bar{\phi}} = 1.0°$), incremental uncertainty in N_γ is small. For greater than about $1°$, incremental uncertainty in N_γ rapidly becomes large, and uncertainty in $\bar{\phi}$ becomes the controlling variable.

(4) For combined vertical and horizontal loads, a FS based on either V or H individually may be an inadequate characterization of safety when the loads are uncertain.

5.2.2 Analytical Modeling of Stability

The procedure of the preceding section for predicting stability is a partly theoretical, partly empirical approach based on the calibration of a simple formulae to observed case histories. Another approach is purely analytical. That is, the geometry of the foundation design and sedimentary zoning is modelled and various potential failure surfaces examined to identify the weakest.

Procedures for analyzing stability directly are usually based on finite element techniques or on limiting equilibrium procedures. Because FEM models are essentially addressed to deformations, they are considered in Section 5.3.2. Attention here is focused on limiting equilibrium models, as for example the various methods of slices, in their application to bearing capacity. While such techniques are uncommon in analyzing small footings, they are increasingly used as foundation dimensions increase (e.g., Lauritzsen and Schjectre, 1976). The main focus here is to assess the level of uncertainty in predictions of bearing capacity made with limiting equilibrium models and to compare that with uncertainties using Terzaghi's superposition method.

Most of the work on stability analysis using various methods of slices has been done for slope stability studies. The comparitive accuracy of these methods has been discussed by Whitman and Baily (1967) among other places. In these methods the sliding mass of sediment is arbitrarily divided into vertical slices and a force equilibrium taken on each. This leads to forces along the surface of assumed sliding, which are vectorily added to obtain a resisting force, and compared to the total driving force to obtain a factor of safety.

The problem with methods of slices, and the reason for there being several such methods, is that the physical system is indeterminant. Unless deformation properties of the sediment are considered, assumptions must be made to reduce the number of unknowns, and different assumptions lead to different factors of safety. Therefore, even if strength parameters for the sediment are well-known, modeling errors are possibly substantial. However, because the sediment properties are never well-known it is difficult to separate out parameters and model error in case studies.

Furthermore, sediment parameter estimates are often made with the modeling procedure in mind and may change with changes of model.

Probabilistic analysis of slice models have been made by a comparitively small number of workers (e.g.; Yuceman and Tang, 1975; Matsuo 1976; Tobutt and Richards, 1979). Primarily, these have treated soil properties as lumped parameters rather than stochastic variables. Typical results are given in Table 5.3. Alonzo (1976) and Peintinger, et al. (1980) have considered slice models with spatially variable soil properties. These results are also given in the table.

Analyses were performed to see whether similar coefficients of variation are obtained for the bearing capacity case. The geometry of Figure 5.16 was assumed, and various trial failure surfaces investigated. All of the failure surfaces begin as a triangular wedge beneath the footing and extend through a log-spiral into a linear tangent which finally intersects the midline. Soil friction angle ($\tan\bar{\phi}$) was taken to be a stationary random field and $\bar{c}$ was assumed negligible. This is in fact not a good assumption (e.g., Section 5.2.1), as $\bar{\phi}$ reduces with increasing confining pressure. Therefore, the friction angle should be lower immediately beneath the foundation than at other locations on the failure surface. This could be analyzed using a trending mean model of spatial variation, but was not. Reliability coefficients for the minimum reliability failure surface using the modified Bishop and Fellineas methods are shown in Figure 5.17 as a function of autocorrelation length. Summing $r_o \simeq 30m$ leads to $r_o/\beta \simeq 0.3$ and coefficients of variation of FS against stability failure on the order of 6 to 10%. Note, this uncertainty is due only to spatial parameter variation, and not modeling uncertainty.

Table 5.3 — Variations in Calculated Factors of Safety Among Various Method of Slices Procedures*

Slope 3.5:1, Pore pressure factor u/γh=0

	strength factor $\gamma H(\tan\phi)/c$					
	0	2	5	8	20	50
Log Spiral	1.00	1.00	1.00	1.00	1.00	1.00
Ordinary Method	1.00	0.94	0.94	0.95	0.96	0.98
Bishop	1.00	1.00	1.00	1.00	1.00	1.00
Force Equilibrium (Lowe and Karafiath)	1.09	1.02	1.01	1.00	1.00	1.00
Janbu General formula	1.00	--	1.00	--	1.00	1.00
Morgenstern-Price and Spencer F(x)=C	1.00	1.00	1.00	1.00	1.00	1.00

Slope 3.5:1, Pore pressure factor u/γh=0.6

	strentth factor $\gamma H(\tan\phi)/c$					
	0	2	5	8	20	50
Log Spiral	1.00	1.00	1.00	1.00	1.00	1.00
Ordinary Method	1.00	0.91	0.75	0.68	0.57	0.50
Bishop	1.00	1.00	1.00	1.00	0.99	0.99
Force Equilibrium	1.09	1.03	1.02	1.01	1.00	1.00
Janbu	1.00	--	--	--	--	--
Morgenstern-Price	1.00	1.00	1.00	1.00	1.00	1.00

* From Duncan, J.M. and S.G. Wright (1980). Accuracy of equilibrium methods of slope stability analysis," Engineering Geology, v16 (1,2):5-19.
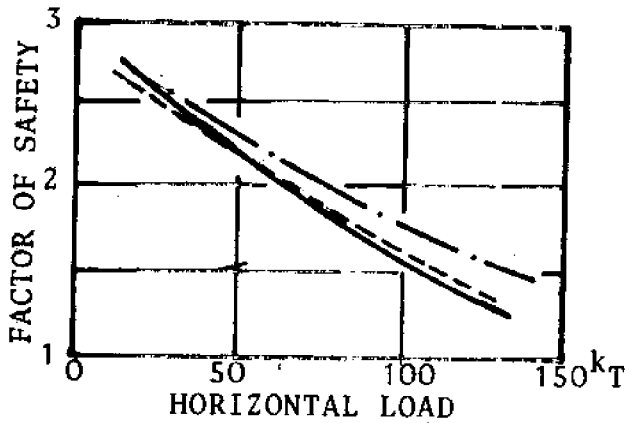
Figure 5.17 -- Comparisons of various stability models for bearing capacity (above from Lauretzsen and Schjetue, 1976) and for slope stability (below, from Whitman and Bailey 1967).
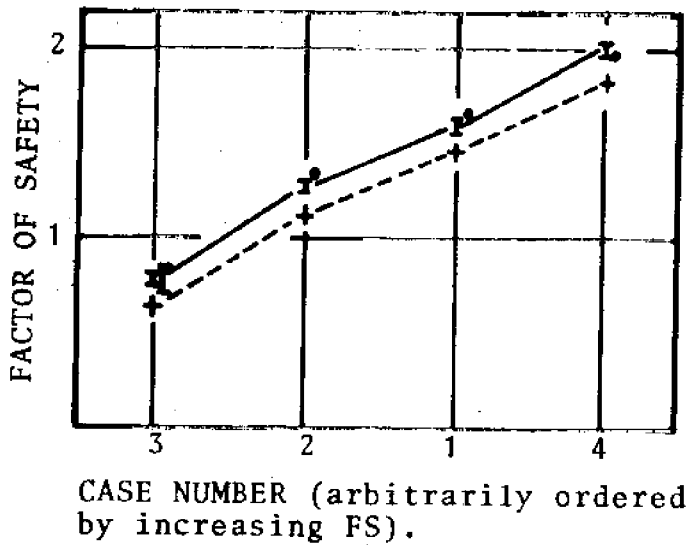
CASE NUMBER (arbitrarily ordered by increasing FS).
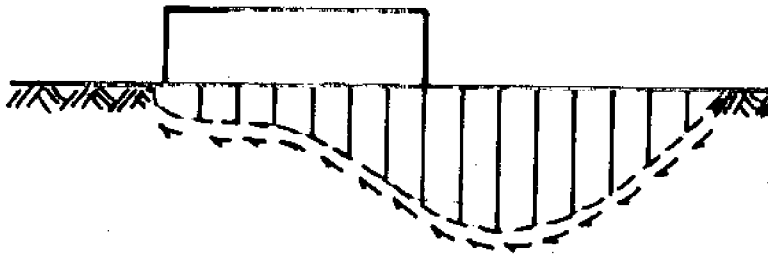
Figure 5.16 -- Typical configuration for stability analysis using methods of slices

5.3   Deformation Modeling

Deformation of the foundation of a gravity structure is induced both
by the static weight of the structure and by transient loading. As the
latter are dynamic, the analysis of deformation under them is more involved
than under the static component itself. This section considers deformations
under static loads, and the influence of lateral (e.g., wave) loads on static
deformation.

Analyses of deformation are made either by simple semi theoretical
procedures calibrated by field data, or by numerical models based on elastic
or elastoplastic theory. The former have the advantage of field verifica-
tion, but the disadvantage of requiring extrapolation outside the domain of
calibration. The latter have the advantage of tailoring analyses directly
to the case at hand, but the disadvantage of being poorly verified by
case histories. These two approaches are discussed in Sections 5.3.1 and
5.3.2, respectively.

Under gravity (and cyclic) loads a structure induces deformations in
the underlying sediment mass which manifest as total and differential settle-
ments of the foundation (Figure 5.18). *Total settlement* means either the
vertical downward movement at a point on the foundation (e.g., δ_1 or δ_2),
or the averaged vertical displacement across a foundation. For flexible
foundations this movement may vary non-uniformly across the foundation area,
whereas for a perfectly rigid foundation the movement must define a plane.
Differential settlement means either the ratio of settlement differences
to their separation (e.g., $|\delta_1 - \delta_2|/\ell$) or the angle induced by the settlement
(e.g., arctan $(|\delta_1 - \delta_2|/\ell)$. In general, differential settlement is the
controling criterion of structural performance, although in deterministic
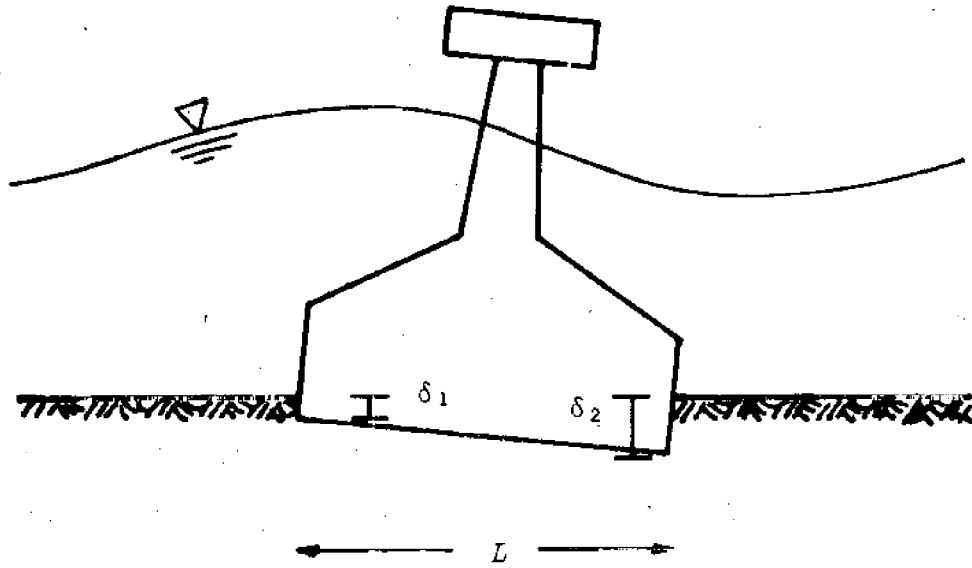
Figure 5.18 -- Illustration of total and differential Settlement for rigid foundation.

modeling differential settlement is difficult to predict. Thus, total settlement is often used as a surrogate criterion. This is not necessarily the case with probabilistic modeling. When structural connections such as piping or anchorages are involved, total settlememt may become a design consideration in its own right.

The Georges Bank site, as discussed earlier, consists of sands and gravelly sands to at least 100m, with minor inclusions of clays and peats. Therefore, delayed consolidation settlement under static loads is not considered here. The only settlements considered are immediate, and assume rapid, complete drainage. The issue of inclusions in an otherwise homogeneous mass are considered in Section 5.3.3.

5.3.1 Simple Settlement Formulae for Sands

A number of settlement formulae for the settlement of foundation on sands have been proposed in the literature. Primarily these formulae are based on variants of elastic theory and have been calibrated to observations on spread footings and model or plate-load tests. The question of extrapolating such results to exceedingly large mat-type footings is at issue, and to date has not been adequately dealt with through empirical verification. In principle, if not in fact, the arguments behind most of the settlement formulae are independent of scale.

Taxonomy of Simple Settlement Formulae

Settlement formulae for foundations on sand can be roughly grouped into five classes: Those based on 1) case penetration resistance, 2) standard penetration blow-counts, 3) laboratory tests, 4) field tests, and 5) elastic theory. This taxonomy is somewhat artificial, but useful. Methods based on finite element analysis or other numerical models are

considered separately. The review and evaluation of these formulae included those listed in Table 5.4.

The purpose of the analysis was to establish the magnitude of modeling error, both bias and random, associated with common formulae. The procedure for doing so was straightforward: empirical data were collected for a number of case studies and relative predictions and actual performances compared. For those formulae for which sufficient data were available, regression analyses were performed. The results are presented as expected regression lines (least square regressions in a classical sense), and as correlations among modeling errors. Joint regressions of model predictions on observed behavior are presented for use in the joint likelihood formulation of model uncertainty of Section 5.1.

In using empirical relationships to asses model uncertainty, both inherent and (regression) parameter uncertainty must be considered.

The expected regression line represents the model bias, while variation about the regression line represents random error. Because the number of data in many cases is insufficient to precisely establish the regression line, uncertainty in the regression parameters must be integrated out to form the broader "predictive" distribution.

It must be emphasized that the present evaluations are based on regression analyses of available data, nothing more. They therefore suffer all the limitations of regression analysis and must be viewed as such. More carefully instrumented case studies or more extensive data might change numerical conclusions. Nevertheless, given the present data, these results are the best that can be objectively inferred from the data alone. The application of these results to new cases rests on an assumption that

Table 5.4 -- Simple Settlement Formulae Considered in Data Evaluation

Buisman-DeBeer (1967)	$\rho = \sum_i \{1.535[(\frac{\sigma_{vi}}{q_c})\Delta z \ \log_{10}(\frac{\Delta\sigma_v + \sigma_{vi}}{vi})]$
Elastic Theory	$\rho = PBI/M$
Egorov (1957)	$\rho = 2aP \sum_{i=1}^{k} \frac{k_i - k_{i-1}}{E_i}$
Meyerhof (1965)	$\rho(in.) = C_w C_d \frac{2P}{N} [\frac{2B}{B+1}]^2$
Schmertmann (1970)	$\rho = \Delta P \int_0^{2B} \frac{I_z}{E_s} \simeq C_1 C_2 \Delta P \sum_0^{2B} \frac{I_z}{E_s} \Delta z$
Terzaghi and Peck (1948)	$\rho(in.) = C_w C_d \frac{3P}{N} [\frac{2B}{B+1}]^2$

a	half-width of footing
B	footing dimension
C_1	correction factor for embedment
C_2	correction factor for creep
C_d	correction factor for depth
C_w	correction factor for groundwater
E_s	subgrade modulus
I_z	influence factor
i	layer number
k_i	coefficient dependent on geometry
M	modulus of compressibility
N	blow count
P	average applied bearing pressure
q_c	cone resistance
ρ	settlement
σ_v	vertical stress

"corrected" means that blow counts or other in situ measurements have been corrected for overburden effect.

the data set on which they are based is homogeneous with the cases to which

they will be applied. In other words, that nature is uniform. This is

never precisely the case, but all engineering is based on similar faith.

In performing the analyses it was assumed that soil properties were

well-known. That is, that errors in penetration resistance, elastic param-

eters, and the like were negligible in comparison to model uncertainties.

In many but far from all of the case studies this may be true. Neverthe-

less, part of the error attributed here to model uncertainty comes in fact

from (geotechnical) parameter uncertainty. Then, if parameter uncertainty

is subsequently added to this model uncertainty the result is conservative.

The magnitude of this conservatism has not been estimated.

Procedure for Analyses and Results

Data on case studies available in the open literature were collected,

and settlement predictions using each of the 8 formulae made. In total these

comprised 48 cases of observed building settlements, and 48 load tests.

Observed settlements and respective predictions of the formulae are given

in Lee and Baecher (1979). In cases for which insufficient information

on geotechnical parameters were available to allow prediction with a par-

ticular formula, no prediction was made.

Univariate regression of predicted on observed settlement (i.e., to

infer the marginal likelihood function of Section 5.1) was made for each

formula, shown by the example of Figure 5.19. Results are given in

Table 5.5. Data on other methods were too few to allow reasonable

regression analyses.

Assuming predictions and observations to be jointly Normal, co-

efficients for the regression of observed on predicted settlement were also

obtained. These are shown in Table 5.6.
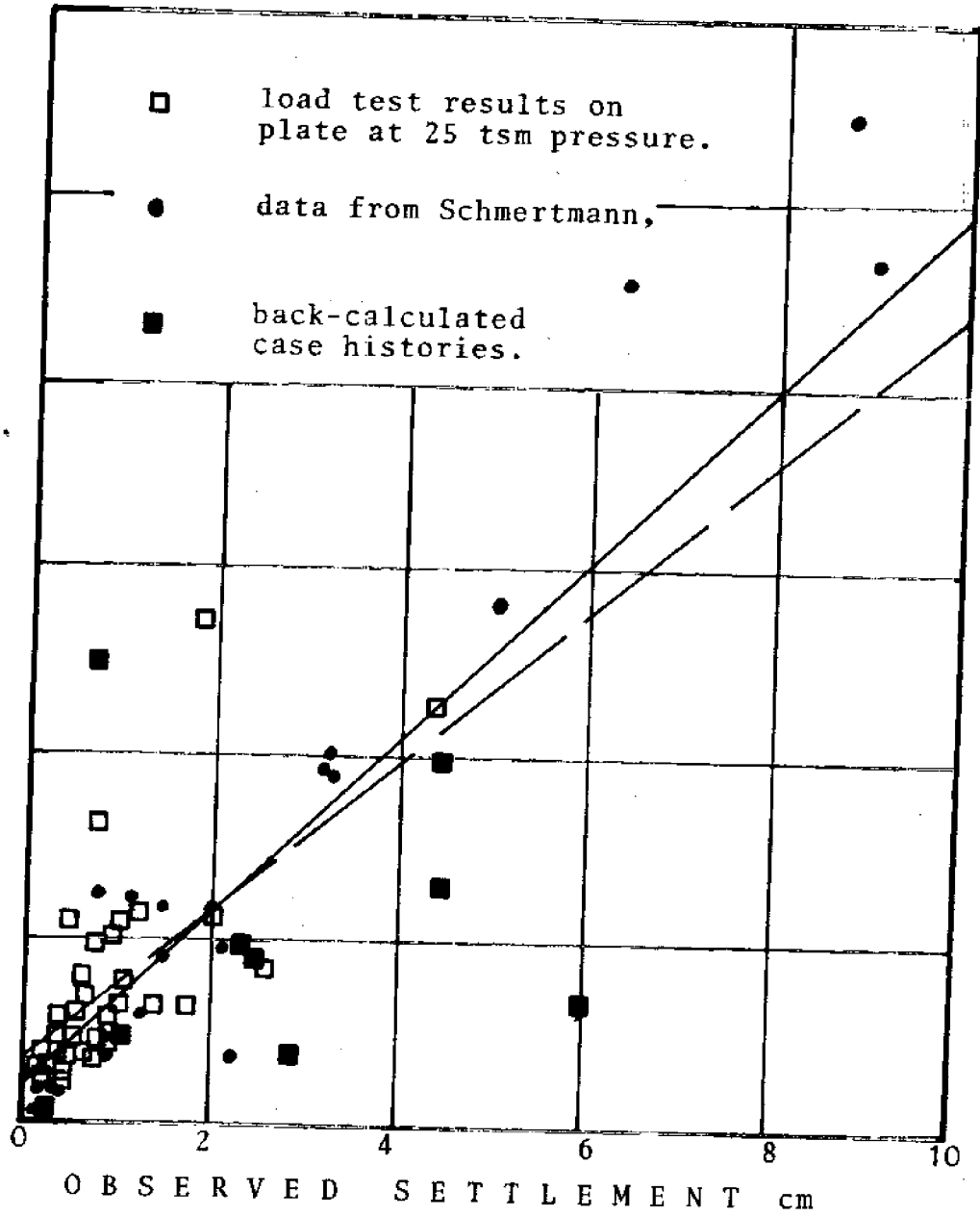
Figure 5.19 -- Relation between observed and predicted total settlement on sand, using Schmertmann's method.

Table 5.5: Regression Results for Marginal Function of Settlement Formulae

Formulae	β_1	β_2	σ_1	σ_2	t_1	t_2	R^2	σ	k
Schmertman	0.754	0.736	0.206	0.045	3.665	16.30	0.773	1.62	80
Buisman-DeB. (corr.)	0.851	0.684	0.594	0.089	1.431	7.71	0.598	3.07	42
Buisman-DeB.	0.483	1.468	0.515	0.112	0.938	13.15	0.663	4.27	90
Terzaghi and Peck (corr. N)	0.319	1.943	0.182	0.227	1.751	8.58	0.615	0.64*	48
Meyerhof	2.226	0.293	0.304	0.091	7.328	3.20	0.109	2.35	87
Meyerhof (corr.)	0.003	1.447	0.077	0.109	0.035	13.23	0.723	0.35	69
Elastic Theory	0.970	0.790	0.152	0.086	6.367	9.20	0.643	0.85	49
Ergorov	-0.047	1.393	1.669	0.084	0.028	16.61	0.968	4.35	11

*For small settlement data only.

Table 5.6 -- Regression results for simple footing settlement
with observed settlement as dependent variable.

Formula	a	b	e^2	n
Schmertmann	-0.28	1.05	2.00	80
Buisman-DeBeer	0.13	0.56	2 45	90
Buisman-DeBeer (corrected)	-0.02	1.13	5.01	42
Terzaghi and Peck (c)	0.16	0.32	0.03	48
Meyerhof	0.842	0.37	8.00	87
Meyerhof (c)	0.08	0.59	0.25	69
Elastic Theory	0.00	1.01	1.20	49
Egorov	0.19	0.71	3.01	11

$$y = a + bx + e$$

[These estimates are made indirectly, using the inverse regression
of predicted on observed settlement.]

Correlations among model uncertainties were examined from the inferred joint likelihood function. The regression model for the joint likelihood

$$\underline{x} = \underline{\beta}_1 + \underline{\beta}_2 y + e \quad , \tag{5.37}$$

where $\underline{x}$ is the vector of model predictions, y the observation, and $\underline{\beta}_1$ and $\underline{\beta}_2$ regression parameters, has the multiNormal error vector

$$e \sim MN(\underline{o}, \underline{\Sigma}) \quad , \tag{5.38}$$

where $\underline{\Sigma}$ is the covariance matrix. Were the models conditionally uncorrelated, the components of e would be independent, and $\underline{\Sigma}$ diagonal. However, $\underline{\Sigma}$ is not diagonal

Pairwise correlations were analyzed to obtain a posterior density function on the correlation coefficient, ρ, using Jeffrey's (1961) approximation,

$$f'(\rho \mid data) \propto \frac{(1-\rho^2)^{(\nu-2)/2}}{(1-\rho r)^{(\nu+1/2)}} \frac{1}{1} \tag{5.39}$$

where r is the sample correlation coefficient and ν the degrees of freedom $(\nu = k-2)$. A typical result is shown in Figure 5.20 for the high correlation between predictions of elastic theory and the Buisman -DeBeer (uncorrected) formulae; similarly in Figure 5.21 for the low correlation between the Buisman-DeBeer (corrected) and Schmertman methods. Most probable pairwise conditional correlations for all 8 models are given in Table 5.1. These are the modes of $f'(\rho \mid data)$.
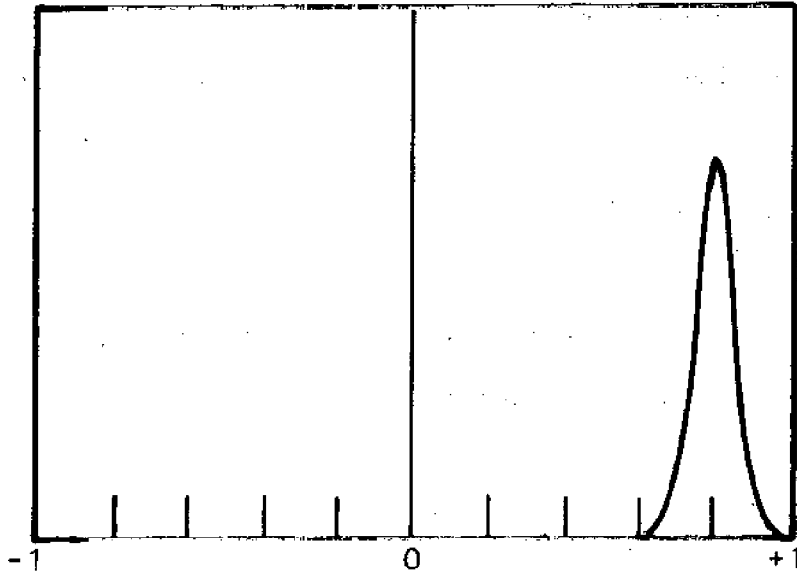
Figure 5.20 -- Empirical conditional correlation between predictions of elastic theory and the Buisman-DeBeer (uncorrected) method.
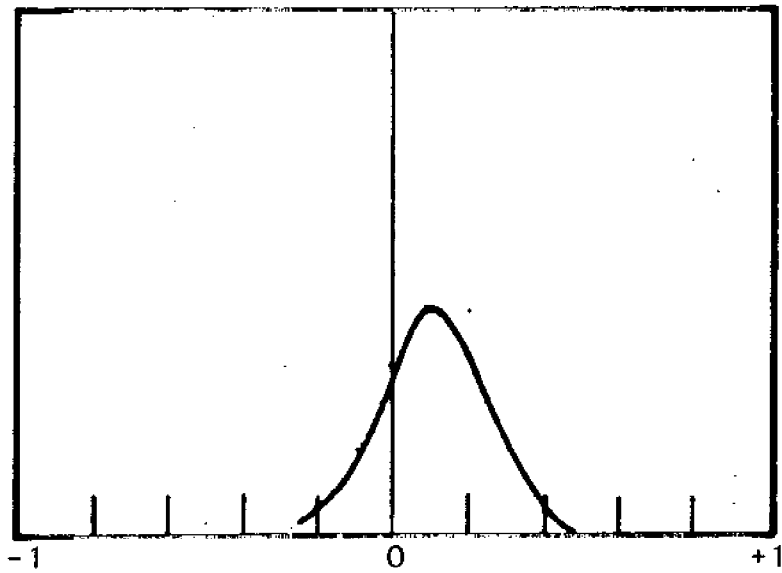
Figure 5.21 -- Empirical conditional correlations between predictions of Buismann-DeBeer (corrected) and Meyerhof Methods.

Differential Settlements

Within deterministic analysis differential settlements cannot be
estimated directly since sediment profiles are assumed (zonally) uniform
and all settlements are predicted to be the same. Therefore, following
Skempton and MacDonald (1956) predictions of differential settlement are
usually estimated to be some fraction of total settlement.

Skempton and MacDonald analyzed 98 case histories to draw conclusions
on the magnitude of differential settlements and on the consequences.
Grant, Christian, and Vanmarke (1972) introduced another 95 cases. In the
present work another 26 cases were identified. The relationship between
maximum differential settlement and maximum settlement is shown in Figure
5.22. These are similar to those relationships reported earlier.

Conclusions on The Accuracy of Simple Settlement Formulae

Neglecting the problem of extrapolating from footings to large mats
or other large foundations, the uncertainty in predictions of total settle-
ment by the methods analyzed would appear to have a coefficient of variation
of 100% or more. This does not include geotechnical parameter uncertainty,
and is corrected for systematic bias. Repeated analysis with more than
one method does not appreciably reduce this uncertainty due to high correla-
tions among models.

5.3.2 Numerical Modeling of Settlement

An alternative to semi empirical settlement formulae is large numerical
modeling. This type of modeling, based primarily on finite element tech-
niques, has to occupy a central role in the analysis of offshore gravity
structures (e.g., Zienkiewitz, et al., 1979).   The reasons are clear.
Analyses can be tailored to the particular design concept and geometry,
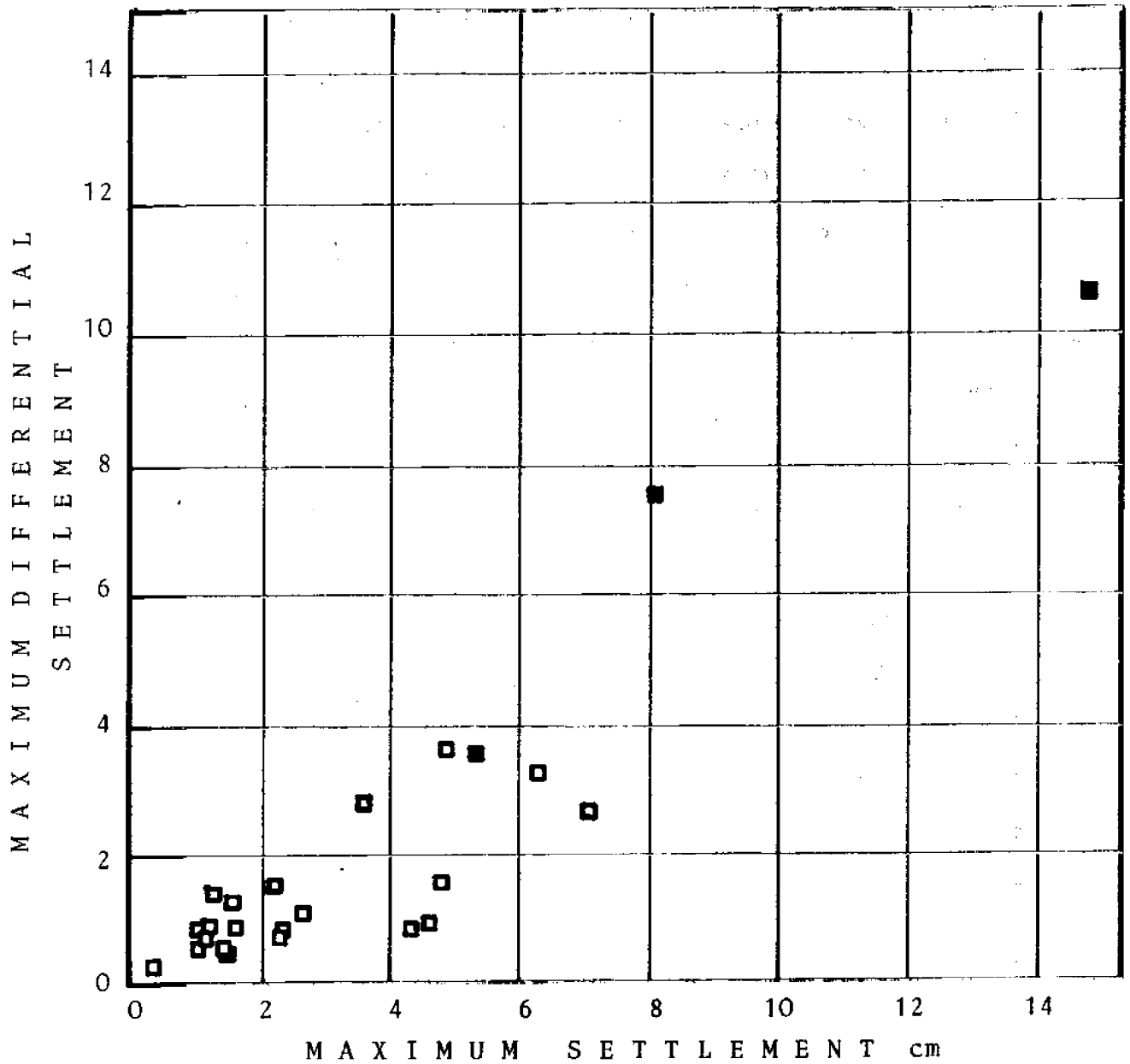
Figure 5.22 -- Additional data showing correlation between differential and total settlement. Open squares, foundations on sand; darkened squares, foundations on fill.

complicated constitutive relations can be incorporated, and a broad variety of loading conditions analyzed. There are also drawbacks: Empirical calibration or verification is difficult, parameter estimates are needed that may be difficult to obtain, and as many or more interrelated parameter estimates are sometimes needed as there are data.

Essentially all present uses of finite element techniques are deterministic. In conjunction with the lack of direct calibration data, this means that uncertainties in predictions of foundation performance are difficult to quantify. Therefore, a finite element technique was developed for incorporating stochastic variation of sediment properties and leading to second moment descriptions of deformations.

Previous Analytical Studies of Settlement Uncertainty

The literature contains several probabilistic models for the prediction of foundation deformations. These works are identifiable within three main groups:

(1) Models for estimating settlement on sand from standard penetration tests (Wu & Kraft (1967), Hilldale (1971), and Ramos (1976)).

(2) Models for estimating the consolidation settlement of clay (Resendiz & Herrera (1970), and Diaz & Vanmarcke (1974)).

(3) Finite element models for deformations of a discretized continuum (Su, et al. (1969), Cornell (1971), and Cambou (1975)).

Deterministic settlement analyses for sand typically use the standard penetration test and empirical models. Probabilistic methods employ similar concepts varying only in quantification of parameter uncertainty.

Hilldale (1971) develops a probabilistic model for total and differ-
ential settlement from approximate second moment analyses. Total settle-
ment is the summation of individual layer settlements from an elastic dis-
tribution of stresses. The spatial correlation of layer compressibilities
employs exponential decay autocorrelation functions. For a vertical
stress increment $\bar{\sigma}_{v_i}$, layer thickness Z_i, and coefficient of volume change
M_{v_i} for the ith layer, Hilldale gives the moments of total settlement as:

$$E[\rho] = \sum_{i=1}^{n} \bar{\sigma}_{v_i} Z_i E[M_{v_i}] \tag{5.40}$$

$$V[\rho] \simeq \sum_{i=1}^{n} \sum_{j=1}^{n} \bar{\sigma}_{v_i} \bar{\sigma}_{v_j} Z_i Z_j \sqrt{V[M_{v_i}]V[M_{n_j}]} \, \rho_{M_{v_i}, M_{v_j}} \tag{5.41}$$

Although developed for the standard penetration test, estimates of the
mean, variance, and covariance of compressibility using any measurement
technique could be used.

Ramos (1976) presents a probabilistic version of the empirical
Terzaghi and Peck (1967) settlement equation to include uncertainties in
the model, penetration resistance, and induced load. Using a multivariate
approximation and assuming the variables are mutually independent, the
expectation and coefficient of variation for total settlement are given as:

$$E[\rho] = K^* E[q_{v,a}]E[F] / E[N_{avg}] \tag{5.42}$$

$$COV[\rho] \simeq \sqrt{COV[q_{v,a}]^2 + COV[F]^2 + COV[N_{avg}]^2} \tag{5.43}$$

where: K^* = deterministic coefficient for effects of water table and

embedment

$q_{v,a}$ = applied vertical stress

N_{avg} = average standard penetration test resistance over B below

the footing

F = model bias correction factor ($E[F] = 0.28$, $COV[F] = 0.4$)

Wu and Kraft (1967) employ an earlier Terzaghi and Peck (1948) empiri-
cal correlation for the load necessary to cause a maximum settlement of one
inch. Based on limited evidence, penetration resistance and model un-
certainty are assumed to be Normally distributed. The distribution of
load necessary for one inch of settlement is then derived.

Resendiz and Herrera (1970) and Diaz and Vanmarcke (1974) develop
second moment probabilistic models for consolidation settlement of clay.
These models follow traditional deterministic settlement methods using a
layered soil profile and compressibility parameters from oedometer tests.
Resendiz and Herrera, however, neglect the spatial correlation of compress-
ibility. Moments for total settlement are similar to those given by
Hilldale (1971), except $\rho_{M_{v_i}, M_{v_j}} = 0$ for all $i \neq j$. Depending on auto-
correlation distance and layer thicknesses, this assumption leads to under-
estimates of the settlement variance: A more comprehensive treatment is
given by Diaz and Vanmarcke. This model yields first order approximations
with consideration of the spatial correlation of several soil properties
($\bar{\sigma}_{vm}$, CR, RR) and soil-structure interaction. The model is, of course,
more difficult to apply than those treating only compressibility as a random
variable.

The application of probabilistic techniques to finite element models has received some attention. Cornell (1971) describes the basic method of applying second moment analyses to finite element models. Cambou (1975) also discusses second moment analyses for finite element models and illustrates the effects of uncertainty in modulus and Poisson's ratio on stress and strain for a simple four element mesh. In particular, Cambou concludes the uncertainty in stress and strain can exceed the uncertainty in soil parameters. Uncertainty in vertical displacement, however, appears relatively insensitive to Poisson's ratio.

Su, et al. (1969) present a linear elastic finite element analysis of stresses around an underground opening with a stochastic simulation of rock properties. Modulus and Poisson's ratio are randomly generated for each element from normal distributions. Although unrelated to settlement problems, the results suggest an important conclusion applicable to approximate second moment analyses. For coefficients of variation as large as 0.20, the simulations show that stresses derived from expected values of uncertain parameters are not significantly different (statistically) from the expected stress from simulation:

$$E[\sigma \{\theta\}] = \sigma(E[\{\theta\}]) \qquad (5.44)$$

where $\{\theta\}$ is a vector of random variables containing modulus and Poisson's ratio. The results also indicate uncertainty in the stresses can exceed uncertainty in the rock properties.

Formulation of Settlement Models

The review of previous studies suggests probabilistic models are essentially extensions of deterministic procedures. The same design models are used, but the parameters are treated as random variables. Consideration of uncertainty is usually limited to inherent spatial variability and measurement error. Although some attempts have been made to include model uncertainty (Ramos, 1976), it is usually neglected.

Except for the finite element models, current methods are one dimensional. Equations expressing the mean and variance are only a function of properties below the point of interest. In other words, the equations of uncertainty are integrated over a line. In a two-dimensional formulation, moments are obtained by integration over the two-dimensional profile (Figure 5.23). Current probabilistic models use a deterministic distribution of stresses. The stress increment is typically calculated from elastic solutions for a homogeneous profile. Finite element models distribute stresses as a function of the random soil properties.

Soil properties for design are usually estimated from a number of laboratory and field tests. These tests provide a mean and variance for soil properties in each layer in a one-dimensional model or each element in a two-dimensional model.

Specimen dimensions are much smaller than the correlation distance of most properties. As a result, properties within a specimen are highly correlated. The dispersion of soil properties among specimens, therefore, is approximately the same as the dispersion of soil properties among points.

Settlement models discretize the soil profile into volumes much larger than the specimen dimensions. For any soil volume, therefore, spatial moments rather than point moments are necessary. Consider some soil property, u, to be a continuous function varying with depth as described by a one-dimensional (line) stochastic process. As shown by Papoulis (1965), the spatial moments are:

$$E[<u>_i] = E[u_i] \tag{5.45}$$

$$V[<u>_i] = \frac{1}{L_i^2} \int_a^b \int_a^b C[u_i,u_i] d\ell_i \, d\ell_i \tag{5.46}$$

$$C[<u>_i,<u>_j] = \frac{1}{L_i L_j} \int_a^b \int_c^d C[u_i,u_j] d\ell_i \, d\ell_j \tag{5.47}$$

Instead of modeling soil properties as a continuous process, Diaz and Vanmarcke (1974) present a convenient discritized form of Equations 5.45 through 5.47. For a known point (specimen) mean $E[u_i]$, variance $V[u_i]$, and correlation coefficient ρ_{u_i,u_j}, the spatial moments for homogeneous layers of constant thickness are:

$$E[<u>_i] = E[u_i] \tag{5.48}$$

$$V[<u>_i] = V[u_i] \left[\frac{1}{n^2} \sum_{a-1}^{n} \sum_{b=1}^{n} \rho u_{i_a},u_{i_b} \right] \tag{5.49}$$

$$C[<u>_i,<u>_j] = \sqrt{V[u_i]V[u_j]} \left[\frac{1}{n^2} \sum_{a=1}^{n} \sum_{b=1}^{n} \rho u_{i_a},u_{j_b} \right] \tag{5.50}$$

where n is the number of specimen size sublayers in each layer. Equation 5.49 shows the spatial variance to be equivalent to the product of the

point variance and a correlation coefficient correction factor. Diaz and
Vanmarcke (1974) treat this factor as a variance reduction factor, Γ_u^2:

$$V[<u>_i] = V[u_i]\Gamma_{u_i}^2 \tag{5.51}$$

or

$$COV[<u>_i] = COV[u_i]\Gamma_{u_i} \tag{5.52}$$

For perfectly correlated properties, $\rho_{u_{i_a},u_{i_b}} = 1.0$ for all a and b and
$\Gamma_u^2 = 1.0$. For perfectly uncorrelated properties, $\rho_{u_{i_a},u_{i_b}} = 0.0$ for all
a $\neq$ b and $\Gamma_u^2 = 1/n$. Actual soil properties have layer variances between
these extremes:

$$V[u_i]/n \overset{\leq}{=} V[<u>_i] \overset{\leq}{=} V[u_i] \tag{5.53}$$

The variance reduction factor is a function of the specimen thickness, layer
thickness, and correlation coefficient. Similarily, spatial covariance can
be written as:

$$C[<u>_i,<u>_j] = \sqrt{V[u_i]V[u_j]}\,\psi_{u_{i,j}}^2 \tag{5.54}$$

where ψ_u^2 is a covariance reduction factor modifying the point covariance to
a spatial covariance. The covariance reduction factor is a function of the
specimen thickness, layer thickness, correlation coefficient, and distance
between volumes in layers i and j.

Two dimensional finite element models require evaluation of spatial
moments for various element geometries and configurations. If the point

(specimen) mean, variance, and correlation coefficient are known for some property u, the two-dimensional spatial mean and variance for homogeneous elements are:

$$E[<u>_i] = E[u_i] \tag{5.55}$$

$$V[<u>_i] = V[u_i]\Gamma_u^2 \tag{5.56}$$

where Γ_u is now taken as a two-dimensional variance reduction factor. Figure 5.23 illustrates the variance reduction factor for a typical triangular element. Both isotropic and anisotropic autocorrelation show increasing Γ_u^2 with increasing b/a for a given ratio of R_o/X or R_v/X. This trend results since an increase in b/a for a given element dimension X increases the correlation between point within the element. As the correlation increases, Γ_u^2 approaches one.

Similarily, two-dimensional covariance reduction factors are shown in Figure 5.24. A typical element configuration is shown. The simulations are also compared with two approximations. The approximations $\exp(-D/R_o)$ or $\exp(-D'/R_v)$ use point variances and element centroids to determine ϕ_u^2. The second approximation, $\Gamma_u^2\exp(-D/R_o)$ or $\Gamma_u^2\exp(-D'/R_v)$, uses spatial variances and element centroids. The degree of approximation varies with how well the correlation between centroids represents the correlation between all points within the elements. The distribution of points around the centroid, therefore, is as important as the distance between centroids. As the correlation within an element increases or as the correlation between elements decreases the approximation improves.

Two-Dimensional Settlement Model

Modeling settlement by a linear elastic two-dimensional finite element
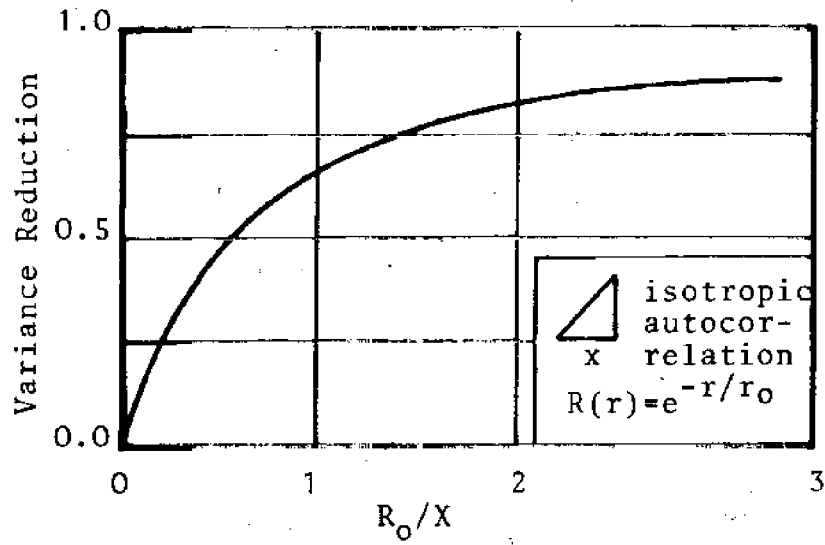
Figure 5.23
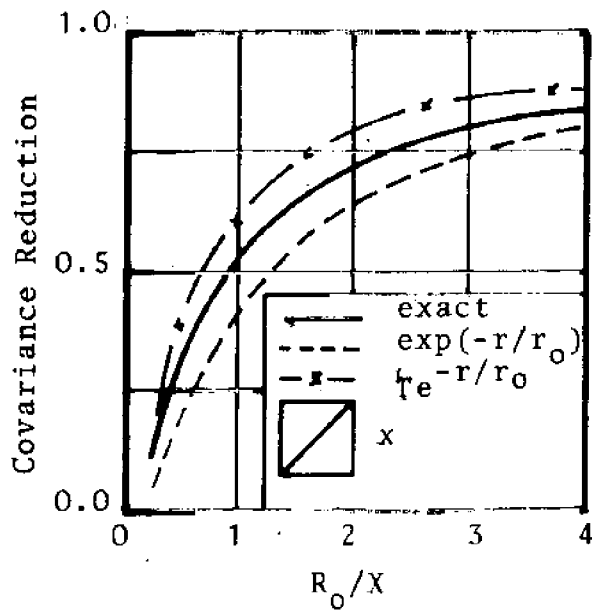
Figure 5.24

model requires solution of the system of equations (Zienkiewicz (1971)):

$$[K]\{\rho\} = \{P\} \tag{5.57}$$

Equation 5.57 relates the vector of unknown displacements $\{\rho\}$ to a vector of forces $\{\rho\}$ through the global stiffness matrix $[K]$. The expectation of the displacement vector from a first order approximation is:

$$E[\{\rho\}] \simeq E[K]^{-1}\{P\} \tag{5.58}$$

First order approximations for the variance and covariance require partial differentiation of the displacement vector with respect to modulus. Differentiating Equation 5.57 yields:

$$[K] \frac{\partial\{\rho\}}{\partial<M>_i} + \frac{\partial[K]}{\partial<M>_i}\{\rho\} = \frac{\partial\{P\}}{\partial<M>_i} \tag{5.59}$$

The force vector $\{P\}$ is independent of modulus reducing Equation 5.59 to:

$$[K] \frac{\partial\{\rho\}}{\partial<M>_i} = - \frac{\partial[K]}{\partial<M>_i}\{\rho\} \tag{5.60}$$

Rewriting Equation 5.60 for $\partial\{\rho\}/\partial<M>_i$ gives:

$$\frac{\partial\{\rho\}}{\partial<M>_i} = - [K]^{-1} \frac{\partial[K]}{\partial<M>_i}\{\rho\} \tag{5.61}$$

Substituting the terms $[K]^{-1}\{\rho\}$ for $\{\rho\}$ yields:

$$\frac{\partial\{\rho\}}{\partial<M>_i} = -[K]^{-1} \frac{\partial[K]}{\partial<M>_i} [K]^{-1}\{\rho\} \tag{5.62}$$

The solution of Equation 5.62 results in a n x m matrix of differentials of the form:

$$
\begin{bmatrix}
\dfrac{\partial \rho_1}{\partial <M>_1} & \dfrac{\partial \rho_1}{\partial <M>_2} & \dfrac{\partial \rho_1}{\partial <M>_3} & \cdots\cdots & \dfrac{\partial \rho_1}{\partial <M>_m} \\[2em]
\dfrac{\partial \rho_2}{\partial <M>_1} & \dfrac{\partial \rho_2}{\partial <M>_2} & & & \dfrac{\partial \rho_2}{\partial <M>_m} \\[1em]
\vdots & & & & \\[1em]
\dfrac{\partial \rho_n}{\partial <M>_1} & \dfrac{\partial \rho_n}{\partial <M>_2} & & & \dfrac{\partial \rho_n}{\partial <M>_m}
\end{bmatrix}
\qquad (5.63)
$$

where n is the number of displacements and m is the number of elements within the finite element mesh. With this matrix of differentials the n x n covariance matrix for total settlement is obtained from the first order approximation:

$$
C[\rho_k , \rho_\ell] \simeq \sum_{i=1}^{m} \sum_{j=1}^{m} \left. \frac{\partial \rho_k}{\partial <M>_i} \right|_{E[<M>_i]} \left. \frac{\partial \rho_\ell}{\partial <M>_j} \right|_{E[<M>_j]} C[<M>_i , <M>_j]
$$

$$(5.64)$$

The major difference between one and two-dimensional models is apparent. One-dimensional settlement is a function of vertical stress, layer thickness, and soil properties along a line below points of interest. Two-dimensional covariance is a function of the stress, soil properties and size of each element in the soil profile through $\partial \rho_k / \partial <M>_i$.

Second moment finite element analysis extends deterministic solutions to yield expressions of uncertainty. Indeed, for a first order approximation of $E[\{\rho\}]$, no additional computation is necessary. The global stiffness matrix only requires evaluation at the mean of modulus for each element. Formulation of the differential matrix and covariance matrix, however, introduce considerable computations. Treating Poisson's ratio deterministically simplifies these calculations. The terms of the global stiffness matrix reduce to the form:

$$k_{s,t} = \sum_{i=1}^{x} <M>_i \, \alpha_i \beta_i \qquad (5.65)$$

$$\frac{k_{s,t}}{\partial <M>} = \sum_{i=1}^{x} \alpha_i \beta_i \qquad (5.66)$$

where $k_{s,t}$ is a term in the global stiffness matrix $[K]$, x is the number of elements contributing to $k_{s,t}$, and α_i and β_i are coefficients from element dimensions and Poisson's ratio.

Assuming Poisson's ratio deterministic results in an underestimate of uncertainty. As shown by Cambou (1975), however, the uncertainty in settlement is relatively insensitive to Poisson's ratio. Specifically, for a deterministic modulus and random Poisson's ratio, Cambou indicates $COV[\rho]/COV[\rho] = 0.15$ and for a random modulus and deterministic Poisson's ratio $COV[\rho]/COV[M] = 0.80$. Although these results are particular to Cambou's model, the relative insensitivity of settlement to Poisson's ratio is apparent. Alternatively, similar results can be qualitatively shown from a second moment analysis of elastic solutions for settlement.

Expressing vertical settlement in the typical form (Poulos and Davis (1974)):

$$\rho \propto \frac{(1 - \nu^2)}{M}$$

(5.67)

and taking a first order approximation for variance yields the expression:

$$V[\rho] \propto \frac{(1 - \nu^2)}{E[M]^2} COV[M]^2 + \frac{4E[\nu]^4}{M^2} COV[\nu]^2$$

$$+ \frac{4(1 - \nu^2)}{E[M]^2} E[\nu]^2 COV[M] COV[\nu] \rho_{\nu,M}$$

(5.68)

Assuming $\rho_{\nu,M} = 1.0$ for maximum uncertainty and using $\nu = 0.33$ for illustration, Equation 5.68 becomes:

$$[\rho] = \left[(0.90 \, COV[M]^2 + (0.05) COV[\nu]^2 \right.$$

$$\left. + (0.40) COV[M] COV[\nu] \right]$$

(5.69)

This result, although qualitative, indicates that uncertainty in settlement is relatively insensitive to uncertainty in Poisson's ratio.

Differential Settlement

For this study the definition of differential settlement is (Figure 5.18):

$$\Delta\rho = |\rho_i - \rho_j|$$

(5.70)

To separate the symmetric settlement component from differential settlement it is convenient to express $\Delta\rho$ for nodes $i = 1$ and $j = 5$ (Figure 5.25).

Since differential settlement is an absolute value, distribution assumptions are necessary. Taken the settlement difference,

$$\Delta\rho_R = \rho_i - \rho_j \tag{5.71}$$

to be $\Delta\rho_R \sim N(0, V[\Delta\rho_R])$, the moments of $\Delta\rho$ become

$$E[\Delta\rho] = \sqrt{2/\pi \ V[\Delta\rho_R]} \tag{5.72}$$

$$V[\Delta\rho] = (1 - (2/\pi)) \ V[\Delta\rho_R] \tag{5.73}$$

Analysis of settlement Uncertainty

This section presents a comparison of one- and two-dimensional models for a uniform vertical strip load. Consideration focuses on two soil profiles:

(1) Homogeneous, constant mean modulus with depth

(2) Nonhomogeneous, modulus increasing as the square root of depth

In both cases Poisson's ratio is deterministic. A value of 0.33, typical of many sands, is assumed. For each profile the models are compared for: (1) the moments of total settlement, (2) correlation of total settlement, and (3) moments of differential settlement. The effects of isotropic and anisotropic autocorrelation are considered for two autocorrelation models.
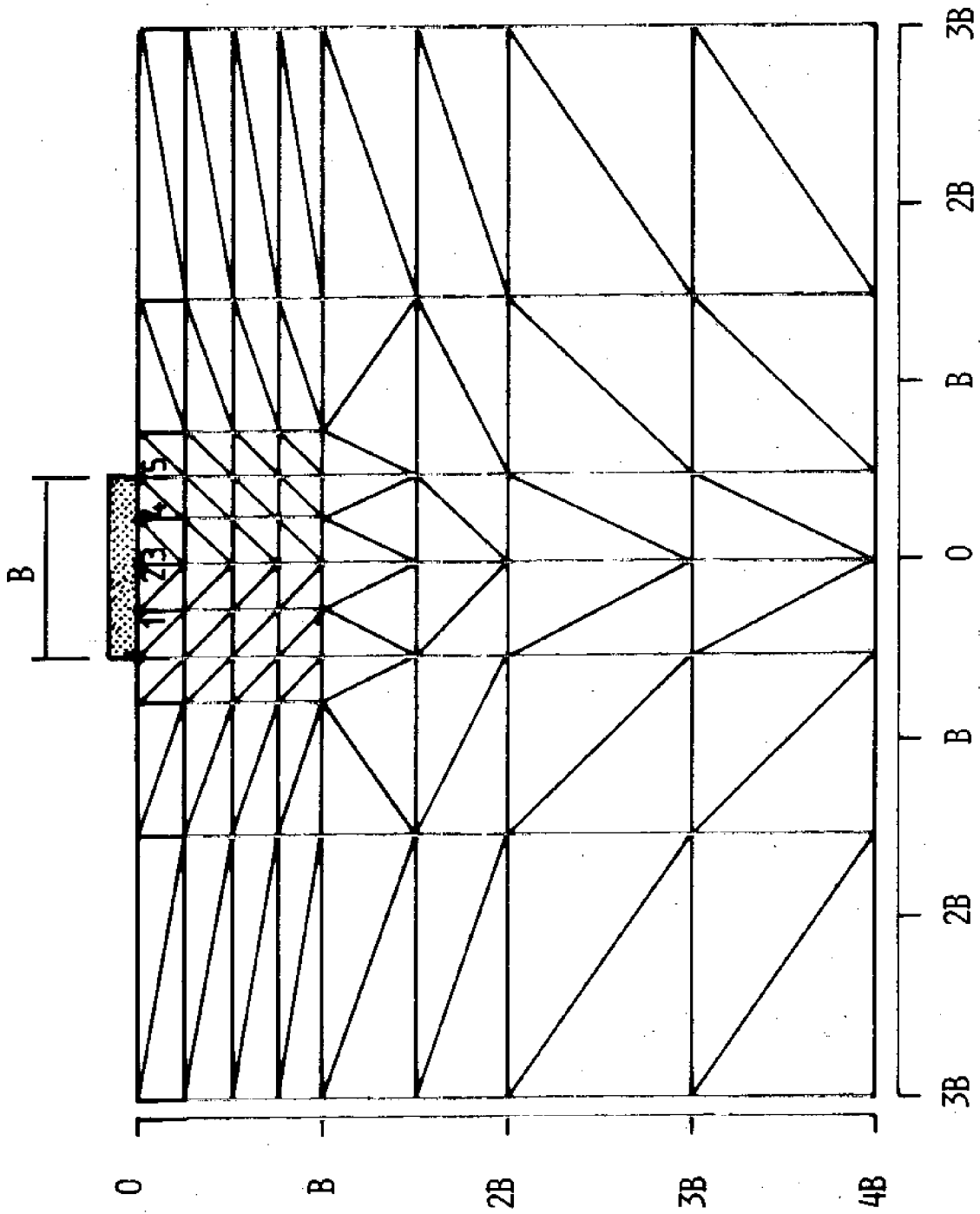
*Figure 5.25 -- Finite Element Net for
two dimensional settlement analyses.*

Profile boundary conditions and first order approximations to the
expected value of settlement are shown in Figures 5.25 and 5.26. The
coarse mesh and tight boundary dimensions minimize cost and computation
requirements. Elastic solutions indicate the stress on any boundary is
$\leq$ 15% of the applied load. In this regard, the finite layer approximates
a half space. The base is a fixed boundary. Lateral boundaries provide
horizontal restraint but allow vertical displacement. The one-dimensional
model uses the same base depth to facilitate comparison. For both
profiles the one-dimensional model yields expected values of settlement
which are 20% to 30% larger than those from the finite element model.
Comparison of the finite element model with half-space and finite layer
solutions shows good agreement.

Comparisons of one- and two-dimensional models for a homogeneous soil
profile are shown in Figure 5.27 through 5.29. Results are normalized
to the coefficient of variation $COV[M]$, autocorrelation distances R_o or
R_v, and the foundation width B. Element covariance is approximated by
applying the autocorrelation function to element or layer centroids.
Autocorrelation functions are shown on the figures.

Figure 5.27 presents a comparison of $COV[M]$ and $COV[\rho]$ for isotropic
autocorrelation structure. Several characteristics emerge:

(1) For $R_o/B = 0$ and $R_o/B \rightarrow \infty$, $COV[\rho] = 0$ and $COV[\rho] \rightarrow COV[M]$.
     These correspond to perfectly uncorrelated and correlated
     values of modulus.

(2) For other values of R_o/B, $COV[\rho]$ is a function of the model.
     The one-dimensional model consistently yields larger values
     than the two-dimensional model.

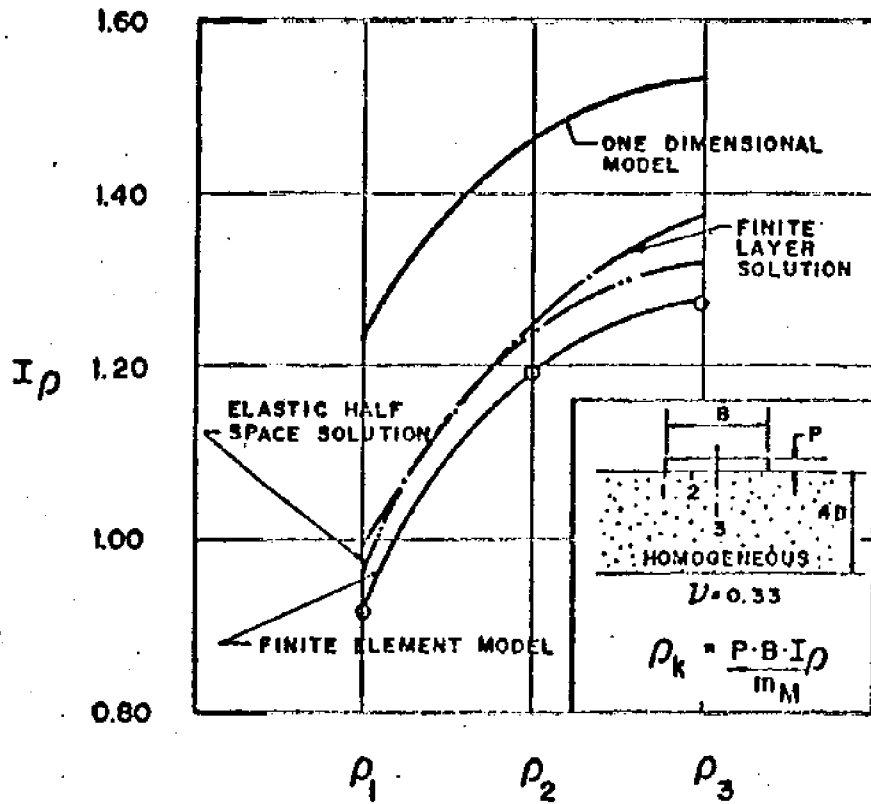*Figure 5.26 -- Expected total settlement for one and two dimensional models.*
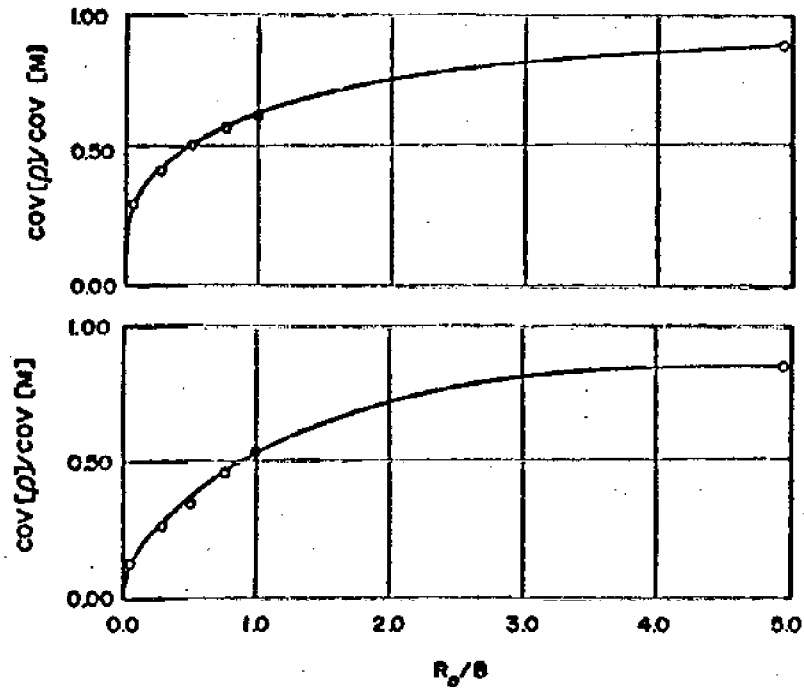
Figure 5.27 -- Normalized coefficient of variantion for one (above) and two (below) dimensional settlement as a function of autocorrelation distance.

(3)   The $COV[\rho]$'s for different points on the foundation are not

the same.   The maximum difference is 10% and varies with R_o/B.

This difference is neglected.

Correlation matrices for five points along the foundation are shown

in Figure 5.28.   In each case, two-dimensional correlation is much larger

than one-dimensional correlation.

Differential settlement is shown in Figure 5.29.   Larger variance

and smaller correlation in the one-dimensional model result in larger

differential settlement.   Both models display the interesting result of a

unique value of R_o which results in the largest differential settlement.

This "worst" autocorrelation distance occurs for R_o/B of 0.75 to 1.0.   For

$R_o/B = 0$, perfectly uncorrelated moduli, or $R_o/B \rightarrow \infty$, perfectly correlated

moduli, differential settlement is zero.

Anisotropic autocorrelation effects on differential settlement for

$R_h = 10R_v$ are shown in Figure 5.30.   Figure 5.31 shows the minor effect of

changing the autocorrelation model.

Comparisons of one- and two-dimensional models for the nonhomogeneous

profile are shown in Figures 5.32.   Analyses are identical to the homogen-

eous soil profile.

While similar characteristics exist, three specific differences emerge.

The nonhomogeneous profile yields larger $COV[\rho]$ for the same $COV[M]$.   The

maximum difference is 25%.   Settlement correlation is also smaller in the

nonhomogeneous profile.   Larger variance and smaller correlation produce

a larger differential settlement influence factor.   The actual moments of

differential settlement depend on the value of modulus.   For $E[M] = E[M_o]$,
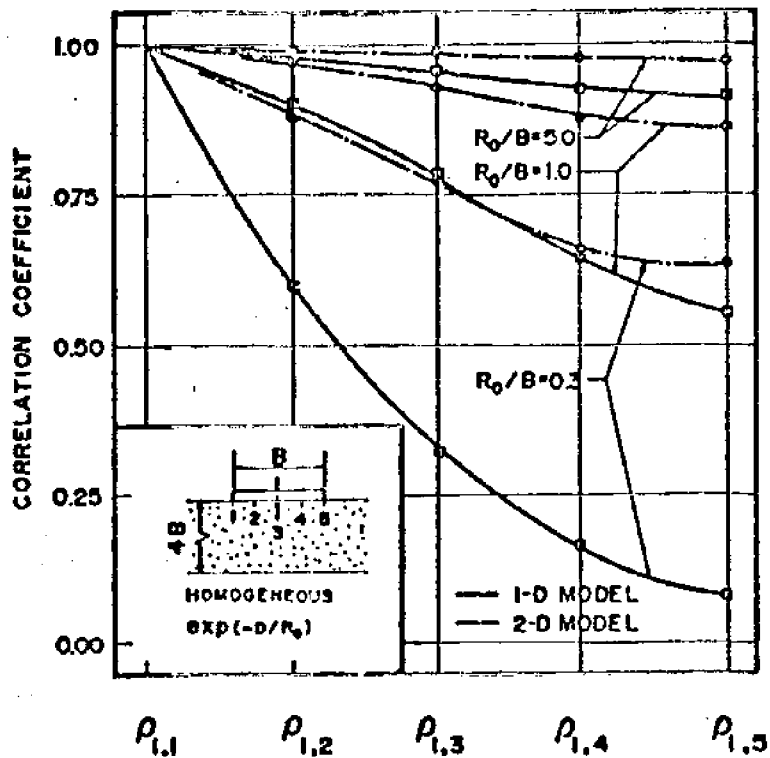
Figure 5.28 -- *Correlations among nodal displacements*
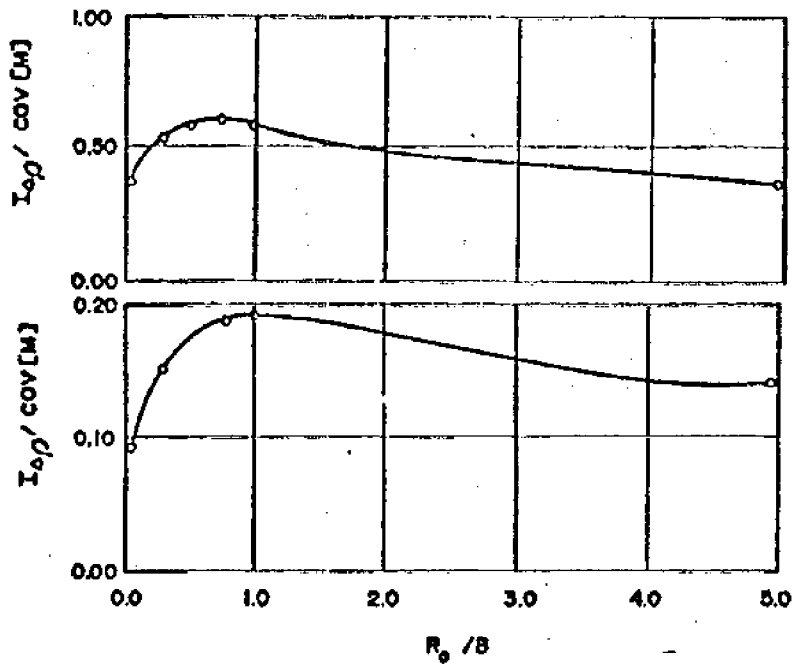
Figure 5.29 -- *Relation of differential settlement for one (above) and two (below) dimensional cases to normalized autocorrelation distance.*
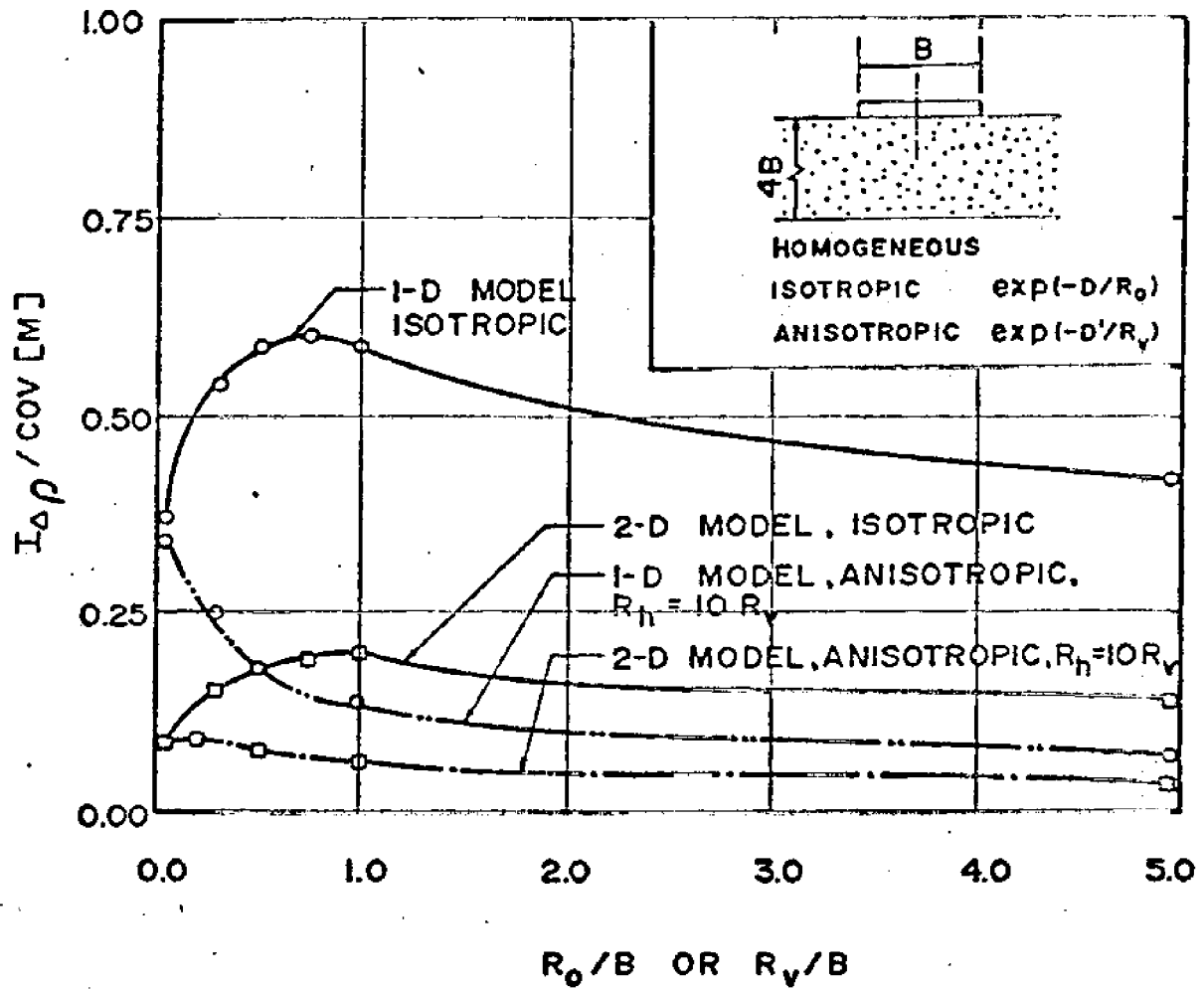
Figure 5.30 -- Effect of anisotropic autocorrelation on differential settlement.
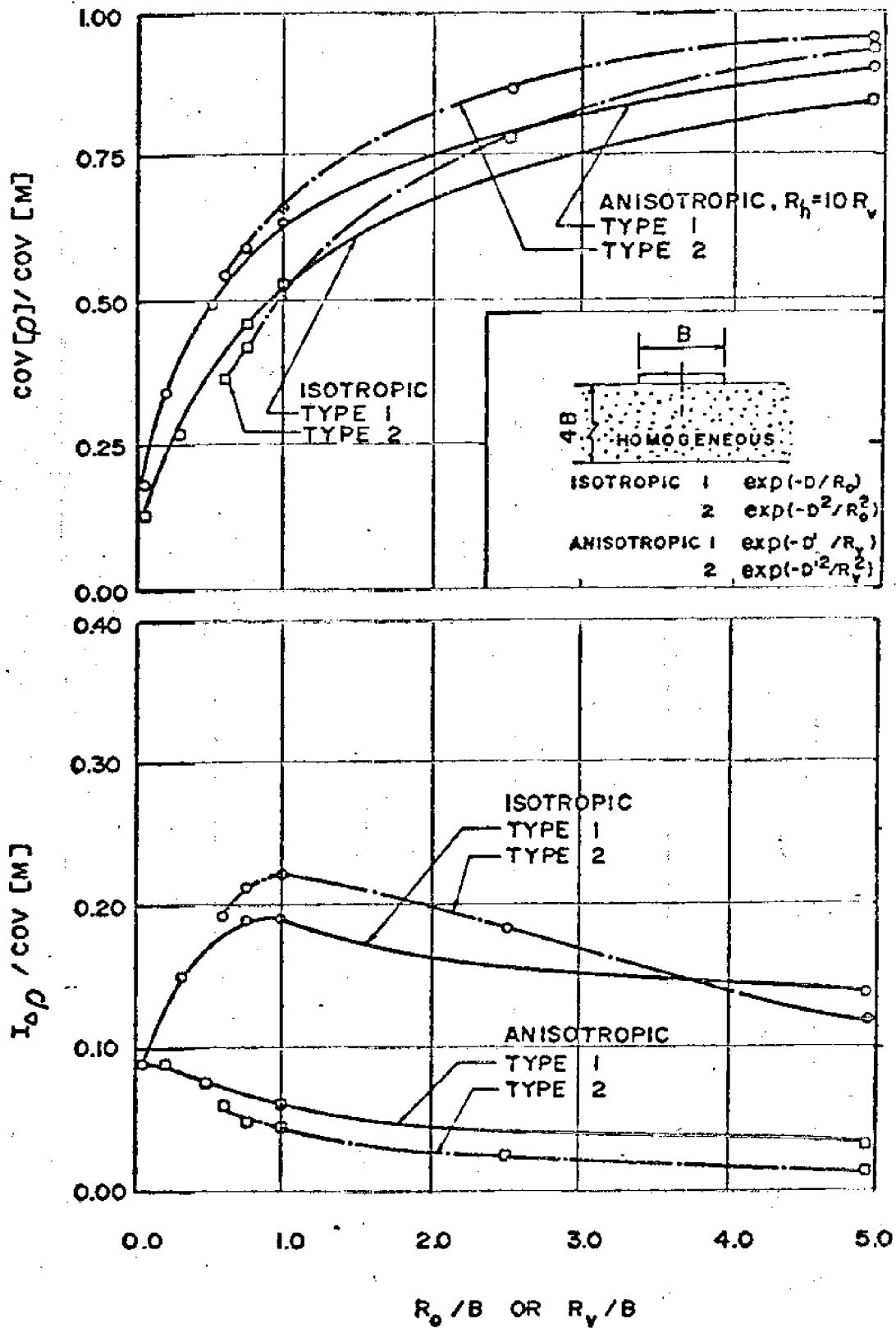
Figure 5.31 -- Effect of autocorrelation model on two dimensional settlement, homogeneous case.
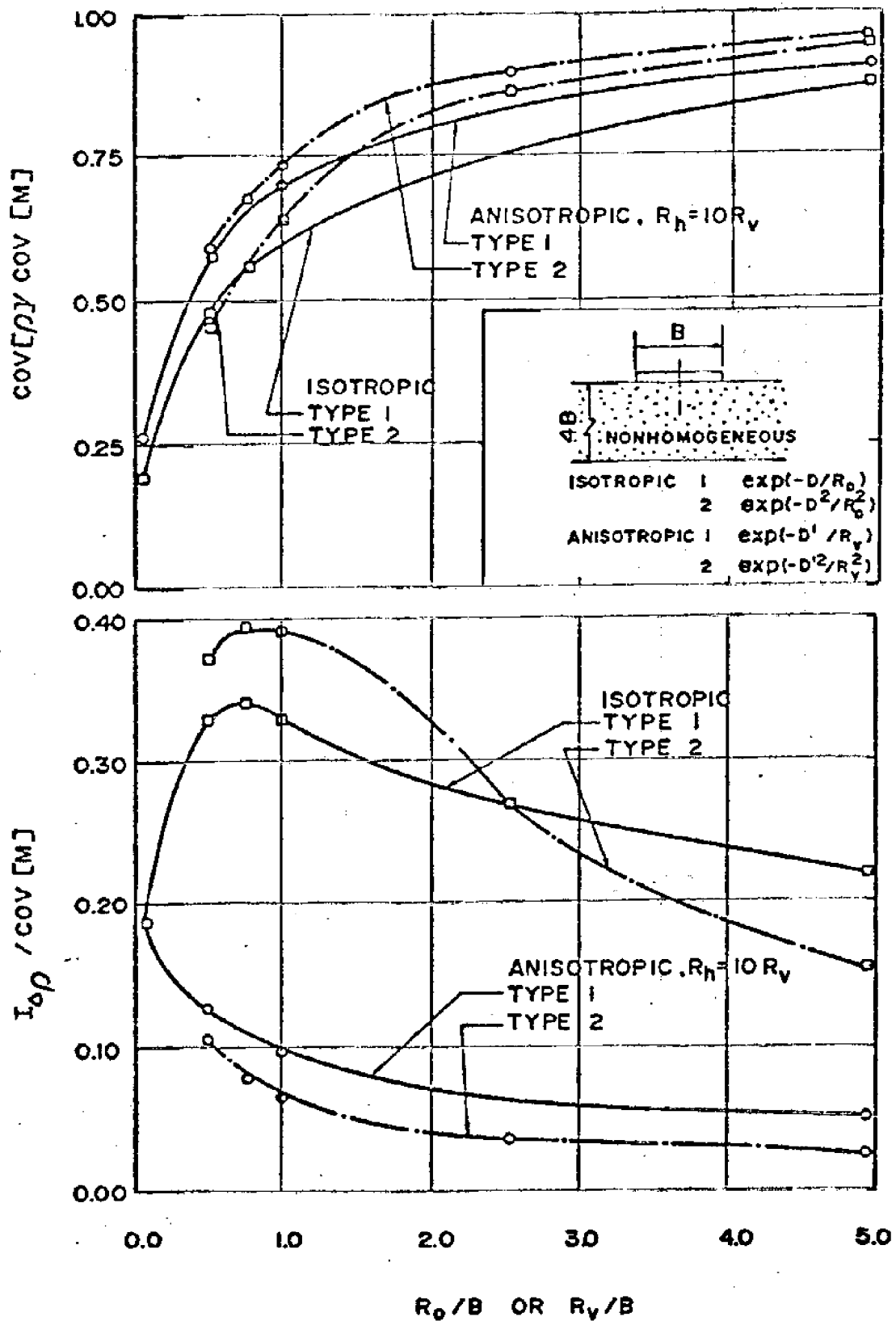
Figure 5.32 -- Effect of autocorrelation model on two dimensional settlement, non-homogeneous case.

the nonhomogeneous profile differential settlement is greater.

The reason for these differences is apparent. Covariance depends more on soil elements near the foundation than distant elements. Small values of modulus near the foundation, therefore, increase covariance proportionally more than the larger distant values of modulus decrease covariance. The net result is an increase of uncertainty in total settlement and larger differential settlement.

Conclusions from Stochastic Analysis

From the two-dimensional analysis of stochastic variability, the COV of total settlement for appropriate magnitudes of the autocorrelation distance (taken as 30m compared to a foundation diameter of 100m, yielding $r_o/B = 0.30$) would appear in the range of 30% of the point COV of sediment properties. The expected differential settlement as a ratio of total settlement would appear to be about 15% of the COV of sediment properties, and the COV of $\Delta\rho$ about 75%. Anisotropic correlation lowers these COV's somewhat, and nonhomogeneous moduli (increasing with depth) increases them.

5.3.3 Effect of Nonhomogeneities on Settlement

The George's Bank site may contain clay or peat inclusions deposited during glacial periods, and given the inefficiencies of geotechnical exploration to detect such inclusions their effect on settlement uncertainties were considered. The model for doing so is somewhat crude, but leads to a first approximation of the effect. More refined models were considered unjustified in a generic analysis of the sort presented here.

Figure 5.33 shows the posterior probability of undetected anomalies existing as a function of the search efficacy of site investigation. Let

Figure 5.33
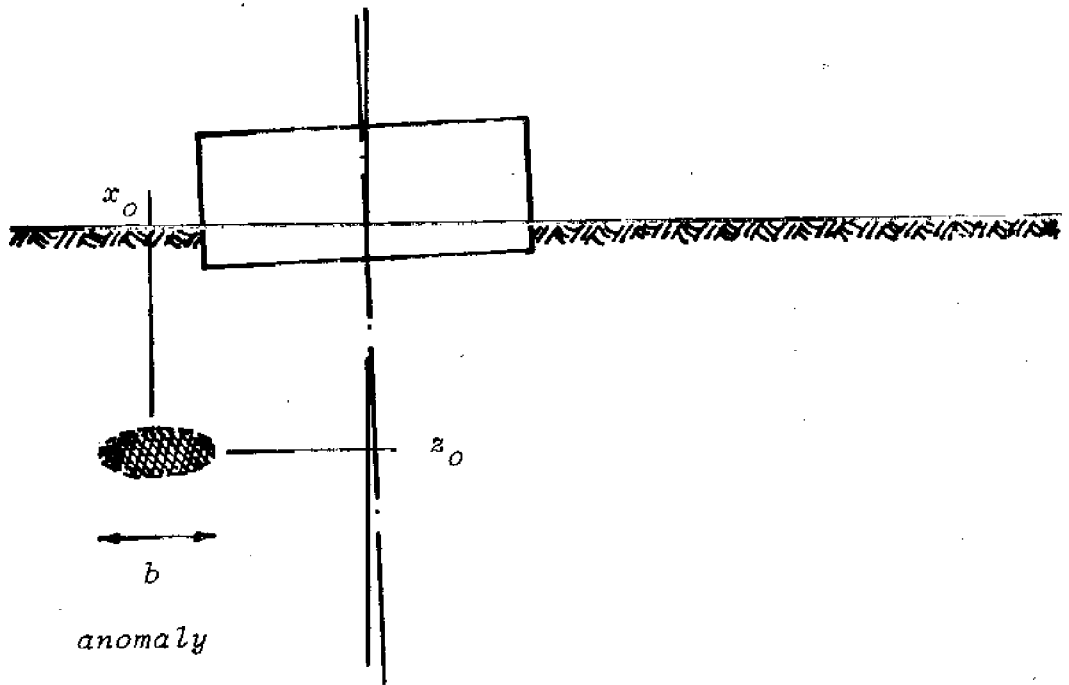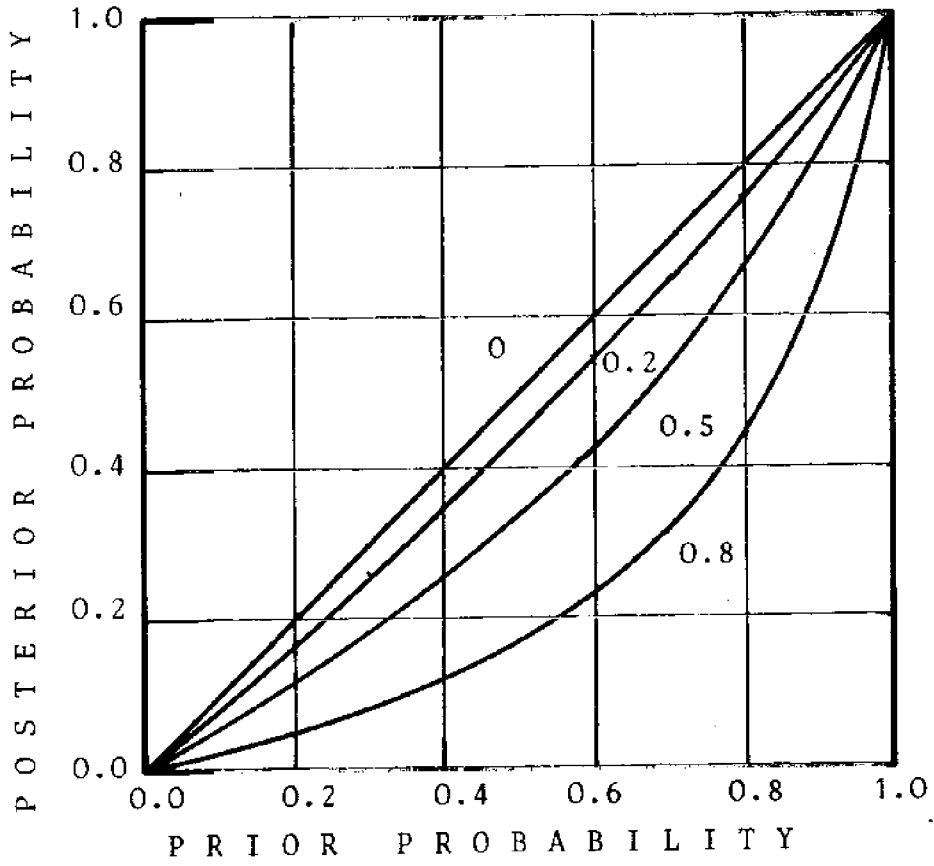
Figure 5.34

this probability be p. Assuming the spatial density of such inclusions to be low, the probability of more than one underlying the site was assumed to be zero. The size of such inclusions, based on accoustic profiles may be about 10m in breadth and as a first cut the size was assumed fixed at this breadth. The location within the sediment profile was assumed random and unformly distributed (Figure 5.34).

Taking the cross section of the inclusion to be approximately elliptical, the differential settlement of the foundation given an inclusion centered at (X_o, Z_o) is shown in the figure. Propagating uncertainty in (X_o, Z_o) through the analysis yields the estimate of inclusion-induced differential settlement shown in Figure 5.35.

Relaxing the assumption of known breadth, inclusion size could be considered uncertain with the same mean. Given lack of information on the distribution of inclusion sizes, the one parameter exponential distribution

$$f(b) = \frac{1}{b_o} \exp(-b/b_o) \tag{5.74}$$

was adopted. Here the mean breadth, b_o, was assumed to equal 10m. This is an arbitrary assumption the primary purpose of which was to test the sensitivity of differential settlement predictions to uncertainty in inclusion size. The result is also shown in Figure 5.35. Obviously, any increase in input uncertainty increases the predictive uncertainty, but the prediction seems not overly sensitive to such changes. The main effect remains the probability that an inclusion exists, and this must be estimated from analysis of the site investigation program, as discussed in Section 4.3.5.
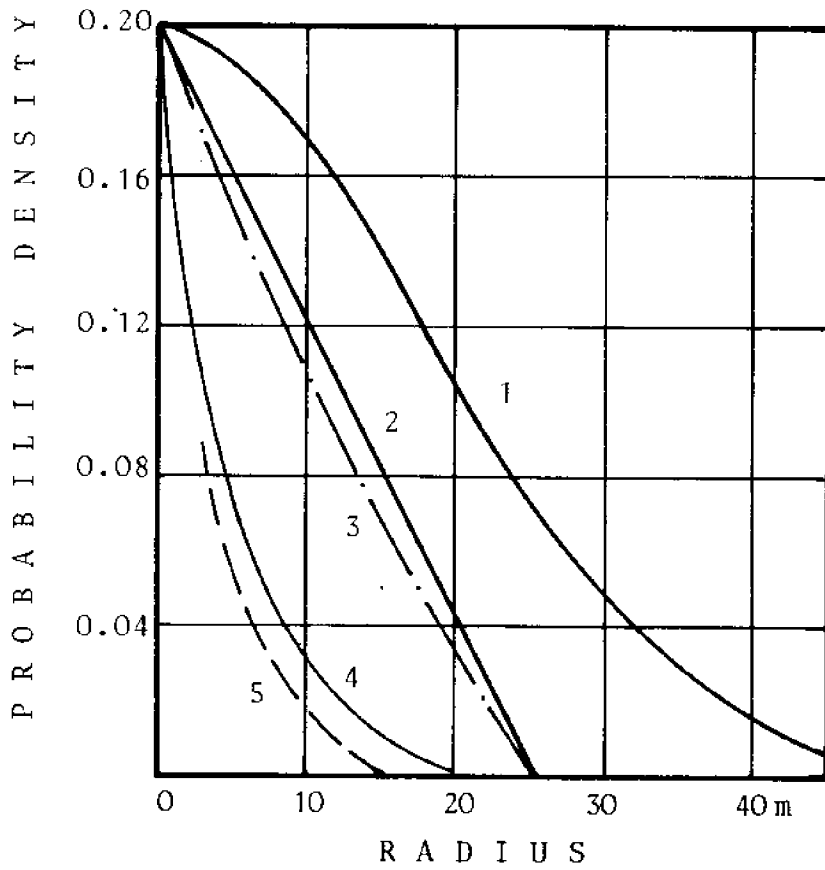
Figure 5.35a -- Posterior probability
distribution of anomaly dimension for
combined borings and geophysics program.
Curve 1: likelihood function for borings;
2: likelihood function for geophysics on
50m spacings; 3: likelihood function
of combined exploration; 4: prior pdf;
5: posterior pdf.
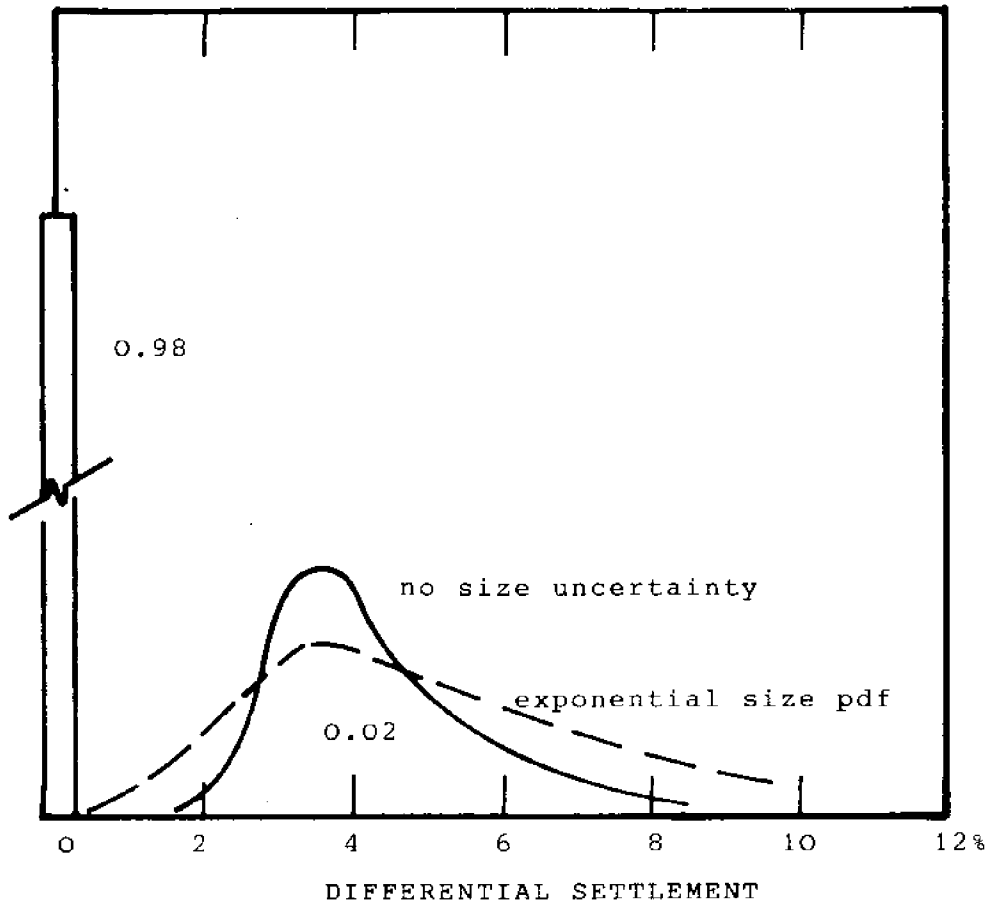
Figure 5.36 -- Predicted differential settlement due to soft inclusions in bottom sediments. Spike at 0% corresponds to probability that no inclusion exists after exploration.

5.4   Dynamic Loading and Sediment Behavior

Most analyses in the present work, as in practice, consider psuedo-static loading under wave action. The reality is, of course, different. As a wave moves past the structure it first exerts force in the direction it is moving, and as it passes the structure it exerts force in the reverse direction. Thus, during a storm the structure is subject to many hours of repeated loading, comprising in total perhaps a thousand or more cycles. The sediments beneath the structure experience cyclic stress reversals of about equal magnitudes during this period, and may behave differently than under static loading.

From extensive work in earthquake engineering it is well known that sands, particularly uniform fine sands, consolidate under cyclic loading. If the period of the cycles is short or if the soil has low permeability, this consolidation leads to an increase in pore water pressure which does not dissipate. Effective stresses drop correspondingly, and if the loading continues, eventually the sand liquifies. In the case of off-shore structures, however, shear failures or large deformations will occur before liquifaction, when the effective stresses are sufficiently reduced and strength correspondingly decreased.

While the phenomenon of pore pressure build up under cyclic loading is well recognized, procedures for dealing with it in design and analysis are not widely agreed upon (e.g., Seed, 1979; Peck, 1979). Experimental results are sensitive to procedural effects, and the primary analytical models are based on simplified assumptions of linear superposition (Bjerrum, 1973). Correlating laboratory measurements to field conditions is made

difficult by the importance of soil fabric to cyclic behavior (Casagrande, 1971), the disturbance introduced in sampling from sand strata, and the imprecision of index properties such as relative density (Tavernas, et al., 1972). Reliability modeling will not significantly improve this situation, as the central problems are ones of mechanistic understanding and not deductive reasoning or quantification of nebulous uncertainties.

The present work has dealt with reliability under dynamic loading only to the extent of incorporating uncertainties in the most widely used event-model, and propogating these uncertainties through to the predictions. For the present, the question of model uncertainties in these predictions seems beyond analytical treatment, and is not incorporated in the reliability calculations. It must be strongly emphasized that the historical record of empirical verification necessary to quantify such inductive uncertainties is almost wholly missing in the case of cyclic effects on sediments under wave loading. Therefore, the conclusions here are at most lower bounds on the actual uncertainty in predicting foundation behavior under these conditions and must be considered tentative.

5.4.1 Pore Pressure Development

Typical results of constant volume cyclic direct shear tests on saturated dense sands are shown in Figure 5.37. Starting from an initial effective consolidation stress σ_o' the shear stress τ is cycled positively and negatively about zero and resulting deformations and pore pressures recorded. With each cycle of loading the pore pressure increases incrementally as the sand grains reorder themselves, and the deformation of the sample increases. Empirically, the increments of pore pressure increase

Figure 5.37
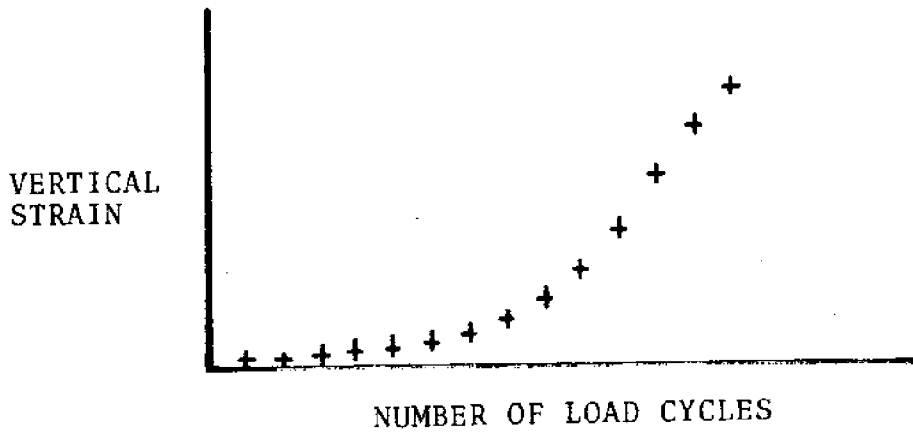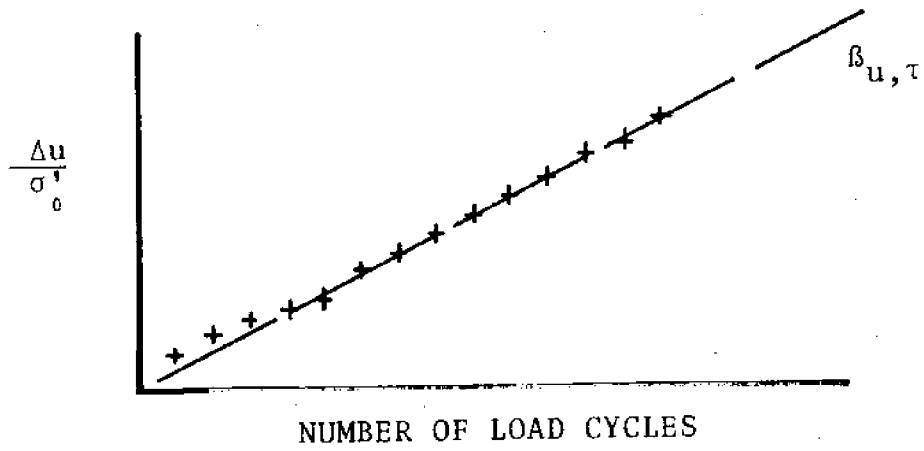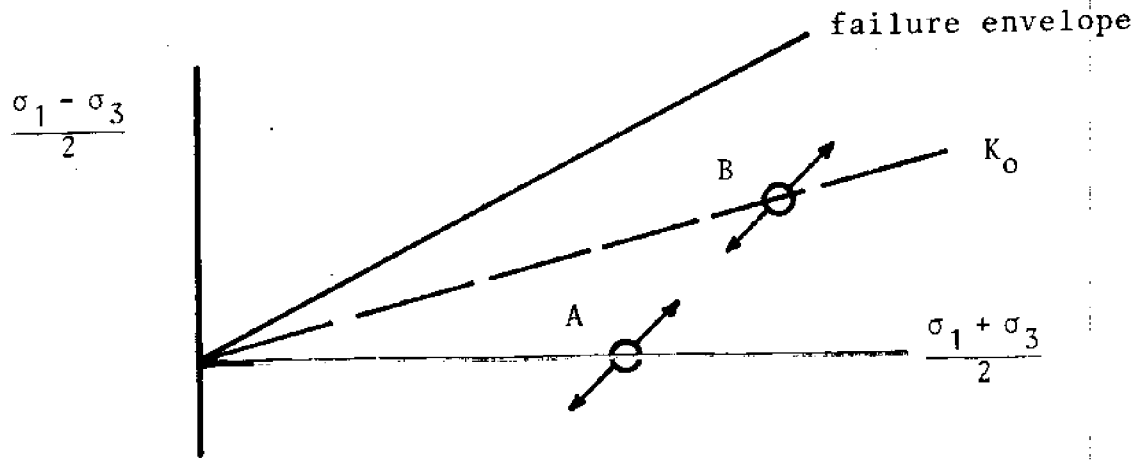
are approximately constant with increasing numbers of cycles, leading eventually to very large deformations of the sample and failure.

The incremental increase of pore pressures per cycle normalized by the consolidation pressure is defined as

$$\beta_u = \frac{\Delta u}{N \sigma_o'} \qquad (5.75)$$

and assumed constant over N. The exponential dependence of β_u on the magnitude of the cycled shear stress τ/σ_o' is shown in Figure 5.38 the higher β_u's corresponding to virgin samples, and lower β_u's corresponding to samples previously experiencing shear stress cycling.

A number of factors affect this generation of pore pressure (e.g., Castro, 1969), and laboratory testing itself is subject to systematic errors (e.g., as noted by Casagrande, 1971, 1980 a redistribution of water content occurs in the sample causing misleading results). Recently Hedberg (1978) and Finn, et al. (1979) have shown the effect of cycling shear stressess about stress states other than $\tau = 0$, such as point B in Figure 5.37. For the present analyses, however, the assumption is made that pore pressure generation is linear in number of cycles and log-linear in cycled shear stress magnitude, and that only the value of $\beta_{u,\tau}$ is in question.

5.4.2 Single Storms

The basic model with which pore pressure development beneath a structure is predicted is the analogue to the Palmgren-Miner formula in fatigue studies. That is, increments of pore pressure development are assumed independent and additive with magnitude proportional to the β_u

of the respective individual wave τ. Thus, for a time streams of wave heights $H_1, \ldots, H_u$ inducing shear stresses $\tau_1, \ldots, \tau_u$ the total pore pressure increase in the foundation sediments is taken as

$$\Delta u = \sum_{i=1}^{m} \beta_{u,\tau_i}^{\sigma} \sigma_o \qquad (5.76)$$

To predict Δu for a particular storm, and therefore the reduction in foundation strength, all that needs be known in addition to β_{u,τ_c} is the distribution of wave heights and number of waves. From Section 3.1.2 the distribution of wave heights given the sea-state parameter H_c has a Rayleigh form.

The number of waves in a storm depends on the duration of the storm, D, and the period of the waves, T, through the joint distribution $f(D,T|H_c)$. Assuming that pore pressures dissipate between storms and that Δu reduce with exposure to storms, only severe storms with large H_c are of interest. Few data have unfortunately been analyzed on storm duration. As discussed in Section 3, extreme storm occurrence seems well modelled as a Poisson process (Russel and Schuëller, 1971), and Houmb (1971) has suggested on this basis that duration may be exponentially distributed. Latter analyses, however (Houmb and Vik, 1977) seem to support more a Weibull distribution of duration for a given sea state H_c, with exponents in the range of 0.5 to 0.8 depending on H_c (Figure 5.39). No empirical work on dependence between T and H_c was found, and in subsequent analyses the relationship is taken as independent except through dependence of the joint pdf of (T,H) on H_c. Build-up and degradation of the storm (Figure 5.40) is ignored. Also, given the large number of waves in a storm (i.e., thousands for a
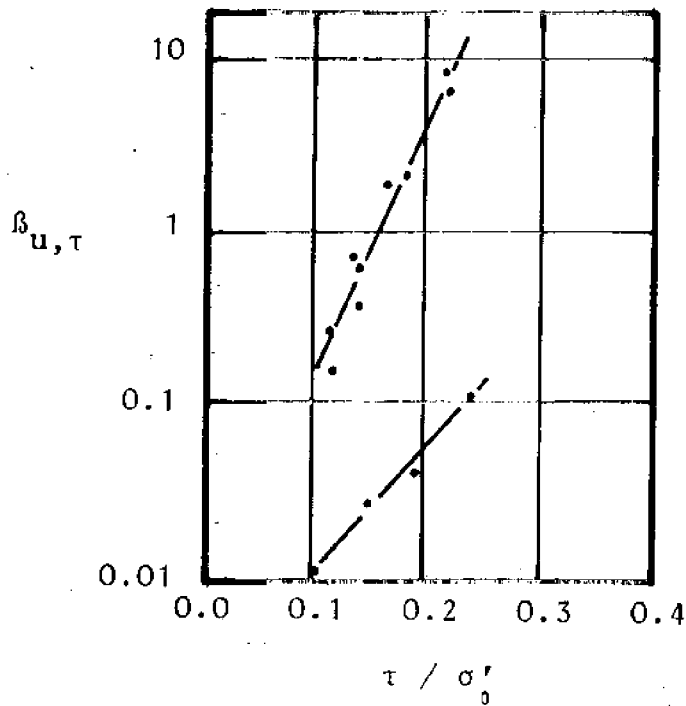
Figure 5.38 -- Relation of pore pressure coefficient $\beta_{u,\tau}$ to magnitude of cycled shear stress (from Bjerrum, 1973). Lower values for presheared specimens. Fine sands at 80% D_r.
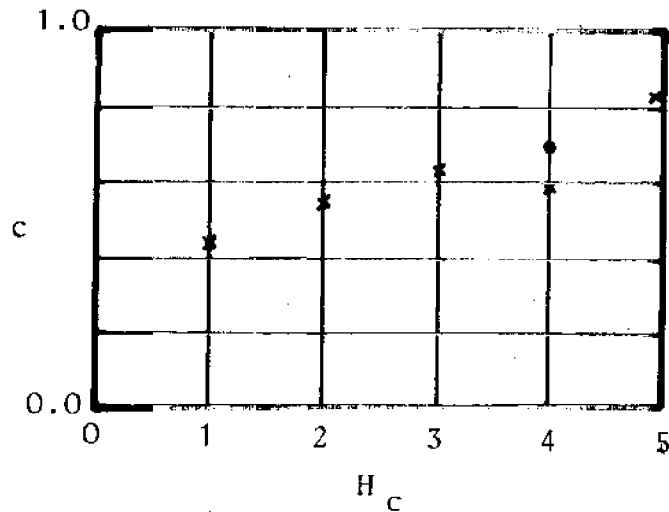
Figure 5.39 -- Empirical relation between exponent of the pdf of storm duration and the significant wave height (From Vik and Houmb, 1977).

long lasting storm on Georges Bank) the dispersion of total number about its mean, due to variations in wave period, is very small and ignored.

Thus, for a storm of given duration and characteristic wave height the build-up of pore pressure beneath the foundation is

$$\frac{\Delta u}{\sigma_o'} = \frac{D}{T} \int_0^\infty \beta_{u,\tau} \tau(H) f(H \mid H_c) dH \quad , \qquad (5.81)$$

where T is the average wave period, $\tau(H)$ the loading transfer function, and $f(H \mid H_c)$ the distribution of wave height. Substituting Morrison's equation for $\tau(H)$ and the dependence of $\beta_{u,\tau}$ on H of Figure 5.38, and then integrating with respect to H gives

$$\frac{\Delta u}{\sigma_o'} = \frac{2Da}{T(2 - \frac{b\tau H_c^1}{\sigma_o^1})} \qquad (5.82)$$

where $\beta_{u,\tau} = a \exp(b\tau/\sigma_o)$. For the Georges Bank test case this becomes

$$\frac{\Delta u}{\sigma_o'} = \frac{2D(1.7 \times 10^{-3})}{T(2 - 2.2 \times 10^{-4} H_c^2)} \qquad (5.79)$$

For a randomly occurring storm D and H_c are dependent Weibull distributed variables, and therefore an analytical transformation into a pdf on $\Delta u/\sigma_o'$ is difficult. Springer (1979) has presented a solution for independent Weibull variables, but this is inapplicable to the present case. Therefore a first-order second-moment approach was used to

WAVE
HEIGHT

H_{100}

H_{50}

H_c

D

PROBABILITY
DENSITY

40 25

10

0   30   60   90 hrs
D U R A T I O N
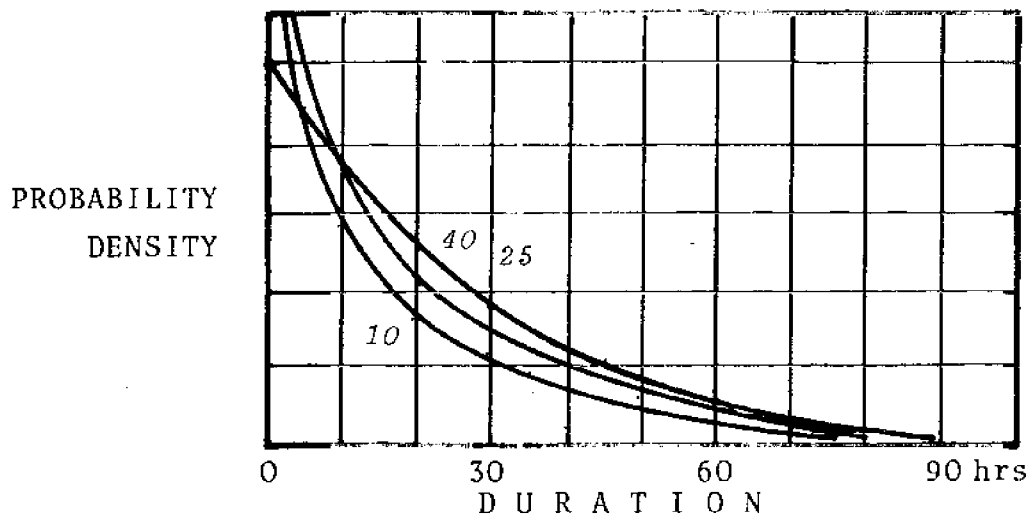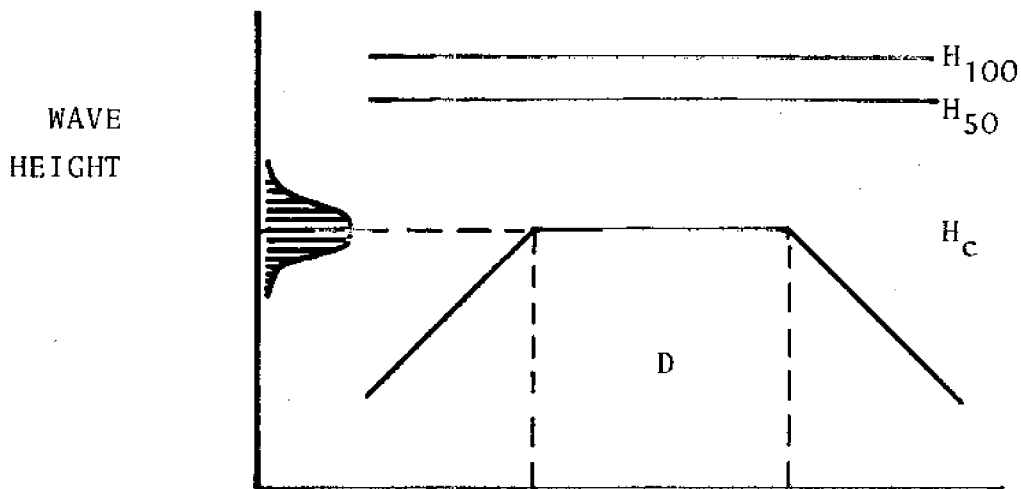
*Figure 5.40 -- Assumed storm occurrence for analysis
of pore pressure build-up. Upper figure shows
significant wave height as a function of time along with
the 100 year and 50 year extreme waves. Lower figure
shows dependence of the pdf of storm duration D on
H_c, for Hc = 10, 25, and 40 feet.*

calculate means and variances for pore pressure build-up. For a randomly occurring storm this yields:

$$E(\Delta u/\sigma_o') = 0.10$$

$$V(\Delta u/\sigma_o') = 0.0009$$

for the statistical descriptions of duration and characteristic wave height at the Georges Bank site, and for the case of simple shear sliding of the foundation.

5.4.3 Recurrence Relations

Making the arbitrary assumption that pore pressure build up is itself logNormally distributed, moment estimation leads to

$$f(\Delta u/\sigma_o') \sim \Lambda(-2.56, 0.77)$$

with a Poisson frequency of occurrence of $\lambda = 0.4$ yr^{-1}, annual exceedance probabilities are shown in Figure 5.41.

5.4.4 Failure Probabilities

To relate pore pressure build-up to increased probabilities of failure the joint distribution of maximum wave height H_m and pore pressure change $\Delta u/\sigma_o'$ must be considered in conjunction with some failure criterion relating H_m and $\Delta u/\sigma$ to performance.

The simplest way to do this is simply to assume a design storm in which, say, the 100-yr. wave height occurs near the end.
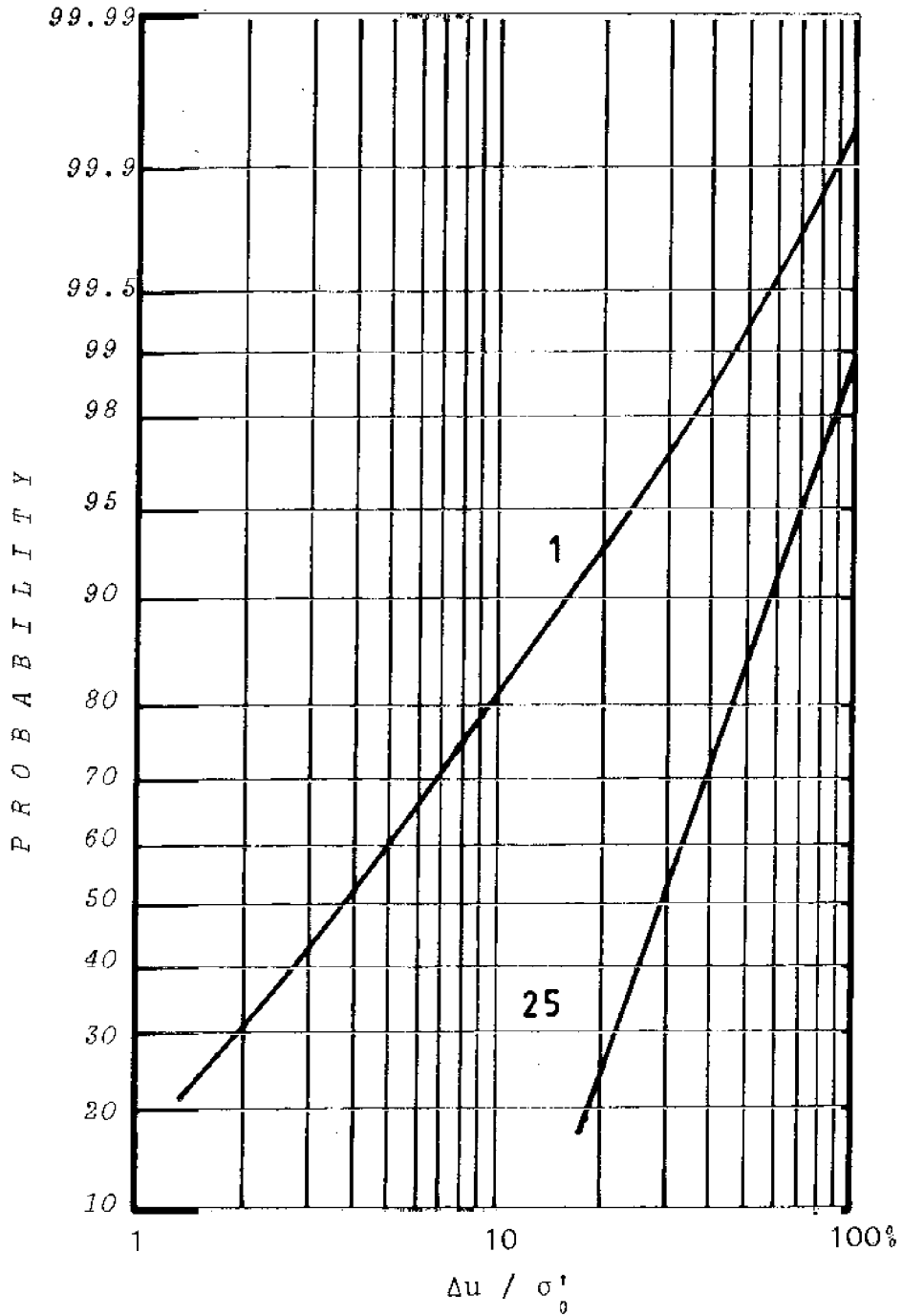
Figure 5.41 -- Exceedence probabilities for pore pressure generation due to cyclic wave loading for 1 and 25 years.

At this point the pore pressures are the highest and reliability can be calculated by adding this uncertain pore pressure to the models of Sections 5.2 and 5.3. Obviously, H_m and $\Delta u / \sigma_o'$ commonly depend on H_c and D, and thus should not be treated as independent, but this introduces few problems.

A more realistic treatment and less conservative assumption is to assume that H_m can occur at anytime throughout the storm. Thus the expected $\Delta u / \sigma_o'$ at the point when H_m occurs will be on the order of half that at the end of the storm.

In the present work no attempts were made to perform such analyses, as the basic mechanisms of pore pressure development under cyclic loading are poorly understood, and the intent of this direction of investigation was primarily to evaluate the magnitude of uncertainty internal to the current method.

5.5 Uncertainty in Predicted Performance

From the above discussions only conclusions on uncertainties in predictions of dynamic performance derive in large measure from limited mechanistic understanding and to that extent have not been treated here.

For well known bottom conditions and sediment parameters, the COV of predictions of limiting equilibrium stability under static design loads is estimated to be about 30%. Typical uncertainty about sediment parameters increases this COV to 60 - 70%. The COV of predictions of total settlement with well known sediment properties is thought to be about 40%, rising to 60% with parameter uncertainty. Respective COV's for differential settlement are thought to be about 30 and 50%.

6.   RISK ANALYSIS

In treating uncertainties of loading and response formally, the question ultimately arises of how they should be aggregated into overall risk and what the risks are. While this would be the ultimate goal of risk and reliability analysis, it is rarely reached. This section addresses current approaches to risk analysis of the geotechnical performance of offshore structures, and what such analyses lead to. The conclusion of this section is that, while much attention has been addressed to geotechnical risk analysis, the difficulties still to be faced are great. More limited goals than complete risk characterization must be accepted if the benefits of such analyses are to be realized.

The following subsections treat in turn the uses and categories of risk analysis, its theoretical structure, the question of aggregating uncertainties into system performance, and finally attempt to define a role for risk analysis in offshore design.

6.1   Uses and Categories of Risk Analysis

Current views on risk analysis for civil works can be broadly grouped in three categories. It is seen alternatively as:

1. A formal procedure with which to aggregate risks defined with respect to some objective function, ultimately to allow as optimization of design and construction decisions.

2. An analytical procedure to allow relative comparisons of uncertainties from different sources and in modes of behavior, and to allow their propagation through engineering calculations to assess cumulative effects.

3. A set of models for studying individual modes of performance
   to estimate from data analysis and theoretical reasoning the
   reliability of each separate component a subsystem.

As Reviewed in Section 2, most current applications are of the third
variety. The present study is an attempt to move toward the second. With
few exceptions (e.g., Fjeld, et al., 1978; Moan 1979), none of which deal
primarily with structural or foundation performance, no comprehensive
risk analyses of the first type have appeared. At current levels of
mechanical understanding of geotechnical behavior and based on the current
empirical record, such comprehensive analyses do not seem possible or
even desirable. This point is taken up further in Section 6.5.

In contrast to these views are the needs of various clients of risk
analysis, which have forced applications into areas for which the models
are poorly suited or inappropriate. The most congruent needs are those
of the designer, primarily concerned with the magnitude of uncertainties
in input parameters and how uncertainties propagate through engineering
calculations. Less congruent are the needs of the owner and insuring
consortium, wanting quantified predictions of frequencies of failures and
associated costs. These approach what analysis can in fact provide, in
considering how design changes marginally reduce probabilities or conse-
quences. Finally and perhaps least congruent are the needs of government
regulators, carrying the public trust of ensuring that the probabilities
and consequences of accidents causing harm to the environmental, social,
and financial well being of the public are acceptably low. These latter
needs require the comprehensive analysis of type 1 above, extended to
include detailed prediction of multiattributed consequences of adverse

performance (e.g., pollution, cost, injury or death, loss of use).

In defining a role for risk analysis in offshore engineering there must be basic criteria against which it is to be judged. These have to do with its relevance to decisions, its integrity, and its validity (Latai, 1977):

1. It should be a practical tool; as such, it should answer questions that are relevant and important.

2. It must be based on a clear statement of the questions to be answered and the risks to be analyzed. It must reflect a profound understanding of the system being analyzed.

3. It must itself be reliable, in that independent groups of analysts should reach approximately the same conclusions when using the same method.

Most current risk analyses only partially satisfy these requirements.

6.2   Structure of Risk Analysis

This section reviews the general organization of risk analysis, focusing on the components and their interrelationships.

Risk may be defined in a general way as a vector $\underline{p} = \{p_1, \ldots, p_n\}$ of probabilities of occurrence of adverse behaviors in n limiting states or modes, and an associated vector $\underline{c} = \{c_1, \ldots, c_n\}$ of consequences conditioned on the occurrence of one or more of the limiting states. The components of $\underline{p}$ and $\underline{c}$ are not necessarily independent, and the components of $\underline{c}$ may be multiattributed (i.e., themselves vectors). To simplify analysis this vector pair is usually replaced by a summary measure, the most common of which are a marginal pdf on consequence cost and the
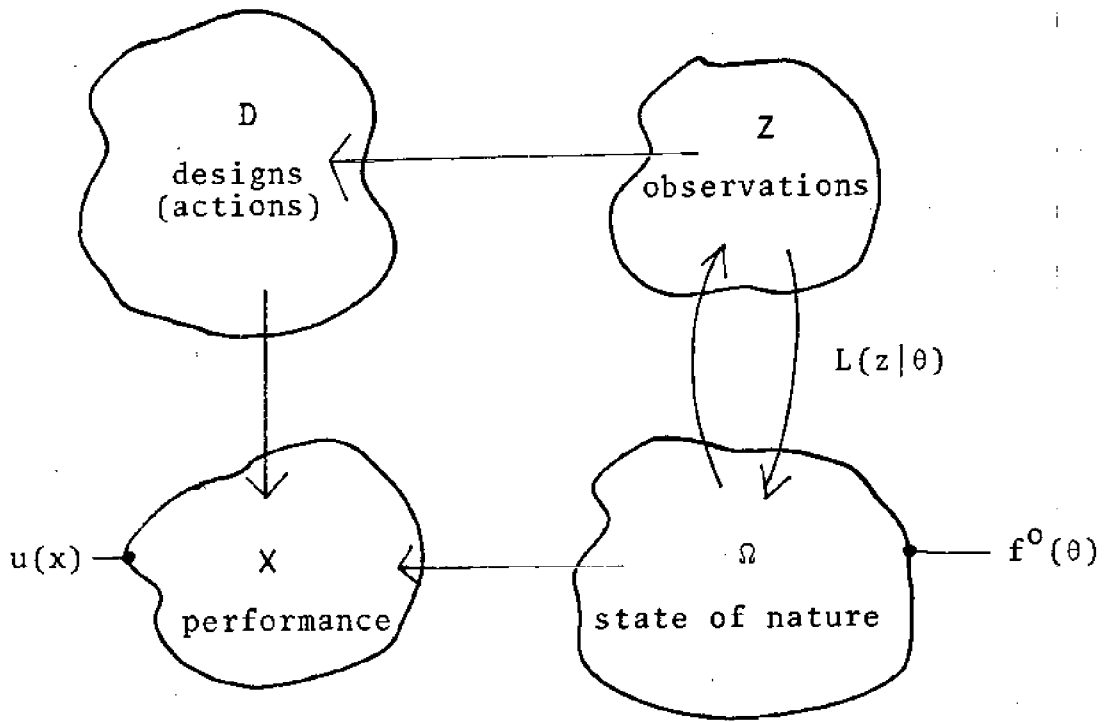
Figure 6.1 -- Paradigm of Risk Analysis (adapted from Barnett, 1974).

product of probability and consequence summed over the limiting states (i.e., expected consequences). For the latter, a non-linear objective function in the sense of cardinal utility (e.g., Keeney and Raiffa, 1976) is sometimes introduced to incorporate risk aversion. For the present work *risk* is taken to be the product of probability and consequence, whether taken directly or transformed into utility. This is in keeping with the civil engineering literature, but differs from usage in, e.g., insurance (Bühlman, 1970) and environmental safety (Lowrance, 1975).

The paradigm of risk analysis is shown in Figure 6.1, around the three fully enumerated spaces which compose its basis: a space of design alternatives D, states of nature Ω, and limiting states X. X is an uncertain mapping from $D \times \Omega$, and has an objective function $u(x)$ defined over it. The important thing to note is that the spaces must be fully enumerated. Any limiting state, state of nature, or consequence not specified cannot be included in a risk analysis. Since it is never possible to do this, risk analyses are necessarily incomplete.

The uncertainties leading to risk enter in the transformation from $D \times \Omega$ to X, and in uncertainty about Ω itself, specified as a probability distribution over the elements $\theta \in \Omega$, $f(\theta)$. This latter uncertainty can be reduced by gathering information, which in the familiar Bayesian procedure enters through a likelihood function $L(z|\theta)$ on the information z, multiplied by a prior distribution $f^o(\theta)$, to give an updated posterior distribution $f'(\theta|z)$. For the present purpose, $f(\theta)$ is said to represent statistical uncertainty, and $f(x \in X | a \in D, \theta \in \Omega)$ to result from reliability analysis. The data z may be from site characterization studies, material testing, hydrographic measurements, or the like, and the function $L(z|\theta)$ is the model through which the data are interpreted.

Beyond the obvious division into $(\mathcal{D}, \Omega, X)$, models enter the risk analysis paradigm in four places:

- $L(z|\theta)$ -- model for interpreting data,

- $f(x|a,\theta)$ -- reliability model,

- $f^{o}(\theta)$ -- model for summarizing initial information,

- $u(x)$ -- model of preferences for consequences.

Each of these is an abstraction, introducing assumptions, amplifications, and inaccuracies; but even more importantly, defining the questions to be analyzed.

The paradigm of risk analysis is a logical structure which proceeds from assumptions to conclusions narrowly, clearly, and indisputably. The analysis is internally either right or wrong by clearly specified rules of mathematical logic. The purpose of this paradigm is to allow a complicated problem to be decomposed into simpler ones, each of which can be dealt with in isolation, and then recombined according to fixed rules to deduce a conclusion. This forces internal consistency among prior information, observations, predictions, preferences, and design decisions; but the analysis itself is only <u>internally</u> objective.

In its entirety, risk analysis is subjective. It is clear, open, and internally consistent; but it is not objective. Important judgments must be made in enumerating the sets $\mathcal{D}$, Ω, and X; in specifying $u(x)$, and $f^{o}(\theta)$; and in modeling $L(z|\theta)$ and $f(x|a,\theta)$. All of these tasks are inductive.

6.3   System Failure Probabilities

The analyses of Sections 2, 3, and 4 have dealt with specific modes of failure and their respective marginal probabilities. If the goal of quantifying overall risk is to be reached, these individual probabilities must be aggregated into a system probability of failure or probability distribution over the spectrum of potential consequences. This is made difficult by two considerations. First, various modes of failure share common input random variables or are functions of distinct but correlated random variables. Second, the sequence of occurrence of events may influence the occurrence of modes of failure and this introduce dependencies among the modes themselves. The reliability of a "geotechnical system" is less difficult to deal with than that of structural systems, because it depends on fewer distinct elements and fewer identifiable sources of uncertainty   (primarily a manifestation of the less sophisticated modelling in geotechnical practice).

At present, there are two general procedures for analyzing the reliability of "geotechnical systems." The first is fault and event free methods and the other is here called basic variable-space method. Fault and event free methods have entered geotechnical engineering via nuclear safety studies and traditional reliability theory (e.g., Barlow, et al., 1976), while basic-variable-space methods have entered via recent work in structural reliability (Rachwitz, 1976). The two methods treat somewhat different problems and are therefore not interchangeable. However, each has important applications in geotechnical analyses.

6.3.1 Fault and Event Tree Analysis

Fault and event trees are analytical techniques for estimating the reliability of complex systems by decomposing them into components, assessing the reliability of each, and fitting the assessments back together. These methods have become a mainstay of present reliability and risk analysis.

Both fault and event tree techniques use a tree structure to describe the interrelations among components of a system being analyzed. Fault trees start with a particular undesired final event (e.g., "complete loss of platform usefulness through structural collapse") and work backward to enumerate all possible ways the final event could occur (Figure 6.2). Event trees start from some initiating event (e.g., "scour action undermines skirt") and project all possible successive events following from it (Figure 6.3). In principle, the two techniques are quite similar.

To determine the probability of an undesired final event, whether from the fault or event tree, the conditional probabilities of faults or events within a chain leading to the final event are multiplied together, and then those from different chains leading to the same final event are added. For computational reasons these fault or event probabilities are usually assumed mutually independent and dichotomous although in principle they need not be. These are inappropriate assumptions in the geotechnical case, where failure modes can interact and processes vary over continuous rather than discrete domains.

The major criticisms of fault/event tree analysis are that:

1. Things are left out: For example, gross human error, unanticipated events, poorly understood physical mechanisms.
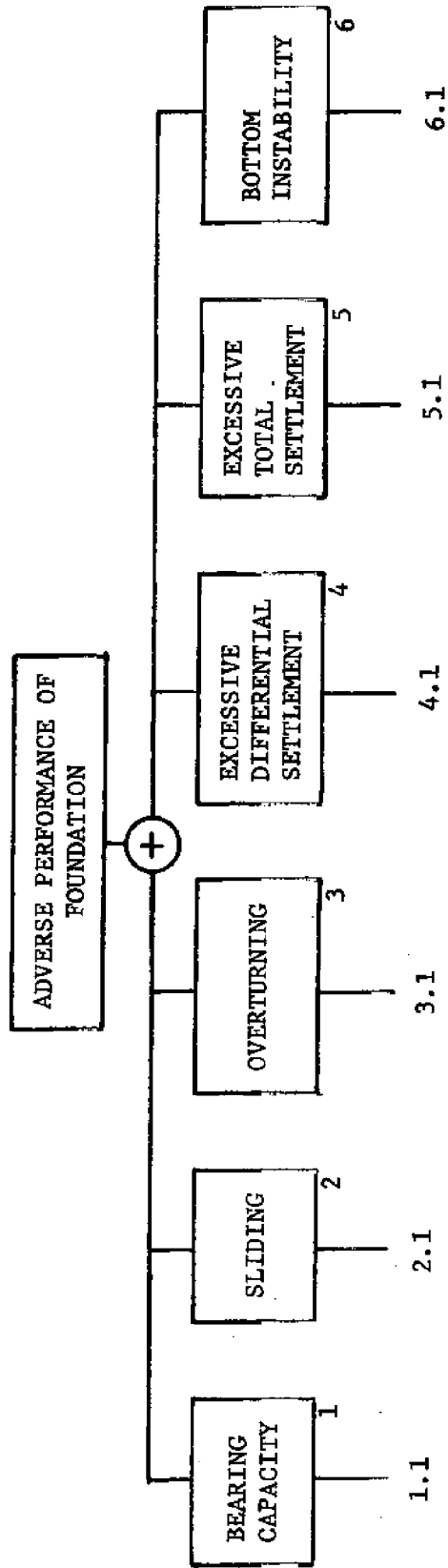
Figure 6.2a — Master fault tree for foundation.
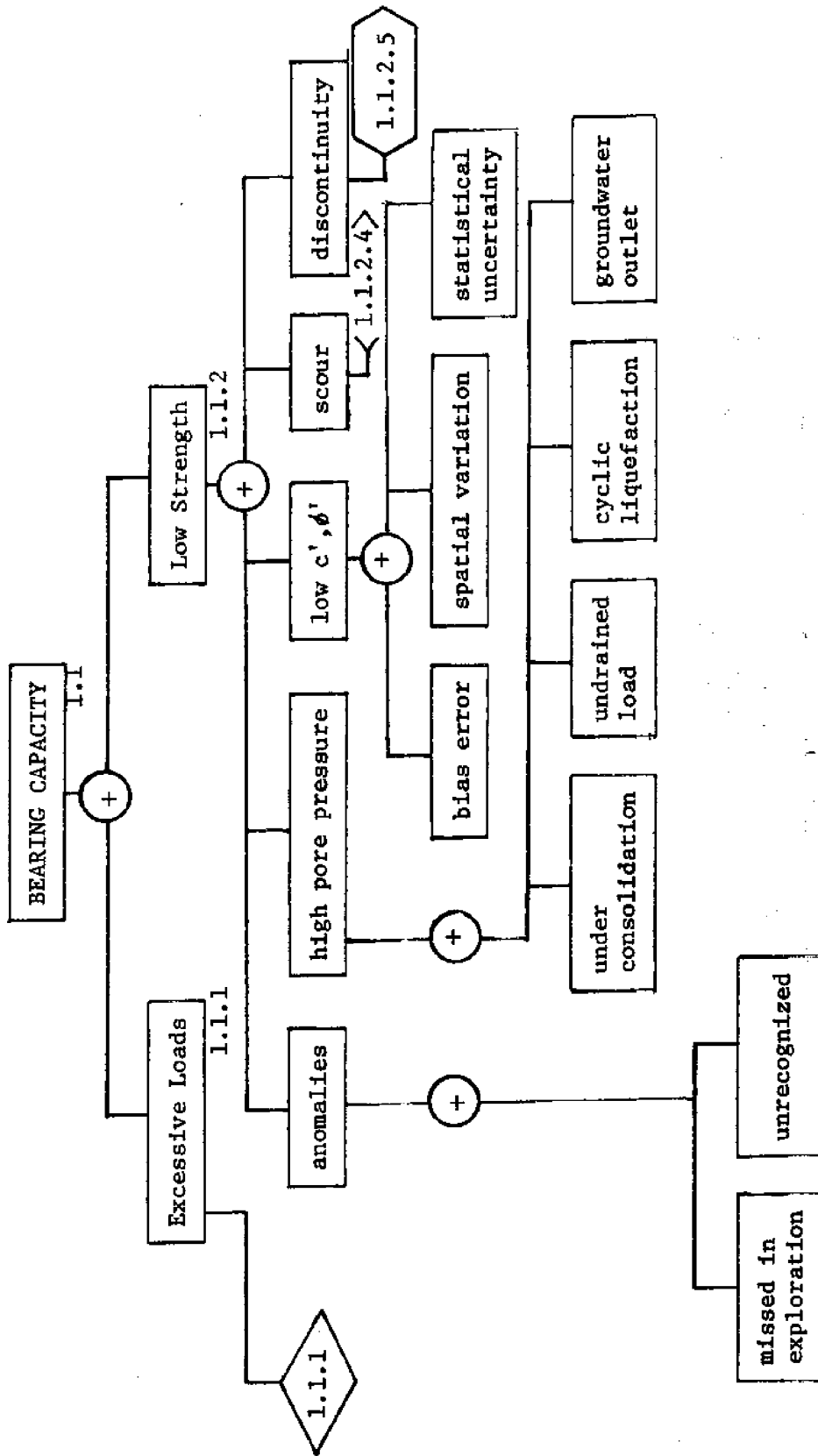
Figure 6.2b -- Sub-fault-tree for bearing capacity
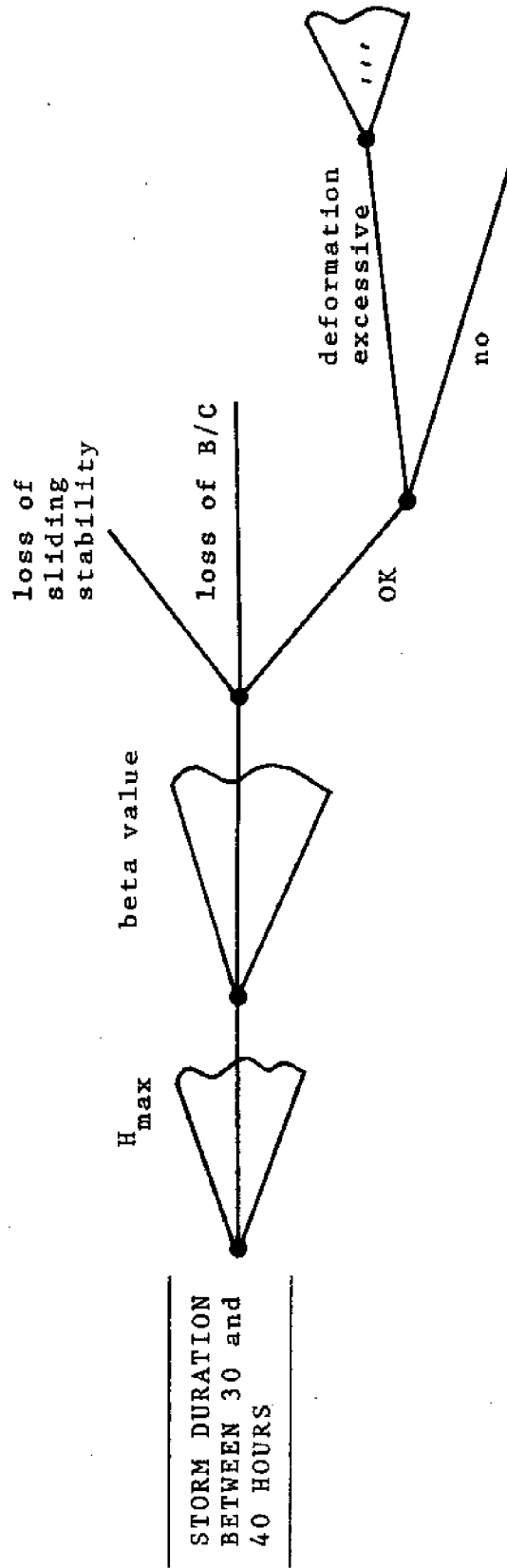
FIGURE 6.3 -- EXAMPLE OF EVENT TREES FOR VARIOUS
SEQUENCES LEADING TO ADVERSE BEHAVIORS.

2. Changes in the use or environment of the structure are

   not anticipated: For example, changes in platform loads,

3. "Common mode" failures in which redundant components have

   correlated failure probabilities are overlooked: For

   example, several members in a tower may all be fabricated

   out of the same defective batch of steel or concrete,

   or high currents may increase lateral loads while at the

   same time scouring the foundation.

4. Time is absent: For example, the sequence of events or

   faults may influence both probabilities and consequences,

   but is not considered.

While the criticisms above apply to the general use of fault/event

trees, difficulties more specific to geotechnical problems are also impor-

ant. The first is that modes of failure interact with one another in ways

that are difficult to account for in f/e trees. Figure 6.4 illustrates

interaction between differential settlement and bearing capacity. Large

differential settlements change the stress distribution along the platform

foundation and thereby increase the probability of local bearing capacity

failure. At the same time, local bearing capacity failure increases the

probability of excessive differential settlements. These cross influences

are generally omitted in f/e trees (also from most deterministic analyses).

The second is that the physical faults or events may themselves be

interrelated in complex ways. For example, for bottom sediments of moder-

ate or low permeability pore pressures are sensitive to the rate of loading.

Thus, loads and resistances may be highly correlated. The simple dichotomies

of f/e tree analysis do not capture the complexity of these interactions.
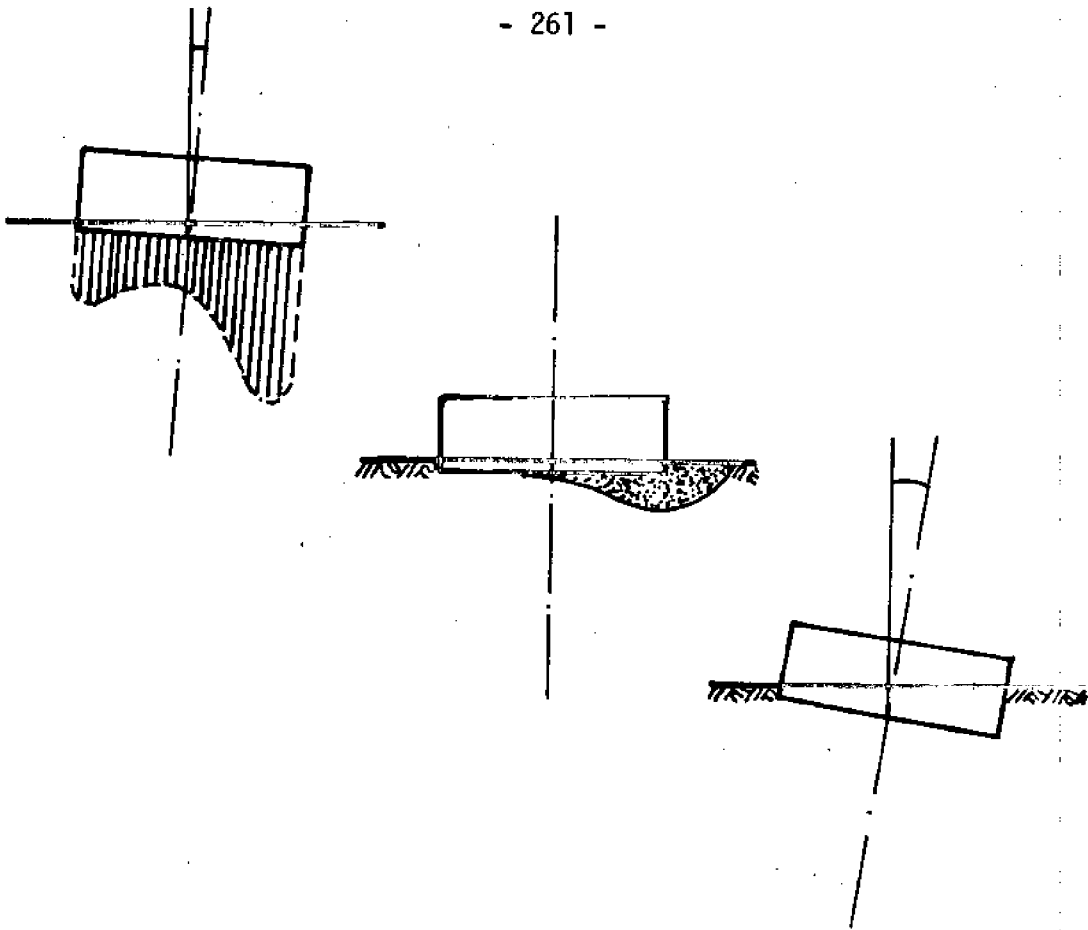
Figure 6.4 -- Interdependence of deformation and stability failure modes. Initial differential displacement leads to nonuniform pressure distribution which leads to local shearing which leads to further differential displacement.

The third is that geotechnical performance is usually sensitive to peculiarities of construction or placement, and designs are often modified during construction in response to initial behavior of the structure and foundation. Although in principle f/e tree analysis could encompass these facts of the problem, the first type are subtle or unknown, and the second usually occur after the risk analyses are complete.

6.3.2 Basic Variable Space Methods

The second method for assessing system reliability is to perform analyses directly in a space defined by the basic uncertain variables, and to specify domains within that space for which the system has exceeded one or more limiting states. Then the probability of reaching a limiting state can be calculated from the probability content of the distribution function of the basic variables outside the safe domain. In principle, this technique can be applied no matter how complex or numerous the basic variables and no matter how complicated their interactions. In practice, computation requirements limit the applicability of the technique, and it is easily used in geotechnical problems only due to the comparitive simplicity of geotechnical models and their limited numbers of parameters.

Figure 6.5 shows the simple case of limiting equilibrium stability of an unembedded foundation on cohesionless sediments with combined and uncertain vertical and horizontal loading. From Section 5.2 an uncertain boundary is calculated separating combinations of horizontal and vertical load leading to instability from those leading to stability. Then the probability of failure is calculated from the volume of the joint density function on H,V outside either of the failure boundaries. Because the boundaries themselves are uncertain, reflecting modeling error, a series
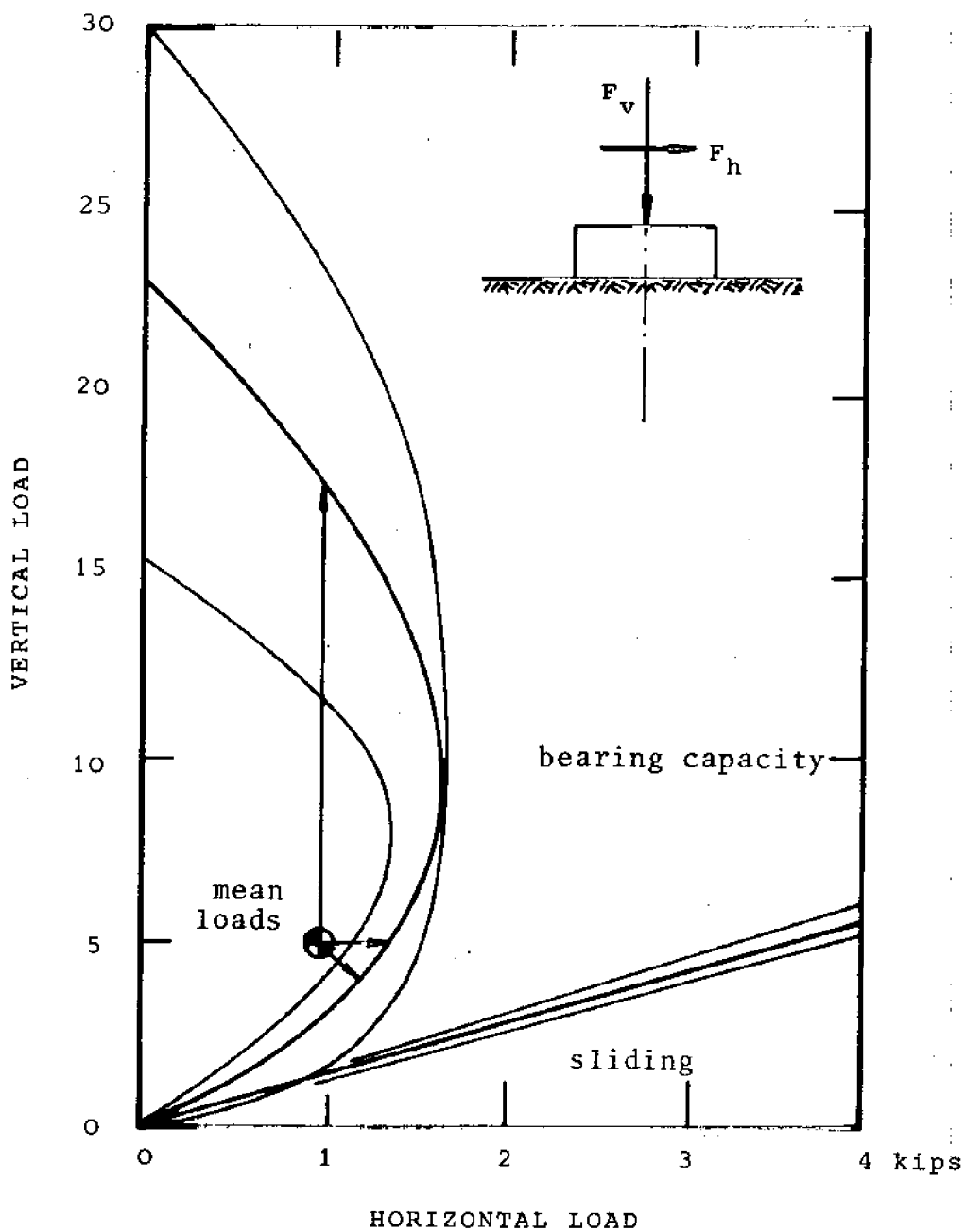
Figure 6.5 -- Basic variable space representation of stability of footing under inclined load. Heavy lines are expected failure boundaries; fine lines are ± one standard deviation.

of conditional probabilities of failure are calculated and combined by the marginal distribution of the boundary locations.*

From a second-moment-point of view a reliability index β can be defined by measuring the distance from the joint expected value of (H, V) to the nearest point on the failure boundaries and normalizing this distance by the standard deviations of the variables. Operationally this is done by rotating the reference to align with the Eigenvectors of the covariance matrix Σ of (H, V), and renormalizing each axis by the resulting standard deviations of the transformed variables. Then the linear distance to the nearest point on the transformed failure boundaries is the reliability index β (Rachwitz, 1976). The rotation leads to a new set of uncertain variables that are mutually independent; the normalization to a set with equal variances. The result is a joint density function whose density contours define concentric (hyper) spheres. Thus, linear distances measure standard deviation units directly. In principle this procedure can be performed in any dimensions as long as the failure boundaries can be transformed. Computationally, a search algorithm is used in higher dimensions to find the nearest point on the transformed boundaries (Rachwitz & Fiesler, 1977).

For geotechnical applications, the main advantages of basic variable space methods over fault and event trees is that they allow easier treatment of continuous variables, and that they allow clear recognition of correlations among failure modes. The major disadvantages are first that computational problems are encountered as the dimension of the basic variable

*An analytically simpler although computationally more difficult way to analyze this problem is to expand the basic variable space to comprise the variables leading to model uncertainty (i.e., N_γ, E_γ, I_γ, $\bar{\theta}$, of Section 5.2), so that in the expanded space the failure boundaries are deterministic. Then the probability of failure is defined by the probability content of the joint distribution function $f(H, V, N_\gamma, E_\gamma, I_\gamma, \phi)$ outside either of these boundaries.

space increases, and that therefore most basic variable space analyses are based on a reliability index measuring only the closest distance from the mean of the basic variables to any of the failure boundaries. This carries no information on probability contributions from other modes of failure. Secondly, spatially varying properties, like bottom parameters, are approximated by random variables in the analyses, leading to numerical errors. Not unexpectedly, the major objections to f/e tree analyses also can be directed at state space techniques: things are left out, changes are not anticipated, time is absent, and modes of failure may not be physically independent of one another.

The most important contribution of state space techniques seems not to be in evaluating overall system failure probabilities, but in evaluating the various ways in which individual types of failures can occur -- e.g., stability failures of various sorts -- and the way basic uncertainties combine to lead to failures. Probabilities estimated in this way may then be further incorporated in f/e tree analyses or other methods of reliability assessment.

6.4   Sources of Uncertainty and Offshore Reliability

From the initial discussion of uncertainties in Section 2 and subsequent enumerations leading to summaries like that of Figure 6.3, the principal sources of uncertainty underlying the geotechnical performance of offshore structures are given in Table 6.1. Unsurprisingly, these are divided into four major groups: uncertainties having to do with environmental loads, bottom conditions, geomechanical models, and omissions or engineering errors. Throughout this work the fourth of these categories

*Table 6.1 -- Principal sources of unctertainty in predictions
of geotechnical performance of offshore gravity structures.*

Environmental loads
<u> </u>

        Wave loads

        Earthquake loads

        Wind Loads

        Current loads

        Extraordinary loads

Load transfer to structure

Bottom conditions

        Strength parameters -- drained, undrained

        Deformation properties

        Anomalous details

Modeling

        Stability -- static   Theoretical uncertainty

        Deformations -- static   Boundary and initial conditions

                          Structural relations

        dynamic response   Omissions

Omissions

Gross errors

has been neglected, even though in practice it may be an important contri-butor to the overall frequency of structural or foundation failure (e.g., Flint and Baker, 1976; Yam, et al., 1980).

From a risk analysis point of view, the interesting thing about these uncertainties is 1) their high implicit correlation, and 2) their combined effect yielding high interdependence of failure modes. The result is that failure through various modes of behavior are both physically and statistically correlated. Addition of failure mode probabilities inde-pendently can greatly over estimate system failure probabilities. Further-more, because estimates of bottom conditions from measurements, predictions of behavior through geomechanical models, and other aspects of design share common assumptions, calibrating data, and other sometimes subtle influences, the analytical combination of these uncertainties under an assumption of independence can strongly bias systems failure probability estimates.

In the present work a Georges Bank site has been used as an example application. Results of the generic analyses are shown in Table 6.2, in which the total variance in the predictions of performance are divided by component contributions of the general classes: environ-mental loads, bottom conditions, and models.

*Table 6.2 -- Approximate reliability indices and variance
conponents for the generic analysis of the Georges Bank site*

MODE OF FAILURE	β 100 yr.	VARIANCE CONTRIBUTIONS %		
		loads	bottom	model
Stability--static				
bearing capacity	2.4	1.0	25	74
sliding	17	76	10	14
Stability--dynamic	$1.8^{\S}$	--	--	--
Excessive Settlement	$(0.6)^{+}$	33	25	42
Differential Settlement	(0.5)	33	25	42

§   Based only on static case with pore pressure development.

+   COV's: ß values are a function of criterion of excessive
total or differential settlement

6.5   The Role of Risk Analysis for Offshore Structures

At present levels of technical capability comprehensive risk analyses

leading to overall design optimization are not possible. Attempts to produce

such analyses meet with at least three obstacles: inadequate mechanistic

understanding of important failure modes, importance of a priori

unidentified (perhaps unidentifiable) geological or construction details,

and complex interdependence of failure modes. Further, given large sta-

tistical uncertainties and modeling errors, calculations lead to nominal

probabilities of failures which do not correspond to realized frequencies.

The purpose of any engineering analysis is to contribute to efficient

design, in which the frequency and consequences of failures are balanced

against design, construction, and operational costs. Risk and reliability

analyses, if seen in a more modest role than complete rationalization of

uncertainty, in fact seem to offer this contribution if used appropriately.

The purpose of their use is not to quantify uncertainty but to lead to

better design. They do this by allowing complicated problems to be

decomposed into simpler ones, which can be directly treated and recombined

in a logically consistent way.

At present, the primary roles for (geotechnical) risk analyses of

offshore structures seems to be,

1. Statistical analysis of site characterization data and the

     planning of site investigation programs. This is an area of

     application for which well developed mathematical results are

     available, in which many (but not all) questions are well

     posed, and which to date has benefitted little from techniques

     and procedures in routine use in other branches of engineering.

2. Uncertainty analysis of individual failure modes (limiting states) and the balancing of cost against changes in reliability indices. Even though reliability analyses lead only to nominal probabilities, because most objective functions are linear with respect to probabilities of failure (e.g., expected utility) partial optimization is possible. Further, for most engineering analyses estimates of uncertainties up to second moments are now possible and at least the variances of parameter estimates, loads, and modeling errors should be propagated through calculations to establish variances of predictions. Again, this practice is common in many branches of engineering.

3. The identification of individual and compound sources of uncertainty to which uncertainties in predicted performances are most sensitive. This is an exploratory type of analysis that allows site investigation and analytical studies to be improved, whether or not formal risk analysis is used in making design decisions. Risk analyses allow significant improvement over traditional sensitivity studies in that important dependencies among uncertainties, correlations of failure modes, and the cost of reducing uncertainty can be combined and incorporated.

Promises of comprehensive risk analysis now appearing in the literature and being made at conferences appear misdirected, in that they will only lead to a failure of expectations by the practicing profession and to a rejection of analytical techniques that, while not truly comprehensive, do offer substantial improvements to practice. A change of

direction of current efforts toward implementation and the development

and testing of practical tools of risk analysis would seem the best policy

at present.

7.   CONCLUSIONS

Three principle conclusions have been drawn from the present attempt to quantify geotechnical risks in offshore structures.

First, comprehensive analyses of geotechnical uncertainties and the risks these uncertainties lead to through imprecise or inaccurate prediction of engineering performance is not now possible in the sense of arriving at aggregate probabilities of levels of adverse performance that may reasonably be expected to reflect realized frequencies. This does not mean that attempts are risk analysis or that a reliability-based approach to geotechnical analysis carry no benefit. Certain categories of uncertainty and prediction can be rationally treated through reliability methods even though comprehensive analyses are not possible. Central uncertainties in offshore design stem from ignorance rather than natural randomness, and the statistical or probabilistic statements made about them can only be interpreted in this way.

Second, for those categories of performance about which physical understanding is good, model and statistical parameter uncertainties appear to be of about equal importance to overall uncertainty. Further, the dominance sometimes attributed to uncertainties in wave loading is not supported by the present study.

Third, for those aspects of geotechnical performance about which physical understanding is good and for which reasonably validated models exist, (first order) reliability indices against major adverse performance (loss of stability, severe deformation) appear to be of the order 2 to 3.

This would correspond to annual probabilities in the range 10^{-4} to 10^{-5}, which appear lower than the sparce historical record (for pile supported platforms) would suggest.

In general, the development of quantified procedures for handling geotechnical uncertainties has advanced rapidly in recent years. Nevertheless, the promises of many proponents of such methods of complete rationalization of uncertainty seem unattainable in light of the subjective nature of many uncertainties and the inadequacy of present understanding of specific aspects of soil behavior. The potential contribution of quantified procedures for assessing uncertainties and incorporating them in analyses seems great, as long as their role within the overall issue of design and safety is not exaggerated. The most urgently needed work at present is to verify such methods in application to actual cases.

REFERENCES

Ackoff, R.L., et al. (1962). Scientific Method: Optimizing Applied Research Decisions. New York: John Wiley and Sons, Inc.

Agterberg, F.P. (1974). Geomathematics. New York: Elesevier North-Holland Inc.

Agterberg, F.P. (1970). "Autocorrelation functions in geology," Proceedings Colloquim on Geostatistics, ed. D.F. Merriam, Lawrence: University of Kansas.

Aitchison, J. and A.C. Brown. (1957). The Lognormal Distribution, Cambridge University Press.

Alonso, E.E. (1976). "Risk analysis of slopes and its application to slopes in Canadian sensitive clays," Geotechnique, 26(3):453-472.

American Institute for Steel Construction. (1970). Manual of Steel Construction. (7th Ed.), New York.

American Petroleum Institute. (1978). "API recommended practice for planning, designing, and constructing fixed offshore platforms," API-RP-2A, 9th Edition. Dallas.

American Association of Civil Engineers Committee on Reliability of Offshore Structures. (1979). "Applications of reliability methods in design and analysis of fixed offshore platforms," Committee report, presented at ASCE Specialty Conference on Structural Reliability and Safety, Tuscon.

Andersen, K.H. (1972). "Bearing Capacity of Shallow Foundations on Cohesionless Soils," Internal Report No. 51404-1. Norwegian Geotechnical Institute.

Ang, A. H-S and C.A. Cornell. (1974). "Reliability bases of structural safety and design," Journal Structural Division, ASCE, Vol. 100, No. ST9.

Baecher, G.B. (1978). "Analyzing exploration strategies," Site Characterization, ed. C.H. Dowding, NSF-ASCE.

Baecher, G.B. (1972). "Site Exploration: A Probabilistic Approach." Ph.D. dissertation, Massachusetts Institute of Technology.

Baecher, G.B. and T. Ingra, (in press). "Settlement analysis by stochastic FEM," ASCE (GT).

Bakr, A.A., L.W. Gelhar, A.L. Gutjahr, and J.R. MacMillian. (1978). "Stochastic analysis of spatial variability in subsurface flows," Water Resources Research, 14:263-71.

Barlett, M.S. (1955). An Introduction to Stochastic Processes, New York: Cambridge University Press.

Battjes, J.A. (1978). Probabilistic aspects of ocean waves," Proceedings of International Research Seminar on Safety of Structures Under Dynamic Load. Norwegian Institute of Technology, Trondheim.

Battjes, J.A. (1972). "Long-term wave height distribution at seven stations around British Isles," Deutche-Hydrographischer Zeitschrift, Jahrgang 25, Vol. 4.

Battjes, J.A. (1972). "Run-up distributions of waves breaking on slopes," ASCE, Vol. 97, (WW 1):91-114.

Bea, R.G. (1975). "Development of safe environmental criteria for offshore structures, Proceedings Oceanology International Conference, Brighton, England.

Bea, R.G. (1974). "Gulf of Mexico hurricane wave heights," Offshore Technology Conference, Preprints, Vol. II, pp 791-810, Houston.

Bea, R.G. (1973). "Selection of environmental criteria for offshore platform design," Offshore Technology Conference, Preprints, Vol. II, pp 185-196, Houston.

Bea, R. G. and P.W. Marshall. (1974). "Failure modes of offshore structures, Proceedings, ASCE-EMD Special Conference on Probability Methods in Engineering, Stanford, Calfornia.

Benjamin, J.R. and C.A. Cornell. (1970). Probability, Statistics, and Decision for Civil Engineers, New York: McGraw-Hill Book Company.

Bjerrum, L. (1973). "Geotechnical problems involved in foundations of structures in the North Sea," Geotechnique, Vol. 23, No. 3.

Bonneau, E. (1971). Statistique des maximums absolus d'un processus aléatoire stationnaire, Gaussien et centré, Rech. Aérosp. No. 1971-3, pp 169-171, May-June.

Borgman, L.E. (1973). "Probabilities for the highest wave in hurricane," Journal Waterways, Harbors and Coastal Engineering, ASCE, Vol. 99, No. WW. May, pp 185-207.

Borgman, L.E. (1972). "Statistical models for ocean waves and wind forces," Advance in Hydroscience, 139-81, New York: Academic Press.

Borgman, L.E. (1967). "Spectral analysis of ocean waves on piling," Journal Waterways and Harbours Division, ASCE, Vol. 93, No. WW2, Paper 5247, pp. 129-156.

Borgman, L.E. (1965). "Wave forces on piling for narrow-band spectra," Journal Waterways Harbor Division, ASCE, Vol. 91, No. WW3, Paper No. 4443.

Borgman, L.E. (1963). "Risk criteria," ASCE, vol. 89, No. WW3, pp. 1-35.

Box, G.E. and G. Jenkins. (1976). Time Series Analysis and Forecasting, San Francisco: Holden-Day, Inc.

Bras, R.L. and I. Rodriguez-Iturbe. (1975). Rainfall-Runnoff as a Spatial Stochastic Process. Massachusetts Institute of Technology, Dept. of Civil Engineering, Technical Report No. R75-5.

Bretschneider, C.L. (1959). "Wave Variability and Wave Spectra for Wind Generated Gravity Waves," U.S. Army Corps of Engineers, B.E.B., Technical Memorandum 118.

Buhlman, H. (1970). Mathematical Methods in Risk Theory, New York: Springer-Verlag.

Bureau of Land Management. (1976). Draft Environmental Impact Statement-Proposed OCS North Atlantic Region Development, Washington, D.C.: U.S. Department of the Interior.

Cambou, B. (1975). "Application of first order uncertainty analysis in the finite elements method in linear elasticity," Proceedings, Second International Conference on Application of Statistics and Probability in Soil and Structural Engineering, Aachen, Germany.

Caquot, A. and J. Kerisel. (1953). "Sur le terme de surface dans le calcul des fondations en milieu pulverulent," Proceedings Third International Conference on Soil Mechanics and Foundations, Vol. 1, Zurich.

Cartwright, D.E. and M.S. Longuet-Higgins. (1956). "On estimating the mean energy of sea waves from the highest waves in a record," Proceedings Royal Society, London, A, 247, pp. 22-48.

Cartwright, D.E. and M.S. Longuet-Higgins. (1956). "The statistical distribution of the maxima of a random function," Proceedings Royal Society of London, A. 237, pp. 212-232.

Casagrande, A. (1965). "Role of the calculated risk in earthwork and foundation engineering," Journal Soil Mechanics and Foundations Division, ASCE, Vol. 91, No. SM4.

Cavanie, A., M. Arhan, and R. Ezraty. (1976). "A statistical relationship between individual heights and periods of storm waves," Proceedings, BOSS'76, Vol. II, 13.5 pp. 354-360.

Chakrabarti, Subrata K. (1978). "Wave forces on multiple vertical cylinders," Journal of the Waterway, Port Coastal and Ocean Division, ASCE, Vol. 104, No. WW2 Proc. Paper 13727, May, pp. 147-161.

Chakrabarti, S.K. (1975). "Second-order wave force on large vertical cylinder," ASCE, 101, WW3, pp. 311-317.

Chakrabarti, S.K. and R.P. Cooley. (1977). "Statistical distribution of periods and heights of ocean waves," Journal of Geophysical Research, 82 9, pp. 1363-1368.

Chakrabarti, Subrata K., Allan L. Wolbert, and William A. Tam. (1976). "Wave forces on vertical circular cylinder," Journal of the Waterways, Harbors and Coastal Engineering Division, ASCE, Vol. 102. No. WW2, Proc. Paper 12140, May, pp. 203-221.

Chen, W.F. (1975). Limit Analysis and Soil Plasticity, New York: Elsevier North-Holland, Inc.

Cornell, C.A. (1971). "First order uncertainty analysis in soils deformation and stability," Proceedings First Intl. Conf. on Applications of Statistics and Probability to Soil and Structural Engineering, Hong Kong.

Cornforth, D.H. (1964). "Some experiments on the influence of strain conditions on the strength of sand," Geotechnique, Vol. 14, No. 2.

Corotis, R.B., A.S. Azzouz, and R.J. Krizek. (1975). "Statistical evaluation of soil index properties and constrained modulus," Proceedings Second International Conference on Application of Statistics and Probability in Soil and Structural Engineering, Aachen, Germany.

Cramer, H., and M.R. Leadbetter. (1967). Stationary and Related Stochastic Processes. New York: John Wiley and Sons, Inc.

DeBeer, E.E. and B. Ladanyi. (1961). "Etrude experimentale de la capacite portante du sable sous des fondations circulaires etablies en surface," Proceedings Fifth International Conference on Soil Mechanics and Foundation Engineering, Vol. 1, Paris.

DeBeer, E.E. (1967). "Bearing capacity and settlement of shallow foundations on sand," Proceedings Fifth International Conference on Soil Mechanics and Foundation Engineering, Vol. 1, Paris.

DeBeer, E.E. (1970). "Experimental determination of the shape factors and Bearing capacity factors of sant," Geotechnique, Vol. 23, No. 4.

Dhillon, G.S. (1961). "The settlement, tilt, and bearing capacity of footings undercentral and eccentric loads," Journal National Buildings Organization, Vol. 6.

Diaz, J. and E.H. Vanmarcke. (1974). "Settlement of Structures on Shallow Foundations: A Probabilistic Approach," Massachusetts Institute of Technology, Department of Civil Engineering, Research Report, R74-9.

Ditlevsen, O. (1980). Uncertainty Modeling with Applications to Multidimensional Civil Engineering Systems. New York: McGraw-Hill Book Company, Inc.

Emery, K. and E. Uchups. (1965). "Structure of Georges Bank," Marine Geology.

Eastwood, W. (1955). "The bearing capacity of eccentrically loaded foundations on sandy soils," The Structural Engineer, Vol. 23, No. 6.

Feda, J. (1961). "Research on the bearing capacity of loose soil," Proceedings Fifth International Conference on Soil Mechanics and Foundation Engineering, October, pp. 1486-1496.

Fjeld, S. (1978). "Reliability of offshore structures," Journal of Petroleum Engineering, October, pp. 1486-1496.

Flint, A.R., et al. (1976). "Rationalization of Safety and Serviceability Factors in Structural Codes," Construction Industry Research and Information Association (CIRIA), Report 63.

Flint, A.R. and M.J. Baker. (1976). "Risk Analysis for Offshore Structures-- the Aims and Methods," Design and Construction of Offshore Structures, London.

Focht, J.A. and C.M. Kraft. (1977). "Progress in Marine Geotechnical Engineering," ASCE V. 103, 10, pp. 1097-1119.

Forristall, G.Z. (1978). "On the Statistical Distribution of Wave Heights in a Storm," Journal of Geophysical Research, Vol. 83, No. C5, pp. 2353.

Fredlund, D.G. and E. Dahlman. (1971). "Statistical geotechnical properties of glacial Lake Edmonton sidiments." Proceedings First International Conference on Application of Statistics and Probability to Soil and Structural Engineering, Hong Kong.

Freudenthal, A.M. (1956). "Safety and Probability of Structure Failure," Transactions ASCE, 121:1337.

Freudenthal, A.M. (1947). "The Safety of Structures," Transactions ASCE, V. 112.

Freudenthal, A.M. and W.S. Gaither. (1969). "Design Criteria for fixed Offshore Structures," Offshore Technology Conference, Preprints, pp. S623-646, Houston, Texas.

Gelb, A. (Ed.) (1974). Applied Optimal Estimation, Cambridge, MA: M.I.T. Press.

Geisel, M.S. (1970). "Comparing and Choosing Among Parametric Statistic Models," Ph.D. dissertation, University of Chicago.

Golder, H.G. (1941). "The ultimate bearing capacity of rectangular footings," Journal Institution of Civil Engineers, Vol. 17.

Graham, J. and J.G. Stuart. (1971). "Scale and boundary effects in foundation analysis," Journal Soil Mechanics and Foundation Engineering Division, ASCE, Vol. 97. No. SM11.

Gregoriu, M. (1976). "A Decision Theoretic Approach to Model Selection For Structural Reliability," Ph.D. thesis, Massachusetts Institute of Technology.

Gumbel, E.J. (1958). Statistics of Extremes, New York: Columbia University Press.

Hammitt, G.M. (1966). "Statistical Analysis of Data from a Comparative Laboratory Test Program Sponsored by ACIL," United States Army Engineering Waterways Experiment Station, Corps of Engineers, Miscellaneous Paper No. 4-785.

Hansen, B.H. (1976). "Modes of failure under inclined eccentric loads," Proceedings Behavior of Offshore Structures, Norwegian Geotechnical Institute.

Hansen, J.B. (1961). "A General Formula for Bearing Capacity," Danish Geotechnical Institute, Bulletin No. 11, Copenhagen.

Hansen, J.B. and N.H. Christensen. (1969). "Discussion of theoretical bearing capacity of very shallow footings by Lawrence Larkin," Journal Soil Mechanics and Foundation Division, ASCE, Vol. 95, No. SM6.

Haring, R.E. et al. (1976). "Extreme wave parameters based on continental shelf storm wave records," 15th International Coastal Engineering Conference, Preprint, Honolulu, Hawaii.

Harr, M.E. (1977). Mechanics of Particulate Media-A Probabilistic Approach New York: McGraw-Hill Book Company, Inc.

Harrison, J.M. (1963). "Nature and significance of geological maps," The Fabric of Geology, ed. C.C. Albritton, Jr., Reading, MA: Addision-Wesley.

Hasofer, A.M. and N.C. Lind. (1974). "Exact and Invariant second moment code format," Journal Engineering Mechanics Division, ASCE. Vol. 100, No. EM1.

Hathaway, J.C., et al. (1979). "U.S. Geological Survey core drilling on the Atlantic Shelf," Science, Vol. 206, No. 4418, pp. 515-527.

Hilldale-Cunningham, C. (1971). "A Probabilistic Approach to Estimating Differential Settlement," M.S. Thesis, Massachusetts Institute of Technology.

Hitchings, G.A., H. Bradshaw, and T.D. Labiosa. (1976). "The planning and execution of offshore site investigations for a North Sea gravity platform," Offshore Technology Conference, Paper No. 2430.

Höeg, K. (1976). "Foundation engineering for fixed offshore structures," BOSS'76, Proceedings, Trondheim, Vol. 1, pp. 39-69.

Höeg, K. and R.P. Mirarka. (1975). "Probabilistic Analysis and Design of a Retaining Wall," Norwegian Geotechnical Institute, Publication 107, Oslo.

Höeg, K. and W.H. Tang. (1978). "Probabilistic Considerations in the Foundation Engineering for Offshore Structures," Norwegian Geotechnical Institute, Publication No. 120.

Hogarth, R. (1975). "Cognitive processes and the assessment of subjective probability distributions," Journal of the American Statistical Association, Vol. 70, No. 350.

Houmb, O.G. (1971). "On the duration of storms in the North Sea," 1st Conference on Port and Ocean Engineering under Arctic Conditions, Trondheim, Vol. 1, pp. 423-439.

Huff, J.R. (1974). "Rig casualties--statistics and analysis," Proceedings Offshore North Sea, Stavanger.

Institut pour L'Encouragement de la Recherche Scientifique dans L'Industrie et L'Agriculture, (1950). "Travaux de la Commission d'Etude des Fondations de Pylones de la Societe Intercommunale Belge d'Electricite," Brussels.

Jahns, H.O. and T.D. Wheeler. (1972). "Long term wave probabilities based on hindcasting of severe storms," Offshore Technology Conference, Paper No. 1590.

Janbu, N.L., L. Bjerrum, and B. Khaernsli. (1956). Veiledning ved losnig av fundamenterings oppgaver," Norwegian Geotechnical Institute.

Jenkins, G.M. (1961). "General considerations in the analysis of spectra," Technometrics, Vol. 3, No. 2, pp. 133-66.

Kameda, H. and T. Koike. (1975). "Reliability Analysis of deteriorating structures," Reliability Approach in Structural Engineering, ed. A.M. Freudenthal, et al., Tokyo: Maruzen Co., pp. 61-78.

Kaplan, E.L. and P. Meier. (1958). "Nonparametric estimation from incomplete observations," JASA, 53: 457-81.

Kaufman, A. (1979). "Personal Communication. Lawrence Livermore Laboratories.

Kay, T.N. (1977). "Factor of safety for piles in cohesive soils," Proceedings Ninth International Conference on Soil Mechanics and Foundation Engineering, Tokyo, Vol. 1, pp. 584-92.

Kay, J.N. (1976). "Safety factor evaluation for single piles in sand," ASCE, 102(GT10).

Kay, J.N. (1976). "Sheet pile interlock tension--probabilistic design," ASCE, 102(GT5), pp. 411-424.

Keeney, R. and H. Raiffa. (1976). Decision Analysis with Multiple Objectives. New York: John Wiley and Sons.

Kelley, W.E. (1971). "Monte carlo approach to seepage in jointed rock." Proceedings thirteenth U.S. National Symposium on Rock Mechanics, University of Illinois.

Kendall, M.G. and A. Stuart (1976). The Advanced Theory of Statistics, London: Hafner, Vol. 2, 3, 3rd Ed.

Keulegan, G.H. and L.H. Carpenter. (1958). "Forces on cylinders and plates in an oscillating fluid," Journal of Research, National Bureau of Standards, Vol. 60, pp. 423-40.

Keynes, J.M. (1921). A Treatise on Probability, London.

Khintchine, A.J. (1960). Mathematical Methods in the Theory of Queueing, London: Griffin.

Kim, Y.Y. and H.C. Hibbard. (1975). "Analysis of simultaneous wave force and water-particle velocity measurements," Offshore Technology Conference, Paper No. 2192.

Ko, H-Y, and L.W. Davidson. (1973). "Bearing capacity of footings in plane strain," Journal Soils Mechanics and Foundation Division, ASCE, Vol. 99, No. SM1.

König, G. (1970). Die Tragfä higheit von Pfählen, Der Baningenieur, Vol. 45, No. 1, pp. 23-29.

Koopman, L.H. (1974). The Spectral Analysis of Time Series, New York: Academic Press.

Kotzias, P.C. and A.C. Stamotopoulos. (1975). "Statistical quality control at Kastrahi earth dam," ASCE, 101(GT 9).

Koutsoffas, D. and J.A. Fischer. (1976). "In situ undrained strength of two marine clays," ASCE, 102(GT9), pp. 989-1005.

Kraft, L.M. (1974). "The behavior of strip foundation on a statistically heterogeneous clay," unpublished.

Kraft, L.M. (1968). "Probability application in soil engineering," Ph.D. thesis, Ohio State University.

Kraft, L.M. and L. Mukhopadhyay. (1977). "Probabilistic analysis of ex-
cavated earth slopes," Proceedings, Ninth International Conference
on Soil Mechanics and Foundation Engineering, Tokyo, Vol 2, pp.
109-116.

Kraft, L.M. and T. Mukhopadhyay. (1972). "The behavior of statistically
heterogeneous excavated earth slopes," Alabama Highway Research HPR
Dept. 67-A, p. 205.

Kraft, L.M. and J.D. Murff. (1975). "A probabilistic investigation of foun-
dation design for offshore gravity structures," Proceedings Offshore
Technology Conference, Dallas, Texas.

Kraft, L.M. and R.L. Perkins. (1979). "Construction eyed from the ground
up, Offshore, November, pp. 57-63.

Kraft, L.M., Jr., and J. Yeung. (1974). "Deformations of statistically
heterogeneous earth structures." Geotechnical Engineering, Vol. 5,
No. 1, pp. 39-52.

Kurzmann, E. (1978). "The reliability of estimating rock excavation costs
in tunneling specifications." Rock Mechanics, Supplement 7, pp. 53-65.

Ladd, C.C. (1977). "Stress-deformation and strength characteristics,"
Proceedings Ninth International Conference on Soil Mechanics and
Foundation Engineering, Tokyo.

Lambe, T.W. (1973). "Predictions in soil engineering," Geotechnique, Vol.
23, No. 2, pp. 149-202.

Langejan, A. (1965). "Some aspects of the safety factor in soil mechanics
considered as a problem of probability," Proceedings Sixth Internation-
al Conference on Soil Mechanics and Foundation Engineering, Vol. 2,
Montreal.

Laakso, L.R. (1976). "The Effects of Environmental Risk on the Design of
Offshore Gravity Platforms," M.S., Thesis, Massachusetts Institute
of Technology.

Latai, D. (1977). "Fault Trees and Fault Tree Data for Land Disposal of
High Level Radioactive Wastes--A Critical Review," unpublished
manuscript.

Lauritzsen, R. and K. Schjetne. (1976). "Stability Calculations for Offshore
Gravity Structures," Norwegian Geotechnical Institute, Publication
Nr. 113.

Lebeque, Y. (1972). "Pouvoir portant du sol sous une charge inclinee,"
Institute Technique de Batiment et des Travaux Publics, Annles Serie:
Sols et Fondations, 88.

Lee, I.K. (1965). "Footings subjected to moments," Proceedings Sixth Inter-
national Conference on Soil Mechanics and Foundation Engineering,
Montreal, Vol. 2.

Lee, K.L. (1970). "Comparison of plane strain and triaxial tests on sand," Journal Soil Mechanics and Foundation Division, ASCE, Vol. 96, No. SM3.

Lewis, R.S. and R.E. Sylvester. (1975). "Shallow Sedimentary Framework of Georges Bank," United States Geological Survey, Draft Report.

Leung, P. and G.B. Baecher. (1979). "Model Uncertainty in Geotechnical Predictions." M.I.T. Department of Civil Engineering, Technical Report.

Longuet-Higgins, M.S. (1957). "The statistical analysis of a random, moving surface," Transactions, Royal Society of London, Serial A, 249, pp. 321-387.

Longuet-Higgins, M.S. (1952). "On the statistical distribution of the heights of sea waves," Journal of Marine Research, XI, 3, pp. 245-266.

Lowrance, W.W. (1976). Of Acceptable Risk. Los Angeles: William Kaufmann, Inc.

Lumb, P. (1975). "Spatial variability of soil properties," Proceedings Second International Conference on Application of Statistics and Probability to Soil and Structural Engineering, Aachen, pp. 397-422.

Lumb, P. (1974). "Applications of statistics in soil mechanics," Soil Mechanics: New Horizons, I.K. Lee ed., Newnes-Butterworth pp. 44-112.

Lumb, P. (1971). "Precision and accuracy of soil tests," Proceedings First International Conference on Application, Statistics, and Probability to Soil and Structural Engineering, Hong Kong.

Lumb, P. (1970). "Safety factors and the probability distribution of soil strength," Canadian Geotechnical Journal, Vol. 7, No. 3.

Lumb, P. (1967). "Statistical methods in soil investigations," Proceedings Fifth Australian-New Zealand Conference on Soil Mechanics and Foundation Engineering, Vol. 1, New Zealand.

Lumb, P. (1966). "Variability of natural soils," Canadian Geotechnical Journal, Vol. 3, No. 2.

Marr, W.A. and J. Hedberg. (1978). "Exploration Methods for Offshore Foundations," M.I.T. INTEVEP Offshore program report.

Marshall, P.W. (1976). "Risk factors for offshore structures," ASCE Conference, Civil Engineering in the Oceans, San Francisco, Calif.

Marshall, P.W. (1968). "Risk evaluation for offshore structures," ASCE, 94, ST 12.

Marshall, P.W. and R.G. Bea. (1976). Failure modes of offshore platforms," BOSS'76, Proceedings.

Marshall, P.W. and R.G. Bea. (1974). "Failure modes of offshore structures," ASCE-EMD Specialty Conference on Probability Methods in Engineering, Stanford, California.

Matern, B. (1960). Spatial Variation, Comm. Swedish Forestry Research Institute, 49: 1-144.

Matheran, G. (1971). The Theory of Regionalized Variables and Its Applications. Les Cahiers du Centre de Morphologie Mathetiques de Fontainebleu, No. 5.

Matsuo, M. (1976). "Reliability in Embankment Design," Massachusetts Institute of Technology, Department of Civil Engineering, Research Report R76-33.

McClelland, B. (1972). "Techniques used in soil sampling at sea," Offshore, March, pp. 51-57.

Meyerhof, G.G. (1976). "Concepts of safety in foundation engineering ashore and offshore," Proceedings Behavior of Offshore Structures, Norwegian Geotechnical Institute, Oslo.

Meyerhof, G.G. (1970). "Safety factors in soil mechanics," Canadian Geotechnical Journal, Vol. 7, No. 4.

Meyerhof, G.G. (1963). "Some recent research on the bearing capacity of foundations," Canadian Geotechnical Journal, Vol. 1, No. 1.

Meyerhof, G.G. (1961). "Some problems in the design of rigid retaining walls," Proceedings Fifteenth Canadian Soil Mechanics Conference. Ottawa.

Meyerhof, G.G. (1955). "Influence of roughness of base and groundwater conditions on the ultimate bearing capacity of foundations," Geotechnique, Vol. 5, No. 3.

Meyerhof, G.G. (1953). "The bearing capacity of foundations under eccentric and inclined loads," Proceedings Third International Conference on Soil Mechanics and Foundation Engineering, Vol. 1, Zurich.

Meyerhof, G.G. (1951). "The ultimate bearing capacity of foundations," Geotechnique, Vol. 2.

Mizuno, T. (1953). "On the bearing power of soil under a uniformly distributed circular load," Proceedings Third International Conference on Soil Mechanics and Foundation Engineering, Vol. 1, Zurich.

Moan, T. (1979). "Risk assessment of mobile rig operations," Norwegian Institute of Technology, Division of Marine Structures, Report SK/R46.

Moan, T., K. Syvertsen, and S. Haver. (1977). "Dynamic analysis of gravity platforms subjected to random wave excitation," Proceedings STAR Symposium: Energy Research in the Oceans, SNAME Spring Meeting, San Francisco.

Moe, G. and S.B. Crandall. (19xx). "Extremes of Morison-Type wave loading on a single pile," Journal of Engineering for Industry, to appear.

Moran, Proctor, Mueser, Rutledge. (1954). "Feasibility report on Texas towers: Part 1," Report to Department of the Navy, Bureau of Yards and Docks.

Morse, R.K. (1971). "The importance of proper soil units for statistical analysis," Statistics and Probability in Civil Engineering, Hong Kong University Press, distributed by Oxford University Press, London.

Moses, F. (1979a). "Bayesian calibration of platform reliability," Proceedings ASCE Special Conference on Probabilistic Mechanics and Structure Reliability, Tucson.

Moses, F. (1979b). "System reliability analyses of platform structures," Proceedings ASCE Special Conference on Probabilistic Mechanics and Structure Reliability, Tucson.

Moses, F. (1977). "Safety and Reliability of offshore structures," International Research Seminar on the Safety of Structures under Dynamic Loading, Trondheim.

Moses, F. (1976). "Reliability of structural systems," BOSS'76, Proceedings, Vol. I, pp. 912-923.

Morison, J.R. and R.C. Crooke. (1953). "The Mechanics of Deep Water, Shallow Water, and Breaking Waves." Beach Erosion Board, Technical Memorandum No. 40.

Morison, J.R., M.P. O'Brien, J.W. Johnson and S.A. Schaaf. (1950). "The force exerted by surface waves on piles," Petroleum Transactions, Vol. 189.

Muhs, H. and K. Weiss. (1974). "Inclined load tests on shallow strip footings," Degebo Heft, No. 30.

Myers, J., C.H. Holm, and R.F. McAllister. (1969). Handbook of Ocean and Underwater Engineering, New York: McGraw-Hill Book Company, Inc.

Nash, K.L. (1953). "The shearing resistance of a closely graded sand," Proceedings Third International Conference on Soil Mechanics and Foundation Engineering, Vol. 1, Zurich.

Netherlands Steering Committee on Offshore Structures' Problems. (1980). "Probabilistic reliability analysis for offshore structures," Final Report, English Edition.

Nolte, K.G., (1973). "Statistical methods for determining extreme sea states," Proceedings Second Conference on Port and Ocean Engineering under Arctic Conditions, Reykjavik, pp. 705-742.

Nolte, K.G. and F.H. Hsu. (1979). "Statistics of large waves in a sea state." ASCE, 105, WW4, pp. 389-404.

Nolte, K.G. and F.H. Hsu. (1972. "Statistics of ocean wave groups," Offshore Technology Conference, Paper No. 1688.

Noorany, I. (1972). "Underwater soil sampling and testing—a State of the art review," Underwater Soil Sampling, Testing, and Construction Control, ASTM STP501.

Noorany, I. and S.F. Gigieushi. (1970). "Engineering properties of submarine soils: state of the art review," ASCE, Vol. 96, SM5, pp. 1735-61.

Nordquist, J.E. (1979). "Subjective Probability in Geotechnical Engineering," M.S. Thesis, Massachusetts Institute of Technology.

Norske Det Veritas. (1979). "Rules for the design, construction and inspection of offshore structures," Oslo.

Nucci, L.A. and G.B. Baecher. (1979). "Error in Two-Color Maps," Massachusetts Institute of Technology, Department of Civil Engineering Report R79-11.

Ochi, M.K. (1973). "On prediction of extreme values," Journal of Ship Research, Vol. 17, No. 1.

Ovesen, N.K. (1975). "Centrifugal testing applied to bearing capacity problems for footings on sand," Geotechnique, Vol. 25, No. 2.

Papoulis, A. (1965). Probability, Random Variables, and Stochastic Processes, New York: McGraw-Hill Book Company, Inc.

Parzen, E. (1961). "Mathematical considerations in the estimation of spectra," Technometrics, Vol. 3, No. 2, pp. 167-190.

Peck, R.B. (1967). "Bearing capacity and settlement: certainties and uncertainties," Proceedings of a Symposium on Bearing Capacity and Settlement of Foundations, Durham, North Carolina: Duke University.

Peck, R.B. (1969). "Advantages and limitations of the observational method in applied soil mechanics," Geotechnique, Vol. 19, No. 2.

Potyondy, J.G. (1961). "Skin friction between various soils and construction materials." Geotechnique, Vol. 11.

Poulos, H.G. and E.H. Davis. (1974). "Elastic solutions for soil and rock mechanics, New York: John Wiley & Sons, Inc.

Prakash, S. and S. Saran. (1971). "Bearing capacity of eccentrically loaded footings," Journal Soil Mechanics and Foundation Division, ASCE, Vol. 97, No. SM1.

Purkayastha, R.D. and R.A. Char. (1977). "Stability analysis for eccentrically loaded footings," Journal Geotechnical Division, ASCE, Vol. 103, No. GT6.

Raiffa, H. and R.L. Schlaifer. (1964). Applied Statistical Decision Theory, Cambridge, MA: M.I.T. Press.

Raman, Harihara, and Venkatanarassiah, Paruchuri. (1976). "Forces due to nonlinear waves on vertical cylinders," Journal of the Waterways, Harbors and Coastal Engineering Division, ASCE, Vol. 102, No. WW3, Proc. Paper 12326, August, pp. 301-316.

Ramberg, S.E. and J.M. Neidzwecki. (1979). "The Sensitivity of Wave Force Computations to Method and to Hydrodynamic Approximations," Naval Research Laboratory Memorandum Report.

Resendiz, D. and I. Herrera. (1969). "A probabilistic formulation of settlement controlled design," Proceedings Sixth International Conference on Soil Mechanics and Foundation Engineering, Vol. 3, Mexico City.

Rice, S.O. (1944). Mathematical Analysis of Random Noise, Bell, System Technical Journal, Vol. 23, pp. 282-332 and (1945) Vol. 24, pp. 46-156.

Richards, A.F., ed. (1967). Marine Geotechnique: Proceedings of the 1966 International Conference in Marine Geotechnique. Champaign, Ill: University of Illinois Press.

Rodriquez-Hurbe, I. and J.M. Menia. (1974). "The Design of Rainfall Networks in Time and Space," Massachusetts Institute of Technology Parsons Laboratory, Research Report R74-6.

Salmon, W.C. (1966). Philosophy of Science, University of Pittsburg Press.

Saran, S., S. Prakash, and A.V. Murty. (1971). "Bearing capacity of footings under inclined loads," Soils and Foundations, Vol. 11, No. 1.

Sarpkaya, T. (1975). "Forces on cylinders and spheres in a sinusoidally oscillating fluid." Journal of Applied Mechanics, March, pp. 32-7.

Schueller, G.I. and H.S. Choi. (1977). "Offshore platform risk based on a reliability model," Offshore Technology Conference, OTC 3028.

Schueller, G.I. (1972). "A probabilistic method for predicting velocities and accelerations of water wave particles. Offshore Technical Conference, Preprints, Vol. 1, pp. 951-964.

Schueller, G.I. (1975). "On the reliability of the spectral method for the design of offshore structures," Proceedings XVI 'th Congress of International Association for Hydraulic Research, Sao Paulo, July.

Schueller, G.I. (1976). "Risk criteria for the design of fixed platforms," Proceedings Second International LAHR Symposium on Stochastic Hydraulics, Lund, Sweden, August 2-4.

Schultze, E. (1971). "The general significance of statistics for the civil engineer." Proceedings Second International Conference on Application of Statistics and Probability in Soil and Structural Engineering, Aachen, Germany.

Schultze, E. (1971). "Frequency distributions and correlations of soil properties," Proceedings First International Conference on Application of Statistics and Probability in Soil and Structural Engineering, Hong, Kong, pp. 371-387.

Selig, E.T. and K.E. McKee. (1961). "Static and dynamic behavior of small footings," Journal Soil Mechanics and Foundation Division, ASCE, Vol. 87, No. SM6.

Shepard, F.P. (1948). Submarine Geology, New York: Harper and Row Publishers, Inc.

Singh, A. and K.L. Lee. (1970). "Variability of soil parameters," Proceedings Eighth Annual Conference on Geological and Soil Engineering, Idaho.

Singh, A. (1971). "How reliable is the Factor of Safety in Foundation Engineering," Statistics and Probability in Civil Engineering, Hong Kong University Press, distributed by Oxford University Press, London.

Spring, B.H. and P.L. Monkmeyer. (1975). "Interaction of plane waves with vertical cylinders," Proceedings Fourteenth International Conference on Coastal Engineering, ASCE.

Springer, M.D. (1979). The Algebra of Random Variables, New York: John Wiley and Sons, Inc.

Stahl, B. (1977). "Offshore structure reliability engineering," Petroleum Engineer, October.

Stahl, B. (1975). "Probabilistic methods for offshore platforms," Proceedings of Annual Meeting Division Products, American Petroleum Institute, Dallas, Texas, April 7-9.

Stahl, B. and K.A. Blenharu. (1976). "Offshore platform reliability--a parameter study," Proceedings National Structural Engineering Conference on Methods of Structural Analysis, Madison, Wisconsin.

Stahl, B. and A.E. Knapp. (1976). "Evaluation of an offshore platform using probabilistic methods," ASCE-EMD Specialty Conference on Probabilistic Methods in Engineering, Stanford, California.

Stone, L.D. (1975). Theory of Optimal Search, New York: Academic Press.

Su, Y.L., Y.J. Wang, and R. Stefanko. (1969). "Finite element analysis of underground stresses utilizing stochastically simulated material properties," Proceedings Eleventh United States Symposium on Rock Mechanics, Berkeley, California.

Tang, Wilson H. (1979). "Probabilistic evaluation of penetration resistances," Journal of the Geotechnical Engineering Division, ASCE Vol. 105, No. GT10, Proc. Paper 14902, October, pp. 1173-1191.

Teng, W.C. (1962). Foundation Engineering, Englewood Cliffs, New Jersey: Prentice-Hall, Inc.

Terzaghi, K. (1943). Theoretical Soil Mechanics, New York: John Wiley & Sons, Inc.

Terzaghi, K. and R.B. Peck. (1967). Soil Mechanics in Engineering Practice, New York: John Wiley & Sons, Inc., 2nd edition.

Thom, H.C.S. (1971). Asymptotic extreme-value distributions of wave heights in the open ocean, Journal of Marine Research, Vol. 29, No. 1, pp. 19-27.

Thompson, E.F. (1974). "Results from CERC wave measurement programs," International Symposium on Ocean Wave Measurements and Analysis, ASCE.

Tran-Vo-Thiem. (1970). "Force Portante Limite des Fondations Superficielles a Charge Inclinee et Excentree," Congresso Brasileiro de Mecanica dos Solos Engenharia de Fundacoes, Vol. 1, Guanabara.

Tung, C.C. (1975). "Statistical properties of wave force," Journal Engineering Mechanics Division, ASCE, Vol. 101, No. EM1, February, pp. 1-11.

Twerksy, V. (1952). "Multiple scattering of radiation by an arbitrary configuration of parallel cylinders. Journal of the Accoustic Society of America, Vol. 24, pp. 42-6.

Vanmarke, E.H. (1977). "Probabilistic modeling of soil profiles," ASCE, Vol. 103, No. GT11, pp. 1277-1246.

Veneziano, D. (1979). "Statistical estimation and data collection: A review of procedures for civil engineers," Proceedings, Third International Conference on Application of Statistics and Probability in Soil and Structural Engineering, Sydney.

Veneziano, D. (1976). "Basic principles and methods of structural safety," Bulletin D'Information, No. 112, Joint Committee on Structural Safety, Comite Europeen Du Beton.

Veneziano, D. (19xx). Personal Communication.

Veneziano, D. and E. Faccioli. (1975). "Bayesian design of optimal experiments for the estimation of soil properties," Proceedings, Second International Conference on Application of Statistics and Probability in Soil and Structural Engineering, Aachen.

Veneziano, D., P.K. Kitanidis, and C.S. Queirioz. (1977). "Two Problems in Spatial Sampling," Massachusetts Institute of Technology, Department of Civil Engineering, Research Report R77-29.

Verghese, A.C. (1972). "Bearing capacity theory from experimental results," Journal Soil Mechanics and Foundation Division, ASCE, Vol. 98, No. SM12.

Vesic, A. (1963). "Bearing capacity of deep foundations in sand," Highway Research Board Record, Vol. 39.

Vesic, A. (1973). "Analysis of ultimate loads of shallow foundations," Journal Soil Mechanics and Foundations Division, ASCE, Vol. 99, No. SM1.

Vesic, A. (1974). "Bearing capacity of shallow foundations," Foundation Engineering Handbook, ed. H.F. Winterkorn and H-Y Fang, New York: Van Nostrand Rheinhold Company.

Vik, I. and O.G. Hounb. (1977). "On the duration of a sea state," Inter-National Research Seminar on Safety of Structure Under Dynamic Loads, Norwegian Institute of Technology, Trondheim.

Vivitrat, V. (1978). "Exploration and evaluation of engineering properties for foundation design of offshore structures." Ph.D. Thesis, Massachusetts Institute of Technology; and MIT Seagrant Technical Report No. MITSG 79-8.

Weiss, K. (1973). "Die Formbeiwerte in der Grundbruchgleichung fur nicht= bindige Boden," Degebo Heft, No. 29.

Whittle, P. (1963). Prediction and Regulation, New York: Van Nostrand, Co.

Wilson, John. (1978). Personal Communication.

Wood, E.G. (1974). "A Bayesian Approach to Analyzing Uncertainty Among Stochastic Models," IIASA Research Report, RL-74-16. Laxenburg, Austria.

Wu, T.H. and L.M. Kraft. (1967). "The probability of foundation safety," Journal Soil Mechanics and Foundation Division, ASCE, Vol. 93, No. 29.

Wu, T.H. (1974). "Uncertainty, safety, and decision in Soil Engineering," Journal Geotechnical Division, ASCE, Vol. 100, No. GT3.

Yüceman, M.S., W.H. Tang, and A.H-S Ang. (1973). "A Probabilistic Study of the Safety and Design of Earth Slopes," Structural Research Series, No. 402. Civil Engineering Studies, University of Illinois.

Zaharescue, E. (1961). "The eccentricity sense influence of the inclined load on the bearing capacity of rigid foundations," Journal National Buildings Organization, Vol. 6.

Zienkiewicz, O.C. (1971). The Finite Element Method in Engineering Science, New York: McGraw-Hill Book Company, Inc.

Zienkiewitz, O.C., R.W. Lewis, and K.G. Stagg (ed.) (1978). Numerical Models in Offshore Engineering, New York: Wiley-Interscience.